UC San Diego

UC San Diego Electronic Theses and Dissertations

Title

Reconstructing Foraging Ecology of a Top Predator through Stable Isotope Analysis of Teeth and Bones

Permalink

https://escholarship.org/uc/item/41n8n959

Author

Bowen, Kelly R.

Publication Date

2024

Supplemental Material

https://escholarship.org/uc/item/41n8n959#supplemental

Peer reviewed|Thesis/dissertation

eScholarship.org Powered by the California Digital Library
University of California

UNIVERSITY OF CALIFORNIA SAN DIEGO

Reconstructing Foraging Ecology of a Top Predator through Stable Isotope Analysis of Teeth and Bones

A Dissertation submitted in partial satisfaction of the requirements
for the degree Doctor of Philosophy

in

Biology

by

Kelly R. Bowen

Committee in charge:

Professor Carolyn Kurle, Chair
Professor Ronald Burton
Professor Elsa Cleland
Professor Kaustuv Roy

2024

Copyright

Kelly R. Bowen, 2024

All rights reserved.

The Dissertation of Kelly R. Bowen is approved, and it is acceptable in quality and form for publication on microfilm and electronically.

University of California San Diego

2024

DEDICATION

This dissertation is lovingly dedicated to my family:

My parents, Robert and Marcia Flanders, for guiding my journey and turning my childhood dreams into reality.

To my husband, John Bowen, whose endless love and support in every way have been my foundation.

TABLE OF CONTENTS

DISSERTATION APPROVAL PAGE iii

DEDICATION iv

TABLE OF CONTENTS v

LIST OF FIGURES viii

LIST OF TABLES xi

LIST OF SUPPLEMENTAL FIGURES xiii

LIST OF SUPPLEMENTAL TABLES xiv

LIST OF SUPPLEMENTAL FILES xv

ACKNOWLEDGEMENTS xvi

VITA xix

ABSTRACT OF THE DISSERTATION xx

Chapter 1 : Effects of pre-treatment, historical age, and sample characteristics on the stable isotope analyses of killer whale (*Orcinus orca*) bone 1

1.1 Abstract 1

1.2 Introduction 2

1.3 Materials and Methods 5

1.4 Results 10

1.5 Discussion 12

1.6 Acknowledgements 19

1.7 References 27

Chapter 2 : Considerations for stable isotope analysis of marine mammal dentin growth layer groups 32

2.1 Abstract 32

2.2 Introduction 33

2.3 Materials and Methods 36

2.4 Results 42

2.5 Discussion 44

2.6 Acknowledgements 50

1.7 References 56

Chapter 3 : Stable isotope values from organisms in the North Pacific Ocean: A reference for trophic ecology studies 59

3.1 Stable isotope value reference library 59

3.2 Acknowledgements 62

3.3 References: Main text 69

3.4 References: Table 3.1 70

Chapter 4 : Reconstructing historical ecology of North Pacific transient killer (*Orcinus orca rectipinnus*) whales using stable isotope analysis of dentin 78

4.1 Abstract 78

4.2 Introduction 79

4.3 Materials and Methods 84

4.4 Results 98

4.5 Discussion 103

4.6 Acknowledgements 111

4.7 References 149

Chapter 5 : Historical reconstruction of northern and southern resident killer whale (*Orcinus orca ater*) diets through stable isotope analysis of dentin 159

5.1 Abstract 159

5.2 Introduction 160

5.3 Materials and Methods 164

5.4 Results 176

5.5 Discussion 180

5.6 Acknowledgements 187
5.7 References 212
CONCLUSIONS 221

LIST OF FIGURES

Figure 1.1. Boxplots of the (A) $\delta^{13}C$, (B), $\delta^{15}N$, and (C) C:N values from killer whale bone samples (n = 34) under an untreated control (C on the x-axis) and three experimental conditions: lipid-extracted (LE), demineralized (D), and both demineralized and lipid-extracted (DLE).. ... 21

Figure 1.2. The C:N values from killer whale bones (n = 28) plotted against the year a specimen was collected. The treatment groups included the untreated control (C; blue circle), demineralized (D; red triangle), lipid-extracted (LE; yellow square), and both demineralized and lipid-extracted (DLE; purple plus). 22

Figure 2.1. Sampling schemes for the three objectives of our study illustrated with the cut surface of tooth halves and visible growth layer groups (GLGs). A gray backdrop indicates the tooth half has been etched and penciled, with a white center indicating an open pulp cavity. 52

Figure 4.1. Map centered in the North Pacific Ocean, showing killer whale specimen collection locations. Blue markers indicate individuals we categorized as 'Alaska' (AK) transient killer whales, and orange markers indicate individuals we categorized as 'California' (CA) transient killer whales. Map created with Datawrapper. 113

Figure 4.2. A 1000 dpi scanned image of a killer whale tooth that has been bisected, polished, etched with formic acid, and highlighted with graphite. Visible growth layer groups (GLGs) represent one year of time. 114

Figure 4.3. The $\delta^{15}N$ values over time for Alaska transient killer whale dentin, divided by pre-1970 (green triangles) and post-1970 (purple circles) growth layer groups. Individuals are connected by a dashed gray line. 115

Figure 4.4. The $\delta^{15}N$ values by age for Alaska (AK) and California (CA) transient killer whales, divided by pre-1970 (green triangles) and post-1970 (purple circles). Individuals are connected by a dashed gray line..... 116

Figure 4.5. The $\delta^{13}C$ values by age for Alaska (AK) and California (CA) transient killer whales, divided by pre-1970 (green triangles) and post-1970 (purple circles). Individuals are connected by a dashed gray line..... 117

Figure 4.6. SIBER ellipses for Alaska (AK, black) vs California (CA, red) killer whales (A) and 'before' (black) and 'after' (red) within AK transients (B). 118

Figure 4.7. Trophic position of Alaska (AK; blue diamonds) and California (CA; orange triangles) over time as estimated from a calculating using the $\delta^{15}N$ values of trophic and source amino acids from dentin..... 119

Figure 4.8. The relationship between the $\delta^{15}N_{Phe}$ values from dentin and the estimated year that the sampled growth layer group was estimated to represent for Alaska (AK; blue diamonds) and California (CA; orange triangles) killer whales. 120

Figure 4.9. The $\delta^{15}N_{Bulk}$ values are shown against the $\delta^{15}N_{Phe}$ values (A, source amino acid) and the $\delta^{15}N_{Pro}$ values (B, trophic amino acid) of dentin from Alaska (AK; blue diamond) and California (CA; orange triangle) killer whale teeth. 121

Figure 4.10. The $\delta^{15}N_{Pro}$ values (trophic amino acid) are shown against the $\delta^{15}N_{Phe}$ values (source amino acid) of dentin from Alaska (AK; blue diamond) and California (CA; orange triangle) killer whale teeth. 122

Figure 4.11. Histogram of the specialization index (*S*) values for Alaska (AK; blue top sections) and California (CA; orange lower sections) individuals calculated from the $\delta^{15}N$ values of dentin, where *S* is the within-individual variation (from growth layer groups) divided by the between-individual variation. 123

Figure 4.12. Isospace plot produced in MixSIAR showing the distributions of stable isotope values from the two primary prey groups: whales (dashed lines) and pinnipeds (solid lines). .. 124

Figure 4.13. Mean estimated proportion that each prey group, pinnipeds (blue top sections) and baleen whales (orange bottom sections), contribute to the diets of each California (B) and Alaska (B) killer whale individual. Red dashed lines in (B) separate time periods: leftmost is pre-1970, middle is during 1970s, and rightmost is post-1970. 125

Figure 5.1. Map centered on the west coast of the United States showing collection location of resident killer whale specimens (blue = Southern resident, orange = Northern resident). Map created using Datawrapper. 189

Figure 5.2. A visual representation of the two-way interaction (time:age) that significantly predicted the $\delta^{13}C$ values from dentin collected from the growth layer groups (GLGs) in teeth from archived Southern resident killer whale (SRKW) skulls (n = 11 individuals; 65 GLGs).. 190

Figure 5.3. The $\delta^{13}C$ values from dentin collected from the growth layer groups (GLGs) in teeth from archived Northern resident killer whale NRKW skulls (n = 6 individuals; 22GLGs) are shown across the years each sampled GLG was estimated to represent. Each connected line represents one individual. 191

Figure 5.4. A visual representation of the three-way interaction (time:age:sex) that significantly predicted the $\delta^{15}N$ values from dentin collected from the growth layer groups (GLGs) in teeth from archived Southern resident killer whale (SRKW) skulls (n = 11 individuals; 65 GLGs).. 192

Figure 5.5. A visual representation of the three-way interaction (time:age:sex) that significantly predicted the $\delta^{15}N$ values from dentin collected from the growth layer groups (GLGs) in teeth from archived Northern resident killer whale (NRKW) skulls (n = 6 individuals; 22 GLGs).. . 193

Figure 5.6. There were no significant relationships between total adult spawning Chinook salmon abundance in Puget Sound and the $\delta^{15}N$ values from dentin collected from the growth layer groups (GLGs) in teeth from archived (A) Northern resident and (B) Southern resident killer whale skulls. 194

Figure 5.7. Estimations of the mean contribution of Chinook salmon to the diets of individual Northern resident (NR; orange triangles) and Southern resident (SR; blue circles) over time using MixSIAR. Error bars represent the standard deviations. 195

Figure 5.8. Trophic positions are shown across time for both Northern resident (NR; orange triangles) and Southern resident (SR; blue circles) killer whales. 196

Figure 5.9. The relationship between (A) the $\delta^{15}N_{bulk}$ and $\delta^{15}N_{Phe}$ (source amino acid values and (B) the $\delta^{15}N_{bulk}$ and $\delta^{15}N_{Pro}$ (trophic amino acid) values from dentin collected from the growth

layer groups (GLGs) in teeth from archived Northern resident (NR; orange triangles) and Southern resident (SR; blue circles) killer whale skulls. 197

Figure 5.10. The $\delta^{15}N_{Phe}$ (source amino acid) values from dentin collected from the growth layer groups (GLGs) in teeth from archived Northern resident (NR; orange triangles) and Southern resident (SR; blue circles) killer whale skulls shown across time. 198

LIST OF TABLES

Table 1.1. Results of Tukey's HSD *post-hoc* tests after a repeated measures ANOVA analyzing the δ^{13}C values of killer whale bone samples (n = 34) under three treatment conditions and a control. C = control/untreated, D = demineralized, LE = lipid-extracted, and DLE = both demineralized and lipid-extracted. 23

Table 1.2. The mean (±SD) δ^{13}C, δ^{15}N, and C:N values for killer whale bone samples (n = 34) across three treatments and a control are shown alongside the change in the δ^{13}C ($\Delta\ \delta^{13}$C) and δ^{15}N ($\Delta\delta^{15}$N) values for each treatment relative to the control. C = control/untreated, D = demineralized, LE = lipid-extracted, and DLE = both demineralized and lipid-extracted. 24

Table 1.3. Results of Tukey's HSD *post-hoc* tests after a repeated measures ANOVA analyzing the C:N values from killer whale bone samples (n = 34) under a normal score transformation using the Elfving method. C = control/untreated, D = demineralized, LE = lipid-extracted, and DLE = both demineralized and lipid-extracted. 25

Table 3.1. The mean δ^{13}C and δ^{15}N values (± SD, or SE where noted) for six major taxonomic groups are compiled from published literature. In the "Tissue" column, "LE" indicates the samples were lipid-extracted to remove fats which are depleted in their δ^{13}C values and create a source of bias. 64

Table 3.2. Summary of single δ^{13}C and δ^{15}N values (± SD) for each species, excluding samples from the Gulf of California due to elevated δ^{15}N values for animals collected in that region. In the event of paired samples (Table 1) from a study, the values for muscle tissue were used. 65

Table 3.3. Summary of single δ^{13}C and δ^{15}N values (± SD) for broad taxonomic groups in the North Pacific Ocean. Values represent primarily soft tissues, except for Mustelidae (sea otters) which are represented by whiskers and bone collagen. See main text and Carlisle *et al.* (2015) for methodology. 68

Table 4.1. The metadata for specimens used in this study, including the specimen ID (* = duplicate teeth analyzed and stable isotope values averaged), alternate catalogue IDs or other identifiers, the collection year, the sex of the animal (F = female, M = male), the method of confirmation for ecotype. 126

Table 4.2. Sampling scheme for compound-specific isotope analysis of amino acids (CSIA-AA). We aimed to sample one growth layer group (GLG) from each of two individuals for each decade. Within decades, we aimed to sample from the earlier and latter half. Locations for the individuals were assigned to either California (CA) or Alaska (AK). 127

Table 4.3. The specimen IDs, estimated year and age represented by the sampled growth layer group (GLG), and the final δ^{13}C and δ^{15}N values for each GLG. See Bowen and Kurle in prep for other previous age estimates of these same teeth and discussions related to aging uncertainty. 128

Table 4.4. Summary statistics for the stable isotope values of dentin from 36 transient killer whales sampled in this study. We first calculated a mean for each individual animal from all growth layer groups (GLGs) sampled, and then we averaged the individual means to identify the '*Means of individual means*' for killer whales 137

Table 4.5. Results from ANOVAs of four separate linear mixed models (LMMs) to investigate the effect of time (categorical) and age (continuous), with all possible interactions, on transient killer whale $\delta^{13}C$ and $\delta^{15}N$ values.. 138

Table 5.1. Metadata for the killer whale specimens used in this study. * = animals that spent some amount of time in captivity, with those years being excluded from our analyses. † = Known wild animals with an assigned pod number. 199

Table 5.2. The killer whales from which tooth specimens were used for measuring the $\delta^{15}N$ values of amino acids through compound-specific isotope analysis of amino acids (CSIA-AA). GLG = growth layer group removed from each tooth, NR = Northern resident killer whales, SR = Southern resident killer whales..... 200

Table 5.3. The stable isotope values of dentin collected from the growth layer groups (GLGs) in teeth from archived Northern resident killer whale (NRKW) and Southern resident killer whale (SRKW) skulls. 201

Table 5.4. Results of linear mixed models to assess the effect of time (year), age, and sex on the $\delta^{13}C$ and $\delta^{15}N$ values from dentin collected from the growth layer groups in teeth from archived Southern resident killer whale (SRKW) and Northern resident killer whale (NRKW) skulls. Significance levels: *** = 0.001 – 0, ** = 0.01 – 0.001, * = 0.05 – 0.01 202

Table 5.5. Results of linear mixed models used to determine the significance of time (year), age, and sex on the $\delta^{13}C$ and $\delta^{15}N$ values from dentin collected from the growth layer groups in teeth from archived Southern resident killer whale (SRKW) and Northern resident killer whale (NRKW) skulls. 204

LIST OF SUPPLEMENTAL FIGURES

Figure S4.1. The mean δ^{15}N values with standard deviation error bars are shown for each of 10 amino acids: four source amino acids (left, purple) and six trophic amino acids (right, green). 139

Figure S4.2. The δ^{13}C values of both Alaska (AK) and California (CA) transient killer whales are shown across ages for males (blue triangles) and females (red circles). Trend lines are shown for all data points in that category, and dashed grey lines indicate sampled growth layer groups within an individual. 140

Figure S4.3. Boxplots of the δ^{13}C values (all sampled growth layer groups) pre- and post-1970 for males (blue) and females (red) in both Alaska (AK) and California (CA) transient killer whale populations. 141

Figure S5.1. The mean δ^{15}N values with standard deviation error bars are shown for each of 10 amino acids: four source amino acids (left, purple) and six trophic amino acids (right, green). 206

LIST OF SUPPLEMENTAL TABLES

Table S1.1. Collection details for the 34 killer whale (*Orcinus orca*) bones sampled and analyzed for their $\delta^{13}C$, $\delta^{15}N$, and C:N values. Each specimen sample was analyzed under three treatment with an untreated control: demineralized, lipid-extracted, and demineralized and lipid-extracted together. 26

Table S2.1. Catalogue numbers for the 25 killer whale (*Orcinus orca*) teeth used in this study are listed in addition to the objective(s) for which the teeth were utilized as described in the main text. * = specimen used for triplicate test. 53

Table S2.2. Catalogue numbers, other associated metadata, and stable isotope values are reported for specimens used towards objective II in the main manuscript to examine variability among 12 duplicate teeth and 1 set of triplicate teeth. 54

Table S4.1. The specimen IDs (* = from external sources not measured in our study), ecotype (O = offshore, R = resident, T = transient), sex (NA = not available, F = female, M = male), and the $\delta^{13}C$ and $\delta^{15}N$ values of the specimen used in our ecotype prediction model. 142

Table S4.2. The output of our ecotype prediction model from stable isotope data using a multinomial regression analysis with input data from known ecotypes (Table S4.1). Offshore, resident, and transient columns show the probability that the specimen belongs to that ecotype. 144

Table S4.3. The $\delta^{15}N$ values from compound-specific isotope analysis of amino acids (CSIA-AA) separated into 'source' amino acids and 'trophic' amino acids. 145

Table S4.4. The mean and standard deviation (SD) for the $\delta^{13}C$ and the $\delta^{15}N$ values of two primary prey groups we examined in our study, pinnipeds and mysticetes, used as input for a MixSIAR analysis. Values were calculated from the meta-analysis in Chapter 3. 146

Table S4.5. Results of linear mixed models used to investigate the effects of sex, time, and age on Alaska (AK) and California (CA) killer whales. Significance codes are: *** < 0.001, ** < 0.01, * < 0.05. 147

Table S4.6. Results from Analysis of Variance tests (ANOVAs) used to assess which variables in the linear mixed model (Table S4.5) were significant predictors of $\delta^{13}C$ and $\delta^{15}N$ values in Alaska (AK) and California (CA) killer whales. Significance codes are: *** < 0.001, ** < 0.01, * < 0.05. 148

Table S5.1. We report details for the compound-specific isotope analysis of amino acids (CSIA-AA) results for each of the 11 specimens sampled, including specimen ID (* = specimen not included in the linear mixed model analyses of bulk isotope analyses), alternate catalogue IDs, resident type (NR = Northern resident, SR = Southern resident) 207

Table S5.2. We report the specimens used in this study (* = time in captivity, † = assigned wild ID), alternate catalogue IDs, the sex of the individual, resident type (SR = Southern resident, NR = Northern resident), the estimated age of the growth layer group (GLG) from which dentin was extracted, the estimated year the GLG represents. 208

LIST OF SUPPLEMENTAL FILES

Bowen_specimen_details.docx : see Table S1.1

Bowen_stable_isotope_reviewl.xlsx : see Table 3.1

ACKNOWLEDGEMENTS

My journey has been shaped by the support of many, for which I am profoundly grateful. To my advisor, Carolyn Kurle, I share my most sincere gratitude. She provided me with the opportunity to pursue this path, and her guidance, expertise, and unwavering support have been instrumental to reaching this point. Beyond her scientific supervision, she has shown me (and all of those around her) genuine patience, kindness, and encouragement. She radiates warmth and care through her natural ability to connect with others that I aspire to emulate in my own professional and personal interactions. I thank her for being both a brilliant advisor and a compassionate mentor.

I also express my thanks to my committee members: Elsa Cleland, Kaustuv Roy, and Ron Burton. Elsa and Kaustuv have been supporting me since my first year, and Ron so very kindly undertook me despite his best efforts at nudging towards retirement. I also thank Jon Shurin and Kelton McMahon for their support with my statistical analyses and data interpretation. My research was also rooted in the generosity of the natural history collections who allowed me to destructively sample their killer whale teeth, and I thank each and every person who was involved in those specimen loans.

I am extending an immense thank you to my parents, Marcia and Robert. Their love and support have been the foundation upon which this achievement rests, in addition to the value of curiosity, hard word, and perseverance that they instilled in me. This dissertation is as much a testament to their sacrifices and dedication as it is to mine. I am forever grateful for everything they have done to help me reach this goal. My siblings (Andrew, Chris, Gordon, and Christian) have also been constant companions, providing me with brotherly comic relief during stressful times and encouragement when I needed it most. Collectively, they have all played a unique and

irreplaceable role in supporting me. I offer a special thanks to my brother Andrew and his wife Tina for not only their heartfelt support but also their financial and logistical support throughout the years. My academic pursuits would not have been possible without it.

I would like to express my heartfelt gratitude to my husband, John, whose love and support have been my foundation throughout this journey. He has spent countless long nights helping me in every way, from building tools that would progress my projects to searching for owls as a relaxing way of relieving research anxieties. He was by my side for many of my tooth-collection trips, making each expedition not only productive but an adventure to be remembered. I am also very grateful for the family I gained through John, who have consistently shown me kindness, generosity, and a genuine curiosity about my work.

Lastly, I could not forget my sweet pets, Keaton the dog-like cat and Kaija the cat-like dog. They became my loyal companions when I was pursing my Master's far from home and have been with me every step of the way ever since. Their playful personalities and unconditional love have brought so much joy and balance into my life. I am thankful to both of them for being there during the long hours of writing and research, keeping me company during late nights, and reminding me to take breaks, sometimes by physically closing my computer when they feel like it.

Chapter 1, in full, is a reprint of material as it appears in "Bowen KR, Kurle CM. Effects of pre-treatment, historical age, and sample characteristics on the stable isotope analyses of killer whale (*Orcinus orca*) bone. *Rapid Commun Mass Spectrom* 2024;38(19):e9874". The dissertation author was the primary investigator and author of this paper.

Chapter 2, in full, has been submitted for publication of the material as it may appear in Rapid Communications in Mass Spectrometry, 2024, Bowen, KR; Kurle, CM. The dissertation author was the primary investigator and author of this paper.

Chapter 3, in part, has been submitted for publication of the material as it may appear in Marine Mammal Science, 2024, Bowen, KR; Kurle, Carolyn. The dissertation author was the primary investigator and author of this paper.

Chapter 4, in full, is currently being prepared for submission for publication of the material. Bowen, Kelly; Kurle, Carolyn. The dissertation author was the primary investigator and author of this material

Chapter 5, in full, is currently being prepared for submission for publication of the material. Bowen, Kelly; Kurle, Carolyn. The dissertation author was the primary investigator and author of this material.

VITA

2016 Bachelor of Science in Biology, Pacific Lutheran University

2018 Master of Science in Marine Science, University of New England

2024 Doctor of Philosophy in Biology, University of California San Diego

PUBLICATIONS

Bowen KR, Kurle CM. Effects of pre-treatment, historical age, and sample characteristics on the stable isotope analyses of killer whale (*Orcinus orca*) bone. *Rapid Commun Mass Spectrom* 2024;38(19):e9874.

Flanders KR, Olson ZH, Ono KA. Utilizing next-generation sequencing to identify prey DNA in western North Atlantic grey seal *Halichoerus grypus* diet. *Mar Ecol Prog Ser* 2020;655:227-40.

McCosker C, **Flanders K**, Ono K, Dufault M, Mellone D, Olson Z. Metabarcoding fecal DNA reveals extent of *Halichoerus grypus* (gray seal) foraging on invertebrates and incidence of parasite exposure. Northeast Nat 2020;27(4):681-700.

Dufault MN, Olson ZH, Mellone DM, **Flanders KR**, Ono KA. Flatfish may be underestimated in the diet of gray seals (*Halichoerus grypus*). *Can J Zool* 2021;99(3):227-34.

ABSTRACT OF THE DISSERTATION

Reconstructing Foraging Ecology of a Top Predator through Stable Isotope Analysis of Teeth and Bones

by

Kelly R. Bowen

Doctor of Philosophy in Biology

University of California San Diego, 2024

Professor Carolyn Kurle, Chair

Interpreting the ecological role of top marine predators requires understanding lifelong foraging and distribution patterns; however, predation events are rarely observed and reliable collection of samples over the life of a fully-aquatic mammal is difficult. Stable isotope analysis (SIA) of archived tissues offers the opportunity to retroactively study long-term foraging ecology of elusive animals, particularly with biologically inert teeth or bone. My dissertation provides a

framework for analyzing and interpreting decades of foraging patterns for a ubiquitous top marine predator, the killer whale (*Orcinus orca*), with the aims of using the past to inform future ecosystem studies and conservation strategies.

In Chapter 1, I identify the appropriate experimental conditions to isolate collagen from powdered killer whale bone in preparation for SIA. I also demonstrate that the historical age of the specimen and the characteristics of the bone will not bias stable isotope values. In Chapter 2, I formally analyze assumptions in existing literature regarding sampling protocols and the effects of common treatments on SIA of dentin from teeth. In Chapter 3, I conduct a literature review to establish a library of stable isotope values for consumers in the North Pacific, which provides a foundation for my forthcoming chapters. I also generated new stable isotope values to represent the variation found within a species from age, sex, geographic location, and other parameters. In Chapter 4, I address a long-standing ecological hypothesis regarding the role of transient killer whales (*Orcinus orca rectipinnus*) in a historic ecosystem collapse throughout the North Pacific. In Chapter 5, I explore the historical differences in foraging ecology between two groups of resident killer whales (*Orcinus orca ater*) to investigate this potential driver of disparate population trajectories. My study aids in understanding the extent of dietary plasticity in resident killer whales, a key component to protecting these ‘Endangered’ and ‘Threatened’ populations.

My dissertation research contributes to our understanding of the ecology and ecosystem impacts of a top predator, as well as the broader field of utilizing archived teeth and bones of marine mammals for SIA.

Chapter 1 : Effects of pre-treatment, historical age, and sample characteristics on the stable isotope analyses of killer whale (*Orcinus orca*) bone

Rapid Communications in Mass Spectrometry, 2024

1.1 Abstract

RATIONALE: Stable isotope analysis of bone provides insight into animal foraging and allows for ecological reconstructions over time, however pre-treatment is required to isolate collagen. Pre-treatments typically consist of demineralization to remove inorganic components and/or lipid-extraction to remove fats, but these protocols can differentially affect stable carbon (δ^{13}C) and nitrogen (δ^{15}N) isotope values depending on the chemicals, tissues, and/or species involved. Species-specific methodologies create a standard for comparability across studies and enhance understanding of collagen isolation from modern cetacean bone.

METHODS: Elemental analyzers coupled to isotope ratio mass spectrometers were used to measure the δ^{13}C and δ^{15}N values of powdered killer whale (*Orcinus orca*) bone that was intact (control) or subjected to one of three experimental conditions: demineralized, lipid-extracted, and both demineralized and lipid-extracted. Additionally, C:N ratios were evaluated as a proxy for collagen purity. Lastly, correlations were examined between control C:N ratios vs. historical age and control C:N ratios vs. sample condition.

RESULTS: No significant differences in the δ^{15}N values were observed for any of the experimental protocols. However, the δ^{13}C values were significantly increased by all three experimental protocols: demineralization, lipid-extraction, and both treatments combined. The most influential protocol was both demineralization and lipid-extraction. Measures of the C:N ratios were also significantly lowered by demineralization and both treatments combined, indicating the material was closer to pure collagen after the treatments. Collagen purity as indicated via C:N ratio was not correlated with historical age nor sample condition.

CONCLUSIONS: If only the δ^{15}N values from killer whale bone is of interest for analysis, no pre-treatment seems necessary. If the δ^{13}C values are of interest, samples should be both demineralized and lipid-extracted. As historical age and specimen condition are not correlated with sample contamination, all samples can be treated equally.

1.2 Introduction

Analysis of the stable carbon (δ^{13}C) and nitrogen (δ^{15}N) isotope values in organismal tissues is an important tool in ecology for understanding animal habitat use, foraging habits, and trophic relationships[1–5]. In particular, stable isotope analysis of marine mammal tissues is increasingly prevalent[6] as the method can overcome the difficulties inherent to obtaining other types of foraging data from cryptic, at-sea species. One method by which to understand long-term temporal and spatial ecological patterns in the foraging and habitat use patterns of marine vertebrates involves serial sampling and stable isotope analysis of archived samples. This can be especially valuable for adding historical perspective to current patterns in the context of a rapidly changing oceanographic environment.

The stable isotope values measured from serially sampled material from accretionary hard structures such as teeth and bones provide particularly valuable data, as they enable insights into an animal's long-term (potentially lifelong) foraging patterns[7]. While teeth can offer annual resolution via distinct dentine layering, bones reflect an accumulation of foraging information over years[8,9] and can be collected from all marine mammal species even if they do not possess teeth. In addition, bone is a relatively accessible and consistent sample material from which to obtain biogeochemical data, as hard structures are more resistant to decomposition than soft tissues, and bone remains have accumulated in natural history collections for centuries. Incorporating stable isotope data of bones from individuals across time and regions can

collectively, and retroactively, build an ecological understanding of past baselines, current patterns, and future trajectories.

Bone is comprised of ~67% inorganic minerals (*e.g.*, bioapatite) and ~33% organic protein, primarily Type I collagen, by dry weight[10]. Importantly, the production of collagen is limited to dietary protein sources, whereas bioapatite is synthesized through a combination of dietary proteins, carbohydrates, and lipids[11,12]. Collagen is also less susceptible to environmental contamination (diagenesis) than bioapatite[11–13], the latter of which readily absorbs external minerals and ions. To most accurately reflect the stable isotopes incorporated from the protein component of the diet, collagen must first be isolated from the inorganic bioapatite and non-target organic molecules, such as lipids and humic acids, which would introduce bias. Lipids are depleted in ^{13}C and artificially lower measured $\delta^{13}C$ values in tissues[1], and humic acids originate from exogenous soil and do not represent dietary sources of carbon.

There are three primary considerations for treatment of bone to isolate collagen[7,14]: removal of the inorganic bioapatite (called demineralization, acidification, or decalcification), removal of lipids (lipid-extraction or delipidation), and removal of humic acids if the bones were buried or likely to be contaminated with decomposing organic soil matter. To verify that a treated sample has been reduced to pure collagen, one can measure the percent carbon (%C), percent nitrogen (%N), and the atomic carbon:nitrogen ($C:N_{atomic}$) ratio[14–16], the latter being the most commonly used metric. The widely accepted values are %C greater than 13, %N greater than 4.8, and a $C:N_{atomic}$ range within 2.9 to 3.6[7,16]. Note that Van Klinken[17] and Guiry and Szpak[14] have proposed a narrower range of acceptable C:N ratios, depending on collagen yield, taxa, and sample age.

Many different chemical methodologies have been utilized to isolate collagen, with varying effects on carbon and nitrogen content[18–21]. For example, hydrochloric acid (HCl), ethylenediaminetetraacetic acid (EDTA), and formic acid (CH_2O_2) have been used as demineralizing agents[22,23], and chloroform-methanol and petroleum ether have been used to lipid-extract bone samples[21]. Sodium hydroxide and ultrafiltration have been used to treat archaeological marine mammal bones for humic acid contamination from soil[24], though this is generally not a concern for modern marine mammal bones or bones that were collected before environmental burial and thus are not considered further in this study.

Previous research has shown inconsistent effects of demineralization, lipid-extraction, and both protocols combined on the $\delta^{13}C$ and $\delta^{15}N$ values from teeth and bone depending on the chemicals, tissues, and species involved. For example, some studies have recommended against experimental demineralization after reporting no significant differences in the $\delta^{13}C$ and $\delta^{15}N$ values of untreated bone[25], but others concluded experimental demineralization or a mathematical correction is necessary for accurate stable isotope measurements[22,26]. Lipid-extraction, again either experimentally or mathematically, is generally recommended for obtaining the $\delta^{13}C$ values from marine mammal bones that most accurately reflect those of their dietary proteins. This is because marine mammal bones have a high fat content and the $\delta^{13}C$ values of lipids are considerably lower than those of proteins, so need to be removed to avoid obscured results[27,28]. Lipid extraction is not required if one is only interested in the $\delta^{15}N$ values from collagen[25,26]. Overall, there are few studies detailing the effects of collagen isolation specifically for modern marine animals, and the recommendations differ. Another complicating factor is the potential interaction between demineralization and lipid-extraction chemicals when used jointly[25,29]. As a result of the multiple chemical methodologies, different findings between

taxa, and unpredictable isotopic interactions, it has been recommended that species-specific protocols be investigated for stable isotope analysis of bone collagen[25,26,30].

In this study, we tested killer whale (*Orcinus orca*) bone samples under three treatment protocols alongside an untreated bone control: (1) demineralized with hydrochloric acid (HCl), (2) lipid-extracted with petroleum ether, and (3) both demineralized and lipid-extracted. Our first aim was to assess the effects of each treatment on the $\delta^{13}C$, $\delta^{15}N$, and $C{:}N_{atomic}$ values, and in doing so, identify the treatment which most effectively isolates bone collagen for killer whales. Because our specimens were collected over the span of approximately 200 years, we were also able to investigate a second aim: whether there was a correlation between stable isotope values across the treatments and historical age of the specimen. We hypothesized that it may be more difficult to extract pure collagen due to degradation and contamination in specimens that were collected decades ago as opposed to recently. Lastly, we observed variation in individual bone powder characteristics (*e.g,* texture, color) which we hypothesized could be related to contamination, possibly lipids or fungi, where samples with a grittier texture and darker color may have a higher contamination load. Our third aim was to identify if a correlation exists between control $C{:}N_{atomic}$ values, as an indication of lipid or other contamination, and bone powder characteristics. Our study provides a framework for any future stable isotope studies involving killer whale bone and contributes to the broader understanding of bone collagen isolation and stable isotope analysis.

1.3 Materials and Methods

We evaluated the $\delta^{13}C$, $\delta^{15}N$, and $C{:}N_{atomic}$ values from 34 killer whale bone specimens obtained from nine archived collections (Table S1.1) under a control condition and three experimental conditions used to isolate collagen and/or remove lipids from powdered bone. The

killer whales lived in the North Pacific between the mid-late 1800s and 2016, with one exception that was collected on an unknown date. Some individuals had been captured and placed in captivity at some point in their life.

We took 31 bone samples from the skull: 28 from the occipital condoyle and three from dentary bone. We also took one bone sample each from a scapula, a hyoid, and a rib, for a total of 34 killer whale bone samples. We preferentially chose skulls for sampling consistency since the head is often saved for museum collections when it is not feasible to salvage an entire skeleton. Furthermore, the back of the skull (*e.g.*, the occipital condoyle) provides a discreet location for destructive sampling. For all skull samples and the scapula, we collected bone powder using a Dremel® tool (Racine, WI) at the lowest speed. We discarded the outermost shavings of bone to reduce contamination, and we rinsed and soaked the drill bit in 70% ethanol or isopropyl alcohol in between sampling. For the dentary, hyoid, and rib bones, we pulverized a small fragment in a manual coffee grinder which was sterilized with 10% bleach for at least 10 minutes, rinsed in water, and dried between specimens.

Experimental treatments

We subjected bone samples to three experimental treatments alongside an untreated control: demineralization (D; HCl treatment), lipid-extraction (LE; petroleum ether treatment), and both demineralization and lipid-extraction (DLE). We extracted 65 mg of untreated bone powder from a specimen, then allocated 20 mg to each of the three treatments. We subsampled ~1.5 mg from the remaining five mg of untreated bone powder to use for the control condition.

For demineralization, we placed 20 mg of bone powder in 10 mL of 0.5M HCl within a 15 mL glass tube. We covered the vials, left them for 48 hours at room temperature in a fume

hood, and then visually inspected the samples for evidence that the reaction had completed (*e.g.*, a lack of bubbles that would indicate ongoing carbon dioxide release and the transition of the powder from opaque to translucent). All samples appeared to be fully decalcified within the allotted 48-hour time period, at which point we centrifuged the samples and decanted the HCl. We rinsed each sample in ultra-pure water (MilliQ, Darmstadt, Germany), centrifuged each again at 12,000g, and decanted the water five times before lyophilizing the remaining solid for 48 hours. For the lipid-extraction treatment, we placed 20 mg of untreated bone powder into 15-mL glass tubes with 10 mL of petroleum ether. We placed the tubes in an ultrasonic bath set to 60°C and 40 KHz for 10 minutes, then centrifuged them at 12,000g for five minutes. We decanted the petroleum ether, and in all cases the supernatant was a very pale yellow, suggesting that the reaction had successfully extracted the lipids without need for further petroleum ether exposure. After decanting the petroleum ether, we added 10 mL of ultra-pure water to each tube for sonication under the same settings for another 10 minutes. Finally, we centrifuged the tubes for another 10 minutes, decanted the water, and dried the samples in either a drying oven at ~43°C or in a lyophilizer for 48 hours. Although our drying method was constrained due to logistics, and this variable has not been explicitly tested for marine mammal bone at this time, note that Kaehler and Pakhomov[31] found no significant differences in the δ^{13}C or δ^{15}N values based on freeze- or oven-drying for tissues from a marine vertebrate, invertebrate, and kelp species. For the combination treatment, we first demineralized and dried the allocated 20 mg of bone powder, then lipid-extracted and re-dried the sample as described above.

Stable isotope analyses

We weighed ~1.5 mg of sample from each of the three treatments and the single control condition into 5x9 mm tin capsules for stable isotope analysis. Our samples were analyzed in two laboratories: the University of California Santa Cruz (UCSC) Stable Isotope Laboratory using a CE Instruments NC2500 Elemental Analyzer coupled to a ThermoFisher Scientific DELTAplus XP isotope ratio mass spectrometer via a CONFLO III interface and the University of New Mexico (UNM) Center for Stable Isotopes using a Costech ECS 4010 Elemental Analyzer coupled to a ThermoFisher Scientific Delta V Advantage mass spectrometer via a CONFLO IV interface. All four conditions for 26 of the 34 killer whale bone samples were measured at UCSC, and all four conditions for the remaining 8 samples were measured at UNM, meaning the relative changes in stable isotope values resulting from treatment were likely not due to variation between laboratories. The measured stable carbon and nitrogen isotope ratios are expressed in δ-notation in parts per thousand (‰) relative to international standards, Vienna Peedee Belemnite (VPDB) for δ^{13}C and atmospheric nitrogen for δ^{15}N: $\delta^{13}\mathrm{C}$ or $\delta^{15}\mathrm{N} = [(\mathrm{Rsample} \div \mathrm{Rstandard}) - 1] \times 1000$, where R is the ratio of ^{13}C:^{12}C or ^{15}N:^{14}N for the sample and standard.

Externally-calibrated standard reference materials across the laboratories (IAEA N1, IAEA N2, USGS 43, NBS 21, NBS 22, USGS 24, IU acetanilide, Pugel, and USGS 41) were measured intermittently for quality control and instrument precision. The overall standard deviations from all reference materials were ≤0.1‰ for δ^{13}C values and ≤0.3‰ for δ^{15}N values. As $C:N_{atomic}$ should be used for the purposes of collagen quality control, $C:N_{weight}$ values were converted to $C:N_{atomic}$ values by multiplying by 12/14 where needed[14]. The results for the δ^{13}C, δ^{15}N, and $C:N_{atomic}$ values (hereafter C:N) are reported with subscripts reflecting each treatment: control (C), demineralization (D), lipid-extracted (LE), and both (DLE).

Statistical analyses

We performed all statistical analyses with R v.4.2.1[32]. We used Sharpiro-Wilk and Mauchly's tests to examine the normality and sphericity assumptions, respectively, of a repeated measures analysis of variance (ANOVA). In the event of sphericity violation, the Greenhouse-Geisser correction was applied ('rstatix' package[33]).

The $\delta^{15}N$ values within all groups were distributed normally ($W = 0.96$ to 0.97, $p > 0.05$ for all). The $\delta^{13}C$ values from the lipid-extracted samples showed a minor violation of normality ($\delta^{13}C_{LE}$: $W = 0.89$, $p = 0.002$), however, the other three treatment groups were consistent with a normal distribution ($W = 0.95$ to 0.99, $p > 0.05$ for all). We proceeded with the parametric repeated measures ANOVA, given the robustness to departures from normality[34]. The C:N values showed significant departures from normality for all groups ($W = 0.42$ to 0.80, $p < 0.001$ for all), so we applied a normal scores transformation using the Elfving method via the *blom* function of the 'rcompanion' package[35], after which all group distributions except $C:N_{LE}$ ($W = 0.91$, $p = 0.013$) resembled normality ($W = 0.97$ to 0.99, $p > 0.05$ for all). Thus, we conducted repeated measures ANOVA tests for the $\delta^{13}C$, $\delta^{15}N$, and C:N values separately to investigate the effects of treatment on group means (*e.g.,* means of the $\delta^{13}C_C$, $\delta^{13}C_D$, $\delta^{13}C_{LE}$, and $\delta^{13}C_{DLE}$ values were compared, and likewise for the $\delta^{15}N$ and C:N values). When the repeated measures ANOVA test detected a significant difference among group means at the $\alpha = 0.05$ level, we employed *post-hoc* Tukey's honestly significant difference (HSD) tests with Bonferroni corrections to follow-up with all pairwise comparisons and determine which group means were driving significance. We also used two-way repeated measures ANOVA tests to determine if

there were interaction effects between the demineralization and lipid-extraction treatments for the $\delta^{13}C$, $\delta^{15}N$, and C:N values[25].

To examine the relationship between untransformed C:N (as a proxy for collagen purity) and historical age of the specimen, we used the non-parametric Spearman's correlation coefficient for each treatment. We excluded six specimens from this analysis that did not have a precise collection date (n = 28). Lastly, we evaluated bone condition as a single parameter with three levels, given that texture and color were highly related: fine powder and white color, medium-coarse and cream color, or gritty and beige color. Each sample was assigned a condition, which was converted to a contrast matrix, meaning the categorical assignments were converted to binary variables where 0 = not the assigned condition and 1 = the assigned condition for use in an ANOVA via linear regression. The linear regression model assessed control C:N values as a function of bone condition.

1.4 Results

We detected a global significant difference in the mean $\delta^{13}C$ values of 34 killer whale bones across the three treatments and control condition together ($F_{(1.99, 66)} = 11.30$, $p < 0.001$). The Tukey's HSD *post-hoc* tests showed that the only non-significant comparison was between the $\delta^{13}C_D$ and $\delta^{13}C_{LE}$ values ($q = -0.93$, $p = 1.0$; see Table 1.1 for full output). Focusing on the three experimental treatments (D, LE, and DLE) compared to the control treatment (C), all three treatments resulted in significantly higher $\delta^{13}C$ values (Tukey's HSD test: $p < 0.05$) with reduced variation. The strongest relationship (Tukey's HSD: $q = 4.28$, $p < 0.001$) was between the $\delta^{13}C_C$ ($\bar{x} = -15.2 \pm 2.2$‰, means reported with SD hereafter) and $\delta^{13}C_{DLE}$ ($\bar{x} = -13.9 \pm 1.3$‰) values, meaning both demineralization and lipid-extraction combined resulted in the highest mean $\delta^{13}C$

value with the lowest variance among experimental treatments. The mean $\delta^{15}N$ values of killer whale bone were not significantly affected by any treatments ($F_{(1.65, 54)} = 1.13$, $p > 0.05$).

We also found that mean C:N values differed significantly ($F_{(2.33, 77)} = 41.36$, $p < 0.001$) among treatments. Focusing again on the comparisons of the 3 experimental treatments and the control treatment, *post-hoc* analyses identified that demineralization ($C:N_C$ vs. $C:N_D$; $p < 0.001$) and the combination treatment ($C:N_C$ vs. $C:N_{DLE}$; $p < 0.001$) significantly lowered the C:N mean from the control value of 4.7±1.7 to 4.0 ±1.4 and 3.5±0.4, respectively (Table 1.2; see Table 1.3 for full model output). It is particularly notable that the DLE treatment narrowed C:N variation (SD) to 0.4, as compared to ~1.5 in all other treatments. The distributions of the $\delta^{13}C$, $\delta^{15}N$, and untransformed C:N values across treatments are illustrated in Figure 1.1 and summarized in Table 1.2. Overall, the $\delta^{13}C$ and C:N, but not $\delta^{15}N$, values were significantly affected by treatment, where the control condition had the lowest $\delta^{13}C$ and highest C:N mean values, and the DLE condition had the highest $\delta^{13}C$ and lowest C:N values.

We did not detect a significant interaction term between demineralization and lipid-extraction for the $\delta^{13}C$ ($F_{(1,33)} = 0.022$, $p > 0.05$) or $\delta^{15}N$ ($F_{(1,33)} = 0.032$, $p > 0.05$) values, but there was a significant interaction for C:N values ($F_{(1,33)} = 11.630$, $p < 0.01$), albeit with a very small effect size ($\eta 2 = 0.0097$), meaning the interaction effect explains 0.97% of the variation in C:N values.

There was also no significant correlation between the C:N values (as a collagen proxy) and historical age of the specimens for any treatment (Spearman's correlation ρ for $C:N_C = 0.08$, $C:N_D = -0.16$, $C:N_{LE} = -0.08$, and $C:N_{DLE} = -0.21$; Figure 2). There was also no effect of bone condition on control C:N values ($F_{(2, 31)} = 0.688$, $p > 0.05$).

1.5 Discussion

Effects of treatment on stable isotope values

Our primary aim was to investigate the effects of three treatments (demineralization, lipid-extraction, and both demineralization and lipid-extraction) relative to a control on the $\delta^{13}C$, $\delta^{15}N$, and C:N values of killer whale bone. Our results demonstrated that the $\delta^{15}N$ values from bone were not significantly affected by any of our treatments, suggesting that measurements of the $\delta^{15}N$ values from protein in bone are robust in the presence of lipids and inorganic molecules. The mean C:N value of control bone (4.7 ± 1.7) indicated that the untreated bone contained contaminated collagen(based on the pure collagen range of 2.9-3.6[7,16]), yet the mean $\delta^{15}N$ value of 18.0 ± 2.5‰ was nearly equal to the mean $\delta^{15}N$ value (18.1 ± 2.7‰) for collagen after receiving the DLE treatment. The DLE-treated collagen had a mean C:N value of 3.5 ± 0.4, which is more in alignment with that expected for 'pure' collagen. Given this observation, untreated killer whale bone can likely be used for stable nitrogen isotope analysis, though we caution researchers to give attention to the C:N values from their analyzed bone samples and consider potential contaminating variables (*e.g.*, fossilization, archaeological burial) that could influence stable nitrogen isotope values that were not represented in our relatively modern, museum-housed sample set. However, if the $\delta^{13}C$ values of killer whale bone are of interest, we recommend samples be both demineralized and lipid-extracted. This treatment (DLE) resulted in the lowest mean C:N value across treatments (3.5 ± 0.6) and the value closest to the acceptable range for pure collagen (2.9 to 3.6)[7,16].

The $\delta^{15}N$ values we found in our study align with other studies that suggest pre-treatment is not necessary for relatively modern marine animal bones[25,26,36,37]. However, Borrell *et al.*[36], Pinela *et al.*[37], and Tatsch *et al.*[25] all found no significant differences in the $\delta^{13}C$ values for bones

left intact or treated with demineralization before stable isotope analysis for other cetacean species (*Balaenoptera physalus* or fin whale, *Delphinus* spp. or common dolphins, and Ziphiidae or beaked whales, respectively). Tatsch *et al.*[25] recommended lipid-extraction before analysis of beaked whale $\delta^{13}C$ values, but cautioned against demineralization because of the presence of an interaction effect between both treatments on the $\delta^{13}C$ values. In contrast, we found that demineralization did have a significant effect on the $\delta^{13}C$ values from killer whale bones, and there was no interaction effect between demineralization and lipid-extraction.

All three treatments led to significantly increased $\delta^{13}C$ values from killer whale bone, but the DLE treatment was associated with the most substantial change (Table 1.2). Stable carbon isotope ratios can be used to study animal movement and foraging dynamics[38], and the change of 1.3 ± 2.6‰ we observed between the $\delta^{13}C_C$ and $\delta^{13}C_{DLE}$ values from killer whale bone is biologically significant given variation in $\delta^{13}C$ values observed from different latitudes[39] and trophic levels[39]. As such, experimental treatments should be applied to the $\delta^{13}C$ values from untreated orca bone to avoid potential misinterpretations of killer whale foraging ecology.

The $\delta^{13}C$ values measured in the killer whale bone increased after lipid extraction and after demineralization, whereas the C:N ratios decreased. Lipid extraction and demineralization remove lipids and inorganic bioapatite, which is comprised largely of lipids and carbohydrates (with some protein)[40]. As lipids and carbohydrates contain negligible nitrogen, but are partly structured by carbon (specifically the more abundant light isotope of carbon, ^{12}C)[41], it follows that the C:N ratios of treated bone would decline with the removal of ^{12}C, whereas the nitrogen content would remain relatively constant as removing carbon-based components would decrease their overall presence in the bone material while the nitrogen-based material would remain relatively unchanged. There is then a corresponding increase in the $\delta^{13}C$ (^{13}C:^{12}C) values as ^{12}C

content is removed relative to ^{13}C, whereas the $\delta^{15}N$ values remain stable. Thus, it is likely the removal of the carbon-based lipids and bioapatite that contributed to the changes in C:N ratios[42] we observed in killer whale bone across treatments.

Despite the small effect size, the significance of the interaction term between the demineralization and lipid-extraction treatments for C:N values in our study could also signal the importance of both treatments combined. In other words, the effect of a combined treatment is stronger than would be expected by the additive effect of each treatment alone. Our DLE protocol involved demineralization first and lipid-extraction second, but other studies did the opposite[21,25]. Our reasoning was that the demineralization treatment might cause lipid in the bone to be more available for lipid extraction after demineralization, but future studies could test if the order in which a combined treatment occurs is important. We recommend both treatments be used for analysis of the $\delta^{13}C$ values from killer whale bones, especially when considering that the $\delta^{13}C$ values are sensitive to collagen contaminated with lipids and inorganic molecules[1] and C:N values indicating pure collagen were only reached for bone that had undergone both treatments. The physiological and contextual (*e.g.*, sample size, exact methodology) drivers of the discrepancies between species and studies are not yet clear, but the findings discussed here underscore the need to investigate patterns more widely and identify possible mechanisms for a priori predictions of treatment plans depending on taxa.

One source of potential variation in the $\delta^{13}C$, $\delta^{15}N$, and C:N values in response to the various treatments across multiple studies could be from the use of specific chemicals for each of the treatments. For example, we used petroleum ether for lipid-extraction, and Tatsch *et al.*[25] used a chloroform-methanol solution. Stable isotope studies of bird muscle[43], bird eggs[44], and sea turtle bone[21] indicate that chloroform-methanol more effectively removes lipids (*i.e.*, yields

increased the $\delta^{13}C$ and decreased C:N values relative to a control) because it interacts with both polar and non-polar lipids[45], whereas petroleum ether only removes polar lipids[46]. However, chloroform-methanol has also been shown to remove some non-lipids[46], which may not be ideal for stable isotope analyses. In our study, lipid-extraction via petroleum ether did have a significant effect on the $\delta^{13}C_C$, values, but it was the weakest effect ($p = 0.046$) among all significant comparisons; this could be due to the lower efficacy of petroleum ether as a solvent. Though chloroform-methanol may be more effective for lipid-extraction, it is important to also consider toxicity and accessibility. Petroleum ether is a safer, widely permissible chemical with a simpler protocol, and in our case, still significantly decreased the mean C:N values to approximately the acceptable collagen range (and increased the $\delta^{13}C$ values from the control treatment) when combined with demineralization.

With regard to isotopic variation from different demineralization protocols, Pang *et al.*[23] recommended either liquid solution HCl or EDTA over CH_2O_2 to most effectively remove inorganic material while preserving collagen integrity. Similarly, Wilson and Szpak[22] also found liquid HCl and EDTA performance to be comparable. These findings support our use of HCl as a demineralizing agent for killer whale bone. Though Tatsch *et al.*[25] also used HCl in their investigation of beaked whale bone, they utilized a vaporous form for 24 hours, shorter than our 48 hour exposure to liquid HCl. This procedural difference could have contributed to why we found a significant effect of demineralization on the $\delta^{13}C$ values of killer whale bone, but Tatsch *et al.*[25] did not find the same effect on beaked whale bone.

Another important consideration when applying various pre-treatments to bone specimens is the possibility of altering the $\delta^{13}C$ and $\delta^{15}N$ values of the collagen itself or influencing non-target molecules such that the tissue composition is undetectably changed

without further chemical analyses. In our case, aforementioned studies[22,23] have supported that HCl demineralization does not alter the $\delta^{13}C$ and $\delta^{15}N$ values of bone collagen. Consequences of lipid-extraction techniques are less clear, as some experimental conditions have shown altered $\delta^{15}N$ values as a result of lipid-extraction[47,48]. Despite this, lipid-extraction is still justified given evidence-based knowledge regarding the bias introduced from ^{13}C-depleted lipids[1] and ^{13}C-enriched bioapatite[49], relative to bone collagen. We were unable to conclusively determine that our petroleum ether protocol did not alter the $\delta^{13}C$ and $\delta^{15}N$ values from killer whale bone collagen or the chemical composition of our treated sample material. However, our data show the expected trend of an increase in the $\delta^{13}C$ values of the bone collagen when lipids were removed.

It appeared that some individual specimens in our study were somewhat resistant to decontamination treatments, as their C:N values were never within the range of pure collagen. For example, specimen LACM 30461 showed the highest C:N value across all treatment groups, and even the DLE treatment only brought the C:N value down to 4.7 from 9.5 in the control treatment. Similarly, specimen NMML 79 showed consistently elevated C:N values, ranking in the top five specimens with the highest C:N values for all treatments. Researchers may evaluate those unique cases to decide if exclusion from a study is appropriate. For cetaceans, there is precedence for an acceptable C:N upper limit as high as 4.0[25,50–52]. Higgs *et al.*[27] also suggested that the posterior end of cetacean skulls may have higher lipid content than the anterior; Tatsch *et al.*[25] speculate that a control C:N of 4.0 from the back skull represents relatively low lipid content. We primarily sampled from the occipital condoyle on the back of the skull, and our control killer whale C:N values aligned very closely with those of chloroform-methanol lipid-extracted beaked whales in Tatsch *et al.*[25], with a mean around 3-4 and maximum of 8-9.

Correlations with historical age and bone condition

We also investigated the potential for correlations between the C:N values from killer whale bones subjected to all treatments and the historical ages of the specimens. Although bone is typically highly resistant to degradation in a museum setting, older bones have had more time and opportunities to be exposed to fluctuating temperature, humidity, UV levels, pests, bacteria, and fungi, which can impact diagenesis[53–55] and lead to higher C:N values. Thus, we hypothesized that specimens collected decades in the past would be associated with higher C:N values (indicative of these age-related contaminations) than specimens collected in the 2000s. Our hypothesis was not supported for any of the treatments, meaning degradation and contamination were not significant factors when analyzing isotope values from bones housed for over approximately 100 years in museums.

We also observed variation in the bone condition of individual specimens, ranging from fine and white to gritty and beige. Texture and color could indicate varying levels of contamination; Huculak and Rogers[56] categorized a spectrum of bone colors resulting from humic acid exposure, fungal presence, and sun-bleaching. Bones with a high lipid load may also appear yellowish with a greasy texture, whereas bleached bone would be brittle. We categorized the killer whale bones in our study as fine powder and white, medium-coarse and cream, or gritty and beige. Although bright white specimens may have been either sun-bleached or intentionally bleached in the cleaning process, which degrades collagen[57], we hypothesized that fine white bone powder would exhibit $C:N_C$ values closer to the range of pure collagen than gritty, beige powder. We expected gritty, beige specimens were more likely to be contaminated by high lipid content or potentially fungal growth[54,56]. However, our hypothesis was not supported, as we found no correlation between bone condition and the $C:N_C$ values. To further support that notion,

we categorized specimen NMML 87 as gritty beige and documented on-site that the skull was especially greasy, yet the $C:N_C$ value (4.7) was equal to the mean (4.7) and this specimen responded well to the DLE treatment ($C:N_{DLE}$ = 3.3). Tatsch *et al.*[25] mention that some individuals with a high C:N value (between 8 and 9) could be due to increased body fat, or insufficient skull-cleaning procedures. Our results could indicate skull-cleaning procedures (or the environment prior to specimen collection) are more likely to cause C:N bias than fat content, as our top 3 highest $C:N_C$ values (9.5, 8.4, 8.4) were all from specimens categorized as fine white (*i.e.*, possibly bleached), whereas a notably greasy specimen showed an average C:N value. However, additional studies examining the relationship between stable isotope values and sample preservation techniques are needed for more conclusive interpretations.

Conclusions

Our results suggest that untreated samples may be used for the stable nitrogen isotope analysis of killer whale bone given relatively modern specimens housed in museums. However, we recommend both demineralization and lipid-extraction treatments for killer whale bone before determining its $\delta^{13}C$ values because both treatments change the $\delta^{13}C$ and C:N values for killer whale bone relative to control samples in ways that indicate the resulting material is closer to pure collagen (increased $\delta^{13}C$ and decreased C:N values) than those left untreated. For concurrent analysis of the $\delta^{13}C$ and $\delta^{15}N$ values from killer whale bone, both measurements can be taken from a single sample that has been demineralized and lipid-extracted since the $\delta^{15}N$ values were not affected by the two treatments. Our recommendations for pre-treatment of marine mammal bones before stable carbon isotope analysis differ from those put forth by Tatsch *et al.*[25] for beaked whale bone, but we emphasize again that different chemical agents, treatment

protocols, burial and preservation environments, etc. may influence these findings. Further studies investigating patterns among different taxa and physiological drivers of isotopic changes from chemical treatments are warranted. Additionally, we can recommend all killer whale bone specimens, regardless of historical age and bone condition, undergo the same treatments for stable isotope analysis, as these were not reliable indicators of potential contamination that could require treatment for removal.

1.6 Acknowledgements

We thank the natural history collections and all the staff/curators who made this work possible through specimen loans, including: the American Museum of Natural History (N. Duncan, E. Hoeger); the Beaty Biodiversity Museum – University of British Columbia (M. deRoos, C. Stinson); the California Academy of Sciences (M. Flannery); the Natural History Museum of Los Angeles County (D. Janiger, J. Velez-Juarbe, S. Robson); the Museum of Vertebrate Zoology – University of California Berkeley (C. Conroy); the NOAA Marine Mammal Laboratory (P. Clapham, P. Wade); the Museum of the North – University of Alaska (A. Gunderson, L. Olson); the Smithsonian National Museum of Natural History (M. Hawkins, D. Lunde, M. McGowen, J. Ososky); the Burke Museum of Natural History and Culture – University of Washington (J. Bradley). Thanks also to D. Andreasen, C. Carney, and E. Cano at the University of California Santa Cruz Stable Isotope Laboratory and S. Newsome and V. Atudorei at the University of New Mexico Center for Stable Isotopes for assistance with sample measurements. Additionally, we thank C. Turner Tomaszewicz for facilitating sample analyses and K. Lanigan for help with sample processing. We are also grateful for the time and feedback of two anonymous reviewers to improve this manuscript. Funding and support for K.B. and C.K. were provided by the University of California San Diego (UCSD), the NIH Cell & Molecular

Genetics Graduate Training Program, the PADI Foundation, the Lerner-Gray Fund for Marine Research by the American Museum of Natural History, the Jeanne Marie Messier Memorial Endowed Fund (UCSD), the American Cetacean Society Los Angeles Chapter John E. Heyning Research Grant, and the Association for Women in Science San Diego Chapter.

Chapter 1, in full, is a reprint of material as it appears in "Bowen KR, Kurle CM. Effects of pre-treatment, historical age, and sample characteristics on the stable isotope analyses of killer whale (*Orcinus orca*) bone. *Rapid Commun Mass Spectrom* 2024;38(19):e9874". The dissertation author was the primary investigator and author of this paper.

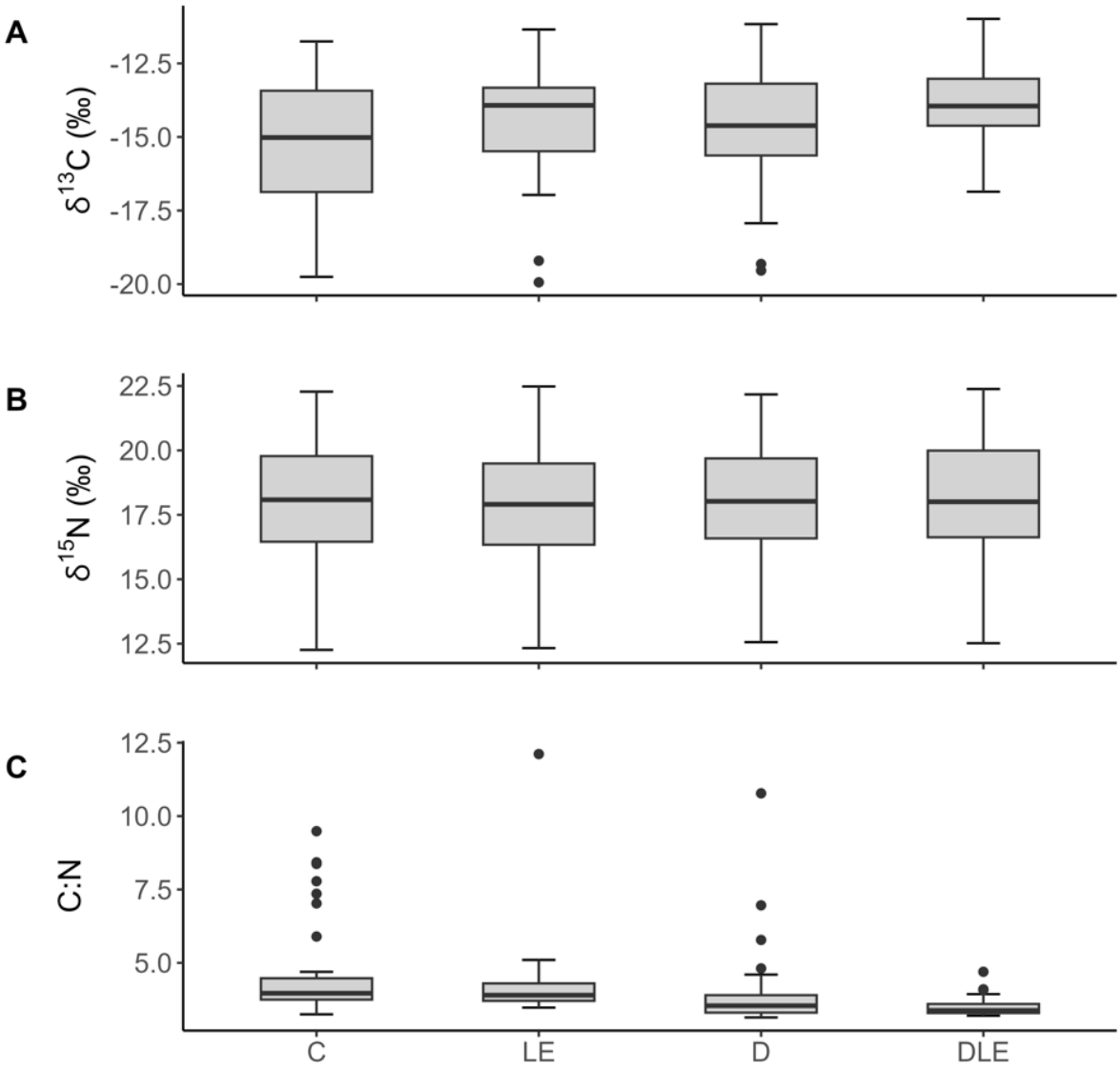


Figure 1.1. Boxplots of the (A) δ^{13}C, (B), δ^{15}N, and (C) C:N values from killer whale bone samples (n = 34) under an untreated control (C on the x-axis) and three experimental conditions: lipid-extracted (LE), demineralized (D), and both demineralized and lipid-extracted (DLE). The shaded boxes illustrate the interquartile range (the lower quartile, median, and upper quartile), and the whiskers extend to the minimum and maximum values. While there were no significant differences in the δ^{15}N values between treatments, the δ^{13}C values from the control samples did vary significantly from the means of all three experimental treatments. The C:N values also significantly differed with the D and DLE treatments, but not the LE treatment.

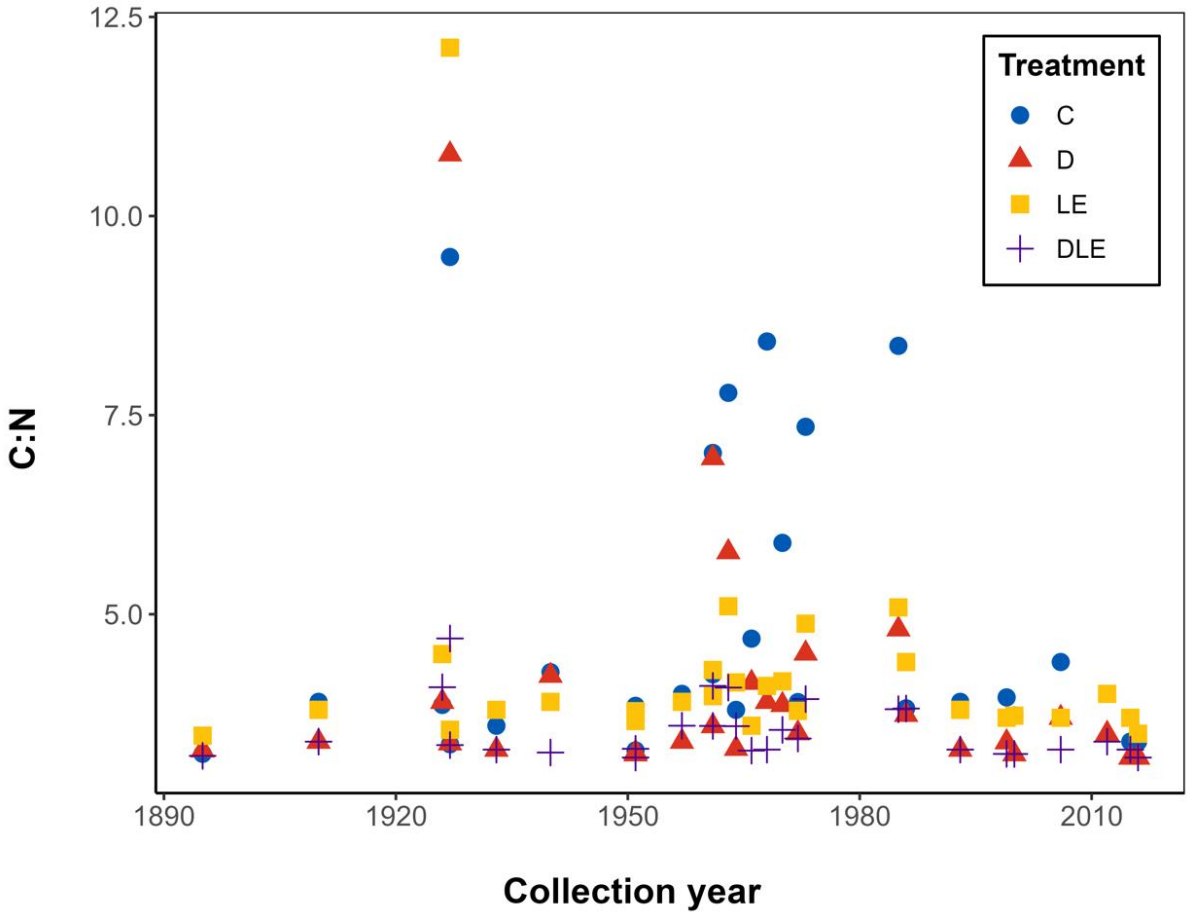


Figure 1.2. The C:N values from killer whale bones (n = 28) plotted against the year a specimen was collected. The treatment groups included the untreated control (C; blue circle), demineralized (D; red triangle), lipid-extracted (LE; yellow square), and both demineralized and lipid-extracted (DLE; purple plus).

Table 1.1. Results of Tukey's HSD *post-hoc* tests after a repeated measures ANOVA analyzing the $\delta^{13}C$ values of killer whale bone samples (n = 34) under three treatment conditions and a control. C = control/untreated, D = demineralized, LE = lipid-extracted, and DLE = both demineralized and lipid-extracted.

$\delta^{13}C$: Tukey's HSD *post-hoc* tests			
Treatment 1	Treatment 2	Statistic	Adjusted *p*-value
C	D	-3.076	0.025
C	DLE	-4.280	< 0.001
C	LE	-2.840	0.046
D	DLE	-3.314	0.013
D	LE	-0.930	1.00
DLE	LE	3.068	0.026

Table 1.2. The mean (±SD) $\delta^{13}C$, $\delta^{15}N$, and C:N values for killer whale bone samples (n = 34) across three treatments and a control are shown alongside the change in the $\delta^{13}C$ ($\Delta\ \delta^{13}C$) and $\delta^{15}N$ ($\Delta\delta^{15}N$) values for each treatment relative to the control. C = control/untreated, D = demineralized, LE = lipid-extracted, and DLE = both demineralized and lipid-extracted.

Treatment	**$\delta^{13}C$ (‰)**	**$\Delta\ \delta^{13}C$**	**$\delta^{15}N$ (‰)**	**$\Delta\ \delta^{15}N$**	**C:N**	**ΔC:N**
C	-15.2 ± 2.2	--	18.0 ± 2.5	--	4.7 ± 1.7	--
D	-14.6 ± 1.9	0.6 ± 3.0	18.2 ± 2.3	0.1 ± 3.6	4.0 ± 1.4	0.7 ± 2.2
LE	-14.5 ± 1.8	0.7 ± 2.9	17.9 ± 2.5	0.1 ± 3.6	4.3 ± 1.5	0.4 ± 2.3
DLE	-13.9 ± 1.3	1.3 ± 2.6	18.1 ± 2.7	0.03 ± 3.7	3.5 ± 0.4	1.2 ± 1.8

Table 1.3. Results of Tukey's HSD *post-hoc* tests after a repeated measures ANOVA analyzing the C:N values from killer whale bone samples (n = 34) under a normal score transformation using the Elfving method. C = control/untreated, D = demineralized, LE = lipid-extracted, and DLE = both demineralized and lipid-extracted.

C:N : Tukey's HSD *post-hoc* tests			
Treatment 1	Treatment 2	Statistic	Adjusted *p*-value
C	D	6.647	< 0.001
C	DLE	8.284	< 0.001
C	LE	0.413	1.00
D	DLE	3.164	0.020
D	LE	-4.877	< 0.001
DLE	LE	-11.836	< 0.001

Table S1.1. Collection details for the 34 killer whale (*Orcinus orca*) bones sampled and analyzed for their $\delta^{13}C$, $\delta^{15}N$, and C:N values. Each specimen sample was analyzed under three treatment with an untreated control: demineralized, lipid-extracted, and demineralized and lipid-extracted together.

Separate file

1.7 References

1. DeNiro MJ, Epstein S. Influence of diet on the distribution of carbon isotopes in animals. *Geochim Cosmochim Acta*. 1978;42(5):495-506. doi:10.1016/0016-7037(78)90199-0

2. Deniro MJ, Epstein S. Influence of diet on the distribution of nitrogen isotopes in animals. *Geochim Cosmochim Acta*. 1981;45(3):341-351. doi:10.1016/0016-7037(81)90244-1

3. Schoeninger MJ, DeNiro MJ. Nitrogen and carbon isotopic composition of bone collagen from marine and terrestrial animals. *Geochim Cosmochim Acta*. 1984;48(4):625-639. doi:10.1016/0016-7037(84)90091-7

4. Ambrose SH, DeNiro MJ. The isotopic ecology of East African mammals. *Oecologia*. 1986;69(3):395-406. doi:10.1007/BF00377062

5. Boecklen WJ, Yarnes CT, Cook BA, James AC. On the use of stable isotopes in trophic ecology. *Annu Rev Ecol Evol Syst*. 2011;42(1):411-440. doi:10.1146/annurev-ecolsys-102209-144726

6. Newsome SD, Clementz MT, Koch PL. Using stable isotope biogeochemistry to study marine mammal ecology. *Mar Mammal Sci*. Published online January 2010. doi:10.1111/j.1748-7692.2009.00354.x

7. Ambrose SH. Preparation and characterization of bone and tooth collagen for isotopic analysis. *J Archaeol Sci*. 1990;17(4):431-451. doi:10.1016/0305-4403(90)90007-R

8. Sealy J, Armstrong R, Schrire C. Beyond lifetime averages: tracing life histories through isotopic analysis of different calcified tissues from archaeological human skeletons. *Antiquity*. 1995;69(263):290-300. doi:10.1017/S0003598X00064693

9. Hedges REM, Clement JG, Thomas CDL, O'Connell TC. Collagen turnover in the adult femoral mid-shaft: Modeled from anthropogenic radiocarbon tracer measurements. *Am J Phys Anthropol*. 2007;133(2):808-816. doi:10.1002/ajpa.20598

10. Koch PL. Isotopic study of the biology of modern and fossil vertebrates. In: Michener R, Lajtha K, eds. *Stable Isotopes in Ecology and Environmental Science*. 2nd ed. Blackwell Publishing Ltd; 2007:99-154. doi:10.1002/9780470691854

11. Lee-Thorp JA, Sealy JC, Van Der Merwe NJ. Stable carbon isotope ratio differences between bone collagen and bone apatite, and their relationship to diet. *J Archaeol Sci*. 1989;16(6):585-599. doi:10.1016/0305-4403(89)90024-1

12. Richards MP. Stable isotope analysis of bone and teeth as a means for reconstructing past human diets in Greece. In: Papathanasiou A, Richards MP, Fox SC, eds. *Archaeodiet in the Greek World: Dietary Reconstruction from Stable Isotope Analysis*. Hesperia supplement. The American School of Classical Studies at Athens; 2015:15-23.

13. Ferretti A, Medici L, Savioli M, Mascia MT, Malferrari D. Dead, fossil or alive: Bioapatite diagenesis and fossilization. *Palaeogeogr Palaeoclimatol Palaeoecol*. 2021;579:110608. doi:10.1016/j.palaeo.2021.110608

14. Guiry EJ, Szpak P. Improved quality control criteria for stable carbon and nitrogen isotope measurements of ancient bone collagen. *J Archaeol Sci*. 2021;132:105416. doi:10.1016/j.jas.2021.105416

15. Neuman RE. The amino acid composition of gelatins, collagens and elastins from different sources. *Arch Biochem*. 1949;24(2):289-298.

16. DeNiro MJ. Postmortem preservation and alteration of in vivo bone collagen isotope ratios in relation to palaeodietary reconstruction. *Nature*. 1985;317(6040):806-809. doi:10.1038/317806a0

17. Van Klinken GJ. Bone collagen quality indicators for palaeodietary and radiocarbon measurements. *J Archaeol Sci*. 1999;26(6):687-695. doi:10.1006/jasc.1998.0385

18. Liden K, Takahashi C, Nelson DE. The effects of lipids in stable carbon isotope analysis and the effects of NaOH treatment on the composition of extracted bone collagen. *J Archaeol Sci*. 1995;22(2):321-326. doi:10.1006/jasc.1995.0034

19. Jørkov MLS, Heinemeier J, Lynnerup N. Evaluating bone collagen extraction methods for stable isotope analysis in dietary studies. *J Archaeol Sci*. 2007;34(11):1824-1829. doi:10.1016/j.jas.2006.12.020

20. Rand A, Bower M, Munkittrick J, Harris A, Burchell M, Grimes V. Comparison of three bone collagen extraction procedures: the effect of preservation on δ^{13}C and δ^{15}N values. *N Atl Archaeol*. 2015;4:93-113.

21. Medeiros L, Da Silveira Monteiro D, Petitet R, Bugoni L. Effects of lipid extraction on the isotopic values of sea turtle bone collagen. *Aquat Biol*. 2015;23(3):191-199. doi:10.3354/ab00628

22. Wilson T, Szpak P. Acidification does not alter the stable isotope composition of bone collagen. *PeerJ*. 2022;10:e13593. doi:10.7717/peerj.13593

23. Pang S, Su FY, Green A, Salim J, McKittrick J, Jasiuk I. Comparison of different protocols for demineralization of cortical bone. *Sci Rep*. 2021;11(1):7012. doi:10.1038/s41598-021-86257-4

24. Szpak P, Krippner K, Richards MP. Effects of sodium hydroxide treatment and ultrafiltration on the removal of humic contaminants from archaeological bone. *Int J Osteoarchaeol*. 2017;27(6):1070-1077. doi:10.1002/oa.2630

25. Tatsch ACC, Secchi ER, Botta S. Effects of acidification, lipid removal and mathematical normalization on carbon and nitrogen stable isotope compositions in beaked whale (Ziphiidae) bone. *Rapid Commun Mass Spectrom*. 2016;30(3):460-466. doi:10.1002/rcm.7457

26. Tomaszewicz CNT, Seminoff JA, Ramirez MD, Kurle CM. Effects of demineralization on the stable isotope analysis of bone samples. *Rapid Commun Mass Spectrom RCM*. 2015;29(20):1879-1888. doi:10.1002/rcm.7295

27. Higgs ND, Little CTS, Glover AG. Bones as biofuel: a review of whale bone composition with implications for deep-sea biology and palaeoanthropology. *Proc R Soc B Biol Sci*. 2010;278(1702):9-17. doi:10.1098/rspb.2010.1267

28. Guilminot E, Lemoine G, Pelé C, Poisson L, Surbled M, Louvet I, Mevellec JY, Rémy L. Re-treatment of whale bones – How to extract degraded fats from weakened bones? *J Cult Herit*. 2014;15(2):128-135. doi:10.1016/j.culher.2013.03.008

29. Bas M, García NA, Crespo EA, Cardona L. Intraskeletal variability in stable isotope ratios of C and N among pinnipeds and cetaceans. *Mar Mammal Sci*. 2020;36(1):375-385. doi:10.1111/mms.12644

30. Clark CT, Horstmann L, Misarti N. Lipid normalization and stable isotope discrimination in Pacific walrus tissues. *Sci Rep*. 2019;9(1):5843. doi:10.1038/s41598-019-42095-z

31. Kaehler S, Pakhomov E. Effects of storage and preservation on the δ13C and δ15N signatures of selected marine organisms. *Mar Ecol Prog Ser*. 2001;219:299-304. doi:10.3354/meps219299

32. R Core Team. R: A language and environment for statistical computing. Published online 2022. https://www.R-project.org/

33. Kassambara A. rstatix: Pipe-friendly framework for basic statistical tests. Published online 2023. https://CRAN.R-project.org/package=rstatix

34. Blanca MJ, Alarcón R, Arnau J. Non-normal data: Is ANOVA still a valid option? *Psicothema*. 2017;(29.4):552-557. doi:10.7334/psicothema2016.383

35. Mangiafico S. rcompanion: Functions to Support Extension Education Program Evaluation. Published online 2023. https://CRAN.R-project.org/package=rcompanion

36. Borrell A, Abad-Oliva N, Gómez-Campos E, Giménez J, Aguilar A. Discrimination of stable isotopes in fin whale tissues and application to diet assessment in cetaceans. *Rapid Commun Mass Spectrom*. 2012;26(14):1596-1602. doi:10.1002/rcm.6267

37. Pinela AM, Borrell A, Aguilar A. Variation in $\delta^{15}N$ and $\delta^{13}C$ stable isotope values in common dolphins (*Delphinus* spp.) worldwide, with particular emphasis on the eastern North

Atlantic populations. *Rapid Commun Mass Spectrom*. 2015;29(9):855-863. doi:10.1002/rcm.7173

38. Gannes LZ, Del Rio CM, Koch P. Natural abundance variations in stable isotopes and their potential uses in animal physiological ecology. *Comp Biochem Physiol A Mol Integr Physiol*. 1998;119(3):725-737. doi:10.1016/S1095-6433(98)01016-2

39. Aurioles D, Koch PL, Le Boeuf BJ. Differences in foraging location of Mexican and California elephant seals: Evidence from stable isotopes in pups. *Mar Mammal Sci*. 2006;22(2):326-338. doi:10.1111/j.1748-7692.2006.00023.x

40. Sullivan CH, Krueger HW. Carbon isotope analysis of separate chemical phases in modern and fossil bone. *Nature*. 1981;292(5821):333-335. doi:10.1038/292333a0

41. Cloyed CS, DaCosta KP, Hodanbosi MR, Carmichael RH. The effects of lipid extraction on $\delta^{13}C$ and $\delta^{15}N$ values and use of lipid-correction models across tissues, taxa and trophic groups. Kurle C, ed. *Methods Ecol Evol*. 2020;11(6):751-762. doi:10.1111/2041-210X.13386

42. Post DM. Using stable isotopes to estimate trophic position: models, methods, and assumptions. *Ecology*. 2002;83(3):703-718. doi:10.1890/0012-9658(2002)083[0703:USITET]2.0.CO;2

43. Doucette JL, Wissel B, Somers CM. Effects of lipid extraction and lipid normalization on stable carbon and nitrogen isotope ratios in double-crested cormorants: implications for food web studies. *Waterbirds*. 2010;33(3):273-284. doi:10.1675/063.033.0302

44. Elliott KH, Elliott JE. Lipid extraction techniques for stable isotope analysis of bird eggs: Chloroform–methanol leads to more enriched 13C values than extraction via petroleum ether. *J Exp Mar Biol Ecol*. 2016;474:54-57. doi:10.1016/j.jembe.2015.09.017

45. Sotiropoulos MA, Tonn WM, Wassenaar LI. Effects of lipid extraction on stable carbon and nitrogen isotope analyses of fish tissues: potential consequences for food web studies. *Ecol Freshw Fish*. 2004;13(3):155-160. doi:10.1111/j.1600-0633.2004.00056.x

46. Dobush GR, Ankney CD, Krementz DG. The effect of apparatus, extraction time, and solvent type on lipid extractions of snow geese. *Can J Zool*. 1985;63(8):1917-1920. doi:10.1139/z85-285

47. Elliott KH, Davis M, Elliott JE. Equations for lipid normalization of carbon stable isotope ratios in aquatic bird eggs. Chiaradia A, ed. *PLoS ONE*. 2014;9(1):e83597. doi:10.1371/journal.pone.0083597

48. Yurkowski DJ, Hussey NE, Semeniuk C, Ferguson SH, Fisk AT. Effects of lipid extraction and the utility of lipid normalization models on $\delta^{13}C$ and $\delta^{15}N$ values in Arctic marine mammal tissues. *Polar Biol*. 2015;38(2):131-143. doi:10.1007/s00300-014-1571-1

49. DeSantis LR, Feranec RS, Southon J, Cerling TE, Harris J, Binder WJ, Cohen JE, Farrell AB, Lindsey EL, Meachen J, Robin O'Keefe F. On the relationship between collagen- and carbonate-derived carbon isotopes with implications for the inference of carnivore dietary behavior. *Front Ecol Evol*. 2022;10:1031383. doi:10.3389/fevo.2022.1031383

50. McConnaughey T, McRoy CP. Food-Web structure and the fractionation of Carbon isotopes in the bering sea. *Mar Biol*. 1979;53(3):257-262. doi:10.1007/BF00952434

51. Gross A, Kiszka J, Van Canneyt O, Richard P, Ridoux V. A preliminary study of habitat and resource partitioning among co-occurring tropical dolphins around Mayotte, southwest Indian Ocean. *Estuar Coast Shelf Sci*. 2009;84(3):367-374. doi:10.1016/j.ecss.2009.05.017

52. Kiszka J, Oremus M, Richard P, Poole M, Ridoux V. The use of stable isotope analyses from skin biopsy samples to assess trophic relationships of sympatric delphinids off Moorea (French Polynesia). *J Exp Mar Biol Ecol*. 2010;395(1-2):48-54. doi:10.1016/j.jembe.2010.08.010

53. Delannoy Y, Colard T, Le Garff E, Mesli V, Aubernon C, Penel G, Hedouin V, Gosset D. Effects of the environment on bone mass: A human taphonomic study. *Leg Med*. 2016;20:61-67. doi:10.1016/j.legalmed.2016.04.006

54. Pinzari F, Cornish L, Jungblut AD. Skeleton bones in museum indoor environments offer niches for fungi and are affected by weathering and deposition of secondary minerals. *Environ Microbiol*. 2020;22(1):59-75. doi:10.1111/1462-2920.14818

55. Procopio N, Mein CA, Starace S, Bonicelli A, Williams A. Bone diagenesis in short timescales: Insights from an exploratory proteomic analysis. *Biology*. 2021;10(6):460. doi:10.3390/biology10060460

56. Huculak MA, Rogers TL. Reconstructing the sequence of events surrounding body disposition based on color staining of bone*. *J Forensic Sci*. 2009;54(5):979-984. doi:10.1111/j.1556-4029.2009.01086.x

57. Kerbl FM, DeVilliers P, Litaker M, Eleazer PD. Physical effects of sodium hypochlorite on bone: An ex vivo study. *J Endod*. 2012;38(3):357-359. doi:10.1016/j.joen.2011.12.031

Chapter 2 : Considerations for stable isotope analysis of marine mammal dentin growth layer groups

2.1 Abstract

RATIONALE: Stable isotope analysis of growth layer groups (GLGs) in mammal dentin is an increasingly prevalent and non-invasive approach to study animal foraging ecology. However, empirical evidence to support assumed proper methodologies for sampling GLGs is lacking. Here, we examine the effects of intra- and inter-tooth variation with respect to targeted GLGs, as well as the effects of common pre-treatments (*e.g.*, formic acid and graphite) to enhance GLG visibility, on stable isotope values (δ^{13}C and δ^{15}N) from dentin.

METHODS: We measured the δ^{13}C and δ^{15}N values of killer whale (*Orcinus orca*) dentin. We used dentin from 37 teeth to compare stable carbon (δ^{13}C) and nitrogen (δ^{15}N) isotope values from multiple locations within a GLG (intra-tooth variation), from corresponding GLGs among teeth of an individual (inter-tooth variation), and from treated and untreated teeth.

RESULTS: We observed no significance differences in the δ^{13}C or δ^{15}N values when sampling a single GLG from multiple locations (intra-tooth variation) or when comparing the same GLG across duplicate teeth of individuals (inter-tooth variation). One tooth in a triplicate set showed a significantly different but likely biologically inconsequential δ^{13}C value. Lastly, formic acid and graphite highlighting to accentuate GLGs did not significantly influence measured stable isotope values.

CONCLUSIONS: We validate several previous assumptions in this field of study. First, dentin samples for stable isotope analysis can be sampled from different locations across a GLG. Second, researchers can compare stable isotope values from the same GLGs of different teeth collected from the same individual in most cases, as the δ^{13}C and δ^{15}N values did not vary with the sampled tooth. Third, a common protocol of formic acid and graphite treatment to enhance

GLG visibility does not bias the $\delta^{13}C$ and $\delta^{15}N$ values from dentin. We also describe factors to consider and cautions associated with these conclusions.

2.2 Introduction

Teeth have been a useful tissue from which to measure stable isotope values of marine mammals for decades[1–4]. Stable nitrogen ($\delta^{15}N$) and carbon ($\delta^{13}C$) isotopes are assimilated into a predator's tissues and can be used to infer their feeding ecology and habitat use[5,6]. Teeth are particularly valuable because they are resistant to decomposition, commonly collected for accession in museums along with skulls, and generally occur as a set where one tooth can be destructively sampled for analysis while preserving the others. Furthermore, odontocetes (toothed whales such as belugas, porpoises, and dolphins) are monophyodonts, meaning they only develop one set of permanent teeth for their entire life[7]. These teeth are characterized by annual, incremental dentin deposits, called growth layer groups[8–10] (GLGs), that gradually fill in the open pulp cavity for most of the animal's life. As a result, stable isotope analysis of metabolically inert dentin from GLGs allows for reconstruction of ecological chronologies over the life of the individual. Researchers can glean an overall age for the animal by sectioning the tooth in half longitudinally and counting GLGs. With this method, specific years of interest can also be targeted for sampling[11].

The exact environmental drivers and physiological mechanisms by which GLGs are distinctly formed are as yet unclear (see discussions in [12–14]), however it is known that GLGs grow horizontally in width as a whole layer during synthesis, as opposed to building vertically from pulp to crown or vice versa. Although there is evidence by Walker and Macko[2] for isotopic homogeneity of dentin through subsampling a mixture from a whole single tooth, it has not, to our knowledge, been empirically demonstrated that stable isotope values are consistent along a

given GLG. This is especially relevant for very large odontocete teeth such as those from sperm whales (*Physeter microcephalus*) or killer whales (*Orcinus orca*) where an isotopic sample represents a very small fraction of an entire GLG. Additionally, pulp stones, cracks in the tooth, occlusion wear, or other factors may dictate where sampling can occur along a GLG and prevent using the same location across GLGs. One of our research goals was to examine stable isotope values taken from two different locations along a single GLG from a given killer whale tooth (*i.e.*, closer to the root and closer to the crown), with the hypothesis that isotope values from both locations should be equivalent because GLGs form as a whole layer along the length of the tooth over the course of a year[11].

Walker and Macko[2] present one of few studies that examined isotopic variation among teeth of an individual. They found very little isotopic variation in eight teeth from a walrus (*Odobenus rosmarus;* but see Stewart and Stewart[15], which did find age estimation differences among walrus teeth) and 12 teeth from a bottlenose dolphin (*Tursiops truncatus*). However, the sample size in Walker and Macko[2] was limited to one animal of each species, and they compared homogenized whole dentin among different teeth rather than individual GLGs. Killer whales have homodont dentition, meaning all teeth are structurally similar, but there is some variation to the extent that teeth located at the very anterior or posterior end of the jaw are substantially smaller than those in the middle. The straightest, largest teeth in the center of the jaw are ideal for age estimation[16], but in some cases, only peripheral smaller or curved teeth are available for the destructive sampling necessary to estimate age and obtain dentin. A second goal of our research using killer whale teeth was to examine isotopic homogeneity of GLGs among teeth of an individual, again with the hypothesis that isotope values should be equivalent in corresponding GLGs among most teeth.

Although GLGs of teeth are a powerful tool for biological and ecological insight, the GLGs themselves can be challenging to delineate. The presence of supernumerary or accessory lines can also complicate the task[9,10,17]. In order to visualize GLGs on the internal face of a half-tooth more clearly, the tooth-halves are often 'etched' in formic acid to produce raised ridges and grooves that define GLGs (reviewed in Read *et al.*[11], although accessory lines can be accentuated in this way as well). Then, a soft graphite pencil is lightly rubbed over the etched surface to highlight the ridges and further aid in GLG identification.

Etching and penciling is a common technique, but the potential effects on stable isotope analysis of dentin are unclear. Numerous studies assumed that formic acid would not significantly influence stable isotope values, despite containing carbon (HCO_2H), because only the surface of the tooth is exposed, and the portion of dentin exposed to the acid is relatively small compared to the entirety of collected dentin for analysis[1,18,19]. Others have attempted to discard the 'outer surface' (undefined in Hanson et al.[20], depth of 100 µm in Knox et al.[21]), though the depth to which formic acid might penetrate is unknown, and it is advantageous to sample as shallow as possible to avoid layers underlying the target. Graphite has either been removed before sampling, although it is uncertain if all the graphite was effectively removed, or the untreated tooth-half was cross-referenced and sampled instead. This can still lead to concerns, as GLGs are less visible on untreated sections, and another source of error is introduced by aging one half of a tooth but sampling from the other.

To the best of our understanding at this time, Stukonytė *et al.*[22] present the only study that has investigated the effects of formic acid and graphite penciling on the stable isotope values of dentin. They found a significant effect of formic acid etching on sperm whale dentin from 30 teeth, leading to an increase of 0.2‰ for both $\delta^{13}C$ and $\delta^{15}N$ values. By cleaning graphite off of

an etched tooth, they found no effect from the presence or absence of graphite. However, the authors caution against the universal application of their findings, given that treatment protocols (*e.g.*, formic acid concentration and exposure time) can differ. In their case, 10% formic acid was used for a duration of 30 hours. A third goal of our study also aimed to examine the effects of 10% formic acid and graphite on stable isotope analysis of dentin, however we used killer whale teeth exposed for 12 hours[19], less than half the time of Stukonytė *et al*.[22]. Additionally, our comparison framework differed (see Methods), as we made comparisons of treated dentin (*e.g.*, etched and penciled) to both untreated dentin and dentin with the 'contaminated' surface layer removed/cleaned.

Overall, we report in this study how stable isotope values from dentin taken from archived killer whale teeth are influenced by two intrinsic variables related to tooth composition (I, II) as well as the external variable of treatments applied to increase the readability of tooth GLGs (III). Specifically, we ask: I. Do the $\delta^{13}C$ and $\delta^{15}N$ values measured from a GLG remain consistent regardless of the area within the GLG from which dentin is sampled? II. Do the $\delta^{13}C$ and $\delta^{15}N$ values measured in dentin from a specific GLG (*e.g.*, the GLG that represents a specific year of the animal's life) remain consistent regardless of the tooth from which the GLG is sampled? III. What are the effects of acid etching and pencil highlighting on the $\delta^{13}C$ and $\delta^{15}N$ values of dentin from killer whale teeth in comparison to (a) dentin with removal of these potential contaminants and (b) dentin never exposed to the contaminants?

2.3 Materials and Methods

In total, we used 37 killer whale teeth representing 24 unique individuals to examine our three objectives (Table S2.1). See Chapters 4 and 5 for more detailed methods on tooth processing and

age estimation, as we used these same killer whale specimens, protocols, and stable isotope data in separate studies with the foundations described there.

Briefly, whole teeth were longitudinally bisected on a modified Bosch® TC10 wet tile saw (Farmington Hills, MI, USA). The cut face of the teeth were manually polished with 400 grit, then 600 grit, wet sandpaper discs to remove saw marks. We then placed the teeth cut face down into 10% formic acid to a depth of 0.5 - 1 cm for 12 hours to decalcify the tooth surface and allow the GLGs to become more visually apparent. After rinsing, soaking, and drying, we used a soft graphite pencil (6B) on the surface of the tooth face to highlight GLG ridges and grooves. We took high-resolution (800-1200 dpi) scans of all tooth faces, and we analyzed the images using GIMP (GNU Image Manipulation Program version 2.10.6) to mark GLG boundaries for every tooth, although the physical tooth was consulted under a microscope in some cases for clarification if needed. All teeth were aged blindly (*i.e.*, no reference to catalog number or other metadata, with the exception of BBM-J18 that was used as a known-age reference tooth) by K.B. across three independent sessions that were evaluated together to form a consensus.

Finally, we collected dentin from targeted GLGs using a computer-controlled micromill (MicroMill2, Elemental Scientific Lasers, Omaha, NE, USA) at the NOAA Southwest Fisheries Science Center (La Jolla, CA). We used drill bits (Brasseler USA Dental Instruments, Savannah, GA, USA) that ranged from 300 µm - 1000 µm depending on the width of the targeted GLG. For a yield of approximately 2 mg of dentin for stable isotope analysis, our drill path was 8 - 10 mm in length and 200 - 350 µm in depth. If the GLG was relatively wide and warranted an 800 or 1000 µm bit, then we could drill a shorter and shallower path to obtain the 1-2 mg of powder. If the GLG was relatively narrow and required a 300 or 500 µm bit, we needed to drill a longer or

deeper line to obtain the minimum amount of dentin. In either case, we subsampled approximately 1.2 mg of dentin from the total yield to package into 5 x 9 mm tin capsules for stable isotope analysis, reported in delta notation:

$$\delta^{13}\mathrm{C} \text{ or } \delta^{15}\mathrm{N} \;=\; [(\mathrm{Rsample} \div \mathrm{Rstandard}) - 1] \times 1000$$

Where R represents the heavy:light ratio for δ^{13}C (^{13}C/^{12}C) or δ^{15}N (^{15}N/^{14}N) for the sample or an international standard as indicated. Standards were Vienna Peedee Belemnite (VPDB) and atmospheric nitrogen for measures of the δ^{13}C and δ^{15}N values, respectively.

Our samples were analyzed primarily in three laboratories: the University of California Santa Cruz Stable Isotope Laboratory using a CE Instruments NC2500 elemental analyzer coupled to a Thermo Scientific DELTAplus XP isotope ratio mass spectrometer via a Thermo-Scientific ConFlo III, the University of California Davis Stable Isotope Facility using a PDZ Europa ANCA-GSL elemental analyzer coupled to a PDZ Europa 20-20 isotope ratio mass spectrometer, and the University of New Mexico Center for Stable Isotopes using a Costech 4010 elemental analyzer coupled to a Thermo Scientific Delta V mass spectrometer via a Thermo-Scientific ConFlo IV. Four of the 161 total samples were analyzed at the University of Florida Light Stable Isotope Mass Spec Lab using a Carlo Erba elemental analyzer coupled to a Thermo Delta V Advantage isotope ratio mass spectrometer via a Thermo-Scientific ConFlo II. The laboratories used a variety of reference standards intermittently for quality control, but in all runs the standard deviations were ≤0.3‰ for δ^{13}C values and ≤0.4‰ for δ^{15}N values. In most cases, the same laboratory analyzed paired samples which were compared for each of our objectives.

Protocols and statistical analyses, all conducted in R[23] (R Core Team 2022) interfaced with R Studio[24], for our three objectives are described below.

I. Do the $\delta^{13}C$ and $\delta^{15}N$ values measured from a GLG remain consistent regardless of the area within the GLG from which dentin is sampled?

To test this question, we took two samples (an "original" sample and a "replicate" sample) from different points along a single GLG (Figure 2.1A). Due to GLG compaction at the root and crown of the tooth, and an increased risk of drilling into an underlying layer, we took the two samples from the middle of the section of the tooth when possible so one sample would not be more likely to contain non-target GLGs than the other. We did this for eight different GLGs, for a total of 16 samples, using seven unique teeth. Sampled GLGs ranged from year four to year 19. For the collection of this dataset, we discarded the surface dentin to a depth of ~25 µm to reduce formic acid and graphite presence, although potential contamination is not a concern in this framework since all samples were treated equally for comparison (see objective III below for testing of formic acid and graphite effects). The $\delta^{13}C$ and $\delta^{15}N$ values for both the original and the replicate groups appeared consistent with normal distributions via the Shapiro-Wilk test ($W(8) = 0.9$, $p > 0.2$ for all), so we proceeded with parametric paired t-tests to assess statistical significance of the mean difference between groups.

*II. Do the $\delta^{13}C$ and $\delta^{15}N$ values measured in dentin from a specific GLG (*e.g., *the GLG that represents a specific year of the animal's life) remain consistent regardless of the tooth from which the GLG is sampled?*

We sampled 106 GLGs total across 12 pairs of teeth to investigate isotopic homogeneity of GLGs among teeth within an individual (Figure 2.1B; Table S2.2). Note that we sampled four teeth from specimen USNM-594671, but treated them as two independent pairs (*i.e.*, Pair 1 and

Pair 2 in Table S2.2) rather than one quadruplicate set. Each pair had a different original catalogue number (*i.e.*, NMML-82 and MML-1966-145) as they were thought to be different specimens, though were later discovered after sampling to be teeth from the same single individual. As a consequence, we did not sample the same corresponding GLGs across all four teeth for fair statistical comparison, only the same corresponding GLGs for each pair. Nonetheless, we retained both pairs in our dataset because they represented a notable comparison between a pair of teeth directly adjacent (Pair 1) and a pair of teeth relatively far apart (Pair 2).

The number of GLGs that we sampled per tooth ranged from one to 8, with the youngest year being four and the oldest year being 25. Again, the outermost dentin to a depth of ~25 µm was discarded for this protocol. We separated the stable isotope data into measurements of GLGs for "Tooth A" and those for "Tooth B" for each pair. We were unable to systematically pair teeth (*i.e.*, collect one middle tooth and one peripheral tooth for every individual, or one left tooth and one right tooth for every individual, *etc.*), but we report tooth positions (and the approximate length of the tooth for a size comparison reference) when known in Table S2.2. We again examined the $\delta^{13}C$ and $\delta^{15}N$ values for normality using the Shapiro-Wilk test. The test showed evidence of non-normality for the $\delta^{13}C$ values of the Tooth A group ($W(53) = 0.95$, $p < 0.01$) and for the $\delta^{15}N$ values of the Tooth B group ($W(53) = 0.92$, $p < 0.01$), so we used a conservative approach with the non-parametric Wilcoxon Signed-Rank test to compare the difference between group means.

We also had access to a single triplicate set of teeth from one individual killer whale and examined this specimen separately. We measured the same five GLGs in all three teeth. The $\delta^{13}C$ values reflected a normal distribution ($W(5) = 0.9$, $p > 0.3$ for all), and the $\delta^{15}N$ values reflected a normal distribution for two of the three teeth ($W(5) = 0.8$, $p > 0.05$ for both) with one sample

showing mild non-normality ($W(5) = 0.7$, $p = 0.04$). Given that ANOVAs are relatively robust to non-normality[25], we used a repeated measures ANOVA to compare the stable isotope values of the five GLGs measured in all three teeth.

III. What are the effects of acid etching and pencil highlighting on stable isotope values of dentin in comparison to (a) dentin with removal of the contaminants and (b) dentin never exposed to the contaminants?

For scenario (a), we utilized four teeth (with two teeth from individual USNM-594671, Table S2.1), where a total of 10 GLGs were sampled twice: a "cleaned" sample in which the outer surface dentin to a depth of ~25 µm was discarded to reduce the presence of formic acid and graphite, and an "uncleaned" (or potentially contaminated) sample in which no dentin was discarded and any surface formic acid and graphite were retained (Figure 2.1C). Thus, we had 20 samples total. Shapiro-Wilk tests showed a significant departure from normality for the $\delta^{15}N$ values of the cleaned and uncleaned groups ($W(10) = 0.8$, $p < 0.05$ for both), but not for the $\delta^{13}C$ values ($W(10) = 0.9$, $p > 0.07$). Accordingly, we used the non-parametric Wilcoxon Signed-Rank test to compare the $\delta^{15}N$ values and the parametric paired t-test for the $\delta^{13}C$ values.

For scenario (b), we examined two GLGs within each of five teeth. Each GLG was sampled from tooth halves treated with formic acid and graphite under the "clean" condition (*i.e.*, with formic acid and graphite from the first ~25 µm discarded) as well as from corresponding tooth halves never exposed to the potential contaminants, for a total of 20 samples (Figure 2.1C). We still discarded the outermost ~25 µm of dentin from the untreated tooth half before collecting the sample to reduce influence from other external contamination such as dust, human oils, *etc*. Although it is more difficult to read GLGs from untreated tooth halves and

ensure the same GLG is being sampled when compared to the treated half, we did intentionally select teeth and specific GLGs with identifying features such that we could be confident about correctly cross-referencing tooth halves. For example, we could use the presence of a pulp stone (a distinct calcified mass embedded in the dentin) within the tooth as a feature to help guide GLG identification. Shapiro-Wilk tests showed evidence of normal distributions for both $\delta^{13}C$ and $\delta^{15}N$ values of treated and untreated groups ($W(10) = 0.9$, $p > 0.05$ for all), so we used paired t-tests to determine if there were differences in isotopic values from dentin apparently cleaned of contaminants and dentin never exposed to the contaminants.

2.4 Results

I. Do the $\delta^{13}C$ and $\delta^{15}N$ values measured from a GLG remain consistent regardless of the area within the GLG from which dentin is sampled?

The paired t-test did not detect a significant difference between original and replicate measurements within a single GLG (Figure 2.1A) for either the $\delta^{13}C$ values ($t(7) = -0.96$, $p = 0.37$) or the $\delta^{15}N$ values ($t(7) = -0.035$, $p = 0.97$). The mean (±SD, hereafter) $\delta^{13}C$ values for the original and replicate samples were -13.8±2.0‰ and -13.8±2.1‰, respectively. The mean $\delta^{15}N$ values for the original and replicate samples were 16.5±2.3‰ and 16.5±1.3‰, respectively.

*II. Do the $\delta^{13}C$ and $\delta^{15}N$ values measured in dentin from a specific GLG (*e.g., *the GLG that represents a specific year of the animal's life) remain consistent regardless of the tooth from which the GLG is sampled?*

The Wilcoxon Signed-Ranks test indicated that there was not a statistically significant difference in the $\delta^{13}C$ ($Z = -1.14$, $p = 0.25$) or $\delta^{15}N$ values ($Z = -0.65$, $p = 0.52$) values measured between Tooth A and Tooth B from the same individual for 12 pairs (Figure 2.1B). The mean

δ^{13}C value (+SD) of all GLGs was the same for both the Tooth A and Tooth B datasets (-13.2±1.0‰) and the mean δ^{15}N values for Tooth A and B groups were 17.5±0.9‰ and 17.5±1.3‰, respectively.

We noted our use of four teeth from specimen USNM-594671, though we could only compare two pairs separately because we were unable to sample the same GLGs across all four teeth. The only exception was GLG 19, which we did measure from all four teeth though the sample size is too small for statistical comparison. However, we did observe that the δ^{13}C values for GLG 19 among all four teeth were between -13.3 and -13.6‰ (SD = 0.2‰), and the δ^{15}N values were between 17.8 and 18.9‰ (SD = 0.5‰).

The repeated measures ANOVA for the triplicate set of teeth also did not detect a significant difference among the δ^{15}N values of the teeth ($F_{(2, 12)} = 3.43$, $p = 0.08$; mean values from 18.7±0.3‰ to 19.0±0.4‰), however there was a significant difference among the δ^{13}C values ($F_{(2,12)} = 8.26$, $p = 0.01$). The mean δ^{13}C values for each of the three teeth were: (1) -13.7±0.4‰, (2) -13.6±0.2‰, and (3) -13.4±0.2‰. Post-hoc paired t-tests indicated that the third tooth was driving the global significance (Tooth 1 to Tooth 3: $t(4) = 3.3$, $p = 0.03$); Tooth 2 to Tooth 3: $t(4) = 3.7$, $p = 0.02$).

III. What are the effects of acid etching and pencil highlighting on the stable isotope values of dentin from killer whale teeth in comparison to (a) dentin with removal of these potential contaminants and (b) dentin never exposed to the contaminants?

For scenario (a), there was no significant difference in the δ^{15}N values of cleaned (*i.e.*, contaminants removed; mean of 18.3±1.3‰) and uncleaned (*i.e.*, contaminates present; mean of 18.2±1.2‰) dentin samples (Figure 2.1C) via the Wilcoxon-Signed Rank test ($Z = -1.27$, $p =$

0.20). Likewise, there was no significant difference between the mean $\delta^{13}C$ values via the paired t-test ($t(9) = 0.44$, $p = 0.67$). The mean $\delta^{13}C$ value of the cleaned and uncleaned samples was -13.1±0.5‰ and -13.1±0.4‰, respectively.

For scenario (b), paired t-tests also showed no evidence of significant differences between dentin that had been cleaned of contaminants and dentin that had never been exposed for either the $\delta^{13}C$ values ($t(9) = 0.87$, $p = 0.41$) or $\delta^{15}N$ values ($t(9) = -0.90$, $p = 0.40$). Mean $\delta^{13}C$ and $\delta^{15}N$ values for the teeth cleaned of potential contaminants were -12.8±1.1‰ and 18.4±1.1‰, compared to -12.9±1.3‰ and 18.6±1.3‰ for the untreated teeth.

2.5 Discussion

I. Do the $\delta^{13}C$ and $\delta^{15}N$ values measured from a GLG remain consistent regardless of the area within the GLG from which dentin is sampled?

Our results support the hypothesis that a given GLG is isotopically uniform throughout a tooth. This might be expected because dentin (representing stable isotopes derived from the diet) is uniformly synthesized as a layer spanning the length of the tooth during GLG formation[12], rather than a progression from the root to the crown that would lead to differing stable isotope values depending on the animal's diet at the time. In the latter case, stable isotope measurements could be dependent on where within the GLG a sample was taken. However, even with the understanding that GLGs form as a whole layer over the span of a year, dentin is a complex structure composed of both mineralized inorganic material and organic collagen. The mineral concentrations in dentin may not be equal throughout a GLG, in part due to the presence and variability of calcospherites (hydroxyapatite or calcium apatite crystals) as well as secondary mineralization by calcium salts[12]. In bone, organic collagen is typically isolated from the inorganic matrix via decalcification[26,27] for stable isotope measurements, but studies have shown

this process is not necessary for modern marine mammal teeth and does not affect isotope values[28,29]. In any case, we found that the potential sources of heterogeneity in dentin were not sufficient to affect the stable isotope values measured in different sections of a GLG.

Another potential factor to consider when sampling a GLG is the concentric nature of the layers and the likelihood of drilling into layers below the target. Because layers are compressed and thinner at the root and the crown of the tooth, samples taken from those regions may need to be shallower than samples taken at the middle of the tooth to avoid underlying layers. In our experimental design, we attempted to control for this issue by drilling two locations in a GLG (to the same depth) that could still be described as the middle region of the tooth. We have found evidence of isotopic ontogenetic changes in adult killer whales (Chapter 4), meaning that accidentally sampling a deeper (*i.e.*, older) GLG could significantly bias the data and interpretations. So while our data suggest there is leniency in the exact sampling point of a GLG, it is advisable to sample from the middle of the tooth when possible or adapt the drill path to be longer but shallower if the sample needs to be taken from the peripheral root or crown regions.

*II. Do the $\delta^{13}C$ and $\delta^{15}N$ values measured in dentin from a specific GLG (*e.g., *the GLG that represents a specific year of the animal's life) remain consistent regardless of the tooth from which the GLG is sampled?*

Overall, our results support that stable isotope values measured from dentin taken from GLGs that represent the same year are not dependent on the exact tooth from which each GLG is sampled. We had 12 pairs of teeth in our dataset, which represented a diversity of position comparisons since we were unable to consistently sample the same two teeth from every individual (Table S2.2). However, where tooth position was known, most pairs of teeth

originated from near the middle of the jaw and were 1-3 positions apart. We did include one pair of teeth (aforementioned specimen ID USNM-594671) that were nearly as far apart as possible, yet the $\delta^{13}C$ and $\delta^{15}N$ values remained similar (Table S2.2).

There was one tooth in a triplicate set that was the only exception to our finding of consistent stable isotope measurements in the same GLGs between teeth, though the differences in the average $\delta^{13}C$ values were only 0.2 or 0.3‰ below those of the other two teeth. Given that meaningful $\delta^{13}C$ increments are ~1-2‰ to infer habitat and feeding patterns[6,30–32], the differences of 0.2-0.3‰ we observed are likely not biologically significant.

An important potential source of error in testing the isotopic consistency of GLGs between teeth of an individual is correctly matching GLGs. Though stable isotope values were not examined, several studies have given attention to whether or not age estimations vary with different teeth from one individual[17,33–36]. If age estimations differ by tooth, the factors that contribute to these differences need to be considered when matching GLGs. For example, Hui[33] found different GLG counts within teeth from bottlenose dolphins because the anterior teeth cease dentin deposition at 10-12 years old, but other teeth showed more than double that count. Kasuya and Matsui[34] similarly found that the anterior and posterior teeth of short-finned pilot whales showed significantly fewer GLGs than teeth from the middle of the jaw, even if the pulp cavity was still open. In contrast, other studies have described similar GLG counts among different teeth from an individual for sperm whales, spinner dolphins (*Stenella longirostris*), pantropical spotted dolphins (*Stenella attenuata*), common dolphins (*Delphinus delphis*), bottlenose dolphins, and long-finned pilot whales (*Globicephala melas*)[17,35,36]

We found that the killer whale teeth within individuals in our study did generally reflect consistent GLG counts. However, we also found that teeth located in the anterior and posterior

sections of the mouth appeared to cease dentin deposition earlier than those positioned in the middle of the mouth due to the closure of the pulp cavity. For example, we counted the same number of GLGs (~25) in a posterior tooth with a nearly closed cavity as we did for a middle tooth with an open pulp cavity still comprising approximately 20% of the cut tooth surface area (aforementioned specimen ID USNM-594671*)*. The matching GLGs between these two teeth could be compared, but we would not have been able to sample older GLGs from the posterior tooth that were only present in the middle tooth. Indeed, we suspect age ~25 may be the point at which the most-posterior teeth fill in, as we found much older animals (~45 GLGs in the middle teeth) with about half as many GLGs in the most-posterior tooth (Bowen, pers. obs.). For that reason, we caution against using very anterior or posterior teeth for aging or stable isotope analysis. Unfortunately the positions of the teeth in our triplicate set were unidentified, but all three were approximately the same size with a similar degree of exposed pulp cavity, meaning an anterior or posterior position in the mouth was unlikely to be a contributing factor to the small but measurable difference in δ^{13}C values.

To summarize, we found that GLG counts were consistent across teeth within an individual and believe GLG matching between two teeth was not a significant contributing source of error to our study, though we acknowledge this should be a consideration when comparing multiple teeth. Our data suggest there is leniency when choosing a particular tooth from which to sample for stable isotope analyses, but researchers should still prioritize a tooth located in the middle of the mouth when possible or otherwise take into account species-specific variation in tooth morphology or GLG patterns. If a killer whale tooth with a closed cavity is collected from the anterior or posterior portion of the mouth for sampling, then the age estimate and isotopic data may not reflect the animal's entire lifetime.

III. What are the effects of acid etching and pencil highlighting on the stable isotope values of dentin from killer whale teeth in comparison to (a) dentin with removal of these potential contaminants and (b) dentin never exposed to the contaminants?

Our data support that acid-etching and pencil highlighting did not significantly affect the $\delta^{13}C$ or $\delta^{15}N$ values of killer whale teeth. We showed this result through comparisons of the same GLGs under two conditions: (a) an "uncleaned" sample which was unaltered and a "cleaned" sample in which formic acid and graphite from the surface had been discarded, and (b) an uncleaned sample from the tooth treated with formic acid and graphite and a sample from the other tooth half which had never been exposed to the chemicals. In both cases, stable isotope values did not differ between the compared samples.

Our results partly agreed with those from Stukonytė *et al*.[22], the only other published study on the effects of formic acid and graphite on teeth from a marine mammal, as they also found no significant effect of graphite on stable isotope values. The authors hypothesize that the amount of graphite is negligible in comparison to the amount of dentin sampled, and the graphite carbon signature is not detectable. For sperm whale and killer whale teeth, removing the graphite layer before collecting dentin for stable isotope analysis does not appear to be necessary.

Though our graphite conclusions were similar, our results for the effect of formic acid on stable isotope values differed from those of Stukonytė *et al*.[22]: they found an increase of 0.2‰ on average for both the $\delta^{13}C$ and $\delta^{15}N$ values in sperm whale teeth etched with formic acid compared to untreated teeth, whereas we found no difference in isotope values for killer whale teeth. A notable change in our methodologies was the amount of time the teeth were exposed to formic acid. The sperm whale teeth were soaked for 30 hours compared to our killer whale teeth

that soaked for 12 hours. Thus, it could be advantageous to limit the duration of the formic acid exposure when targeting GLGs for stable isotope analyses. Teeth are etched with formic acid to expose the GLGs more clearly and etching time is a trade-off between soaking the tooth long enough to obtain clear GLGs and short enough to avoid over-etching, in which the GLGs may be obscured from decalcification activity. Evans and Robertson[37] found that ideal etching time was significantly related to the size of the tooth for sperm whales. In our study, we etched all sizes of killer whale teeth from ~5 cm to ~15 cm in length for 12 hours and qualitatively found equally readable GLGs. Though Stukonytė *et al*.[22] did not specify the size of the sperm whale teeth used, killer whale and sperm whale teeth can be comparable[38] (Bowen, pers. obs.). Researchers should consider optimizing the formic acid etching time of their species and tooth sizes to be as short as possible while still yielding clear GLGs. The concentration of the formic acid is important to consider as well[37], though both our study and Stukonytė *et al*.[22] used 10% formic acid.

Another variable that could influence the effect of formic acid on stable isotope values in dentin is the depth of formic acid penetration given the permeability of the tooth[12]. Klevezal[12] remarks that lower concentrations and smaller sizes of calcospherites can increase permeability. It could be possible that certain species are prone to higher or lower levels of dentin permeability. Relatedly, the depth to which a GLG is sampled or the overall amount of dentin collected could affect whether or not formic acid biases stable isotope measurements. Stukonytė *et al*.[22] suggest 0.9 mg of dentin was extracted and packaged for stable isotope analysis. In contrast, we collected up to approximately 2 mg of dentin and subsampled 1.2 mg for isotope analysis. As in the case with graphite, formic acid may comprise a negligible proportion of the dentin sample if 2 mg is collected, but the effect could differ if only 1 mg is collected since the formic acid could be more prevalent in the sample.

Although Stukonytė *et al.*[22] report a significant increase of 0.2‰ for both $\delta^{13}C$ and $\delta^{15}N$ values in sperm whale teeth from formic acid, it is also important to consider biological context for interpretation. As previously noted, meaningful $\delta^{13}C$ increments are typically on the order of ~1-2‰[6,30–32]. Additionally, 0.2‰ was within our range of stable isotope measurement precision. Stukonytė et al.[22] examined a slightly larger sample size (n = 30 independent samples) than presented here (n = 20 independent samples total for scenarios "a" and "b"), so it is possible we could have detected an effect of formic acid with additional specimens. However, our data suggest that killer whale teeth of any size (excluding those from young calves) can be etched in 10% formic acid for 12 hours, highlighted with graphite pencil, and directly sampled for stable isotope analysis. For good practice, we still recommend discarding the outermost layer of dentin if possible due to any number of surface contamination possibilities. However, this may not be feasible for very narrow GLGs representing the oldest years of a killer whale's life, because all drilled dentin may be needed to have sufficient material for isotope analysis and to maintain the shallowest path possible so as to avoid underlying non-target GLGs. Researchers studying smaller cetacean or pinniped teeth could encounter this same dilemma. Additional studies of different formic acid conditions across species may help establish a framework that can be used for pre-treatment, age estimation, and stable isotope sampling of mammal teeth.

2.6 Acknowledgements

We are grateful to the natural history collections and all the staff/curators who made this work possible through generous specimen loans, including: the Beaty Biodiversity Museum – University of British Columbia (M. deRoos, C. Stinson); the California Academy of Sciences (M. Flannery); Cal Poly Humboldt (formerly Humboldt State University, T. Danufsky, M. Hawkins, P. Goley, A. Bronson, A. Semerdjian); the Natural History Museum of Los Angeles

County (D. Janiger, J. Velez-Juarbe, S. Robson); the NOAA Marine Mammal Laboratory (P. Clapham, P. Wade); the Museum of the North – University of Alaska (A. Gunderson, L. Olson); the Smithsonian National Museum of Natural History (M. Hawkins, D. Lunde, M. McGowen, J. Ososky); the Burke Museum of Natural History and Culture – University of Washington (J. Bradley); the Royal British Columbia Museum (G. Hanke, C. Davies, L. Golding).
Our thanks also to the following for assistance with sample measurements: University of California Santa Cruz Stable Isotope Laboratory (D. Andreasen, C. Carney, and E. Cano); the University of New Mexico Center for Stable Isotopes (S. Newsome, V. Atudorei); University of Florida - Light Stable Isotope Mass Spec Lab (J. Curtis); University of California Davis - Stable Isotope Facility (C. Yarnes, E. Schick).

Finally, we extend our greatest appreciation to numerous researchers at NOAA's Southwest Fisheries Science Center for support that made this work possible, including: D. Weller, J. Seminoff, C. Turner Tomaszewicz, T. Chen, R. Schnug. Also thanks to L. Ballance, J. Shurin, S. Nehasil, and J. Bowen for invaluable additional project support. Funding and support for K.B. and C.K. were provided by the University of California San Diego (UCSD), the NIH Cell & Molecular Genetics Graduate Training Program, the PADI Foundation, the Lerner-Gray Fund for Marine Research by the American Museum of Natural History, the Jeanne Marie Messier Memorial Endowed Fund (UCSD), the American Cetacean Society Los Angeles Chapter John E. Heyning Research Grant, and the Association for Women in Science San Diego Chapter.

Chapter 2, in full, has been submitted for publication of the material as it may appear in Rapid Communications in Mass Spectrometry, 2024, Bowen, KR; Kurle, CM. The dissertation author was the primary investigator and author of this paper.

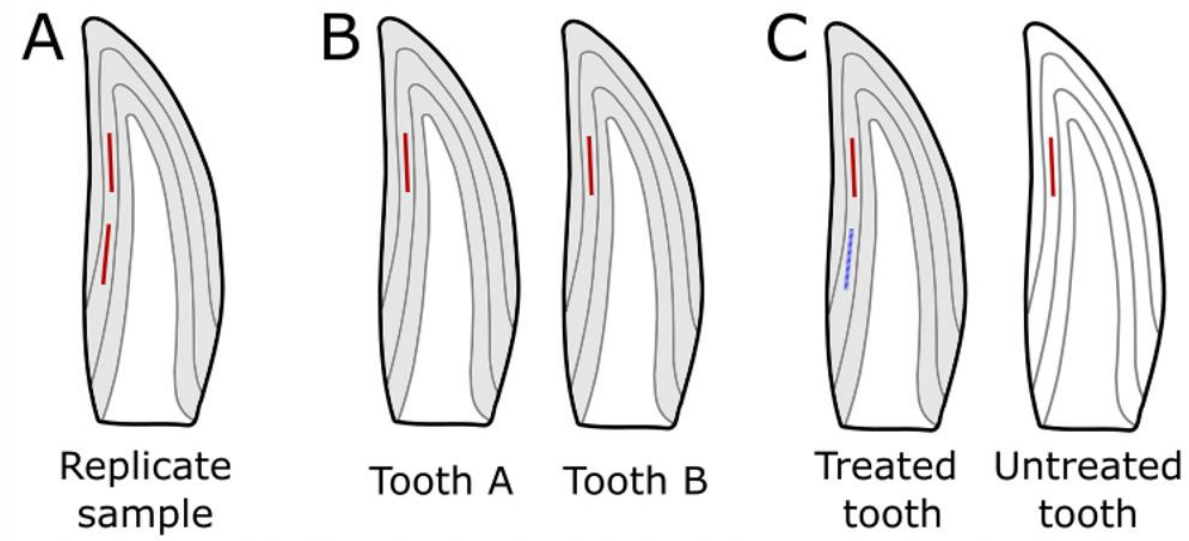


Figure 2.1. Sampling schemes for the three objectives of our study illustrated with the cut surface of tooth halves and visible growth layer groups (GLGs). A gray backdrop indicates the tooth half has been etched and penciled, with a white center indicating an open pulp cavity. Our first objective (A) was to sample two locations within the same GLG of an etched and penciled tooth half, where the solid red lines indicate a representative drill sampling path. Our second objective (B) was to sample the same GLG in two different teeth (Tooth A and Tooth B) from the same individual. Our third objective (C) was twofold: (i) to compare a sample from a GLG with formic acid and graphite intact (red solid line on gray backdrop) to a sample from the same GLG with the formic acid and graphite cleaned away (blue dashed line), and (ii) to compare a sample from a treated GLG with formic acid and graphite intact (red solid line on gray backdrop) to a sample from the same GLG on the other untreated tooth half.

Table S2.1. Catalogue numbers for the 25 killer whale (*Orcinus orca*) teeth used in this study are listed in addition to the objective(s) for which the teeth were utilized as described in the main text. * = specimen used for triplicate test. For the sample IDs, collection abbreviations are as follows: BBM = Beaty Biodiversity Museum; CAS = California Academy of Sciences; HSU = Humboldt State University (previously Humboldt State University); LACM = Natural History Museum of Los Angeles County; N/MML = NOAA Marine Mammal Lab; RBCM = Royal British Columbia Museum; UAM = University of Alaska Museum of the North; UWBM = University of Washington Burke Museum.

Sample ID	**Alternate ID**	**Replicate test (I)**	**Duplicate test (II)**	**"Clean v unclean" test (III-a)**	**"Clean v untreated" test (III-b)**
BBM-J18	--	x			
CAS-16464	--				x
HSU-uncatalogued	--				x
LACM-1790	LACM-52455		x		
LACM-84249	--		x		
MML-3265	--	x			
MML-3774	--	x			
"Namu"	MML-1966		x		
NMML-1850	--				x
RBCM-10001	--	x			x
RBCM-21490	--	x			
RBCM-8386	--			x	
UAM-101747	--				x
USNM-594668	NMML-81, MML-1965-4		x		
USNM-594669	NMML-84, MML-1967-157		x		
USNM-594670	NMML-88, MML-3264		x		
USNM-594671	NMML-82, MML-1966-145		x*	x	
USNM-594672	NMML-89, MML-3266		x		
USNM-594674	NMML-87, MML-3204		x		
USNM-594676	NMML-85, MML-1967-175		x**		
USNM-594678	NMML-79, MML-1963-832			x	
UWBM-82332	--		x		
UWBM-82333	--	x	x		
UWBM-82688	--	x			

Table S2.2. Catalogue numbers, other associated metadata, and stable isotope values are reported for specimens used towards objective II in the main manuscript to examine variability among 12 duplicate teeth and 1 set of triplicate teeth. See Table S1.1 caption for specimen collection abbreviations. For "Tooth position", abbreviations are as follows: single L = left, single R = right, LR = lower right, LL = lower left, UL = upper left. Killer whale teeth positions are sequentially labeled in the jaw, where 1 indicates the most anterior position and 12 indicates the most posterior position.

Sample	Alternate	Tooth position	Tooth length	Age	$\delta^{13}C$	$\delta^{13}C$	$\delta^{15}N$	$\delta^{15}N$	$\delta^{13}C$	$\delta^{15}N$
ID	ID	(A, B, C)	(cm; A, B, C)	line	(Tooth A)	(Tooth B)	(Tooth A)	(Tooth B)	(Tooth C)	(Tooth C)
LACM-1790*	LACM-52455	L11, --	4.4, 5.3	4	-12.6	-12.6	17.0	17.1		
				7	-12.8	-12.6	16.7	16.6		
				10	-13.0	-12.8	16.6	16.8		
				13	-12.8	-12.7	17.1	16.6		
LACM-84249	--	UR7, --	9.2, 8.6	4	-12.0	-12.4	17.7	17.4		
				7	-12.5	-12.4	16.7	17.2		
"Namu"	MML-1966, UWBM-26282	L7, R9	10.7, 10.5	4	-11.8	-11.6	17.0	16.9		
				7	-11.7	-11.4	17.2	17.3		
				10	-11.9	-11.8	17.5	17.1		
				13	-11.7	-11.5	18.2	17.7		
				16	-11.7	-12.0	18.4	17.6		
USNM-594668	NMML-81, MML-1965-4	R8, L7	13.0, 11.8	4	-14.4	-14.1	17.2	17.0		
				7	-14.1	-14.2	17.1	17.1		
				10	-13.8	-14.3	17.3	16.9		
				13	-14.5	-14.6	16.7	17.0		
				16	-14.4	-14.3	17.2	17.6		
				19	-14.7	-14.2	17.2	18.0		
USNM-594669	NMML-84, MML-1967-157	R8, R5	12.2, 12.5	4	-13.7	-13.1	18.7	19.5		
				7	-13.2	-12.8	18.9	19.5		
				10	-13.3	-12.9	19.1	20.0		
				16	-13.5	-13.3	19.6	19.7		
USNM-594670	NMML-88, MML-3264	LL7, R5	7.4, 7.5	5	-12.5	-12.7	17.1	17.1		
USNM-594671 (Pair 1)**	NMML-82, MML-1966-145	R8, R7	12.8, 13.5	4	-13.3	-13.4	17.8	18.4		
				7	-13.2	-13.3	17.6	18.2		
				10	-13.5	-13.7	17.5	18.0		
				13	-13.6	-13.5	17.9	18.3		
				16	-13.6	-13.4	18.2	18.8		
				19	-13.3	-13.6	18.9	17.8		
				22	-13.6	-13.5	18.4	18.3		
				25	-13.4	-13.3	18.3	19.0		

Table S2.2. Continued. Catalogue numbers, other associated metadata, and stable isotope values are reported for specimens used towards objective II in the main manuscript to examine variability among 12 duplicate teeth and 1 set of triplicate teeth. See Table S2.1 caption for specimen collection abbreviations. For "Tooth position", abbreviations are as follows: single L = left, single R = right, LR = lower right, LL = lower left, UL = upper left. Killer whale teeth positions are sequentially labeled in the jaw, where 1 indicates the most anterior position and 12 indicates the most posterior position.

Sample	Alternate	Tooth position	Tooth length	Age	$\delta^{13}C$	$\delta^{13}C$	$\delta^{15}N$	$\delta^{15}N$	$\delta^{13}C$	$\delta^{15}N$
ID	ID	(A, B, C)	(cm; A, B, C)	line	(Tooth A)	(Tooth B)	(Tooth A)	(Tooth B)	(Tooth C)	(Tooth C)
USNM-594671 (Pair 2)**	NMML-82, MML-1966-145	LR4, UL12	13.0, 9.3	11	-13.6	-13.1	18.1	17.8		
				19	-13.6	-13.3	17.8	18.3		
USNM-594672	NMML-89, MML-3266	R8, R7	11.2, 11.3	4	-12.7	-12.6	17.1	17.2		
				7	-11.7	-11.8	17.9	18.0		
				10	-11.6	-11.8	17.7	17.8		
				13	-11.8	-11.8	17.9	18.1		
				15	-11.9	-12.0	18.3	18.3		
				17	-12.2	-12.4	18.0	18.3		
				19	-11.9	-12.3	18.2	18.9		
USNM-594674***	NMML-87, MML-3204	R8, R10	8.6, 7.2	4	-13.3	-13.4	17.8	17.8		
				7	-13.0	-13.0	17.1	17.3		
				10	-13.4	-13.4	17.8	17.7		
				13	-13.0	-12.8	18.6	18.3		
				16	-13.3	-13.3	17.9	17.9		
				19	-13.3	-13.0	18.5	18.4		
				22	-13.2	-13.0	18.7	18.5		
USNM-594676	NMML-85, MML-1967-175	--, --, --	12.6, 11.0, 11.4	4	-13.8	-13.6	18.6	18.8	-13.6	18.9
				7	-13.4	-13.5	18.5	18.5	-13.3	18.4
				10	-13.4	-13.4	19.3	19.4	-13.1	19.0
				13	-13.8	-13.6	19.3	19.4	-13.4	18.9
				16	-14.3	-13.9	18.5	18.8	-13.6	18.4
UWBM-82332	--	--, --	6.0, 5.3	4	-14.8	-15.0	15.5	15.4		
				7	-14.8	-14.9	15.3	13.5		
				10	-14.7	-14.8	15.8	15.3		
				13	-15.2	-15.4	16.7	15.8		
				16	-14.7	-15.2	16.4	13.0		
UWBM-82333	--	--, --	7.2, 7.0	4	-15.3	-15.1	16.2	16.0		
				8	-15.0	-14.7	15.3	15.6		

1.7 References

1. Hobson KA, Sease JL. Stable isotope analyses of tooth annuli reveal temporal dietary records: an example using Steller sea lions. *Marine Mammal Science*. 1998;14(1):116-129. doi:10.1111/j.1748-7692.1998.tb00694.x

2. Walker JL, Macko SA. Dietary studies of marine mammals using stable carbon and nitrogen isotopic ratios of teeth. *Marine Mammal Science*. 1999;15(2):314-334. doi:10.1111/j.1748-7692.1999.tb00804.x

3. Newsome SD, Clementz MT, Koch PL. Using stable isotope biogeochemistry to study marine mammal ecology. *Marine Mammal Science*. Published online January 2010. doi:10.1111/j.1748-7692.2009.00354.x

4. Teixeira CR, Troina GC, Daura-Jorge FG, Simões-Lopes PC, Botta S. A practical guide on stable isotope analysis for cetacean research. *Marine Mammal Science*. 2022;38(3):1200-1228. doi:10.1111/mms.12911

5. DeNiro MJ, Epstein S. Influence of diet on the distribution of carbon isotopes in animals. *Geochimica et Cosmochimica Acta*. 1978;42(5):495-506. doi:10.1016/0016-7037(78)90199-0

6. Deniro MJ, Epstein S. Influence of diet on the distribution of nitrogen isotopes in animals. *Geochimica et Cosmochimica Acta*. 1981;45(3):341-351. doi:10.1016/0016-7037(81)90244-1

7. MD Uhen. Evolution of dental morphology (cetacean). In: *Encyclopedia of Marine Mammals*. Academic Press; :316-318.

8. Nishiwaki M, Yagi T. On the age and the growth of teeth in a dolphin (*Prodelphinus caeruleo-albus*). *Sci Rep Whales Res Inst*. 1953;(8):133-146.

9. Scheffer VB, Myrick AC. A review of studies to 1970 of growth layers in the teeth of marine mammals. *Rep Int Whale Commn*. (3 (special issue)):51-63.

10. Hohn AA, Scott MD, Wells RS, Sweeney JC, Irvine AB. Growth layers in teeth from known-age, free-ranging bottlenose dolphins. *Marine Mammal Science*. 1989;5(4):315-342. doi:10.1111/j.1748-7692.1989.tb00346.x

11. Read FL, Hohn AA, Lockyer CH. A review of age estimation methods in marine mammals with special reference to monodontids. *NAMMCOSP*. 2018;10. doi:10.7557/3.4474

12. Klevezal GA. *Recording Structures of Mammals: Determination of Age and Reconstruction of Life History*. 1st ed. Routledge; 1995. doi:10.1201/9780203741146

13. Boyd IL, Roberts JP. Tooth growth in male Antarctic fur seals (*Arctocephalus gazella*) from South Georgia: an indicator of long-term growth history. *Journal of Zoology*. 1993;229(2):177-190. doi:10.1111/j.1469-7998.1993.tb02630.x

14. Hamilton V, Evans K, Raymond B, Hindell MA. Environmental influences on tooth growth in sperm whales from southern Australia. *Journal of Experimental Marine Biology and Ecology*. 2013;446:236-244. doi:10.1016/j.jembe.2013.05.031

15. Stewart R, Stewart B. Comparison of between-tooth age estimates of Atlantic walrus (*Odobenus rosmarus rosmarus*). *Mar Mamm Sci*. 2005;21(2):346-354.

16. Hohn AA. Age estimation. In: *Encyclopedia of Marine Mammals*. Academic Press; 2009:11-17.

17. Myrick AC. Is tissue resorption and replacement in permanent teeth of mammals caused by stress-induced hypocalcaemia? In: *The Biological Mechanisms of Tooth Eruption and Root Resorption*. EBASCO Media; 1988:379-389. https://www.cabidigitallibrary.org/doi/full/10.5555/19892291525

18. Newsome SD, Koch PL, Etnier MA, Aurioles-Gamboa D. Using carbon and nitrogen isotope values to investigate maternal strategies in northeast Pacific otariids. *Marine Mammal Science*. 2006;22(3):556-572. doi:10.1111/j.1748-7692.2006.00043.x

19. Newsome S, Etnier M, Monson D, Fogel M. Retrospective characterization of ontogenetic shifts in killer whale diets via δ^{13}C and δ^{15}N analysis of teeth. *Mar Ecol Prog Ser*. 2009;374:229-242. doi:10.3354/meps07747

20. Hanson N, Wurster C, Bird M, Reid K, Boyd I. Intrinsic and extrinsic forcing in life histories: patterns of growth and stable isotopes in male Antarctic fur seal teeth. *Mar Ecol Prog Ser*. 2009;388:263-272. doi:10.3354/meps08158

21. Knox TC, Stuart-Williams H, Warneke RM, Hoskins AJ, Arnould JPY. Analysis of growth and stable isotopes in teeth of male Australian fur seals reveals interannual variability in prey resources. *Marine Mammal Science*. 2014;30(2):763-781. doi:10.1111/mms.12078

22. Stukonytė L, Borrell A, Drago M, Lockyer C, Víkingsson G, Aguilar A. Effect of formic acid treatment on carbon and nitrogen stable isotope ratios in sperm whale teeth dentine. *Rapid Comm Mass Spectrometry*. 2023;37(10):e9500. doi:10.1002/rcm.9500

23. R Core Team. R: A language and environment for statistical computing. Published online 2022. https://www.R-project.org/

24. Posit Team. RStudio: Integrated Development Environment for R. Published online 2024.

25. Blanca MJ, Alarcón R, Arnau J. Non-normal data: Is ANOVA still a valid option? *Psicothema*. 2017;(29.4):552-557. doi:10.7334/psicothema2016.383

26. Ambrose SH. Preparation and characterization of bone and tooth collagen for isotopic analysis. *Journal of Archaeological Science*. 1990;17(4):431-451. doi:10.1016/0305-4403(90)90007-R

27. Lee-Thorp JA, Sealy JC, Van Der Merwe NJ. Stable carbon isotope ratio differences between bone collagen and bone apatite, and their relationship to diet. *Journal of Archaeological Science*. 1989;16(6):585-599. doi:10.1016/0305-4403(89)90024-1

28. Brault EK, Koch PL, Gier E, Ruiz-Cooley RI, Zupcic J, Gilbert KN, McCarthy MD. Effects of decalcification on bulk and compound-specific nitrogen and carbon isotope analyses of dentin. *Rapid Comm Mass Spectrometry*. 2014;28(24):2744-2752. doi:10.1002/rcm.7073

29. Groom B. *Effects of Decalcification, Species, and Mammalian Order on Bulk Stable Isotope Values from Marine Mammal Teeth*. University of California San Diego; 2018. https://www.proquest.com/openview/7b61f9e80a3bd2171850ad4a04ac42f4/1?pq-origsite=gscholar&cbl=18750

30. Burton RK, Koch PL. Isotopic tracking of foraging and long-distance migration in northeastern Pacific pinnipeds. *Oecologia*. 1999;119(4):578-585. doi:10.1007/s004420050822

31. Burton RK, Snodgrass JJ, Gifford-Gonzalez D, Guilderson T, Brown T, Koch PL. Holocene changes in the ecology of northern fur seals: insights from stable isotopes and archaeofauna. *Oecologia*. 2001;128(1):107-115. doi:10.1007/s004420100631

32. Aurioles D, Koch PL, Le Boeuf BJ. Differences in foraging location of Mexican and California elephant seals: Evidence from stable isotopes in pups. *Marine Mammal Science*. 2006;22(2):326-338. doi:10.1111/j.1748-7692.2006.00023.x

33. Hui CA. Variability of dentin deposits in *Tursiops truncatus*. *Can J Fish Aquat Sci*. 1980;37(4):712-716. doi:10.1139/f80-090

34. Kasuya T, Matsui S. Age determination and growth of the short-finned pilot whale off the Pacific coast of Japan. *Sci Rep Whales Res Inst*. 1984;35:57-91.

35. Nishiwaki M. Age study of sperm whale based on reading of tooth laminations. *Sci Rep Whales Res Inst*. 1958;13:135.

36. Lockyer CH. A report on patterns of deposition of dentine and cement in teeth of pilot whales, genus Globicephala. *Rep Int Whale Commn*. 1993;14:137-161.

37. Evans K, Robertson K. A note on the preparation of sperm whale (*Physeter macrocephalus*) teeth for age determination. *jcrm*. 2023;3(1):101-107. doi:10.47536/jcrm.v3i1.907

38. Omura H, Nishiwaki M, Ichihara T, Kasuya T. Osteological note of a sperm whale. *Sci Rep Whales Res Inst*. 1962;16:35-45.

Chapter 3 : Stable isotope values from organisms in the North Pacific Ocean: A reference for trophic ecology studies

3.1 Stable isotope value reference library

Trophic ecology research provides insight into ecosystem form and function through an understanding of predator-prey dynamics [1]. Analyses of the stable carbon ($^{13}C/^{12}C$; $\delta^{13}C$) and nitrogen ($^{15}N/^{14}N$; $\delta^{15}N$) isotope values from predator and prey tissues are a useful method by which to study foraging relationships. Stable isotope values increase with each tropic level due to consumer metabolism and the differential assimilation of heavier and lighter isotopes from prey into predator tissues [2–4]. The differences in the stable isotope values between prey and predator tissues due to fractionation can be predictable and is measured as the trophic discrimination factor (TDF). TDFs are dependent upon several variables, including taxonomy (*e.g.*, fish or mammal, etc.), consumer type (*e.g*., carnivore or herbivore), consumer sex (e.g., male or female), diet source (*e.g*., marine or terrestrial) and tissue type (*e.g*., blood or skin, etc.) [5–7].

Although TDFs would ideally be specific to the system being studied, controlled feeding experiments over months to identify TDFs are often prohibitively difficult. Generalized TDFs have been recognized (+1‰ for the $\delta^{13}C$ values and +3.4‰ for the $\delta^{15}N$ values[8]) as a substitute when experimentally-derived TDFs are unavailable, but, when possible, it remains important to compare similar predator and prey tissues to control for the tissue-dependency of TDFs. Stable isotope values can be measured for soft tissues such as skin, blubber, and muscle, as well as hard tissues such as dentin and bone. The isotopic turnover, the rate at which stable isotopes in a tissue are replaced with those metabolized from the diet, varies by tissue type [5]. Blood has a relatively high turnover rate of weeks compared to the slow turnover rate of bone over years [9–11]. Therefore, similar tissues should be compared between predator and prey when possible.

Despite the challenges in standardizing isotope values and TDFs across taxa and tissue types, stable isotope analyses have been used to study trophic ecology at multiple temporal and spatial scales in the Pacific Ocean (among other marine and terrestrial environments). For example, Misarti *et al.* [12] examined stable isotope values of bone collagen from fish and marine mammals in the Pacific Ocean over 4500 years, and Arnoldi *et al.* [13] investigated stable isotope values from invertebrates and fish across the majority of the North Pacific Ocean basin. These studies demonstrate the utility of a multi-taxa approach to understanding food webs and trophic dynamics.

To facilitate food web studies of diverse organisms within the North Pacific Ocean, we curated a database of stable isotope values from consumer species in six broad taxonomic groups: Cetacea (dolphins, porpoises, and whales), Pinnipedia (seals, sea lions, and walruses), Mustelidae (sea otters), Osteichthyes (bony fishes), Chondrichthyes (cartilaginous fishes), and Cephalopoda (squids and octopus). Our database (Table 3.1) is a comprehensive, but not exhaustive, overview of many ecologically important species of interest.

Our first goal was to capture the range of stable isotope values that could represent a species, given measurements from different time periods, regions, life stages, sexes, and tissues. We compiled 254 δ^{13}C and δ^{15}N values (with standard deviations, SD, or standard errors, SE) from 89 taxa across 74 published studies. Our second goal was twofold: to first condense the multitude of stable isotope values across studies into one representative range for that species (*i.e.*, calculate one mean δ^{13}C and δ^{15}N value ± SD from values reported across multiple studies) and further condense the stable isotope values from multiple species into a representative range for that taxonomic group (*i.e.*, calculate one mean δ^{13}C and δ^{15}N value ± SD to represent 'pinnipeds' from multiple species). Some studies could require the fine-scale data shown in

Table 3.1, such as the $\delta^{13}C$ and $\delta^{15}N$ values for juvenile male Northern fur seals, but others may aim to examine a broad taxonomic group, such as the $\delta^{13}C$ and $\delta^{15}N$ values for pinnipeds in the North Pacific.

To compute a single $\delta^{13}C$ and $\delta^{15}N$ value (± SD) from multiple studies and species (Table 3.2), we followed methodology in Carlisle *et al*.[14] For example, we computed a single $\delta^{13}C$ value (± SD) for the pantropical spotted dolphin (*Stenella attenuata*) by resampling 2000 values from a normal distribution with the parameters of study 1 (mean $\delta^{13}C$ value of -16.82 ± 0.69‰[15]) and the parameters of study 2 (mean $\delta^{13}C$ value of -17.3 ± 0.3‰[16]), then combining them into a cumulative distribution, and finally evaluating the mean $\delta^{13}C$ and SD of the cumulative distribution (in this case, our reported $\delta^{13}C$ value for pantropical spotted dolphins is -17.1 ± 0.6‰). We also resampled 2000 values from the $\delta^{13}C$ and $\delta^{15}N$ values ± SD of species with only one representative study to generate a distribution that incorporates the reported variation and remains consistent with our methodology for these generated $\delta^{13}C$ and $\delta^{15}N$ values.

We applied several filters and corrections to our compilation analysis of Table 3.1 to identify the single $\delta^{13}C$ and $\delta^{15}N$ values in Table 3.2. First, we excluded samples if they were collected from the Gulf of California due to bias from elevated $\delta^{15}N$ values in this region [17]. Second, we aimed to compile the $\delta^{13}C$ and $\delta^{15}N$ values that were representative of soft tissues overall, with muscle specifically targeted when possible. We found muscle was the most frequently sampled tissue, allowing for greater consistency when compiling studies among a species. Soft tissues are also more likely to be useful for dietary analyses, since soft tissues are typically consumed by a predator and bones, teeth, or whiskers may be discarded. To this end, we chose muscle samples in cases of measurements from paired tissues in Table 3.1. We also corrected bone or teeth measurements to resemble muscle with the equation: $\delta^{13}C_{muscle}$ =

$\delta^{13}C_{bone/tooth} - 2‰$ (see supplementary material of Kim *et al.*[18], except for sea otters. The studies we report for sea otters sampled bone and whiskers, and the correction factor does not apply to whiskers. For consistency, we complied the hard tissue measurements (whiskers and bone) for sea otters as they were reported. Finally, if a study provided SE rather than SD, we converted SE to SD when calculating our study or species distributions (Table 3.1 reports the original SE values in such cases). We report single condensed stable isotope values (± SD) for each species in Table 3.2, and single condensed stable isotope values (± SD) for broad taxonomic groups in Table 3.3. All computations were conducted in R v. 4.2.1 (R Core Team 2022) using base functions.

Our reference database is informative for future researchers aiming to study trophic relationships within the North Pacific, variation in isotope values within species that may be due to differential life history traits, variation in isotope values across time, and the potential for differences in the trophic discrimination factors among multiple tissues from a species. It is worth emphasizing that we report the original data here to maximize adaptability, but studies that reference this database may consider accounting for or further examining tissue corrections, the Suess effect[19], geographic variation (*i.e.*, changes in the $\delta^{13}C$ values with latitude or the elevated $\delta^{15}N$ values of the Gulf of California[20]) or other appropriate measures for the context of their work.

3.2 Acknowledgements

Funding and support for K.R.B. and C.K. were provided by the University of California San Diego (UCSD).

Chapter 3, in part, has been submitted for publication of the material as it may appear in Marine Mammal Science, 2024, Bowen, KR; Kurle, Carolyn. The dissertation author was the primary investigator and author of this paper

Table 3.1. The mean $\delta^{13}C$ and $\delta^{15}N$ values (± SD, or SE where noted) for six major taxonomic groups are compiled from published literature. In the "Tissue" column, "LE" indicates the samples were lipid-extracted to remove fats which are depleted in their $\delta^{13}C$ values and create a source of bias. A note of "LE corr" indicates that the values reported by the original study were mathematically (and not experimentally) corrected for the presence of lipids. "LE/corr" means that the samples were a mixture of experimentally and mathematically corrected values. The "Year(s)" column reports the general timeframe in which the samples in the study were collected, although some samples do not have a known collection date or it was not reported ("NA"). "Meta" in the "Tissue" or "Year(s)" columns indicates that the measurements reported were part of a meta-analysis consolidating multiple studies. In the sample number column ("N"), two values separated by a comma indicates that the $\delta^{13}C$ and $\delta^{15}N$ measurements, respectively, had different sample sizes. In the "Metadata" column, we note location of sample collection, sex, size, life stage, or other relevant information provided in the study (M: males, F: females, U: unknown sex, SE: standard error).

Separate Supplementary File

Table 3.2. Summary of single $\delta^{13}C$ and $\delta^{15}N$ values (± SD) for each species, excluding samples from the Gulf of California due to elevated $\delta^{15}N$ values for animals collected in that region. In the event of paired samples (Table 3.1) from a study, the values for muscle tissue were used. Additionally, for studies that utilized bone collagen, we converted the values to resemble those from muscle. In the sample number column ("N"), if two values are present, the first indicates the $\delta^{13}C$ sample size and the second indicates the $\delta^{15}N$ sample size. See main text and Carlisle *et al*. (2015) for methodology.

Taxa	$\delta^{13}C$ (‰)	SD	$\delta^{15}N$ (‰)	SD	N
Cetacea (dolphins, porpoises, whales)					
Balaena mysticetus	-20.1	1.5	13.6	0.9	268
Balaenoptera acutorostrata	-18.5	0.8	11.7	1.4	25
Balaenoptera borealis	-19.6	1.6	8.3	1.3	10
Balaenoptera brydei	-16.9	0.6	10.0	1.2	11
Balaenoptera musculus	-16.9	0.0	13.3	0.1	222
Balaenoptera physalus	-18.4	0.8	12.5	1.0	15
Berardius bairdii	-17.8	0.6	16.3	0.8	19
Delphinapterus leucas	-18.4	0.6	16.7	0.6	49
Delphinus capensis	-16.7	0.5	18.4	0.4	39
Delphinus delphis	-17.8	0.3	11.4	0.6	33
Eschrichtius robustus	-16.2	1.1	13.1	1.3	113
Globicephala macrorhynchus	-16.9	0.5	12.2	0.7	18
Grampus griseus	-16.7	0.3	13.1	0.5	8
Megaptera novaeangliae	-17.8	0.8	12.7	1.2	1489, 1488
Orcinus orca	-15.9	1.4	17.2	1.4	123
Phocoena phocoena	-16.2	0.5	15.2	0.8	29
Phocoenoides dalli	-19.7	0.8	11.7	1.1	33
Physeter macrocephalus	-16.3	1.1	17.2	0.7	57
Pseudorca crassidens	-16.2	0.6	12.8	0.6	5
Stenella attenuata	-17.1	0.6	13.6	0.4	36
Stenella coeruleoalba	-17.3	0.6	12.3	0.6	140
Steno bredanensis	-16.9	0.5	12.3	0.6	6
Tursiops truncatus	-16.7	0.8	13.1	0.6	50
Pinnipedia (seals, sea lions, walrus)					
Callorhinus ursinus	-17.6	1.3	16.5	1.5	609, 607
Eumetopias jubatus	-16.2	1.7	17.6	1.2	129
Mirounga angustirostris	-16.0	1.0	18.2	1.1	24
Odobenus rosmarus	-16.9	0.6	12.8	0.8	184
Phoca vitulina	-15.8	1.4	17.7	1.5	106
Zalophus californianus	-15.4	0.5	17.6	1.1	78
Mustelidae (sea otters)					
Enhydra lutris	-13.4	1.5	13.4	1.8	247

Table 3.2. Continued. Summary of single $\delta^{13}C$ and $\delta^{15}N$ values (± SD) for each species, excluding samples from the Gulf of California due to elevated $\delta^{15}N$ values for animals collected in that region. In the event of paired samples (Table 3.1) from a study, the values for muscle tissue were used. Additionally, for studies that utilized bone collagen, we converted the values to resemble those from muscle. In the sample number column ("N"), if two values are present, the first indicates the $\delta^{13}C$ sample size and the second indicates the $\delta^{15}N$ sample size. See main text and Carlisle *et al*. (2015) for methodology.

Taxa	$\delta^{13}C$ (‰)	SD	$\delta^{15}N$ (‰)	SD	N
Osteichthyes (bony fishes)					
Ammodytes hexapterus	-17.5	1.2	11.6	0.6	34
Ammodytidae	-20.3	1.5	11.5	1.2	27
Anoplopoma fimbria	-18.9	1.1	13.7	0.4	24
Atheresthes stomas	-16.8	1.1	15.1	0.8	59
Clupea pallasii	-19.2	0.2	13.0	0.2	393
Engraulis mordax	-17.3	0.9	13.8	0.6	96
Gadus macrocephalus	-17.0	0.9	15.6	1.2	83
Genyonemus lineatus	-15.3	0.2	15.1	0.3	10
Hippoglossus stenolepis	-17.4	1.2	15.3	1.4	1224
Hypomesus pretiosus	-18.6	0.6	13.4	0.1	2
Lampris guttatus	-18.3	0.9	12.1	1.7	30
Mallotus villosus	-19.2	0.8	15.4	0.6	6
Merluccius productus	-17.6	0.4	13.5	0.6	67
Mola mola	-20.5	0.9	7.0	1.8	17
Oncorhynchus gorbuscha	-21.3	0.6	11.3	0.5	244
Oncorhynchus keta	-20.7	0.9	11.7	0.9	195
Oncorhynchus kisutch	-19.1	1.8	14.1	1.6	239
Oncorhynchus nerka	-20.5	1.1	12.1	1.3	313
Oncorhynchus tshawytscha	-18.8	2.2	14.2	1.6	477
Ophiodon elongatus	-17.6	0.9	14.5	2.1	525
Pleurogrammus monopterygius	-18.5	1.4	12.3	1.3	99
Sarda chiliensis	-17.7	0.3	16.2	0.2	12
Sardinops sagax	-18.4	1.3	13.1	0.6	91
Scomber japonicus	-18.1	0.4	14.3	0.3	23
Sebastes spp.	-17.5	0.5	13.0	1.5	172
Seriola lalandi	-17.2	0.6	15.9	0.6	34
Thunnus alalunga	-18.5	1.6	13.2	1.6	914
Thunnus albacares	-15.7	1.1	12.2	3.0	978
Thunnus obesus	-16.0	1.2	14.0	2.9	642
Thunnus orientalis	-18.1	0.5	13.4	1.6	155
Xiphias gladius	-17.2	1.0	14.6	1.8	34

Table 3.2. Continued. Summary of single $\delta^{13}C$ and $\delta^{15}N$ values (± SD) for each species, excluding samples from the Gulf of California due to elevated $\delta^{15}N$ values for animals collected in that region. In the event of paired samples (Table 3.1) from a study, the values for muscle tissue were used. Additionally, for studies that utilized bone collagen, we converted the values to resemble those from muscle. In the sample number column ("N"), if two values are present, the first indicates the $\delta^{13}C$ sample size and the second indicates the $\delta^{15}N$ sample size. See main text and Carlisle *et al*. (2015) for methodology.

Taxa	$\delta^{13}C$ (‰)	SD	$\delta^{15}N$ (‰)	SD	N
Chondrichthyes (cartilaginous fishes)					
Alopias superciliosus	-17.1	0.4	17.0	1.2	7
Carcharhinus falciformis	-17.1	0.4	15.5	1.0	19
Carcharhinus longimanus	-18.8	0.2	14.9	0.8	5
Carcharodon carcharias	-15.7	1.0	19.3	1.6	64
Isurus oxyrinchus	-18.2	0.2	16.4	0.8	10
Lamna ditropis	-18.0	0.7	13.6	1.3	20
Prionace glauca	-18.4	0.8	15.0	1.9	167
Somniosus pacificus	-20.6	0.7	14.0	1.0	160
Sphyrna lewini	-16.1	0.2	15.1	1.1	8
Squalus acanthias	-15.1	0.4	14.6	0.5	43
Cephalopoda (squids and octopus)					
Abraliopsis felis	-18.9	0.5	14.5	0.7	4
Abraliopsis spp.	-19.0	0.5	15.2	0.7	4
Berryteuthis magister	-18.7	1.0	12.5	1.3	427
Dosidicus gigas	-18.2	0.8	14.8	0.8	134
Enteroctopus dofleini	-16.9	0.9	11.4	2.4	32
Eucleoteuthis luminosa	-17.8	0.3	11.2	1.1	3
Gonatopsis borealis	-19.4	1.3	11.2	1.4	23
Gonatopsis spp.	-19.4	0.3	13.6	1.2	7
Gonatus berryi	-17.8	0.1	11.4	0.2	2
Gonatus madokai	-20.7	0.0	13.0	0.0	1
Gonatus onyx	-19.3	0.3	12.7	0.3	6
Loligo opalescens	-17.6	0.7	14.3	1.2	31
Ommastrephes bartramii	-18.4	0.7	11.8	1.3	44
Onychoteuthis borealijaponica	-20.1	0.4	13.2	0.6	14
Onychoteuthis spp.	-18.5	0.2	14.4	0.4	6
Onykia robusta	-18.8	0.6	16.7	0.8	10
Stenouteuthis oualaniensis	-17.6	1.1	10.3	2.3	30, 172

Table 3.3. Summary of single $\delta^{13}C$ and $\delta^{15}N$ values (± SD) for broad taxonomic groups in the North Pacific Ocean. Values represent primarily soft tissues, except for Mustelidae (sea otters) which are represented by whiskers and bone collagen. See main text and Carlisle *et al.* (2015) for methodology.

Taxa	**$\delta^{13}C$ (‰)**	**SD**	**$\delta^{15}N$ (‰)**	**SD**
Cetacea	-17.5	1.4	13.1	2.4
Pinnipedia	-16.3	1.4	16.7	2.2
Mustelidae	-13.5	1.5	13.5	1.8
Osteichthyes	-18.1	1.7	12.6	5.5
Chondrichthyes	-17.5	1.6	15.6	2.0
Cephalopoda	-18.7	1.2	13.1	2.1

3.3 References: Main text

1. Boecklen WJ, Yarnes CT, Cook BA, James AC. On the use of stable isotopes in trophic ecology. *Annu Rev Ecol Evol Syst*. 2011;42(1):411-440. doi:10.1146/annurev-ecolsys-102209-144726

2. DeNiro MJ, Epstein S. Influence of diet on the distribution of carbon isotopes in animals. *Geochimica et Cosmochimica Acta*. 1978;42(5):495-506. doi:10.1016/0016-7037(78)90199-0

3. Deniro MJ, Epstein S. Influence of diet on the distribution of nitrogen isotopes in animals. *Geochimica et Cosmochimica Acta*. 1981;45(3):341-351. doi:10.1016/0016-7037(81)90244-1

4. Hobson KA. Tracing origins and migration of wildlife using stable isotopes: a review. *Oecologia*. 1999;120(3):314-326. doi:10.1007/s004420050865

5. Kurle CM. Interpreting temporal variation in omnivore foraging ecology via stable isotope modelling. *Funct Ecol*. 2009;23(4):733-744. doi:10.1111/j.1365-2435.2009.01553.x

6. Kurle CM, Koch PL, Tershy BR, Croll DA. The effects of sex, tissue type, and dietary components on stable isotope discrimination factors ($\Delta^{13}C$ and $\Delta^{15}N$) in mammalian omnivores. *Isot Environ Health Stud.* 2014;50(3):307-321. doi:10.1080/10256016.2014.908872

7. Stephens RB, Shipley ON, Moll RJ. Meta-analysis and critical review of trophic discrimination factors ($\Delta^{13}C$ and $\Delta^{15}N$): Importance of tissue, trophic level and diet source. *Funct Ecol*. 2023;37(9):2535-2548. doi:10.1111/1365-2435.14403

8. Post DM. Using stable isotopes to estimate trophic position: models, methods, and assumptions. *Ecology*. 2002;83(3):703-718. doi:10.1890/0012-9658(2002)083[0703:USITET]2.0.CO;2

9. Aurioles-Gamboa D, Rodríguez-Pérez M, Sánchez-Velasco L, Lavín M. Habitat, trophic level, and residence of marine mammals in the Gulf of California assessed by stable isotope analysis. *Mar Ecol Prog Ser*. 2013;488:275-290. doi:10.3354/meps10369

10. Buchheister A, Latour RJ. Turnover and fractionation of carbon and nitrogen stable isotopes in tissues of a migratory coastal predator, summer flounder (*Paralichthys dentatus*). Trudel M, ed. *Can J Fish Aquat Sci*. 2010;67(3):445-461. doi:10.1139/F09-196

11. Riofrío-Lazo M, Aurioles-Gamboa D. Timing of isotopic integration in marine mammal skull: comparative study between calcified tissues. *Rapid Comm Mass Spectrometry*. 2013;27(9):1076-1082. doi:10.1002/rcm.6556

12. Misarti N, Finney B, Maschner H, Wooller MJ. Changes in northeast Pacific marine ecosystems over the last 4500 years: evidence from stable isotope analysis of bone collagen from archeological middens. *The Holocene*. 2009;19(8):1139-1151. doi:10.1177/0959683609345075

13. Arnoldi NS, Litvin SY, Madigan DJ, Micheli F, Carlisle A. Multi-taxa marine isoscapes provide insight into large-scale trophic dynamics in the North Pacific. *Prog Oceanogr*. 2023;213:103005. doi:10.1016/j.pocean.2023.103005

14. Carlisle AB, Goldman KJ, Litvin SY, Madigan DJ, Bigman JS, Swithenbank AM, Kline Jr TC, Block BA. Stable isotope analysis of vertebrae reveals ontogenetic changes in habitat in an endothermic pelagic shark. *Proc R Soc B*. 2015;282(1799):20141446. doi:10.1098/rspb.2014.1446

15. Kanaji Y, Yoshida H, Okazaki M. Spatiotemporal variations in habitat utilization patterns of four Delphinidae species in the western North Pacific, inferred from carbon and nitrogen stable isotope ratios. *Mar Biol*. 2017;164(4):65. doi:10.1007/s00227-017-3107-z

16. Endo T, Hisamichi Y, Kimura O, Haraguchi K, Lavery S, Dalebout ML, Funahashi N, Baker CS. Stable isotope ratios of carbon and nitrogen and mercury concentrations in 13 toothed whale species taken from the Western Pacific Ocean off Japan. *Environ Sci Technol*. 2010;44(7):2675-2681. doi:10.1021/es903534r

17. Altabet MA, Pilskaln C, Thunell R, Pride C, Sigman D, Chavez F, Francois R. The nitrogen isotope biogeochemistry of sinking particles from the margin of the Eastern North Pacific. *Deep-Sea Res I: Oceanogr Res Pap*. 1999;46(4):655-679. doi:10.1016/S0967-0637(98)00084-3

18. Kim SL, Tinker MT, Estes JA, Koch PL. Ontogenetic and among-individual variation in foraging strategies of northeast pacific white sharks based on stable isotope analysis. Hughes W, ed. *PLoS ONE*. 2012;7(9):e45068. doi:10.1371/journal.pone.0045068

19. Baxter JM, Walton A. A theoretical approach to the Suess effect. *Proc R Soc Lond A*. 1970;318(1533):213-230. doi:10.1098/rspa.1970.0141

20. Ruiz-Cooley RI, Engelhaupt DT, Ortega-Ortiz JG. Contrasting C and N isotope ratios from sperm whale skin and squid between the Gulf of Mexico and Gulf of California: effect of habitat. *Mar Biol*. 2012;159(1):151-164. doi:10.1007/s00227-011-1795-3

3.4 References: Table 3.1

Alter SE, Newsome SD, Palumbi SR. Pre-whaling genetic diversity and population ecology in Eastern Pacific Gray Whales: Insights from ancient DNA and stable isotopes. Knapp M, ed. *PLoS ONE*. 2012;7(5):e35039. doi:10.1371/journal.pone.0035039

Aurioles-Gamboa D, Rodríguez-Pérez M, Sánchez-Velasco L, Lavín M. Habitat, trophic level, and residence of marine mammals in the Gulf of California assessed by stable isotope analysis. *Mar Ecol Prog Ser*. 2013;488:275-290. doi:10.3354/meps10369

Becker B, Peery M, Beissinger S. Ocean climate and prey availability affect the trophic level and reproductive success of the marbled murrelet, an endangered seabird. *Mar Ecol Prog Ser*. 2007;329:267-279. doi:10.3354/meps329267

Bentzen R, Castellini JM, Gerlach R, Dykstra C, O'Hara T. Mercury concentrations in Alaska Pacific halibut muscle relative to stable isotopes of C and N and other biological variables. *Mar Pollut Bull*. 2016;113(1-2):110-116. doi:10.1016/j.marpolbul.2016.08.068

Bigman JS. *Trophic Ecology of the North Pacific Spiny Dogfish,* Squalus Suckleyi*, off Central California*. Master of Science. California State University Monterey Bay; 2013. https://scholarworks.calstate.edu/downloads/dn39x628v

Bodin N, Pethybridge H, Duffy LM, Lorrain A, Allain V, Logan JM, Ménard F, Graham B, Choy CA, Somes CJ, Olson RJ. Global data set for nitrogen and carbon stable isotopes of tunas. *Ecology*. 2020;102(3):e03265. doi:10.1002/ecy.3265

Bosley KL, Lavelle JW, Brodeur RD, Wakefield WW, Emmett RL, Baker ET, Rehmke KM. Biological and physical processes in and around Astoria submarine Canyon, Oregon, USA. *J Mar Syst*. 2004;50(1-2):21-37. doi:10.1016/j.jmarsys.2003.06.006

Brown B. *Geographic and Ontogenetic Variation in the Trophic Ecology of Lingcod (*Ophiodon Elongatus*) Along the U.S. West Coast*. Master of Science. San Jose State University; 2021. doi:10.31979/etd.5s93-muc8

Burton RK, Koch PL. Isotopic tracking of foraging and long-distance migration in northeastern Pacific pinnipeds. *Oecologia*. 1999;119(4):578-585. doi:10.1007/s004420050822

Busquets Vass GR. *Variability of stable isotopes of nitrogen and carbon in blue whale (*Balaenoptera musculus*) skin.* Master's Thesis. National Polytechnic Institute. Interdisciplinary Center for Marine Sciences.; 2008. https://www.repositoriodigital.ipn.mx/handle/123456789/13664

Busquets-Vass G, Newsome SD, Pardo MA, Calambokidis J, Aguíniga-García S, Páez-Rosas D, Gómez-Gutiérrez J, Enríquez-Paredes LM, Gendron D. Isotope-based inferences of the seasonal foraging and migratory strategies of blue whales in the eastern Pacific Ocean. *Mar Environ Res*. 2021;163:105201. doi:10.1016/j.marenvres.2020.105201

Carlisle AB, Kim SL, Semmens BX, Madigan DJ, Jorgensen SJ, Perle CR, Anderson SD, Chapple TK, Kanive PE, Block BA. Using stable isotope analysis to understand the migration and trophic ecology of northeastern pacific white sharks (*Carcharodon carcharias*). Romanuk TN, ed. *PLoS ONE*. 2012;7(2):e30492. doi:10.1371/journal.pone.0030492

Carlisle AB, Goldman KJ, Litvin SY, Madigan DJ, Bigman JS, Swithenbank AM, Kline Jr TC, Block BA. Stable isotope analysis of vertebrae reveals ontogenetic changes in habitat in an endothermic pelagic shark. *Proc R Soc B.* 2015;282(1799):20141446. doi:10.1098/rspb.2014.1446

Choy CA, Popp BN, Hannides CCS, Drazen JC. Trophic structure and food resources of epipelagic and mesopelagic fishes in the North Pacific Subtropical Gyre ecosystem inferred from nitrogen isotopic compositions. *Limnol Oceanogr*. 2015;60(4):1156-1171. doi:10.1002/lno.10085

Clark CT, Horstmann L, Misarti N. Lipid normalization and stable isotope discrimination in Pacific walrus tissues. *Sci Rep*. 2019;9(1):5843. doi:10.1038/s41598-019-42095-z

Courtney DL, Foy R. Pacific sleeper shark *Somniosus pacificus* trophic ecology in the eastern North Pacific Ocean inferred from nitrogen and carbon stable-isotope ratios and diet. *J Fish Biol*. 2012;80(5):1508-1545. doi:10.1111/j.1095-8649.2012.03261.x

Dehn LA, Follmann EH, Rosa C, Duffy LK, Thomas DL, Bratton GR, Taylor RJ, O'Hara TM. Stable isotope and trace element status of subsistence-hunted bowhead and beluga whales in Alaska and gray whales in Chukotka. *Mar Pollut Bull*. 2006;52(3):301-319. doi:10.1016/j.marpolbul.2005.09.001

Diaz-Gamboa RE. *Trophic relationships of teutophagous cetaceans with the Giant Squid* Dosidicus gigas *in the Gulf of California*. Doctorate in Marine Sciences. National Polytechnic Institute. Interdisciplinary Center for Marine Sciences.; 2009. http://repositoriodigital.ipn.mx/handle/123456789/14199

Doll AC, Taras BD, Stricker CA, Rea LD, O'Hara TM, Cyr AP, McDermott S, Loomis TM, Fadely BS, Wunder MB. Temporal records of diet diversity dynamics in individual adult female Steller sea lion (*Eumetopias jubatus*) vibrissae. *Oecologia*. 2018;188(1):263-275. doi:10.1007/s00442-018-4173-8

Endo T, Hisamichi Y, Kimura O, Haraguchi K, Lavery S, Dalebout ML, Funahashi N, Baker CS. Stable isotope ratios of carbon and nitrogen and mercury concentrations in 13 toothed whale species taken from the Western Pacific Ocean off Japan. *Environ Sci Technol*. 2010;44(7):2675-2681. doi:10.1021/es903534r

Endo T, Hotta Y, Hisamichi Y, Kimura O, Sato R, Haraguchi K, Funahashi N, Baker CS. Stable isotope ratios and mercury levels in red meat products from baleen whales sold in Japanese markets. *Ecotoxicol Environ Saf*. 2012;79:35-41. doi:10.1016/j.ecoenv.2012.01.020

Fauvelle M, Somerville AD. Surf and turf: A dataset of stable isotope values of plants and animals from southern California. *Data in Brief*. 2021;38:107380. doi:10.1016/j.dib.2021.107380

Filatova OA, Witteveen BH, Goncharov AA, Tiunov AV, Goncharova MI, Burdin AM, Hoyt E. The diets of humpback whales (*Megaptera novaeangliae*) on the shelf and oceanic feeding grounds in the western North Pacific inferred from stable isotope analysis. *Mar Mammal Sci*. 2013;29(3). doi:10.1111/j.1748-7692.2012.00617.x

Fujinami Y, Nakatsuka S, Ohshimo S. Feeding Habits of the Blue Shark (*Prionace glauca*) in the Northwestern Pacific Based on Stomach Contents and Stable Isotope Ratios. *Pac Sci*. 2018;72(1):21-39. doi:10.2984/72.1.2

Gorbatenko KM, Kiyashko SI, Lazhentsev AE, Emelin PO, Grishan RP. Bentho-pelagic relations in the deep-water part of the Okhotsk Sea by the data of stable isotopes C and N analysis. *Izv Tihookean naučno-issled rybohoz centra*. 2015;183(4):200-216. doi:10.26428/1606-9919-2015-183-200-216

Gendron D, Aguiniga S, Carriquiry J. δ^{15}N and δ^{13}C in skin biopsy samples: a note on their applicability for examining the relative trophic level in three rorqual species. *jcrm*. 2023;3(1):41-44. doi:10.47536/jcrm.v3i1.898

Gould P, Ostrom P, Walker W. Trophic relationships of albatrosses associated with squid and large-mesh drift-net fisheries in the North Pacific Ocean. *Can J Zool*. 1997;75(4):549-562. doi:10.1139/z97-068

Herman DP, Burrows DG, Wade PR, Durban JW, Matkin CO, LeDuc RG, Barrett-Lennard LG, Krahn MM. Feeding ecology of eastern North Pacific killer whales *Orcinus orca* from fatty acid, stable isotope, and organochlorine analyses of blubber biopsies. *Mar Ecol Prog Ser*. 2005;302:275-291. doi:10.3354/meps302275

Hirons AC, Schell DM, Finney BP. Temporal records of δ^{13}C and δ^{15}N in North Pacific pinnipeds: inferences regarding environmental change and diet. *Oecologia*. 2001;129(4):591-601. doi:10.1007/s004420100756

Hobson KA, Sease JL. Stable isotope analyses of tooth annuli reveal temporal dietary records: an example using Steller sea lions. *Mar Mammal Sci.* 1998;14(1):116-129. doi:10.1111/j.1748-7692.1998.tb00694.x

Hobson KA, Sease JL, Merrick RL, Piatt JF. Investigating trophic relationships of pinnipeds in Alaska and Washington using stable isotope ratios of nitrogen and carbon. *Mar Mammal Sci*. 1997;13(1):114-132. doi:10.1111/j.1748-7692.1997.tb00615.x

Hoekstra PF, Dehn LA, George JC, Solomon KR, Muir DC, O'Hara TM. Trophic ecology of bowhead whales (*Balaena mysticetus*) compared with that of other arctic marine biota as interpreted from carbon-, nitrogen-, and sulfur-isotope signatures. *Can J Zool*. 2002;80(2):223-231. doi:10.1139/z01-229

Horstmann-Dehn L, Follmann EH, Rosa C, Zelensky G, George C. Stable carbon and nitrogen isotope ratios in muscle and epidermis of arctic whales. *Mar Mammal Sci*. 2012;28(2). doi:10.1111/j.1748-7692.2011.00503.x

Hunsicker M, Essington T, Aydin K, Ishida B. Predatory role of the commander squid *Berryteuthis magister* in the eastern Bering Sea: insights from stable isotopes and food habits. *Mar Ecol Prog Ser*. 2010;415:91-108. doi:10.3354/meps08750

Jaime-Rivera M, Caraveo-Patiño J, Hoyos-Padilla M, Galván-Magaña F. Feeding and migration habits of white shark *Carcharodon carcharias* (Lamniformes: Lamnidae) from Isla Guadalupe inferred by analysis of stable isotopes δ^{15}N and δ^{13}C. *Rev Biol Trop*. 2014;62(2):637-647.

Jaume-Schinkel MS. *Food habits of the fin whale* Balaenoptera physalus *in the Gulf of California using stable isotopes of nitrogen and carbon*. Master's Thesis. National Polytechnic Institute. Interdisciplinary Center for Marine Sciences.; 2004. http://repositoriodigital.ipn.mx/handle/123456789/14439

Johnson SP, Schindler DE. Trophic ecology of Pacific salmon (*Oncorhynchus* spp.) in the ocean: a synthesis of stable isotope research. *Ecol Res*. 2009;24(4):855-863. doi:10.1007/s11284-008-0559-0

Kanaji Y, Yoshida H, Okazaki M. Spatiotemporal variations in habitat utilization patterns of four Delphinidae species in the western North Pacific, inferred from carbon and nitrogen stable isotope ratios. *Mar Biol*. 2017;164(4):65. doi:10.1007/s00227-017-3107-z

Kang HY, Lee YJ, Kim C, Kim D, Kim DH, Kim JH, Choi DL, Kang CK. Food web trophic structure at marine ranch sites off the east coast of Korea. *Front Mar Sci*. 2021;8:653281. doi:10.3389/fmars.2021.653281

Kim SL, Tinker MT, Estes JA, Koch PL. Ontogenetic and among-individual variation in foraging strategies of northeast pacific white sharks based on stable isotope analysis. Hughes W, ed. *PLoS ONE*. 2012;7(9):e45068. doi:10.1371/journal.pone.0045068

Kurle CM, Worthy GAJ. Stable isotope assessment of temporal and geographic differences in feeding ecology of northern fur seals (*Callorhinus ursinus*) and their prey. *Oecologia*. 2001;126(2):254-265. doi:10.1007/s004420000518

Kurle C, Worthy G. Stable nitrogen and carbon isotope ratios in multiple tissues of the northern fur seal *Callorhinus ursinus*: implications for dietary and migratory reconstructions. *Mar Ecol Prog Ser*. 2002;236:289-300. doi:10.3354/meps236289

Kurle CM, Sinclair EH, Edwards AE, Gudmundson CJ. Temporal and spatial variation in the δ^{15}N and δ^{13}C values of fish and squid from Alaskan waters. *Mar Biol*. 2011;158(11):2389-2404. doi:10.1007/s00227-011-1741-4

Li Y, Gong Y, Chen X, Dai X, Zhu J. Trophic ecology of sharks in the mid-east Pacific ocean inferred from stable isotopes. *J Ocean Univ China*. 2014;13(2):278-282. doi:10.1007/s11802-014-2071-1

Lian M, Castellini JM, Miller D, Griff B, Vertyankin VV, Dupont J, Broker K, Godard-Codding CA, O'Hara TM. Assessing δ^{13}C, δ^{15}N and total mercury measures in epidermal biopsies from gray whales. *Front Mar Sci*. 2020;7:133. doi:10.3389/fmars.2020.00133

Litz MN, Miller JA, Copeman LA, Teel DJ, Weitkamp LA, Daly EA, Claiborne AM. Ontogenetic shifts in the diets of juvenile Chinook Salmon: new insight from stable isotopes and fatty acids. *Environ Biol Fish*. 2017;100(4):337-360. doi:10.1007/s10641-016-0542-5

Liu AK. *Temporal Variability in the Stable Carbon and Nitrogen Isotope Values from Common Midtrophic Level Species in the Bering Sea*. Master's Thesis. UC San Diego; 2017. https://escholarship.org/uc/item/3x09n333

Madigan DJ, Carlisle AB, Dewar H, Snodgrass OE, Litvin SY, Micheli F, Block BA. Stable isotope analysis challenges wasp-waist food web assumptions in an upwelling pelagic ecosystem. *Sci Rep*. 2012;2(1):654. doi:10.1038/srep00654

Mandi DA. *Trophic Ecology of Northern Sea Otter (*Enhydra Lutris*) in Southcentral and Southwest Alaska Utilizing Stable Isotope Ratios*. Nova Southeastern University; 2002. https://nsuworks.nova.edu/hcas_etd_all/7

Miller T, Bosley K, Shibata J, Brodeur R, Omori K, Emmett R. Contribution of prey to Humboldt squid *Dosidicus gigas* in the northern California Current, revealed by stable isotope analyses. *Mar Ecol Prog Ser*. 2013;477:123-134. doi:10.3354/meps10133

Nakamura I, Sato K. Ontogenetic shift in foraging habit of ocean sunfish *Mola mola* from dietary and behavioral studies. *Mar Biol*. 2014;161(6):1263-1273. doi:10.1007/s00227-014-2416-8

Newsome SD, Tinker MT, Monson DH, Oftedal OT, Ralls K, Staedler MM, Fogel ML, Estes JA. Using stable isotopes to investigate individual diet specialization in California sea otters (*Enhydra lutris nereis*). *Ecology*. 2009a;90(4):961-974. doi:10.1890/07-1812.1

Newsome S, Etnier M, Monson D, Fogel M. Retrospective characterization of ontogenetic shifts in killer whale diets via δ^{13}C and δ^{15}N analysis of teeth. *Mar Ecol Prog Ser*. 2009b;374:229-242. doi:10.3354/meps07747

Ohizumi H, Miyazaki N. Differences in stable isotope ratios of Dall's porpoises (*Phocoenoides dalli*) between coastal and oceanic areas of the North Pacific. *Fish Oceanogr*. 2010;19(4):257-261. doi:10.1111/j.1365-2419.2010.00547.x

Orr AJ, Newsome SD, DeLong R. Variation in stable carbon and nitrogen isotope values from multiple tissues of California sea lions (*Zalophus californianus*). In: Damiani CC, Garcelon DK, eds. *Proceedings of 121 the 7th California Islands Symposium*. Institute for Wildlife Studies; 2009:121-129. https://sbbotanicgarden.org/wp-content/uploads/2022/08/Orr-et-al-2009-CA-sea-lion-isotopes.pdf

Parry M. Trophic variation with length in two ommastrephid squids, *Ommastrephes bartramii* and *Sthenoteuthis oualaniensis*. *Mar Biol*. 2008;153(3):249-256. doi:10.1007/s00227-007-0800-3

Ruiz-Cooley R, Gendron D, Aguíñiga S, Mesnick S, Carriquiry J. Trophic relationships between sperm whales and jumbo squid using stable isotopes of C and N. *Mar Ecol Prog Ser*. 2004;277:275-283. doi:10.3354/meps277275

Ruiz-Cooley RI, Markaida U, Gendron D, Aguíñiga S. Stable isotopes in jumbo squid (*Dosidicus gigas*) beaks to estimate its trophic position: comparison between stomach contents and stable isotopes. *J Mar Biol Ass*. 2006;86(2):437-445. doi:10.1017/S0025315406013324
Satterfield FR, Finney BP. Stable isotope analysis of Pacific salmon: insight into trophic status and oceanographic conditions over the last 30 years. *Prog Oceanogr*. 2002;53(2-4):231-246. doi:10.1016/S0079-6611(02)00032-0

Seymour J, Horstmann-Dehn L, Wooller MJ. Inter-annual variability in the proportional contribution of higher trophic levels to the diet of Pacific walruses. *Polar Biol*. 2014;37(5):597-609. doi:10.1007/s00300-014-1460-7

Sydeman WJ, Hobson KA, Pyle P, McLaren EB. Trophic relationships among seabirds in Central California: Combined stable isotope and conventional dietary approach. *The Condor*. 1997;99(2):327-336. doi:10.2307/1369938

Takai N, Onaka S, Ikeda Y, Yatsu A, Kidokoro H, Sakamoto W. Geographical variations in carbon and nitrogen stable isotope ratios in squid. *J Mar Biol Ass*. 2000;80(4):675-684. doi:10.1017/S0025315400002502

Tawa A, Ishihara T, Uematsu Y, Ono T, Ohshimo S. Evidence of westward transoceanic migration of Pacific bluefin tuna in the Sea of Japan based on stable isotope analysis. *Mar Biol*. 2017;164(4):94. doi:10.1007/s00227-017-3127-8

Todd SK, Holm B, Rosen DAS, Tollit DJ. Stable isotope signal homogeneity and differences between and within pinniped muscle and skin. *Mar Mammal Sci*. 2009;26(1):176-185. doi:10.1111/j.1748-7692.2009.00345.x

Toperoff A. *Examination of Diet of Harbor Porpoise (*Phocoena Phocoena*) from Central California Using Stomach Content and Stable Isotope Analysis from Multiple Tissues*. Master's Thesis. San Jose State University; 2002. https://scholarworks.calstate.edu/concern/theses/pc289p704

Waite JN, Trumble SJ, Burkanov VN, Andrews RD. Resource partitioning by sympatric Steller sea lions and northern fur seals as revealed by biochemical dietary analyses and satellite telemetry. *J Exp Mar Biol Ecol.* 2012;416-417:41-54. doi:10.1016/j.jembe.2012.02.009

Warlick A, Ylitalo G, O'Neill S, Hanson M, Emmons C, Ward E. Using Bayesian stable isotope mixing models and generalized additive models to resolve diet changes for fish-eating killer whales Orcinus orca. *Mar Ecol Prog Ser*. 2020;649:189-200. doi:10.3354/meps13452

Wild LA, Mueter F, Witteveen B, Straley JM. Exploring variability in the diet of depredating sperm whales in the Gulf of Alaska through stable isotope analysis. *R Soc open sci*. 2020;7(3):191110. doi:10.1098/rsos.191110

Witteveen BH, Wynne KM. Trophic niche partitioning and diet composition of sympatric fin (*Balaenoptera physalus*) and humpback whales (*Megaptera novaeangliae*) in the Gulf of Alaska revealed through stable isotope analysis. *Mar Mammal Sci*. 2016;32(4):1319-1339. doi:10.1111/mms.12333

Witteveen B, Worthy G, Roth J. Tracing migratory movements of breeding North Pacific humpback whales using stable isotope analysis. *Mar Ecol Prog Ser*. 2009a;393:173-183. doi:10.3354/meps08231

Witteveen B, Worthy G, Wynne K, Roth J. Population structure of North Pacific humpback whales on their feeding grounds revealed by stable carbon and nitrogen isotope ratios. *Mar Ecol Prog Ser*. 2009b;379:299-310. doi:10.3354/meps07900

Wolf N, Webster SR, Welker JM, Harris BP. Assessing the relationship between diet and size-at-age in Pacific halibut (*Hippoglossus stenolepis*) using $\delta^{13}C$ and $\delta^{15}N$ analysis. *Can J Fish Aquat Sci*. 2019;76(12):2326-2331. doi:10.1139/cjfas-2018-0380

Chapter 4 : Reconstructing historical ecology of North Pacific transient killer (*Orcinus orca rectipinnus*) whales using stable isotope analysis of dentin

4.1 Abstract

Populations of transient killer whales (*Orcinus orca rectipinnus*) along the west coast of North America occupy different habitats, as evidenced by transients in central California that rarely venture north (CA transients) and transients that range from Alaska through Oregon and occasionally California (AK transients). We aimed to characterize the long-term diet of killer whales from CA and AK and address a long-standing hypothesis (the 'sequential megafaunal collapse hypothesis'; SMCH) that predation by AK killer whales contributed to marine mammal declines in the North Pacific during the late 1900s.

We used stable isotope analysis of killer whale teeth from both CA and AK populations to reconstruct transient killer whale diets and understand their ecosystem impacts. We bisected 36 teeth and counted their annual growth layers to determine individual killer whale ages. We sampled dentin from every 3rd year to create a longitudinal dataset of the bulk (n = 270; δ^{13}C and δ^{15}N) and compound-specific (n = 11; δ^{15}N) stable isotope values from killer whales over approximately 120 years to address potential: 1) effects of sex, time, and age on killer whale diets, 2) trophic level changes in killer whales over time relative to the food web baseline, and 3) inter- and intra- specific patterns in their diets.

We found that both populations of killer whales had similar isotopic profiles overall and reflected values consistent with individual specialists. Our linear mixed models identified time as a significant predictor of AK killer whale δ^{15}N values, though support for the SMCH overall was mixed. There were significant ontogenetic changes in the δ^{15}N values of CA killer whales, but those effects varied with time. Our framework provides insight into the long-term ecology of two

transient killer whale populations and informs the study of historical reconstructions of animal diets.

4.2 Introduction

Assessing the trophic ecology of predators is necessary to understand community structure and species trajectories, which in turn informs ecosystem management and conservation policies[1–3]. Marine mammals, in many cases, govern food web dynamics via top-down control, meaning the direct and indirect consequences of foraging contribute to shaping the ecosystem[4–8].

Killer whales (*Orcinus orca rectipinnus*) are ubiquitous marine predators known to drive ecosystem structure through direct and cascade effects in multiple regions of the world[9,10]. A well-known instance of marine top-down control was illustrated in the Aleutian Islands, Alaska during the late 1990s[5]. Increased killer whale predation on sea otters (*Enhydra lutris*) reduced foraging pressure on sea urchins (*Strongylocentrotus polyacanthus*), whose populations grew and devastated kelp forests. Off the western coast of South Africa, killer whale activity reduced the presence of white sharks (*Carcharodon carcharias*), either through direct predation or emigration, which has led to increased occurrences of bronze whalers, a smaller and primarily coastal requiem shark[11]. Similarly, killer whale presence near Southeast Farallon Island, California is also thought to displace white sharks and consequently reduce predation on northern elephant seals (*Mirounga angustirostris*)[12]. Though still under study, killer whale presence also alters the behavior and movement of narwhals (*Monodon monoceros*) in the Arctic[13].

Killer whales inhabit all oceans and they are organized into distinct ecotypes that differ in morphology, genetics, acoustics, social structure, and diet[14–23]. In the North Pacific, mammal-

eating transient killer whales and fish-eating resident killer whales are sufficiently diverged to warrant subspecies designations, *Orcinus orca rectipinnus* and *Orcinus orca ater*, respectively[24]. There are several stocks of transient killer whales recognized in the United States, including the "Gulf of Alaska, Aleutian Islands, and Bering Sea Transient stock" and the "West Coast Transient stock", the latter of which ranges from Alaska through California[25]. However, studies have implied there is a separate California stock: McInnes *et al*.[26] found >83% of killer whales photo-identified in California could not be matched to animals in the Pacific Northwest, a finding supported by Dahlheim and White[27]. Fisheries and Oceans Canada also does not include California killer whales in their definition of the "West Coast Transient stock"[25]. Diet might differ between killer whales residing in Alaska or California; for example, Steller sea lions (*Eumetopias jubatus*) are estimated to comprise up to 20% of Gulf of Alaska transient diet[28], but are uncommon in California waters, and gray whales (*Eschrichtius robustus*) migrating from Alaska to Mexico are thought to be an important prey source for California transients[29,30], though transients in Alaska are known to depredate gray whale calves as well[31].

A contentious, long-standing hypothesis centers on the potential role of transient killer whales as keystone predators in Alaska, known as the sequential megafaunal collapse hypothesis[32] (SMCH). The SMCH was part of an extensive effort to explain an observed decline in pinnipeds and sea otters throughout the North Pacific and Bering Sea and suggests the following ideas: 1) great whales once composed a substantial portion of killer whale diet, 2) industrial whaling by humans peaked in the 1960s and significantly depleted stocks of great whales, 3) killer whales responded to depleted great whale stocks by switching sequentially to seals, sea lions, and otters beginning in the 1970s. Unlike other ecotypes of killer whales that may specialize on particular prey species to the exclusion of other, more available prey[33,34], there

is little evidence of widespread individual specialization on particular marine mammals[18] (*e.g.*, orcas targeting pinnipeds versus cetaceans) within transients observed hunting in British Columbia and Alaska. Thus, it might be expected that transients could readily alter their diet in response to marine mammal prey availability.

As studies began to investigate the causes of the pinniped and otter declines, debate arose regarding the extent to which the collapse was driven by climate regime shifts and resulting nutritional limitation (*i.e.*, bottom-up effects) or potential predation shifts (*i.e.*, top-down effects). Evidence against nutritional limitation, and possibly supporting the SMCH, included that Steller sea lion pups were heavier and experienced higher growth rates in rookeries that were declining compared to those that were increasing in abundance[35,36]. Physiologically, blood chemistry did not support nutritional stress in pups belonging to declining population stocks[37]. Oceanographic shifts were also purportedly not drivers for an overall decrease in prey availability, nor were human fishing activities[38]. However, a number of discrepancies regarding the SMCH were raised[39], including the role that great whales played in killer whale diet historically[40–42], the sequential nature of the declines[40], and incongruent timing between whaling and consequent ecosystem changes[41,43].

An outcome of the debates was that the SMCH was not directly testable without knowledge of killer whale diet before and after industrial whaling. Stable isotope analysis of archived, biologically inert animal tissues is one of few methodologies which enable reconstructions of historical animal diets. Teeth are readily accessible in natural history collections, and they are accretionary structures that preserve the biochemical chronologies of physiological and environmental conditions throughout the animal's life[44–47]. Studies have utilized teeth from pinnipeds and cetaceans to estimate the age of individuals through annual

growth layer groups (GLGs) and to estimate dietary patterns, including weaning age and adult diet composition, through stable isotope analysis[48–51].

Measuring the bulk stable carbon (δ^{13}C) and nitrogen (δ^{15}N) isotope values of GLGs in dentin allows for reconstructions of individual life-long foraging patterns and overall food web structure[45,49,50]. An animal's trophic position and prey preferences are primarily inferred by its δ^{15}N values, where δ^{15}N values increase ~2-5% with each trophic level[52]. Habitat use and movement can be determined with both δ^{13}C and δ^{15}N values, but δ^{13}C values are generally more useful than δ^{15}N values for this purpose. For example, δ^{13}C values are higher in nearshore and benthic habitats compared to offshore and pelagic habitats, and δ^{13}C values generally decline with increasing latitude[49].

The ability to compare inter- and intra-individual variability is another advantage of sampling the δ^{13}C and δ^{15}N values of multiple GLGs within teeth. Populations can vary along a spectrum of individual generalists (*i.e.*, individuals which exploit a diversity of prey sources and utilize the total isotopic niche of a species) to individual specialists[53–56] *(i.e.*, individuals which target a small fraction of the total isotopic niche). To further investigate dietary composition of individuals and the population as a whole, Bayesian stable isotope mixing models can be used to estimate the contributions of prey groups to diets[57] and better understand the targeted prey of specialists or the prey mixtures of generalists.

Two potential limitations to bulk stable isotope analysis are 1) coarse taxonomic resolution (*i.e.*, prey identification is limited to similar trophic groups rather than particular species), and 2) conflation of environmental and physiological effects[58,59] (*i.e.*, stable isotope values from bulk tissues can reflect a mix of the isotopic composition at the base of the food web and effects of consumer metabolism). A burgeoning technique to disentangle baseline effects

from consumer effects is compound-specific isotope analysis of amino acids (CSIA-AA). Amino acids can be classified into source amino acids, those whose isotope values remain relatively unchanged by the consumer's metabolism and thus reflect stable isotope values at the base of the food web, and trophic amino acids, those whose isotope values are altered by a consumer's metabolism and reflect the consumer's trophic level[60]. CSIA-AA allows for delineation between stable isotope values from source and trophic amino acids to more accurately differentiate true consumer dietary changes from changes that reflect variation in isotope values at the base of the food web[59].

In this study, we characterize the diet of transient killer whales collected in Alaska, Canada, or Washington (hereafter 'AK' transients) and California (hereafter 'CA' transients) via bulk (δ^{13}C and δ^{15}N) and CSIA-AA (δ^{15}N) analyses of GLGs in teeth. We analyzed GLGs from 36 individuals aged between 5 and 53 years old, spanning approximately 150 years (mid-1800s to 2022). For each population, we aimed to address: 1) What are the effects of sex, time, and age on killer whale diets, 2) How has trophic position changed over time for killer whales in context of the food web baseline, and 3) What are the inter- and intra-specific patterns in the diet (as measured by degree of individual specialization and broad diet composition estimates)? With those insights, we then consider the potential ecosystem impacts of killer whales.

Our framework also allows us to investigate the SMCH as it relates to AK transients. For aim (1), we would expect AK killer whale bulk isotopic signatures to reflect a higher baleen whale contribution to the diet before the collapse event in the 1970s compared to after, at which point we would expect AK killer whales to predominantly feed at a higher tropic level (*e.g.*, pinnipeds) and show a corresponding upward shift in bulk δ^{15}N values. For aim (2), the CSIA-AA data would support a true trophic shift in AK killer whales via increases in trophic amino

acid values, while source amino acids values would remain relatively constant if changes at the base of the food web were not driving bulk isotope value patterns. We would likely expect no significant ontogenetic shifts in diet nor sex-based diet differences under the SMCH. Although these ideas were not specifically addressed in the SMCH, AK transient killer whales were treated as a whole by the authors and previous evidence of prey sharing[61] suggests a similar diet among individuals of both sexes and various ages. For aim (3), if the SMCH is supported, we would hypothesize that AK transients would exhibit high intra-specific variation, indicating diverse diet compositions (within marine mammal taxa) and a high degree of individual generalization, facilitating prey switching behavior. The crux of the SMCH is the assertion that AK transient killer whales altered the trophic system of the North Pacific through predation of marine mammals. Our study retroactively contributes to decades of transient killer whale ecology as well as constructs a historical baseline by which to contextualize current and future trophic dynamics.

4.3 Materials and Methods

Specimen collection

We sampled the internal growth layer groups (GLGs; n = 270 total) from 36 North Pacific transient killer whale teeth from 10 museum and research collections (Table 4.1). Based on evidence that 86% of killer whales in Alaska also utilize coastal waters off Canada and Washington[27], we categorized 22 teeth as 'AK' transients if they were collected in these waters. Based on evidence that there is a separate population of transient killer whales in California that rarely travels to AK[25–27], we conservatively categorized 14 teeth as 'CA' transients. Approximate collection locations are shown in Figure 4.1. The collection dates of the specimens ranged from the mid-1800s to 2022. Of the 36 teeth, 18 were from males (n = 146 GLGs sampled), 8 were

from females (n = 65 GLGs sampled), and 10 were from individuals of an unknown sex (n = 59 GLGs sampled).

Ecotype classification via modeling

For 23 of the 36 teeth, the ecotype of the animal had been verified by photo-identification, stomach contents, or genetics (Table 4.1). The remaining 13 teeth were of 'unknown' ecotype according to the originating collection database.

The teeth discussed here were part of a larger study that involved known transient, resident, and offshore teeth (the three described North Pacific ecotypes[62]). We used the δ^{13}C and δ^{15}N values of known ecotypes in a multinomial regression analysis to predict the ecotype of unknown samples. Of the unknown samples, 13 were predicted to be transient and are included in this study (Table S4.1, Table S4.2). See the Supplemental Material for details on this analysis.

Specimen preparation

Most teeth were stored dry in the museums, although one (USNM: 594673) was stored in a 30% glycerin/20% alcohol solution to prevent potential desiccation and cracking of the tooth. Before we processed this tooth for analysis, we soaked it in ultra-pure water (MilliQ, Darmstadt, Germany) with daily water changes for three days[63]. Note that Lockyer *et al.*[64] recommended against storage in glycerin solution (5% glycerin, 35% alcohol) due to potential reduced readability of internal GLGs (see Age Estimation below). However, we found that the readability of internal GLGs for the tooth in this study was qualitatively comparable to those from the teeth that were stored dry.

Aging and sampling internal GLGs from animal teeth require cutting them in half longitudinally, which is most easily accomplished using large, straight teeth[65]. Thus, when possible, we sampled the largest, straightest teeth from the center of the jaw. However, in many cases the selection was limited by tooth quality, extraction logistics, or museum preferences. We sectioned whole teeth longitudinally with a 10-inch diamond blade on a Bosch® TC10 wet tile saw (Farmington Hills, MI, USA) outfitted with a custom mount and motorized pulley system to control angle and speed, respectively (see Bowen and Bowen in prep). We targeted a rate of 0.5 cm per minute[64] and the actual average rate was 0.48 cm per minute. Some teeth were already cut, so we sectioned 26 teeth for this study.

The goal when sectioning teeth is to expose the midline as evenly as possible so that all GLGs are visible and minimally distorted. Because some material is lost due to the grinding of the blade, we aligned the teeth slightly off-center so our resulting cut would most closely reflect its true center. We selected the most robust tooth halves for dentin analysis because they best captured the midline of the tooth on the cut face. We manually polished the cut face of each tooth with individual wet sandpaper discs, first 400, then 600, grit to remove sawblade marks and prepare the tooth for reading and targeting individual GLGs for dentin analysis[64]. In the event of a misaligned cut, we ground the tooth down to the midline point using a belt sander (80 grit), then manually polished the face of the tooth using successive increments of increasing grit until we reached the final polish with 600 grit sandpaper discs.

GLGs are defined by alternating regions of more dense and less dense dentin[66]. To enhance the visibility of the GLGs, we immersed each bisected and polished tooth half in 10% formic acid to a depth of 0.5-1.0 cm[67] for 12 hours[48] in separate glass dishes. This process differentially decalcifies the face of the tooth based on density, resulting in a distinct series of

grooves and ridges. We then rinsed the tooth halves in running tap water for approximately 1 hour, soaked them overnight in ultra-pure water[68] and slowly dried them over the span of 3 days to prevent cracking. To achieve this, we first wrapped the teeth individually in damp paper towels and placed each in a separate, sealed glass dish for one day. On the second day, we unclasped the lids but left them atop the dish and loosened the paper towels. On the third day, we removed the lids first, then the paper towels several hours later, to allow the teeth to completely air-dry. When teeth were dry, we gently rubbed over the etched surface of the tooth with a soft graphite pencil (6B) to highlight the ridges that aid in distinguishing GLGs.

Age estimation

We followed a similar protocol as the Fisheries and Oceans Canada Quebec Region laboratory[64] and created and processed high-resolution (800-1200 dpi) scans of all tooth halves using GIMP[69] (GNU Image Manipulation Program version 2.10.6) to mark individual GLGs and determine the age of the tooth (Figure 4.2). We sharpened the images using the "High Pass" and "Sharpen" tools to enhance overall clarity. We made all image adjustments and annotations on independent 'layers' such that the original image was preserved.

Numerous approaches have been used to age layered tissues: a single reader to reduce inconsistencies[68,70], multiple readers to reduce personal biases[20,71], requiring consensus among readers if using multiple readers, using the median or mode among or within readers to determine age (reviews in [64,66,72]), or use of Bayesian statistical modeling[73]. For our study, we aged all teeth blind (*i.e.,* no reference to ecotype, sex, body size, etc.) using one reader (K.B.). We noted multiple readings within a session, and three sessions took place at intervals of at least 14 days (each aging session was annotated via a separate layer on the image in GIMP that could

be toggled between visible and hidden). Our study relied on sampling individual GLGs throughout the life of the animal, so it was more important to resolve each GLG boundary rather than identify an overall age. We reached a consensus image with delineated GLGs by holistically evaluating all three sessions (*i.e.*, GIMP image layers) together to address inconsistencies, and we referred to the physical tooth under a microscope for clarification as needed[64]. Although understanding killer whale aging via teeth is an ongoing effort, see Bowen and Kurle in prep for a discussion on particulars relating to aging KW teeth. Bowen and Kurle in prep also identifies other previous age estimates and related commentary for the same teeth used in this study.

Dentin sampling

We collected dentin from individual GLGs of teeth via a computer-controlled micromill (MicroMill2, Elemental Scientific Lasers, Omaha, NE, USA) at the NOAA Southwest Fisheries Science Center (La Jolla, CA). We first mounted and secured teeth onto the micromill stage using putty, and then we equipped the drill with a carbide bit ranging from 300 µm – 1200 µm (Brasseler USA Dental Instruments, Savannah, GA, USA), depending on the width of the target GLG. We used computer software that interfaces with the micromill to program a user-specified drill path along the targeted GLG. The software also probed the height of the tooth along the drill path to ensure a consistent sampling depth. For all teeth, we discarded the first two drill passes on the top layer of dentin (~25 µm depth) with compressed air to reduce presence of surface contaminants, formic acid, and graphite (although we show in Bowen and Kurle in review that removing the external layer did not significantly impact bulk isotope values, lessening concern of possible contamination. This may be useful if one is collecting material from teeth with very shallow or small GLGs with less available dentin).

To extract ~1-2 mg of dentin for bulk stable isotope analysis, the drill path was ~8-10 mm in length. The curved shape of killer whale teeth means that some GLGs are underneath the layer we are targeting; to avoid accidentally sampling these additional GLGs, we restricted our drilling depth to 200-350 µm[48,63,74]. Newsome *et al.*[48] demonstrated that the weaning process likely occurs during the 3rd year of life and is complete by age 4. Accordingly, age 4 was the first sampled GLG we incorporated into our analyses to reflect isotope values incorporated into tooth dentin during prey foraging. Subsequently, we sampled teeth aged 10 or younger every other year (*e.g.*, GLG 4, 6, 8, 10) and teeth aged older than 10 years every 3 years in general (*e.g.*, 4, 7, 10, 13, etc).

To capture more fine-scale interpretations of potential variations in killer whale foraging patterns through time, we aimed to sample a GLG from at least one individual from each decade when possible (n = 11 total; n = 6 for AK transients and n = 5 for CA transients; Table 4.2) and analyzed them for CSIA-AA. To select candidate teeth for CSIA-AA, we prioritized those that were known-age to reduce temporal error associated with aging, though in some cases the chosen tooth was aged for this study without age verification. Then, to reduce the influence of confounding environmental variables, we targeted GLGs that were incorporated into the tooth of each animal during years of neutral oceanographic conditions in the Pacific Ocean (*i.e.*, neither El Niño nor La Niña years). Lastly, we selected GLGs closest to the end-of-life when possible to reduce potential aging error because we are certain that the final GLG of life corresponds to the known collection year. We also controlled for potential differences in the diets of juvenile vs. adult killer whales by avoiding GLGs that reflected data incorporated when the animal was younger than 10 years old.

For CSIA-AA, we collected ~35 – 45 mg of dentin from a drill path ~30 mm in length and ~1,100 - 1,400 µm in total depth using either a 500 µm or 800 µm bit. As noted above, killer whale teeth are curved, meaning that is it possible to drill into GLGs below the target. We made our drill paths as long and shallow as possible to minimize depth and the possibility of reaching a non-target GLG while still acquiring the minimum amount of dentin required for CSIA-AA, which is much greater than that required for bulk analyses. We also again discarded the top layer with compressed air to reduce surface contaminants.

Per recommendation in Brault *et al*.[75] for CSIA-AA, ~35 – 45 mg of dentin was demineralized in 0.5N hydrochloric acid for ~1 hour at room temperature and ~23 hours at 4°C in a refrigerator. We then centrifuged the samples at 12,000 rpm for five minutes, removed the HCl with a pipette, and rinsed the sample five times with ultra-pure water including centrifugation after each rinse. Lastly, the samples were aspirated via pipette once more and lyophilized for 48 hours. The yield of approximately 1 - 1.3 mg of demineralized dentin was packaged in glass vials to be analyzed.

-Stable isotope analyses

Approximately 1.2 mg of untreated dentin for each sampled GLG was packaged into 5x9 mm tin capsules for bulk $\delta^{13}C$ and $\delta^{15}N$ analysis. Previous studies have shown demineralization and lipid-extraction are not necessary for bulk analyses of marine mammal dentin[75,76], so we did not pre-treat dentin for bulk isotope analyses (but see below).

Our samples were analyzed in four laboratories: the University of California Santa Cruz - Stable Isotope Laboratory using a CE Instruments NC2500 elemental analyzer coupled to a Thermo Scientific DELTAplus XP isotope ratio mass spectrometer via a Thermo-Scientific

ConFlo III, the University of New Mexico Center for Stable Isotopes using a Costech 4010 elemental analyzer coupled to a Thermo Scientific Delta V mass spectrometer via a Thermo-Scientific ConFlo IV, the University of California Davis - Stable Isotope Facility using a PDZ Europa ANCA-GSL elemental analyzer coupled to a PDZ Europa 20-20 isotope ratio mass spectrometer, and the University of Florida Light Stable Isotope Mass Spec Lab using a Carlo Erba elemental analyzer coupled to a Thermo Delta V Advantage isotope ratio mass spectrometer via a Thermo-Scientific ConFlo II. Stable isotope values are expressed in δ-notation as parts per thousand (‰) following the equation:

$$\delta X = [(R_{sample} \div R_{standard}) - 1] \times 1000,$$

where X is either ^{13}C or ^{15}N and R is the ratio of ^{13}C:^{12}C or ^{15}N:^{14}N for the sample or international standard. The international standards were Vienna Peedee Belemnite (VPDB) for $\delta^{13}C$ and atmospheric nitrogen for $\delta^{15}N$. The mean standard deviations (SD) from all reference materials across all labs were ≤0.2‰ for $\delta^{13}C$ values and ≤0.3‰ for $\delta^{15}N$ values.

A small subset of specimens (n = 5; Table 4.1) used in this study were also part of a separate effort to examine intra-tooth variation in age determination and stable isotope values (see Bowen and Kurle in review). We found no significant differences between the $\delta^{13}C$ or $\delta^{15}N$ values of replicate teeth, so stable isotope values were averaged for the same GLGs across teeth (*e.g.*, GLG 4 reported here is an average of the stable isotope measurements for GLG 4 in replicate tooth 1 and replicate tooth 2). Averaged GLG stable isotope values are reported for two replicate teeth from specimens USNM: 594668, USNM: 594671, and USNM: 59466. Three replicate teeth were averaged for specimen USNM: 610855.

The CSIA-AA for $\delta^{15}N$ values was performed by the University of California Davis - Stable Isotope Facility (see [77,78]). Proteins in killer whale dentinal collagen were first hydrolyzed

in acid to free the amino acids (6 M HCl, 70 min, 150°C under N_2 headspace). N-acetyl amino acid methyl ester derivatives were then injected at 260°C (splitless, 1 min) and separated in a DB-35 (Agilent Technologies) column (60 m x 0.32 mm inner diameter, 1.5 µm film thickness; constant flow 2 mL/min). The temperature protocol was as follows: 70°C (hold 2 min); 140°C (15°C/min, hold 4 min); 240°C (12°C/min, hold 5 min); and 255°C (8 °C/min, hold 35 min).

Gas chromatography/combustion/isotope ratio mass spectrometry was then performed using a Thermo Trace GC 1310 gas chromatograph coupled to a Thermo Scientific Delta V Advantage isotope-ratio mass spectrometer via a GC IsoLink II combustion interface with a NiO/CuO/NiO reactor at 1000°C. Water was removed using a Nafion dryer before isotope ratio mass spectrometry, and CO_2 was removed post-combustion using a liquid N_2 trap.

The primary isotopic reference material for the $\delta^{15}N$ measurements was air, and secondary references included the following: IAEA-600, USGS-40, USGS-41, USGS-42, USGS-43, USGS-61, USGS-64, and USGS-65. Amino acid $\delta^{15}N$ measurements were calibrated and scale-normalized using these reference materials. Samples were measured in duplicate (we report the mean CSIA-AA $\delta^{15}N$ values of the duplicate measurements), and the expected measurement error was ≤1.0‰. For our analysis, the mean SD of sample replicates was ≤0.5‰, and the mean SD for the reference material replicates was ≤0.6‰. The mean absolute accuracy for calibrated references materials was also ≤0.6‰.

-Corrections to the $\delta^{13}C$ *values for Suess Effect and lipids*

We made corrections to the bulk $\delta^{13}C$ values of killer whale dentin in our study to account for the Suess effect (and the Laws effect simultaneously) and, where appropriate, an influence of lipids.

The Suess effect refers to a decrease in global atmospheric $\delta^{13}C$ concentration (and thus a decreased ^{13}C:^{12}C ratio or $\delta^{13}C$ values) from the onset of the industrial revolution and the increased release of $\delta^{13}C$ -depleted CO_2 from burning fossil fuels[79]. Numerous methods have been applied to correct for the Suess effect, but Clark *et al.*[80] have developed an approach which 1) applies an updated and more accurate correction, given the tendency for commonly used methods to overcorrect, 2) establishes a framework for region-specific corrections as appropriate for marine environments, and 3) also accounts for the Laws effect, which is a change in phytoplankton fractionation from changing aqueous CO_2 concentrations. Clark *et al.*[80] also built an R package, SuessR[81], which utilizes sample $\delta^{13}C$ values, collection year, and collection region as input to generate Suess and Laws corrections as output. Currently, SuessR is only configured for four regions: the Bering Sea, the Aleutian Islands, the Gulf of Alaska, and the Subpolar North Atlantic.

We used the SuessR package with R version 4.2.1[82] to correct the $\delta^{13}C$ values of killer whale dentin for the Suess and Laws effects. We standardized $\delta^{13}C$ values to the default preindustrial year of 1850. Of our specimens, 13 were collected in the Bering Sea, Aleutian Islands, or Gulf of Alaska and were assigned accordingly for SuessR. The remaining 29 specimens were collected in Canada, Washington, and California. Despite these locations falling outside of SuessR regions, we still chose to utilize SuessR for the correction to remain consistent across samples. The net corrections for the three configured North Pacific locations showed a difference of less than 0.01% in Clark *et al.*[80], supporting our assumption that nearby Canada, Washington, and California waters are likely operating under sufficiently similar ecological conditions. We assigned the 29 specimens to the Gulf of Alaska for SuessR purposes, being the geographically closest option.

Lastly, lipids are depleted in ^{13}C and bias $\delta^{13}C$ values, so are frequently removed from study tissues before stable carbon isotope analysis. Previous studies indicate that lipids are not present in sufficient quantities within dentin from cetacean teeth[75,76]. However, a portion of our samples (137/270 measurements) exhibited C:N ratios greater than 3.5 ($\bar{x}$ of samples with C:N > 3.5 was 3.67 ± 0.13), which indicates potentially concerning lipid levels[83] and suggests that lipid contamination of dentin may vary by species or other specimen characteristics. We thus applied a small correction factor to the $\delta^{13}C$ values[84] from our affected samples following Pereira *et al*.[85], as they had similar results to ours for teeth from bottlenose dolphins (*Tursiops truncatus*).

Statistical analyses

All statistical analyses were conducted in R version 4.2.1[82] via RStudio[86].

- <u>The effects of sex, time, and age on diet</u>

To examine whether sex, time, and age were significant predictors of the bulk $\delta^{13}C$ and $\delta^{15}N$ values of killer whale dentin GLGs, we used separate linear mixed models (LMMs) followed by Type III Analysis of Variance tests (ANOVAs) with Satterthwaite's method for each isotope. Sex was a categorical variable where the animal was assigned ‘male’, ‘female’, or ‘NA’ if unknown. We also chose to treat time as a categorical variable, either ‘before’ the year 1970 or ‘after’ (and inclusive of, hereafter) 1970, to test the SMCH hypothesis. Springer *et al*.[32] suggest that industrial whaling activity substantially slowed in the early 1970s because whale stocks had been depleted, and pinniped populations began to decline from the 1960s and 1970s on. We therefore assumed that 1970 was a reasonable demarcation for the purported killer whale dietary changes. Broadly categorizing time also reduces potential error associated with aging via GLGs.

Although our treatment of time was motivated by the SMCH and AK transients, we also applied it to CA transients because 1) there is evidence that a regime shift in the 1970s impacted the North Pacific[87], and 2) temporal dietary changes would be comparable between the two populations. Age was treated as a continuous variable. Sex, time, and age were all fixed variables, whereas specimen ID was incorporated as a random effect variable to account for multiple samples (*i.e.*, GLGs) from the same individuals. We used the lmerTest package[88] in R to construct and evaluate our models. For all models, we visually assessed assumptions via diagnostic plots: residuals vs fitted (linearity), normal Q-Q (normality), scale-location (homoscedasticity), and residuals vs leverage (influential points). We found three potentially influential data points with consistently high Cook's distance scores, which we removed from further analysis.

To further investigate transient killer whale diet, we used the R package SIBER (Stable Isotope Bayesian Ellipses in R[89,90]) to quantify isotopic niche space and overlap between AK and CA transients and between 'before' and 'after' time periods for AK transients. SIBER utilizes isotopic values (mean δ^{13}C and δ^{15}N values per individual here) in a Bayesian framework to estimate standard ellipses (SEA), a measure of variance for multivariate data, which define isotopic niche space[89]. An advantage of standard ellipses is that they can be corrected for sample sizes (SEAc). Overlap between ellipses can be calculated by drawing from the posterior distributions of the ellipses. We report SEAc to represent isotopic niche space, and we report ellipse overlap as a mean from the distribution of 10,000 posterior draws of the fitted ellipses[91].

<u>- Trophic position calculations from CSIA-AA δ^{15}N data</u>

Three amino acids are considered 'source' amino acids because they fractionate very little with increasing trophic level and thus reflect changes in the $\delta^{15}N$ values at the base of the food web[59]: phenylalanine (Phe), lysine (Lys), and methionine (Met). In contrast, seven 'trophic' amino acids are influenced by the consumer's metabolism[59]: Aspartic acid + asparagine (Asx), isoleucine (Ile), alanine (Ala), glutamic acid + glutamine (Glx), leucine (Leu), proline (Pro), and valine (Val). The $\delta^{15}N$ values for these amino acids are reported in Table S4.3 and Figure S4.1, except for Ile because those measurements fell below the limit of quantification

We calculated trophic positions (TP) for the subset of killer whale specimens that were analyzed for CSIA-AA using the equation:

$$TP = 1 + [(\delta^{15}N_{Pro} - \delta^{15}N_{Phe} - \beta_{Pro/Phe})/TDF_{Pro\text{-}Phe}]$$

We use Pro rather than the traditional Glx[59] for TP calculations, as Pro is thought to provide more realistic estimations for marine mammals[73,92]. In the equation, the $\delta^{15}N_{Pro}$ and $\delta^{15}N_{Phe}$ values are our measurements from killer whale dentin, $\beta_{Pro/Phe}$ is a constant equal to 3.1‰ that represents the difference between the $\delta^{15}N_{Pro}$ and $\delta^{15}N_{Phe}$ values of the primary producer in the ecosystem[93] (*e.g.*, marine phytoplankton), and $TDF_{Pro\text{-}Phe}$ ('trophic discrimination factor') is a constant equal to 4.5‰ that represents the difference in TDF[92] (*i.e.*, the $\delta^{15}N$ offset between consumer and prey) for Pro minus that for Phe). Finally, we used linear regression models to examine relationships between bulk and CSIA-AA $\delta^{15}N$ values, TP, and time.

- Inter- and intra-specific patterns in the diet

We also aimed to examine dietary differences within and among individuals for both the CA and AK transient killer whale populations. First, we used the '*varcomp*' (variance component) function of the predictmeans package[94] in R to calculate the variance attributable to

specimen ID (*i.e.*, among individual differences) and the residual term (*i.e.*, within individual differences) given the linear mixed model[55,95]. Since δ^{15}N values are more reflective of diet than δ^{13}C values, we assessed the δ^{15}N models only for AK and CA transients separately. If most of the variation falls within individuals, the population is considered to be composed of generalists feeding on a diversity of prey. If variation is mostly driven by differences among individuals, the population is likely composed of specialists. Given transients are specialists in the sense that they primarily consume marine mammals, our analysis investigates whether individual transients may show preferences for particular marine mammal groups (*e.g.*, baleen whales versus pinnipeds).

To complement our variance component analysis, we also calculated a specialization index (*S*) for the δ^{15}N values of each individual[95–97]. The total niche width (TNW) is a metric derived from the sum of variation within (WIC) and between (BIC) individuals[54]. The degree of individual specialization can be expressed as WIC/TNW, where a value closer to 0 indicates that a population is comprised of individual specialists (*i.e.*, individuals that utilize a small fraction of the species' overall dietary resources) and a value closer to 1 indicates individual generalists (*i.e.*, individuals that capitalize on a diversity of dietary resources). We defined WIC as the SD of isotope measurements of GLGs within an individual/tooth, and BIC as the SD among the mean isotope measurements of all teeth. Following Hückstädt *et al.*[96], we defined an individual with an *S* of less than 0.2 as an extreme specialist, meaning the individual is utilizing less than 20% of the species' available prey resources. Similarly, an *S* of greater than 0.5 (50%) was considered a generalist.

Lastly, we used the Bayesian stable isotope mixing model (MixSIAR) package[57,98,99] in R to estimate the contributions of marine mammal prey groups (sources) to transient killer whale diet (consumers) using stable isotope values. In an effort to constrain this analysis to the context

of the SMCH, we simplified the prey groups to only mysticetes and pinnipeds (Table S4.4; see Bowen and Kurle in review for details). Our analysis is not meant to comprehensively describe transient killer whale diet, but rather attempt to elucidate 1) whether the contribution of mysticetes or pinnipeds in particular have changed over time for AK transients, and 2) differences in relative contributions of these prey groups to CA or AK transient diet. We used trophic discrimination factors that have been identified for bone protein in cetaceans[100] as a reasonable approximation for killer whale dentin: 3.11 ‰ ± 0.27 for $\delta^{13}C$ values, and 2.03 ‰ ± 0.71 for $\delta^{15}N$ values. We ran the mixing model with no informative priors using specimen ID as a random factor and location (AK or CA) as a fixed factor under the "long" run setting (three chains; chain length of 300,000; burn-in of 200,000; thinning interval of 100). We used the Gelman-Rubric diagnostic to assess convergence, where all values were less than 1.05[101].

4.4 Results

We measured the bulk $\delta^{13}C$ and $\delta^{15}N$ values, and the CSIA-AA of $\delta^{15}N$ values, from multiple GLGs within dentin from transient killer whales collected in the North Pacific to characterize dietary patterns (Table 4.3). Overall, we sampled 36 teeth from animals with a maximum estimated age of 53 years old. Between two and 14 GLGs were sampled for each individual, totaling 270 samples used for our analyses. The average age for male animals (n = 18) was 26 years old (range 7 to 45). The average age for female animals (n = 8) was 30 years old (range 14 to 53). The average age for the animals of undetermined sex (n = 10) was 21 years old (range 5 to 43). We categorized 14 teeth with 108 sampled GLGs as CA transients and 22 teeth with 162 sampled GLGs as AK transients. Within the AK transients, there were 38 GLGs representing the 'before' time period (before 1970), and 124 GLGs representing the 'after' time period (inclusive of and after 1970). Summary statistics are reported in Table 4.4. Overall, there

were no significant differences between the mean $\delta^{13}C$ ($t(34) = 0.12$, $p = 0.90$)) or $\delta^{15}N$ ($t(34) = 0.21$, $p = 0.84$)) values of CA and AK transient killer whales.

Effect of sex, time, and age on diet

For the $\delta^{15}N$ values of both AK and CA populations, and the $\delta^{13}C$ values for the AK transients, sex was not a significant predictor in the full LMMs for the 26 animals of known sex (Table S4.5, Table S4.6). For the $\delta^{13}C$ values of the CA transients, although sex was not significant as a main effect, there were significant two-way and three-way interactions (Table S4.5, Table S4.6). The $\delta^{13}C$ values tend to increase with age for males, but decrease with age for females (Figure S4.2). In contrast, the median $\delta^{13}C$ values increased for both males and females from pre- to post-1970 (Figure S4.3), but the variation in males especially decreased substantially. For subsequent analyses to assess the effects of time and age, we dropped sex as a variable in the model because we had 10 individuals (n = 59 GLGs) for which sex was undetermined. By removing sex as a variable, we could include the additional 10 individuals and increase sample size.

We found the only significant predictor for the $\delta^{15}N$ values of AK transient killer whales was the main effect of time (Table 4.5). The mean of the $\delta^{15}N$ values of all GLGs (Table 4.4) in the 'before' category ($\bar{x} = 19.0 +/ 1.3$) is nearly equal to that of the 'after' category ($\bar{x} = 19.3 +/ 1.7$). However, mean values mask variations among individuals (ranges in Table 4.4; see next section). To address this, we calculated the average slope for each individual in Figure 4.3 (*i.e.*, the average ontogenetic change in the $\delta^{15}N$ value for each individual, irrespective of absolute values). If an animal lived through 1970, we calculated the average slope before 1970 and the average slope after 1970 separately. The overall average slope for animals living before 1970

was 0.02‰ per year of the animal's life, compared to -0.03‰ for after 1970. For CA transients, time was not a significant predictor of their δ^{15}N values, but both age and the interaction age:time were significant predictors (Table 4.5). The δ^{15}N values increased with age overall, though the ontogenetic increase was greater before 1970 than after (Figure 4.4).

For AK transients, again the main effect of time was the only significant predictor of their δ^{13}C values (Table 4.4) and we calculated the slopes of individuals to investigate that effect. The average individual living after 1970 experienced a 3x increase in their δ^{13}C values (0.03% per year) than the average individual living before 1970 (0.01%; Figure 4.5). Neither time nor age were significant predictors of the δ^{13}C values for CA transients (Table 4.4).

We also generated SIBER ellipses to compare isotopic niche space between AK and CA transients, as well as within the 'before' and 'after' time frames for AK transients (Figure 4.6). The standard ellipse area for AK transients (SEAc = 3.99%) was nearly twice the size of the CA transients (SEAc = 2.06%), where the additional area was due to a wider range of the δ^{13}C values. There was a substantial overlap area (1.81%), with the CA ellipse falling almost entirely within the AK ellipse. The ellipse differences within AK transients 'before' and 'after' the marine mammal declines were driven by their δ^{15}N values. The overall standard ellipse area for AK transients 'before' the collapse event (SEAc = 4.38%) was slightly larger than 'after' (SEAc = 3.60%), with an overlap area of 1.76%.

Trophic position calculations from CSIA-AA δ^{15}N data

The TPs for six AK and five CA transients ranged from 3.6 to 4.3 (mean of 3.9±0.3) and 3.2 to 3.9 (mean of 3.5±0.3), respectively. For both AK and CA transients, there was a downward trend in TP over time (Figure 4.7), although there was no significant linear

relationship for either AK transients (R^2 = 0.21, $F_{(1,4)}$ = 1.1, p = 0.36) or CA transients (R^2 = 0.48, $F_{(1,3)}$ = 2.74, p = 0.20).

The range of the source amino acid ($\delta^{15}N_{Phe}$) values was 3.7‰ (min = 13.1‰, max = 16.8‰) and 4.3‰ (min = 13.2‰, max = 17.5‰) for AK and CA transients, respectively. Linear regression fits (Figure 4.8) again showed no significant relationships between the $\delta^{15}N_{Phe}$ values and time for both AK transients (R_2 = 0.50, $F_{(1,4)}$ = 4.1, p = 0.11) and CA transients (R^2 = 0.02, $F_{(1,3)}$ = 0.0061, p = 0.94), however there was an increasing trend for AK transients.

We also examined linear correlations between the $\delta^{15}N_{Phe}$ (the source AA) and $\delta^{15}N_{bulk}$ values, as well as the $\delta^{15}N_{Pro}$ (the trophic AA) and $\delta^{15}N_{bulk}$ values (Figure 4.9). The relationships between the $\delta^{15}N_{Phe}$ vs. $\delta^{15}N_{bulk}$ values (R^2 = 0.82, $F_{(1,3)}$ = 13.23, p = 0.036) and the $\delta^{15}N_{Pro}$ vs $\delta^{15}N_{bulk}$ values (R^2 = 0.98, $F_{(1,3)}$ = 160.0, p = 0.001) for CA transients were both statistically significant, but the $\delta^{15}N_{Pro}$ values were a stronger explanatory variable for the bulk $\delta^{15}N$ values from the CA transients. Neither the $\delta^{15}N_{Phe}$ vs. $\delta^{15}N_{bulk}$ values (R^2 = 0.57, $F_{(1,4)}$ = 5.2, p = 0.084) nor the $\delta^{15}N_{Pro}$ and $\delta^{15}N_{bulk}$ values (R^2 = 0.36, $F_{(1,4)}$ = 2.22, p = 0.21) were significantly correlated for AK transients. Lastly, we found $\delta^{15}N_{Pro}$ were largely independent of $\delta^{15}N_{Phe}$ for AK transients (R^2 = 0.012, $F_{(1,4)}$ = 0.049, p = 0.84), but were highly related to $\delta^{15}N_{Phe}$ for CA transients (R^2 = 0.87, $F_{(1,3)}$ = 19.40, p = 0.022; Figure 4.10).

Inter- and intra-specific patterns in the diet

Our variance component analysis of the $\delta^{15}N$ value LMMs suggested both AK and CA transient populations are composed of highly specialist foragers, with 90.7% and 92.9% of random variation, respectively, being attributable to differences among individuals. This pattern

can also be visualized in Figures 3 and 4, where some individuals are foraging consistently higher in the food web (*i.e.*, measured by relatively higher δ^{15}N values) compared to others.

Our *S* calculations also support the notion that transients show individual specialization. The average *S* for AK transients was 0.23±0.07 (range 0.10 – 0.35), and the average *S* for CA transients was 0.19±0.09 (range 0.01 – 0.39). Huckstadt *et al*.[96] defines extreme specialists as those that score less than 0.2 on the *S* index scale, meaning these transient killer whales are very nearly in this category of highly specialist consumers by isotopic values. There were 6/22 individuals in the AK group and 10/20 individuals in the CA group that were categorized as 'extreme' specialists, and there were no individuals categorized as a generalist (an *S* of greater than 0.5) for either group (Figure 4.11).

To gain further insight into the dietary specialization we detected through stable isotopes of transient killer whale dentin, we used MixSIAR to generate proportional estimates of diet composition (reported as means ± SD). Our aim was to investigate relative patterns of the two prey groups most relevant to the hypotheses (*e.g.*, pinnipeds and mysticetes; Figure 4.12) in context of location, time frame, and individual specialization indices. Overall, pinnipeds dominated the diet for both AK and CA transients at an estimated mean of 99.3% (± 0.7) and 99.2% (±1.0), respectively (Figure 4.13). Mysticetes comprised only 0.7% (±0.7) and 0.8% (± 1.0) on average for AK and CA transients, respectively. Diet compositions were highly similar between AK and CA transients, with a reliance on pinnipeds and a low estimated contribution from mysticetes.

Within the AK transients, we broadly examined how dietary estimates differed over time (Figure 4.3). Although there were only two individuals that lived entirely before 1970, the mean estimated contribution of mysticetes was 7.8% (±10), compared to 7.0% (±18.7) for animals that

lived entirely after 1970 (n = 15). However, it is important to consider the influence of strong individual specialization in our samples. The two pre-1970 individuals showed a range in mean mysticete diet contribution, from 14.8% (±8.3) to 0.7% (±1.5). Similarly, one post-1970 individual (RBCM 21490) consumed an estimated 72.8% (±4.9) mysticetes and another (AMMSN: 2020-023) consumed an estimated 17.5% (±15.3). Excluding those animals, the mean estimated contribution of mysticetes to killer whale diet post-1970 was 1.1% (± 1.2) with a range of 0.2% to 4.1%.

4.5 Discussion

Effect of sex, time, and age on diet

There were significant interaction effects of sex:age, sex:time, and sex:age:time for the δ^{13}C values of CA killer whales. Transient killer whales generally form matrilineal pods consisting of 1-2 adult females and a few of their offspring[102,103]. Males sometimes remain in the matrilineal pod, but may also disperse after sexual maturity and forage alone or with another male[103]. The increase we observed in the δ^{13}C values with age in males, as opposed to the decrease in females, is likely a result of divergent social behavior between the sexes. An increase in the δ^{13}C values indicates males in our study were perhaps forging at a higher latitude or further inshore (or upon prey that forage further inshore) than females. While the median male and female δ^{13}C values increased from pre- to post-1970s, the two sexes showed opposite changes in variability: the range of δ^{13}C values became more constrained for males and slightly more diffuse for females. This may again be related to social behavior. Eastern North Pacific gray whales and California sea lions (*Zalophus californianus*) are two primary prey sources for modern CA transients[104] that lack population estimates pre-1970, but have increased in

abundance overall since then[105]. With increasingly available prey, male killer whales hunting alone may be less likely to expend energy roaming, resulting in more consistent δ^{13}C values.

Excluding sex as a variable in the proceeding models to increase sample size, neither age nor time were significant predictors of the δ^{13}C values for CA transients, but time was a significant predictor for those from the AK transients. Again, the increase in the δ^{13}C values pre-1970 would suggest the animals foraged at higher latitudes or targeted prey further inshore. After the 1970s, foraging moved further to lower latitudes or further offshore, inferred from lower δ^{13}C values. This finding could be in contrast to the SMCH, as northern fur seals (*Callorhinus ursinus*) and Steller sea lions are generally higher (~2‰) in their δ^{13}C values than baleen whales such as fin whales (*Balaenoptera physalus*) and minke whales (*Balaenoptera acutorostrata*), though there are some exceptions (Bowen and Kurle in review).

Our LMMs showed that age and the interaction between age:time were significant predictors of the δ^{15}N values of CA transients. The δ^{15}N values increased with age both pre- and post-1970s, but the increase was greater pre-1970, implying that CA transients once experienced more diverse ontogenetic changes than in modern times. As gray whales and California sea lions are more common than they were in 1970[105], CA transients may have narrowed their dietary preferences in more recent years. Dall's porpoise (*Phocoenoides dalli*) is another important prey species[104] with substantially lower δ^{15}N values than other cetaceans and pinnipeds (Bowen and Kurle in review). Small porpoises may have been easier and more available prey for young killer whales pre-1970s, until they were older and more capable of hunting whale calves and pinnipeds, which are prey with higher δ^{15}N values (Bowen and Kurle in review).

The effect of time was the only predictor of the δ^{15}N values for AK transients, as individuals tended to increase in their δ^{15}N value pre-1970, whereas individuals living post-1970

displayed the opposite trend. This could support the SMCH prediction that the δ^{15}N values would increase pre-1970 as killer whales transitioned from lower- δ^{15}N whales to higher- δ^{15}N pinnipeds and perhaps decrease in the decades post-1970 if killer whales return to foraging on baleen whales as populations recover. However, the overall magnitude of the δ^{15}N changes in either time-period only amount to ~0.5 – 1‰ over the average lifespan of a killer whale in our dataset, which represents less than a trophic level.

Our SIBER analysis would also seem to refute the principles of the SMCH. Though the difference is not considerable, there was a greater range of δ^{15}N values in the pre-1970 ellipse than in the post-1970 ellipse, suggesting killer whales were previously foraging on a wider diversity of prey. The SMCH would purport that diet diversity would increase post-1970, motivated by the lack of baleen whale availability and exploitation of alternative food sources.

Nonetheless, there are some observations from our data (Figure 4.3) that could favor the SMCH. There was one individual (RBCM: 10001) that lived during the critical time period from ~1950 to ~1980 and exhibited continuously increased δ^{15}N values throughout its life (14.6‰ to 19.7‰; 5.1‰ range), possibly indicating prey-switching from a lower trophic level to a higher trophic level. Indeed, RBCM: 10001 was documented with harbor seal (*Phoca vitulina*) claws in his stomach at stranding, supporting a diet involving pinnipeds inferred by the δ^{15}N values at that time. Additionally, there were two specimens (RBCM: 21490 and NMML: 1865) with substantially lower δ^{15}N values for their entire lives relative to every other individual in our study. It could be that these animals preferred baleen whales. The same individuals also showed substantially lower δ^{13}C values than other killer whales, supporting the idea that they may have been foraging further offshore for baleen whales (although a diet of Dall's porpoise could yield a similar result).

There are two ways these outlying animals could be important for adding support to the SMCH, despite the fact that they lived after the collapse of baleen whale populations. First, they may represent killer whales with a prey preference for baleen whales. One of the arguments against the SMCH was that great whales have never been known to comprise a large portion of killer whale diet[40,43]. Although our dataset did not reflect killer whales with low δ^{15}N values before 1970, as the SMCH would predict, that may be an artifact of sampling. We only had access to two specimens that lived entirely before 1970, despite our extensive sampling efforts, as older historical specimens are scarce in natural history collections. Our data demonstrate that transient killer whales can exhibit stable isotope values as low as 14-15%, possibly aligning with a mysticete-based diet. Second, discussions of the SMCH include the idea that predators will revert to their originally preferred prey if a switch is driven by low prey abundance[39,43]. The two animals with low δ^{15}N values lived post-1970, but could represent a lineage that switched back to baleen whales as their populations began to recover[105].

Together, the isotope results from three specimens in our dataset (RBCM: 10001, RBCM: 21490, and NMML: 1865) could also support the claim in Springer *et al.*[32] that as few as 27 killer whales could cause a collapse of Steller sea lions if they switched from a reliance on baleen whales. As mentioned, the two animals with low δ^{15}N values demonstrate that some killer whales could show a strong preference for baleen whales, and RBCM: 10001 represents one example of a killer whale potentially switching from a baleen diet to a one consistent with Steller sea lions. There are at least ~580 transient killer whales in Alaska as of 2020, with a studied subset showing stable abundance since 1984[25], and we sampled 22 transient killer whale teeth. If we extrapolate from our dataset and assume a similar total population size in the 1970s, there

could have been ~26 killer whales that switched to pinnipeds for prey, which is perhaps sufficient to drive ecological re-organization.

Lastly, our results showed no significant differences between the $\delta^{13}C$ and $\delta^{15}N$ values of CA and AK transients through both a direct comparison of the isotope values as well as with our SIBER analyses. We did observe a wider range of $\delta^{13}C$ values in AK transients, consistent with a larger latitudinal range. AK transient killer whales also exhibited a lower minimum $\delta^{15}N$ value than CA transients, though the CA transients showed a higher maximum $\delta^{15}N$ value. Diet composition may still differ between CA and AK animals, as they likely consume different cetacean and pinniped species, but differences were not detectable from an isotopic perspective.

Trophic position calculations from CSIA-AA $\delta^{15}N$ data

The SMCH posits that AK killer whale TP would be lower pre-1970, implying a diet of baleen whales, and rising post-1970 congruent with an increase in pinniped consumption. Due to sampling limitations, we were unable to sample dentin representing years prior to 1969 for AK transients. We might expect to observe consistently high TPs onward from 1970 if killer whales were primarily consuming pinnipeds by that point, though a decrease in TPs over time could indicate killer whales again incorporating more baleen whales into their diet as those populations recover. Our results were more consistent with the latter case, as the second highest TP (4.2) was associated with 1972, which could reflect an individual consuming primarily pinnipeds. There was a decreasing (but non-significant) trend over time, similar to our $\delta^{15}N_{bulk}$ data, with the lowest TP (3.6) being associated with the most recent year sampled (2001). This decreasing temporal trend in TPs could indicate an increase in baleen whales or sea otters in the diet, either

of which could be feasible under the SMCH, but it could also be influenced by other low-TP cetacean prey such as Dall's porpoise.

TP calculations indexed to the base of the food web, while valuable, rely on parameters β and TDF, which involve assumptions and uncertainties[106]. We also examined the direct relationships of $\delta^{15}N_{Phe}$ and $\delta^{15}N_{Pro}$ with $\delta^{15}N_{bulk}$ to better understand the contributions of source and trophic AAs to $\delta^{15}N_{bulk}$ values. Neither relationship was significant for AK transients, however the $\delta^{15}N_{Phe}$ (source AA) values explained more variation in the $\delta^{15}N_{bulk}$ values (57%) than the $\delta^{15}N_{Pro}$ values (trophic AA; 36%). Also, the $\delta^{15}N_{Phe}$ explained very little of the variation in the $\delta^{15}N_{Pro}$ values (1%), meaning true dietary changes can be attributed to the influence of $\delta^{15}N_{Pro}$ on $\delta^{15}N_{bulk.}$

There was also an increasing trend (though again non-significant) of $\delta^{15}N_{Phe}$ over time. However, transient killer whales are frequently moving and can travel along the entire U.S. west coast[25]. The $\delta^{15}N$ values of nitrate, which provides nitrogen for primary production at the base of the food web, can vary as much as ~4‰ (the same range as our $\delta^{15}N_{Phe}$ values) from AK to CA[107]. Furthermore, the differences that our data show in the measured $\delta^{15}N_{Phe}$ values are consistent with possible minor trophic fractionation of $\delta^{15}N_{Phe}$, which shows variability of up to 1.6‰[59]. These variations inherent to a top predator with a wide range complicate interpretation of source and trophic drivers, though it appears both play a role in AK transient killer whales. Finally, we acknowledge our sample size was limited, which is of particular importance considering the high degree of dietary variation among individuals suggested by our bulk $\delta^{15}N$ values.

The mean TP for the six CA transients was slightly lower than those for the AK transients (3.5 vs 3.9), though there was a downtrend trend in TP over time for both groups. Such a trend in

the CA transients could imply an increasing reliance on migrating gray and minke whales, as increases in their populations have been documented in more recent years[30] relative to the 1940s and 1950s. Killer whales foraging at a higher trophic level may have been consuming pinnipeds such as harbor seals, elephant seals, and California sea lions.

The relationship between the $\delta^{15}N_{Phe}$ values and year was notably weaker for CA transients compared to AK transients, which could be related to the narrower latitudinal range of apparent CA stock killer whales or different nitrogen cycling dynamics. For the CA transients, there were significant positive linear correlations between both the $\delta^{15}N_{Phe}$ and $\delta^{15}N_{bulk}$ values and the $\delta^{15}N_{Pro}$ and $\delta^{15}N_{bulk}$ values, with the $\delta^{15}N_{Pro}$ values explaining more variation (98%) than $\delta^{15}N_{Phe}$ (86%). However, when comparing $\delta^{15}N_{Phe}$ and $\delta^{15}N_{Pro}$, there was a significant relationship, with the $\delta^{15}N_{Phe}$ values explaining 91% of the variation in $\delta^{15}N_{Pro}$ values. Altogether, these results strongly suggest that variation in baseline or source $\delta^{15}N$ values are driving $\delta^{15}N_{bulk}$ values in CA transients.

Inter- and intra-specific patterns in the diet

We found a remarkable degree of individual specialization in both AK and CA transient killer whales through variance component analyses of the linear models as well as our *S* calculations. This is particularly interesting, as killer whales are not generally thought to specialize within their marine mammal prey[18]. However, there has been some evidence that a small and localized stock of AK killer whales, the AT1 transients that reside primarily in Prince William Sound, may specialize on harbor seals and Dall's porpoise[28]. Specific individuals in the Gulf of Alaska stock have also been observed harassing Steller sea lions[28], which could align with specimens in our study whose $\delta^{15}N$ values were consistently in the 20-21‰ range. Other

studies have also shown marine mammals are frequently categorized as specialists[55,85,96,108]. Our data suggest that transient killer whales may be far more specialized foragers than previously thought.

A high degree of individual specialization could both support and refute the SMCH. Specialized foraging would support the notion that some killer whales could have relied heavily on baleen whales, but it could also hinder prey-switching tendencies. Foraging habits of killer whales are culturally ingrained within matrilineal lines[109]. One individual transient killer whale that was captured in 1970 starved to death, being unable to recognize or unwilling to accept fish as a food source. Though this is an extreme example, it could challenge the notion that transient killer whales easily switched from baleen whales to pinnipeds in a relatively short time frame as baleen whales became scarce.

Our constrained MixSIAR analysis did not support the SMCH through a notable decrease in baleen whale and increase in pinniped consumption throughout time, though our two individuals that exhibited lower δ^{15}N values specimens did reflect a relatively high baleen whale contribution as expected. There were also no patterns in the estimated pinniped and baleen whale contributions to CA transient diet.

Conclusions

Our study provided mixed interpretations for the SMCH (Table 4.6). Overall, if we interpret the SMCH to mean that we should observe (1) a reliance on baleen whales pre-1970 and (2) a switch to and maintenance of pinniped reliance post-1970, our findings do not support the related predictions. However, if we accept that (1) a rapid switch to pinnipeds occurred very near 1970, and (2) killer whales have been gradually incorporating baleen whales again as those

populations recover, then our findings could support the related predictions. These conclusions may also be dependent on behaviors of individual killer whales; for example, if only some killer whales rely on baleen whales or only some killer whales engaged in prey-switching, for which we show evidence of both.

We also found AK and CA transients to be isotopically very similar, though the drivers of the $\delta^{15}N_{bulk}$ values differed in each system. AK transients were influenced by both source and trophic changes, perhaps related to their wide range, whereas CA transients were primarily influenced by source or baseline changes in the environment. Finally, we observed a greater degree of individual specialization in CA and AK transient killer whales than previous studies have suggested. This finding could inform future studies that examine the role of killer whale predation in ecosystems. It would be valuable to continue stable isotope studies of killer whale teeth, particularly as killer whale field research efforts have increased in recent years, and we can better correlate field observations, stomach contents, stable isotope values, and other measurements of diet.

4.6 Acknowledgements

We are grateful to the natural history collections and all the staff/curators who made this work possible through generous specimen loans, including: the Beaty Biodiversity Museum – University of British Columbia (M. deRoos, C. Stinson); the California Academy of Sciences (M. Flannery); Cal Poly Humboldt (formerly Humboldt State University, T. Danufsky, M. Hawkins, P. Goley, A. Bronson, A. Semerdjian); the Natural History Museum of Los Angeles County (D. Janiger, J. Velez-Juarbe, S. Robson); the NOAA Marine Mammal Laboratory (P. Clapham, P. Wade); the Museum of the North – University of Alaska (A. Gunderson, L. Olson); the Smithsonian National Museum of Natural History (M. Hawkins, D. Lunde, M. McGowen, J.

Ososky); the Burke Museum of Natural History and Culture – University of Washington (J. Bradley); the Royal British Columbia Museum (G. Hanke, C. Davies, L. Golding).
Our thanks also to the following for assistance with sample measurements: University of California Santa Cruz Stable Isotope Laboratory (D. Andreasen, C. Carney, and E. Cano); the University of New Mexico Center for Stable Isotopes (S. Newsome, V. Atudorei); University of Florida - Light Stable Isotope Mass Spec Lab (J. Curtis); University of California Davis - Stable Isotope Facility (C. Yarnes, E. Schick).

Finally, we extend our greatest appreciation to numerous researchers at NOAA's Southwest Fisheries Science Center for support that made this work possible, including: D. Weller, J. Seminoff, C. Turner Tomaszewicz, T. Chen, R. Schnug. Also thanks to L. Ballance, J. Shurin, S. Nehasil, and J. Bowen for invaluable additional project support. Funding and support for K.B. and C.K. were provided by the University of California San Diego (UCSD), the NIH Cell & Molecular Genetics Graduate Training Program, the PADI Foundation, the Lerner-Gray Fund for Marine Research by the American Museum of Natural History, the Jeanne Marie Messier Memorial Endowed Fund (UCSD), the American Cetacean Society Los Angeles Chapter John E. Heyning Research Grant, and the Association for Women in Science San Diego Chapter.

Chapter 4, in full, is currently being prepared for submission for publication of the material. Bowen, Kelly; Kurle, Carolyn. The dissertation author was the primary investigator and author of this material

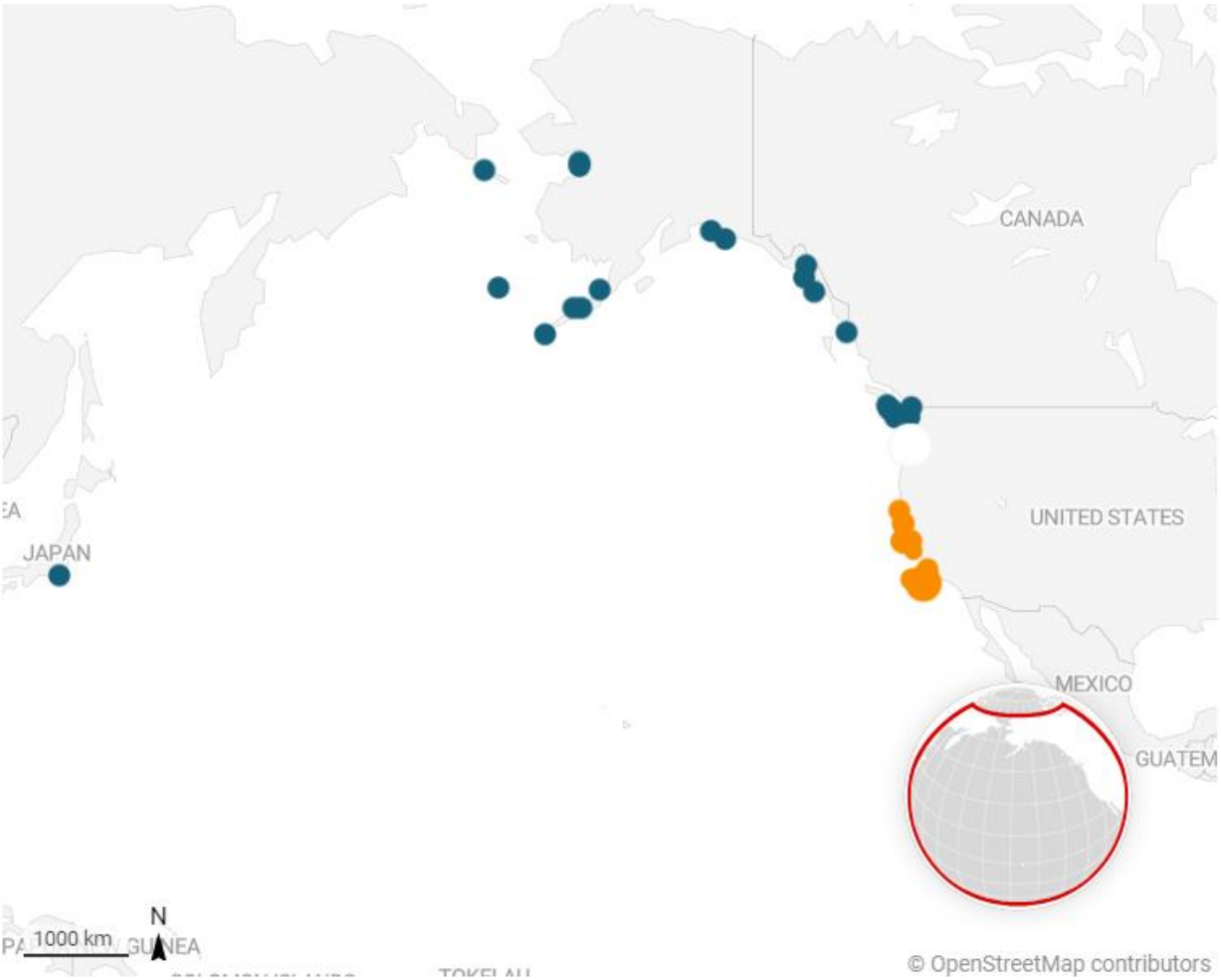


Figure 4.1. Map centered in the North Pacific Ocean, showing killer whale specimen collection locations. Blue markers indicate individuals we categorized as ‘Alaska’ (AK) transient killer whales, and orange markers indicate individuals we categorized as ‘California’ (CA) transient killer whales. Map created with Datawrapper.



Figure 4.2. A 1000 dpi scanned image of a killer whale tooth that has been bisected, polished, etched with formic acid, and highlighted with graphite. Visible growth layer groups (GLGs) represent one year of time.

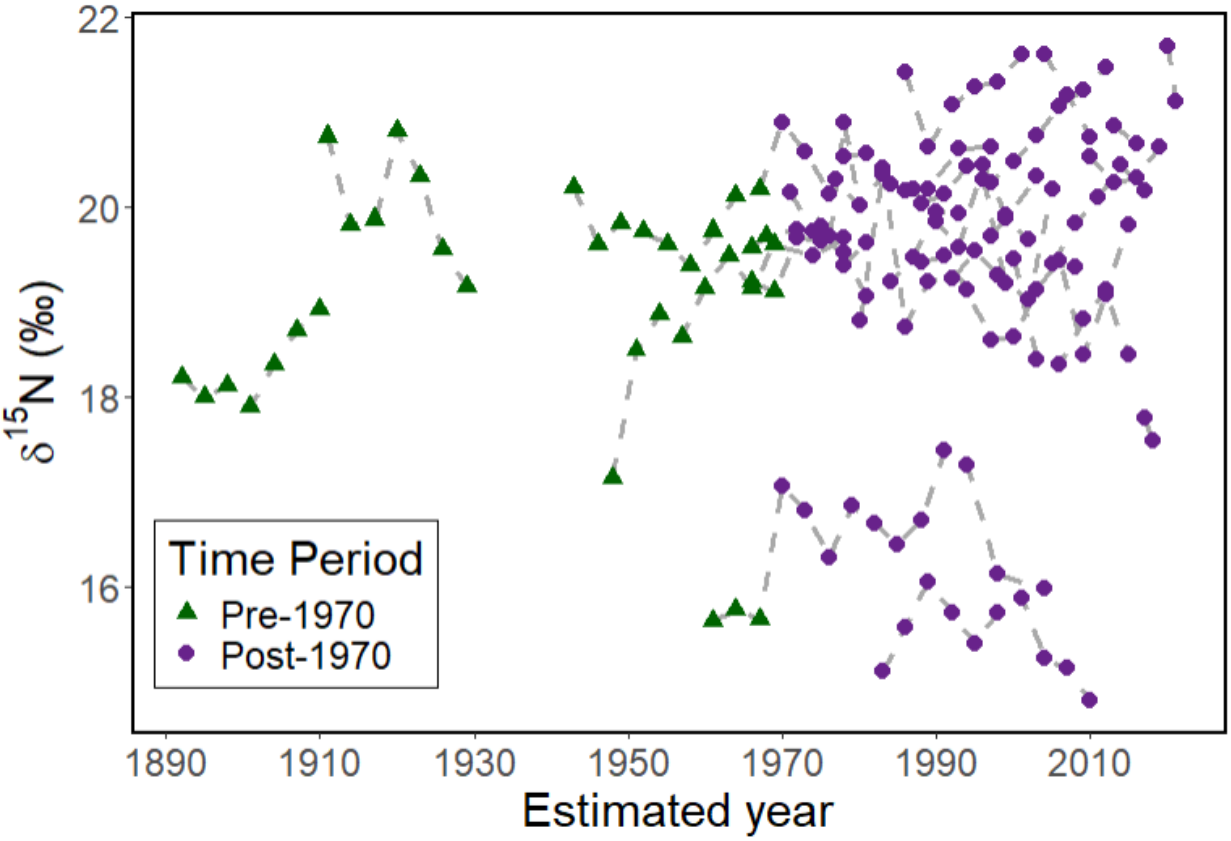


Figure 4.3. The δ^{15}N values over time for Alaska transient killer whale dentin, divided by pre-1970 (green triangles) and post-1970 (purple circles) growth layer groups. Individuals are connected by a dashed gray line.

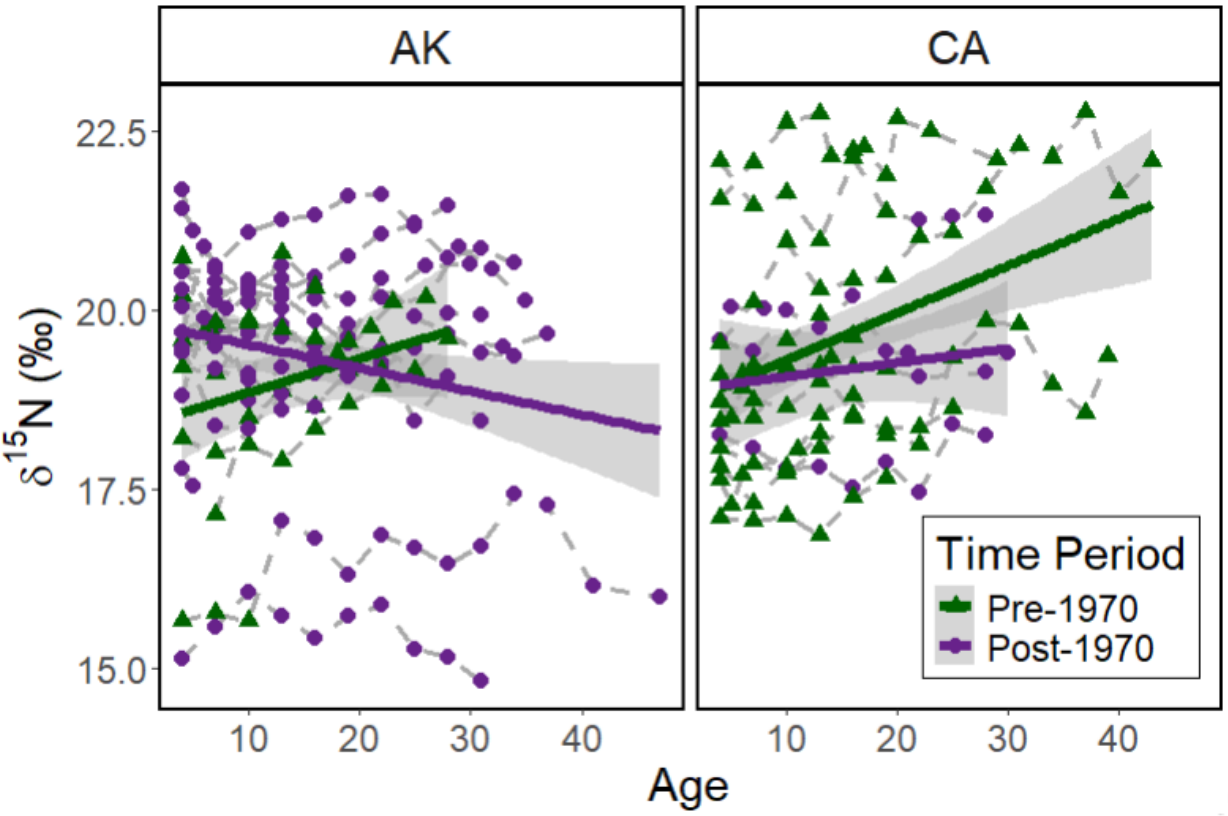


Figure 4.4. The δ^{15}N values by age for Alaska (AK) and California (CA) transient killer whales, divided by pre-1970 (green triangles) and post-1970 (purple circles). Individuals are connected by a dashed gray line. Trend lines show patterns for all growth layer groups sampled in a time period, however the linear mixed models showed a significant interactive effect of age:time for only CA transient killer whales when accounting for random variation due to individual.

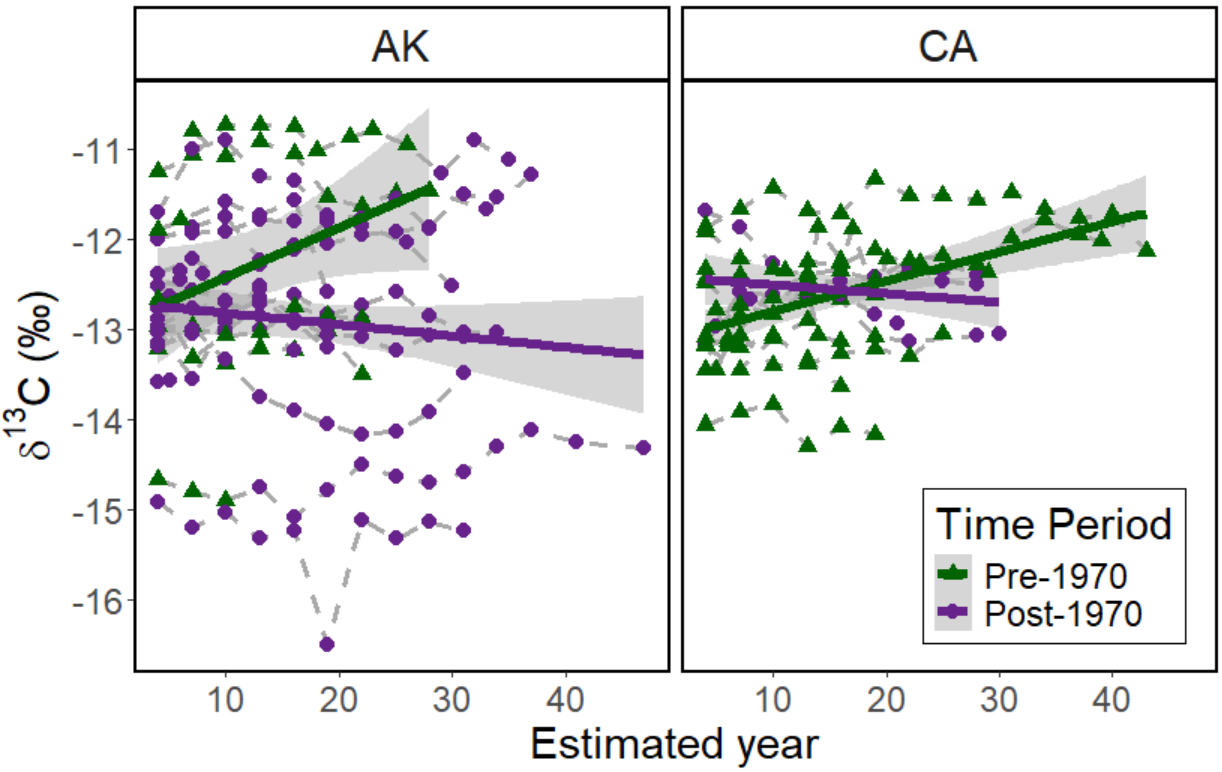


Figure 4.5. The $\delta^{13}C$ values by age for Alaska (AK) and California (CA) transient killer whales, divided by pre-1970 (green triangles) and post-1970 (purple circles). Individuals are connected by a dashed gray line. Trend lines show patterns for all growth layer groups sampled in a time period, however the linear mixed models showed a significant effect of time for only the AK transient killer whales.

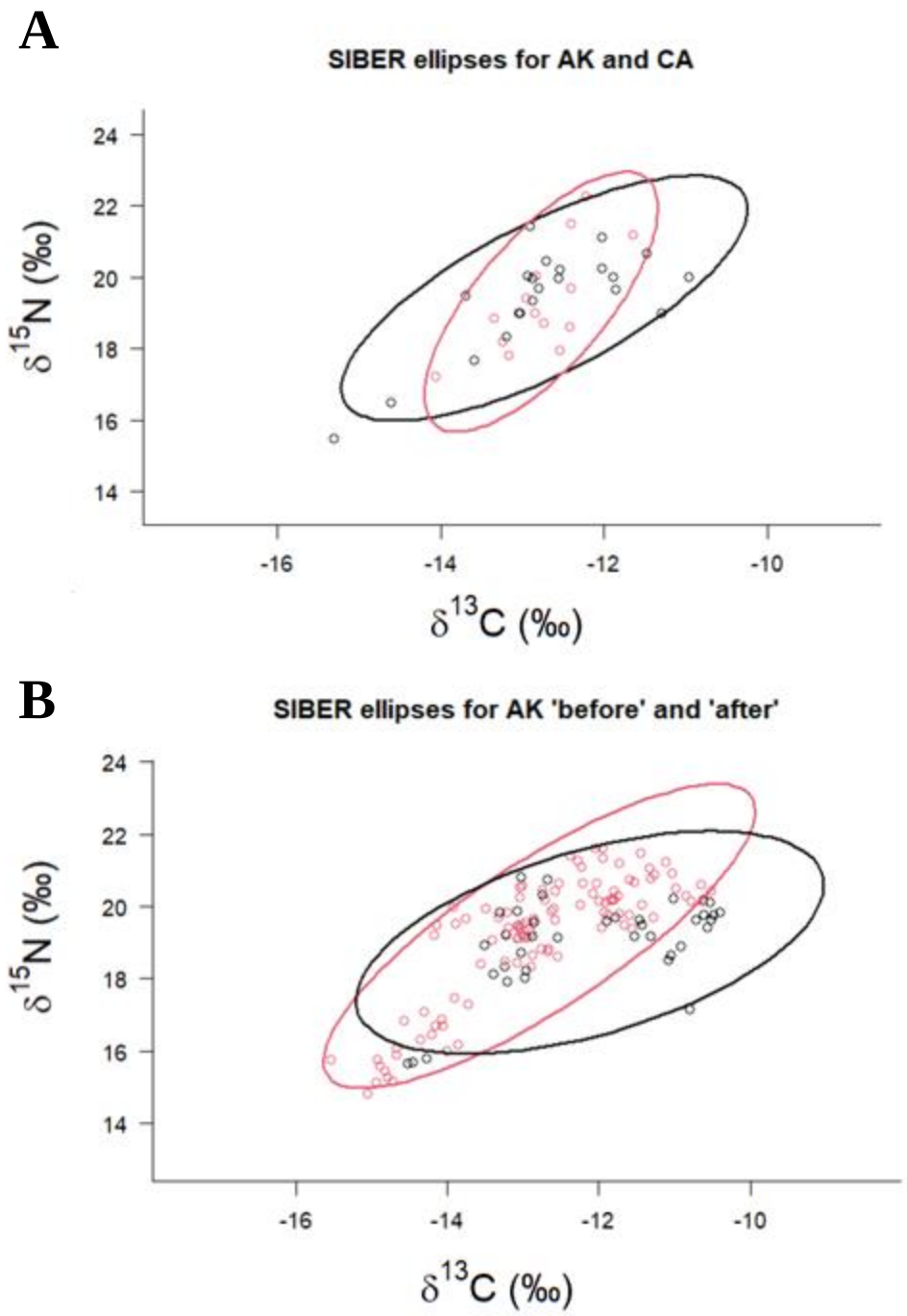


Figure 4.6. SIBER ellipses for Alaska (AK, black) vs California (CA, red) killer whales (A) and 'before' (black) and 'after' (red) within AK transients (B).

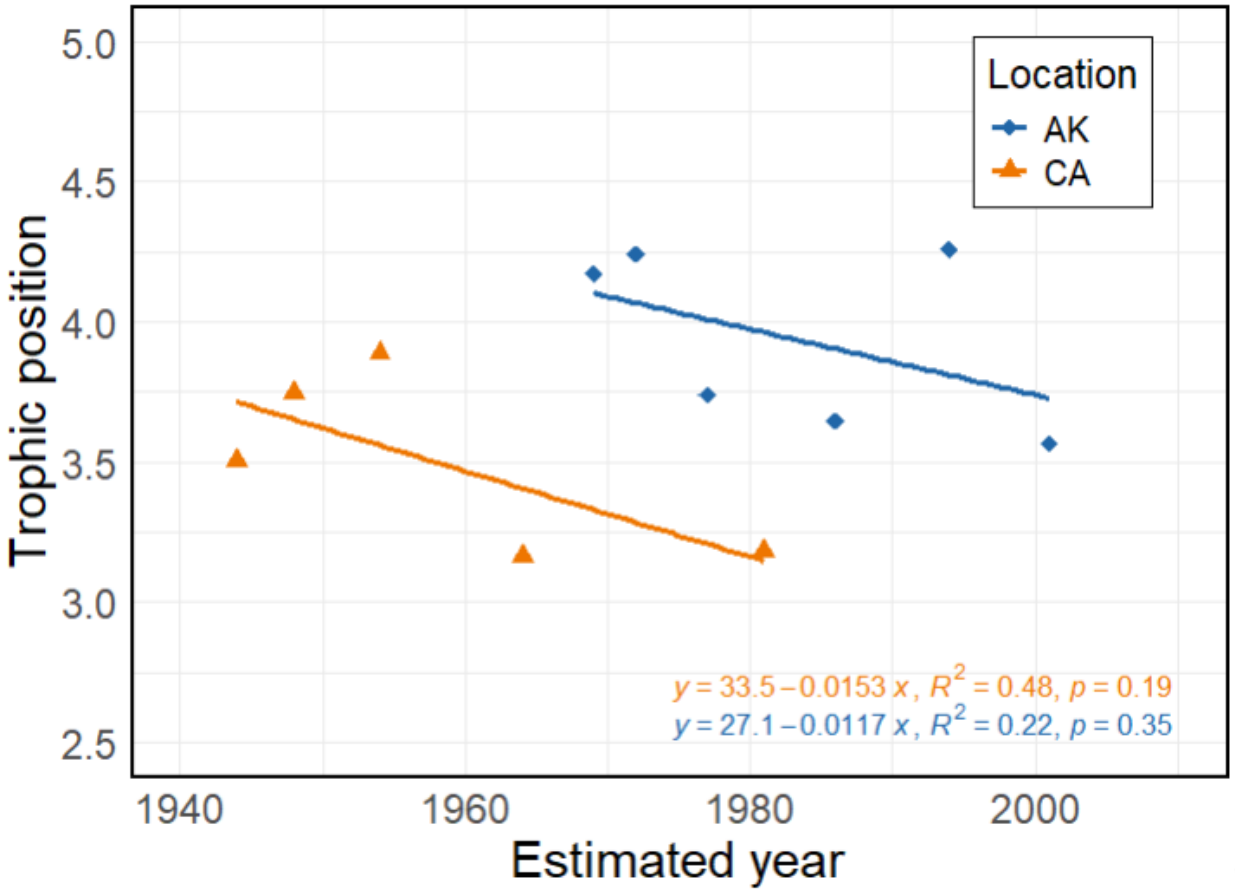


Figure 4.7. Trophic position of Alaska (AK; blue diamonds) and California (CA; orange triangles) over time as estimated from a calculating using the δ^{15}N values of trophic and source amino acids from dentin.

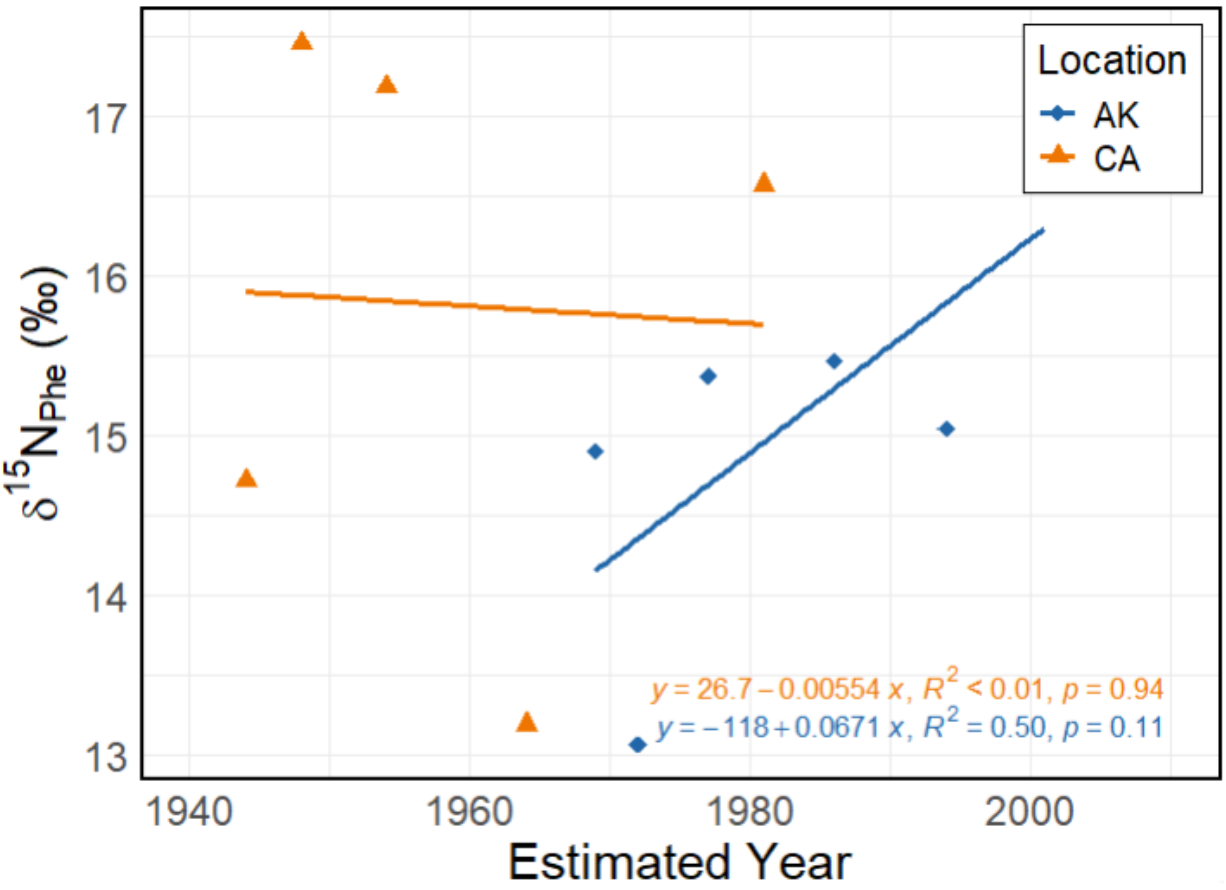


Figure 4.8. The relationship between the $\delta^{15}N_{Phe}$ values from dentin and the estimated year that the sampled growth layer group was estimated to represent for Alaska (AK; blue diamonds) and California (CA; orange triangles) killer whales.

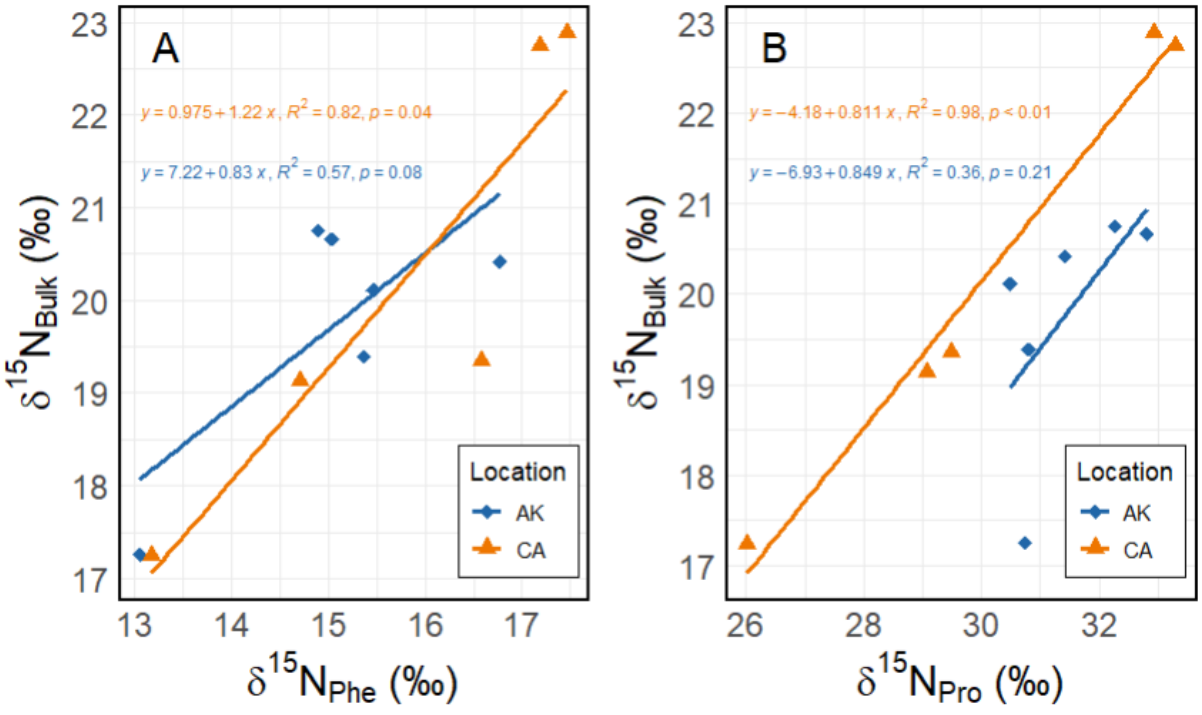


Figure 4.9. The $\delta^{15}N_{Bulk}$ values are shown against the $\delta^{15}N_{Phe}$ values (A, source amino acid) and the $\delta^{15}N_{Pro}$ values (B, trophic amino acid) of dentin from Alaska (AK; blue diamond) and California (CA; orange triangle) killer whale teeth.

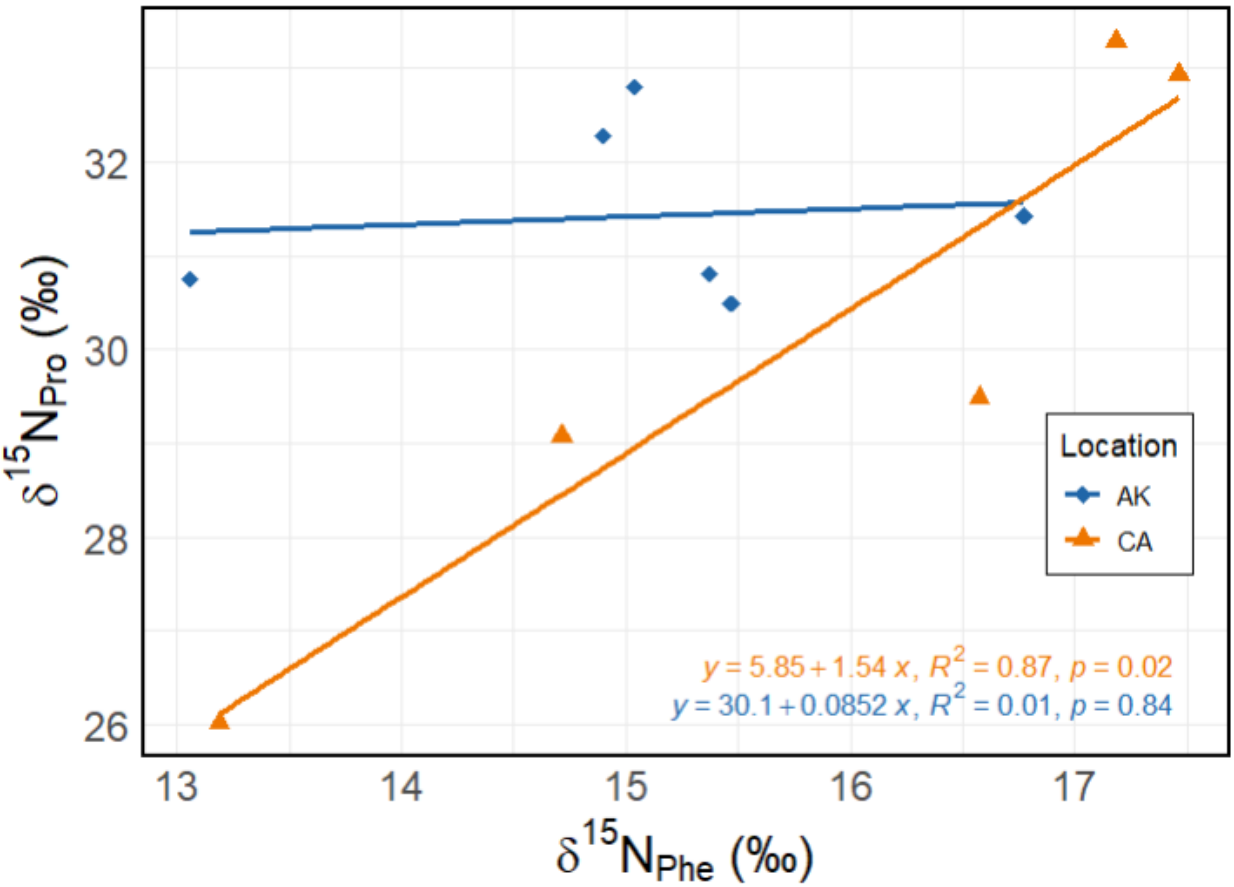


Figure 4.10. The $\delta^{15}N_{Pro}$ values (trophic amino acid) are shown against the $\delta^{15}N_{Phe}$ values (source amino acid) of dentin from Alaska (AK; blue diamond) and California (CA; orange triangle) killer whale teeth.

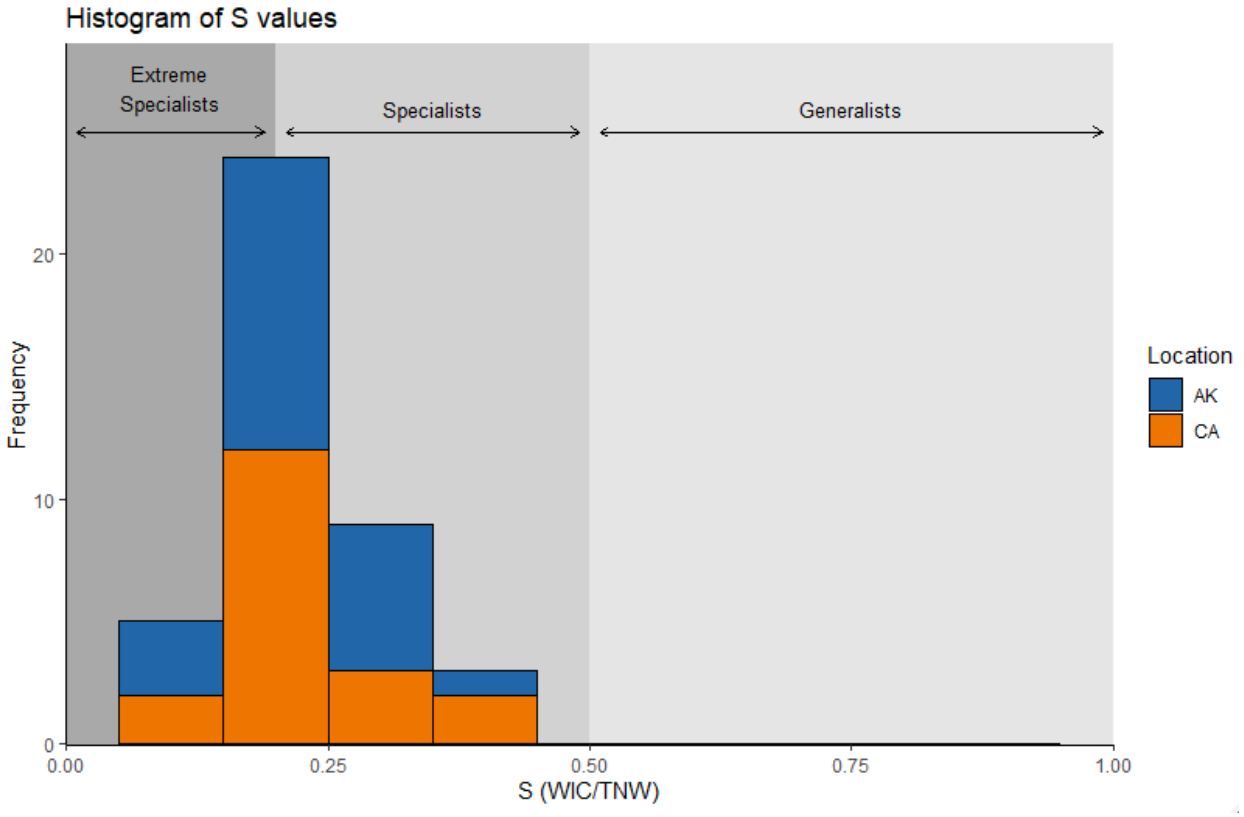


Figure 4.11. Histogram of the specialization index (*S*) values for Alaska (AK; blue top sections) and California (CA; orange lower sections) individuals calculated from the δ^{15}N values of dentin, where *S* is the within-individual variation (from growth layer groups) divided by the between-individual variation. The very similar distributions between AK and CA individuals indicates killer whales are specialists within marine mammals.

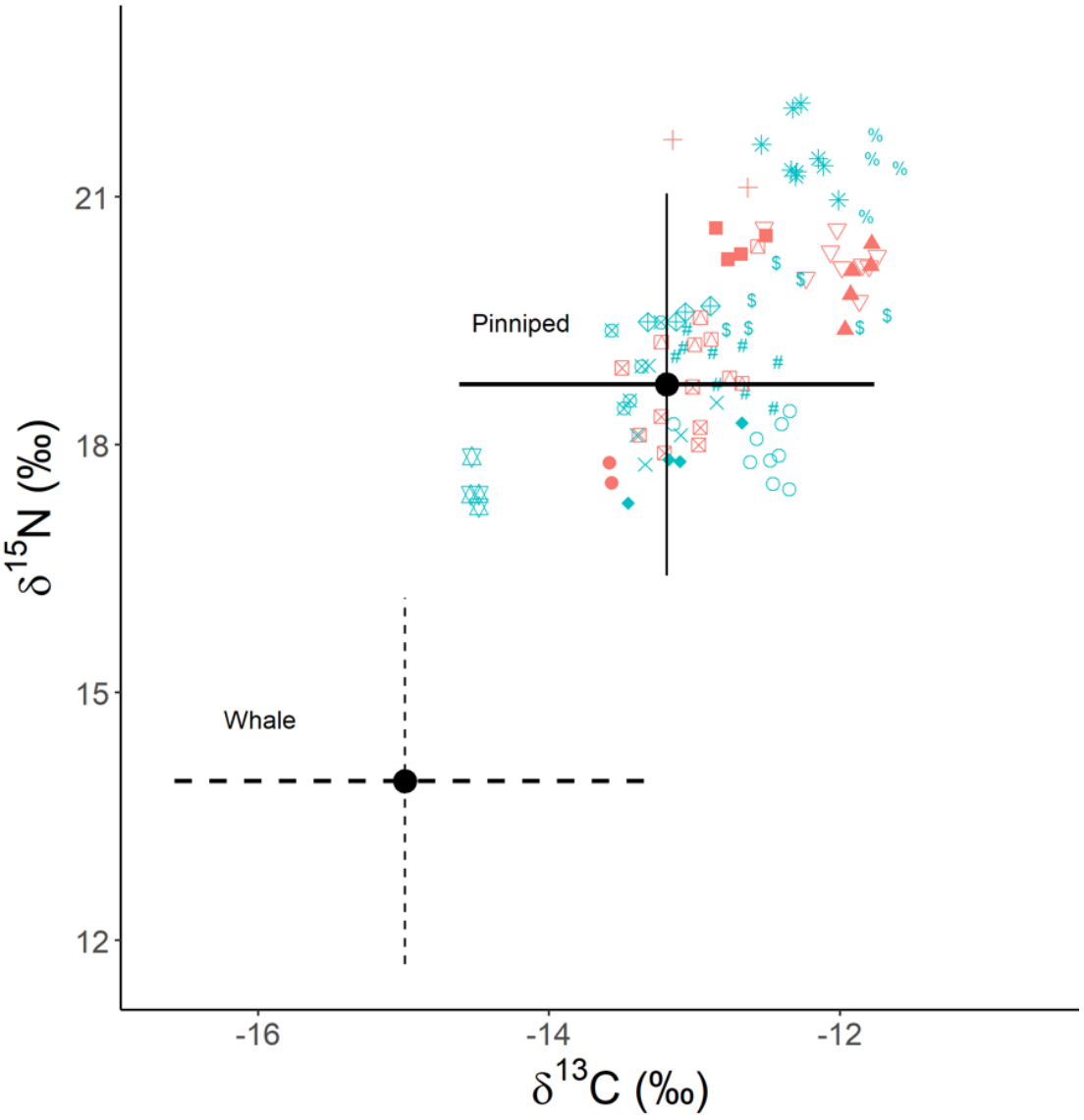


Figure 4.12. Isospace plot produced in MixSIAR showing the distributions of stable isotope values from the two primary prey groups: whales (dashed lines) and pinnipeds (solid lines). Individual data points represent stable isotope measurements from growth layer groups (GLGs; symbols are multiple GLGs from an individual) of Alaska (red) and California (blue) killer whale teeth.

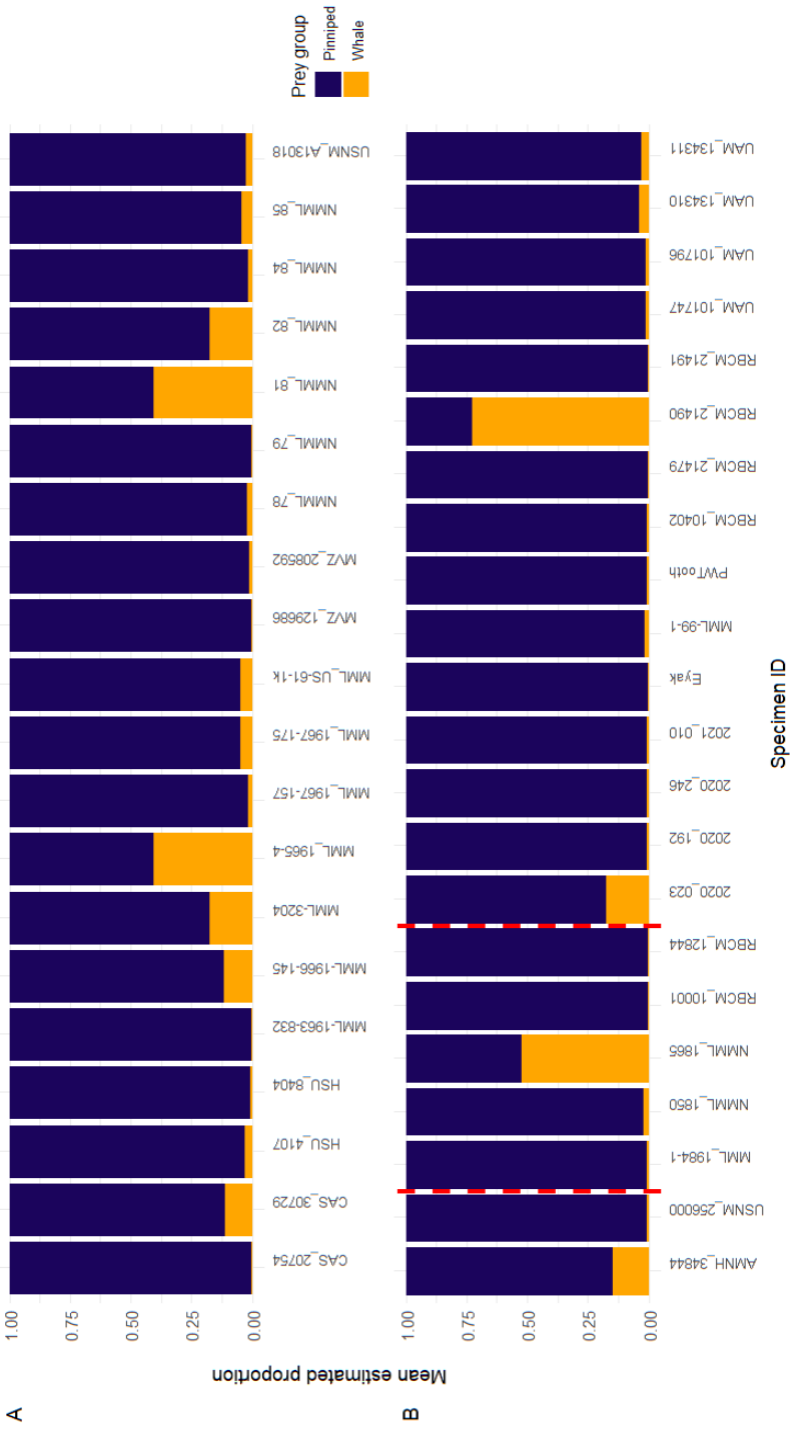


Figure 4.13. Mean estimated proportion that each prey group, pinnipeds (blue top sections) and baleen whales (orange bottom sections), contribute to the diets of each California (B) and Alaska (B) killer whale individual. Red dashed lines in (B) separate time periods: leftmost is pre-1970, middle is during 1970s, and rightmost is post-1970.

Table 4.1. The metadata for specimens used in this study, including the specimen ID (* = duplicate teeth analyzed and stable isotope values averaged), alternate catalogue IDs or other identifiers, the collection year, the sex of the animal (F = female, M = male), the method of confirmation for ecotype, and the location we categorized the animal into for analysis (AK = Alaska, CA = California).

Specimen ID	Alternate ID	Collection year	Sex	Ecotype	Location
AMMSN: 2020-023		2020	M	Model	AK
AMMSN: 2020-192		2020	M	Photo-ID	AK
AMMSN: 2020-246		2020	F	Model	AK
AMMSN: 2021-010		2021	NA	Model	AK
AMNH: 34844		1910	F	Model	AK
CAS: 20754		1976	M	Model	CA
CAS: 30729		2015	M	Model	CA
BBM: "Eyak"		2000	M	Photo-ID	AK
HSU: 4107		1980	F	Model	CA
HSU: 8404		2005	F	Photo-ID	CA
USNM: 611102	MML: 3204	1966	M	Model	CA
MML: 1999-1		1999	NA	Model	AK
MML: 1984-1		1984	NA	Model	AK
MVZ: 129686		1962	M	Genetics	CA
MVZ: 208592		1997	M	Model	CA
NMML: 1850		2002	F	Photo-ID	AK
USNM: 594673	NMML: 1865	2010	F	Genetics	AK
USNM: 594667	NMML: 78 ; MML: US-61-1k	1961	M	Genetics	CA
USNM: 594678	NMML: 79 ; MML: 1963-832	1963	M	Genetics	CA
USNM: 594668*	NMML: 81 ; MML: 1965-4	1965	M	Genetics	CA
USNM: 594671*	NMML: 82 ; MML: 1966-145	1966	M	Genetics	CA
USNM: 594669*	NMML: 84 ; MML: 1967-157	1967	M	Genetics	CA
USNM: 610855*	NMML: 85 ; MML: 1967-175	1967	F	Genetics	CA
NMML: PW		2017	NA	Photo-ID	AK
RBCM: 10001		1979	M	Photo-ID	AK
RBCM: 10402		1981	M	Genetics	AK
RBCM: 12844		1976	M	Genetics	AK
RBCM: 21479		2016	M	Photo-ID	AK
RBCM: 21490		2013	M	Photo-ID	AK
RBCM: 21491		2013	F	Photo-ID	AK
UAM: 101747		2006	NA	Model	AK
UAM: 101796		2006	NA	Genetics	AK
UAM: 134310		2016	NA	Genetics	AK
UAM: 134311		2016	NA	Genetics	AK
USNM: 256000		1930	NA	Model	AK
USNM: A-13018		~mid-1800s	NA	Genetics	CA

Table 4.2. Sampling scheme for compound-specific isotope analysis of amino acids (CSIA-AA). We aimed to sample one growth layer group (GLG) from each of two individuals for each decade. Within decades, we aimed to sample from the earlier and latter half. Locations for the individuals were assigned to either California (CA) or Alaska (AK).

Decade	Specimen sampled	Targeted GLG year(s)	Estimated age	Location
1940 - 1949	USNM: 594667	1944	23	CA
	USNM: 594678	1948	30	CA
1950 - 1959	MVZ: 129686	1954	13	CA
	USNM: 594668	1959	15	CA
1960 - 1969	RBCM: 12844	1968+1969	27+28	AK
1970 - 1979	NMML: 1865	1972	15	AK
	NMML: 1850	1977	15	AK
1980 - 1989	HSU: 8404	1981	11	CA
	PW	1986	12	AK
1990 - 2001	RBCM: 21479	1994	12	CA
	RBCM: 21491	2001	17	AK

Table 4.3. The specimen IDs, estimated year and age represented by the sampled growth layer group (GLG), and the final $\delta^{13}C$ and $\delta^{15}N$ values for each GLG. See Bowen and Kurle in prep for other previous age estimates of these same teeth and discussions related to aging uncertainty.

Specimen ID	Estimated year	Estimated age	Final corrected $\delta^{13}C$ (‰)	$\delta^{15}N$ (‰)
AMMSN: 2020_023	2017	4	-13.6	17.8
AMMSN: 2020_023	2018	5	-13.6	17.5
AMMSN: 2020_192	2005	4	-12.0	19.4
AMMSN: 2020_192	2008	7	-11.9	19.8
AMMSN: 2020_192	2011	10	-11.9	20.1
AMMSN: 2020_192	2014	13	-11.8	20.4
AMMSN: 2020_192	2017	16	-11.8	20.2
AMMSN: 2020_246	2010	4	-12.5	20.5
AMMSN: 2020_246	2013	7	-12.8	20.2
AMMSN: 2020_246	2016	10	-12.7	20.3
AMMSN: 2020_246	2019	13	-12.9	20.6
AMMSN: 2021_010	2020	4	-13.2	21.7
AMMSN: 2021_010	2021	5	-12.6	21.1
AMNH: 34844	1892	4	-13.0	18.2
AMNH: 34844	1895	7	-13.0	18.0
AMNH: 34844	1898	10	-13.4	18.1
AMNH: 34844	1901	13	-13.2	17.9
AMNH: 34844	1904	16	-13.2	18.3
AMNH: 34844	1907	19	-13.0	18.7
AMNH: 34844	1910	22	-13.5	18.9
CAS: 20754	1952	4	-12.5	22.1
CAS: 20754	1955	7	-12.4	21.5
CAS: 20754	1958	10	-12.8	21.6
CAS: 20754	1961	13	-12.2	21.0
CAS: 20754	1964	16	-12.3	22.1
CAS: 20754	1967	19	-12.1	21.4
CAS: 20754	1970	22	-12.3	21.3
CAS: 20754	1973	25	-12.5	21.3
CAS: 20754	1976	28	-12.5	21.3
CAS: 30729	1989	4	-13.1	18.3
CAS: 30729	1992	7	-12.6	18.1
CAS: 30729	1995	10	-12.6	17.8
CAS: 30729	1998	13	-12.5	17.8
CAS: 30729	2001	16	-12.5	17.5
CAS: 30729	2004	19	-12.4	17.9
CAS: 30729	2007	22	-12.4	17.5
CAS: 30729	2010	25	-12.3	18.4
CAS: 30729	2013	28	-12.4	18.3

Table 4.3. Continued. The specimen IDs, estimated year and age represented by the sampled growth layer group (GLG), and the final $\delta^{13}C$ and $\delta^{15}N$ values for each GLG. See Bowen and Kurle in prep for other previous age estimates of these same teeth and discussions related to aging uncertainty.

Specimen ID	Estimated year	Estimated age	Final corrected $\delta^{13}C$ (‰)	$\delta^{15}N$ (‰)
BBM: "Eyak"	1971	4	-12.0	20.2
BBM: "Eyak"	1974	7	-11.9	19.7
BBM: "Eyak"	1977	10	-11.7	20.3
BBM: "Eyak"	1980	13	-12.2	20.0
BBM: "Eyak"	1983	16	-12.1	20.3
BBM: "Eyak"	1986	19	-11.8	20.2
BBM: "Eyak"	1989	22	-11.8	20.2
BBM: "Eyak"	1993	26	-12.0	20.6
BBM: "Eyak"	1997	30	-12.5	20.6
HSU: 4107	1953	4	-12.5	18.5
HSU: 4107	1956	7	-12.8	18.7
HSU: 4107	1959	10	-12.7	18.6
HSU: 4107	1962	13	-12.6	19.0
HSU: 4107	1965	16	-12.7	19.2
HSU: 4107	1968	19	-13.1	19.2
HSU: 4107	1971	22	-13.1	19.1
HSU: 4107	1977	28	-13.1	19.1
HSU: 4107	1979	30	-13.0	19.4
HSU: 8404	1974	4	-11.7	19.6
HSU: 8404	1977	7	-11.9	19.4
HSU: 8404	1980	10	-12.3	20.0
HSU: 8404	1983	13	-12.6	19.7
HSU: 8404	1986	16	-12.6	20.2
HSU: 8404	1989	19	-12.8	19.4
HSU: 8404	1991	21	-12.9	19.4
MML: 1965-4	1958	4	-14.5	17.2
MML: 1965-4	1960	6	-14.5	17.4
MML: 1965-4	1962	8	-14.5	17.4
MML: 1965-4	1964	10	-14.5	17.9
MML: 1967-157	1958	4	-13.3	19.5
MML: 1967-157	1961	7	-13.1	19.5
MML: 1967-157	1964	10	-12.9	19.7
MML: 1967-157	1966	12	-13.1	19.6

Table 4.3. Continued. The specimen IDs, estimated year and age represented by the sampled growth layer group (GLG), and the final $\delta^{13}C$ and $\delta^{15}N$ values for each GLG. See Bowen and Kurle in prep for other previous age estimates of these same teeth and discussions related to aging uncertainty.

Specimen ID	Estimated year	Estimated age	Final corrected $\delta^{13}C$ (‰)	$\delta^{15}N$ (‰)
MML: 1967-175	1955	4	-13.4	19.0
MML: 1967-175	1958	7	-13.4	18.5
MML: 1967-175	1961	10	-13.2	19.5
MML: 1967-175	1964	13	-13.6	19.4
MML: 1967-175	1967	16	-13.5	18.4
MML: 1984-1	1966	4	-11.9	19.6
MML: 1984-1	1968	6	-11.8	19.7
MML: 1984-1	1972	10	-11.6	19.8
MML: 1984-1	1975	13	-11.7	19.8
MML: 1984-1	1978	16	-11.6	19.4
MML: 1984-1	1981	19	-12.6	19.6
MML: US-61-1k	1948	4	-13.6	18.0
MML: US-61-1k	1951	7	-13.3	18.1
MML: US-61-1k	1954	10	-12.5	18.5
MML: US-61-1k	1957	13	-12.7	19.5
MML: US-61-1k	1960	16	-12.6	19.1
MML: 1963-832	1954	4	-11.8	20.8
MML: 1963-832	1957	7	-11.6	21.4
MML: 1963-832	1959	9	-11.8	21.5
MML: 1963-832	1962	12	-11.8	21.8
MML: 1966-145	1948	7	-13.1	18.1
MML: 1966-145	1952	11	-13.4	18.1
MML: 1966-145	1957	16	-13.3	19.0
MML: 1966-145	1960	19	-13.3	17.8
MML: 1966-145	1964	23	-12.8	18.5
MML: 3204	1954	4	-13.2	17.8
MML: 3204	1957	7	-13.5	17.3
MML: 3204	1960	10	-13.1	17.8
MML: 3204	1963	13	-12.9	18.3
MML: 99-1	1980	4	-12.8	18.8
MML: 99-1	1983	7	-12.6	20.4
MML: 99-1	1986	10	-12.7	18.7
MML: 99-1	1989	13	-13.0	19.2
MML: 99-1	1992	16	-13.2	19.2
MML: 99-1	1995	19	-13.0	19.5
MML: 99-1	1998	22	-12.9	19.3

Table 4.3. Continued. The specimen IDs, estimated year and age represented by the sampled growth layer group (GLG), and the final $\delta^{13}C$ and $\delta^{15}N$ values for each GLG. See Bowen and Kurle in prep for other previous age estimates of these same teeth and discussions related to aging uncertainty.

Specimen ID	Estimated year	Estimated age	Final corrected $\delta^{13}C$ (‰)	$\delta^{15}N$ (‰)
MVZ: 129686	1934	4	-11.9	21.6
MVZ: 129686	1937	7	-12.2	22.0
MVZ: 129686	1940	10	-12.3	22.6
MVZ: 129686	1943	13	-12.4	22.7
MVZ: 129686	1944	14	-11.9	22.2
MVZ: 129686	1946	16	-12.2	22.2
MVZ: 129686	1947	17	-11.9	22.3
MVZ: 129686	1949	19	-12.6	21.9
MVZ: 129686	1950	20	-12.2	22.7
MVZ: 129686	1953	23	-12.3	22.5
MVZ: 129686	1959	29	-12.4	22.1
MVZ: 208592	1993	5	-13.0	20.0
MVZ: 208592	1996	8	-12.7	20.0
NMML: 1850	1966	4	-13.2	19.2
NMML: 1850	1969	7	-13.0	19.1
NMML: 1850	1972	10	-13.3	19.7
NMML: 1850	1975	13	-13.8	19.6
NMML: 1850	1978	16	-13.9	19.5
NMML: 1850	1981	19	-14.1	19.1
NMML: 1850	1984	22	-14.2	19.2
NMML: 1850	1987	25	-14.1	19.5
NMML: 1850	1990	28	-13.9	19.9
NMML: 1850	1993	31	-13.5	19.9
NMML: 1865	1961	4	-14.7	15.7
NMML: 1865	1964	7	-14.8	15.8
NMML: 1865	1967	10	-14.9	15.7
NMML: 1865	1970	13	-14.8	17.1
NMML: 1865	1973	16	-15.1	16.8
NMML: 1865	1976	19	-14.8	16.3
NMML: 1865	1979	22	-14.5	16.9
NMML: 1865	1982	25	-14.6	16.7
NMML: 1865	1985	28	-14.7	16.5
NMML: 1865	1988	31	-14.6	16.7
NMML: 1865	1991	34	-14.3	17.4
NMML: 1865	1994	37	-14.1	17.3
NMML: 1865	1998	41	-14.3	16.2
NMML: 1865	2004	47	-14.3	16.0

Table 4.3. Continued. The specimen IDs, estimated year and age represented by the sampled growth layer group (GLG), and the final $\delta^{13}C$ and $\delta^{15}N$ values for each GLG. See Bowen and Kurle in prep for other previous age estimates of these same teeth and discussions related to aging uncertainty.

Specimen ID	Estimated year	Estimated age	Final corrected $\delta^{13}C$ (‰)	$\delta^{15}N$ (‰)
NMML: 78	1925	4	-13.1	17.6
NMML: 78	1926	5	-13.4	17.3
NMML: 78	1927	6	-13.2	17.7
NMML: 78	1932	11	-12.3	18.0
NMML: 78	1934	13	-12.4	18.5
NMML: 78	1937	16	-12.4	18.8
NMML: 78	1940	19	-12.5	18.3
NMML: 78	1943	22	-12.2	18.1
NMML: 78	1946	25	-12.2	19.3
NMML: 78	1949	28	-12.3	19.8
NMML: 78	1952	31	-12.0	19.8
NMML: 78	1955	34	-11.8	19.0
NMML: 78	1958	37	-11.9	18.6
NMML: 78	1960	39	-12.0	19.4
NMML: 79	1922	4	-11.9	19.5
NMML: 79	1925	7	-11.7	20.1
NMML: 79	1928	10	-11.4	21.0
NMML: 79	1931	13	-11.7	20.3
NMML: 79	1934	16	-11.7	20.4
NMML: 79	1937	19	-11.3	20.5
NMML: 79	1940	22	-11.5	21.0
NMML: 79	1943	25	-11.5	21.1
NMML: 79	1946	28	-11.6	21.7
NMML: 79	1949	31	-11.5	22.3
NMML: 79	1952	34	-11.7	22.1
NMML: 79	1955	37	-11.8	22.8
NMML: 79	1958	40	-11.7	21.6
NMML: 79	1961	43	-12.1	22.1
NMML: 81	1948	4	-14.1	17.1
NMML: 81	1951	7	-13.9	17.1
NMML: 81	1954	10	-13.8	17.1
NMML: 81	1957	13	-14.3	16.9
NMML: 81	1960	16	-14.1	17.4
NMML: 81	1963	19	-14.2	17.6

Table 4.3. Continued. The specimen IDs, estimated year and age represented by the sampled growth layer group (GLG), and the final $\delta^{13}C$ and $\delta^{15}N$ values for each GLG. See Bowen and Kurle in prep for other previous age estimates of these same teeth and discussions related to aging uncertainty.

Specimen ID	Estimated year	Estimated age	Final corrected $\delta^{13}C$ (‰)	$\delta^{15}N$ (‰)
NMML: 82	1944	4	-13.2	18.1
NMML: 82	1947	7	-13.1	17.9
NMML: 82	1950	10	-13.4	17.7
NMML: 82	1953	13	-13.4	18.1
NMML: 82	1956	16	-13.3	18.5
NMML: 82	1959	19	-13.2	18.4
NMML: 82	1962	22	-13.3	18.4
NMML: 82	1965	25	-13.0	18.6
NMML: 84	1955	4	-13.2	19.1
NMML: 84	1957	6	-13.1	19.1
NMML: 84	1958	7	-12.7	19.2
NMML: 84	1961	10	-12.8	19.6
NMML: 84	1964	13	-12.6	19.9
NMML: 84	1965	14	-13.1	19.3
NMML: 84	1967	16	-13.1	19.6
NMML: 85	1954	4	-13.4	18.7
NMML: 85	1957	7	-13.2	18.5
NMML: 85	1960	10	-13.1	19.2
NMML: 85	1963	13	-13.3	19.2
NMML: 85	1966	16	-13.6	18.5
PWTooth	1978	4	-13.0	20.5
PWTooth	1981	7	-13.0	20.6
PWTooth	1984	10	-13.0	20.2
PWTooth	1987	13	-12.7	20.2
PWTooth	1990	16	-12.6	19.8
PWTooth	1993	19	-12.8	19.6
PWTooth	1996	22	-12.7	20.4
PWTooth	1999	25	-12.6	19.9
PWTooth	2002	28	-12.8	19.7
PWTooth	2005	31	-13.0	19.4
PWTooth	2008	34	-13.0	19.4

Table 4.3. Continued. The specimen IDs, estimated year and age represented by the sampled growth layer group (GLG), and the final $\delta^{13}C$ and $\delta^{15}N$ values for each GLG. See Bowen and Kurle in prep for other previous age estimates of these same teeth and discussions related to aging uncertainty.

Specimen ID	Estimated year	Estimated age	Final corrected $\delta^{13}C$ (‰)	$\delta^{15}N$ (‰)
RBCM: 10001	1948	7	-10.8	17.2
RBCM: 10001	1951	10	-11.1	18.5
RBCM: 10001	1954	13	-10.9	18.9
RBCM: 10001	1957	16	-11.0	18.6
RBCM: 10001	1960	19	-11.5	19.2
RBCM: 10001	1963	22	-11.6	19.5
RBCM: 10001	1966	25	-11.5	19.2
RBCM: 10001	1969	28	-11.5	19.6
RBCM: 10001	1974	33	-11.7	19.5
RBCM: 10001	1978	37	-11.3	19.7
RBCM: 10402	1976	4	-12.9	19.7
RBCM: 10402	1978	6	-12.4	20.9
RBCM: 10402	1980	8	-12.4	20.0
RBCM: 12844	1943	4	-11.3	20.2
RBCM: 12844	1946	7	-11.1	19.6
RBCM: 12844	1949	10	-10.7	19.8
RBCM: 12844	1952	13	-10.7	19.7
RBCM: 12844	1955	16	-10.8	19.6
RBCM: 12844	1958	18	-11.0	19.4
RBCM: 12844	1961	21	-10.9	19.8
RBCM: 12844	1964	23	-10.8	20.1
RBCM: 12844	1967	26	-10.9	20.2
RBCM: 12844	1970	29	-11.3	20.9
RBCM: 12844	1973	32	-10.9	20.6
RBCM: 12844	1976	35	-11.1	20.1
RBCM: 21479	1986	4	-12.4	21.4
RBCM: 21479	1989	7	-12.2	20.6
RBCM: 21479	1992	10	-12.4	21.1
RBCM: 21479	1995	13	-12.3	21.3
RBCM: 21479	1998	16	-12.1	21.3
RBCM: 21479	2001	19	-12.0	21.6
RBCM: 21479	2004	22	-11.9	21.6
RBCM: 21479	2007	25	-11.9	21.2
RBCM: 21479	2010	28	-11.9	20.7
RBCM: 21479	2013	31	-11.5	20.9
RBCM: 21479	2016	34	-11.5	20.7

Table 4.3. Continued. The specimen IDs, estimated year and age represented by the sampled growth layer group (GLG), and the final δ^{13}C and δ^{15}N values for each GLG. See Bowen and Kurle in prep for other previous age estimates of these same teeth and discussions related to aging uncertainty.

Specimen ID	Estimated year	Estimated age	Final corrected δ^{13}C (‰)	δ^{15}N (‰)
RBCM: 21490	1983	4	-14.9	15.1
RBCM: 21490	1986	7	-15.2	15.6
RBCM: 21490	1989	10	-15.0	16.1
RBCM: 21490	1992	13	-15.3	15.7
RBCM: 21490	1995	16	-15.2	15.4
RBCM: 21490	1998	19	-16.5	15.7
RBCM: 21490	2001	22	-15.1	15.9
RBCM: 21490	2004	25	-15.3	15.3
RBCM: 21490	2007	28	-15.1	15.2
RBCM: 21490	2010	31	-15.2	14.8
RBCM: 21491	1988	4	-11.7	20.0
RBCM: 21491	1991	7	-11.0	20.1
RBCM: 21491	1994	10	-10.9	20.4
RBCM: 21491	1997	13	-11.3	20.3
RBCM: 21491	2000	16	-11.3	20.5
RBCM: 21491	2003	19	-11.7	20.8
RBCM: 21491	2006	22	-11.8	21.1
RBCM: 21491	2009	25	-11.5	21.2
RBCM: 21491	2012	28	-11.9	21.5
UAM: 101747	1997	4	-12.5	19.7
UAM: 101747	1999	6	-12.4	19.9
UAM: 101747	2003	10	-12.7	20.3
UAM: 101796	1996	4	-13.0	20.3
UAM: 101796	1999	7	-12.8	19.2
UAM: 101796	2002	10	-12.9	19.0
UAM: 101796	2005	13	-12.5	20.2
UAM: 134310	1988	4	-13.2	19.4
UAM: 134310	1991	7	-13.1	19.5
UAM: 134310	1994	10	-13.0	19.1
UAM: 134310	1997	13	-12.5	18.6
UAM: 134310	2000	16	-12.9	18.6
UAM: 134310	2003	19	-13.1	19.1
UAM: 134310	2006	22	-13.1	19.4
UAM: 134310	2009	25	-13.2	18.5
UAM: 134310	2012	28	-13.1	19.1
UAM: 134310	2015	31	-13.1	18.4

Table 4.3. Continued. The specimen IDs, estimated year and age represented by the sampled growth layer group (GLG), and the final $\delta^{13}C$ and $\delta^{15}N$ values for each GLG. See Bowen and Kurle in prep for other previous age estimates of these same teeth and discussions related to aging uncertainty.

Specimen ID	Estimated year	Estimated age	Final corrected $\delta^{13}C$ (‰)	$\delta^{15}N$ (‰)
UAM: 134311	2000	4	-13.0	19.5
UAM: 134311	2003	7	-13.5	18.4
UAM: 134311	2006	10	-12.9	18.3
UAM: 134311	2009	13	-12.7	18.8
UAM: 134311	2012	16	-12.9	19.1
UAM: 134311	2015	19	-13.2	19.8
USNM: 256000	1911	4	-12.7	20.7
USNM: 256000	1914	7	-13.3	19.8
USNM: 256000	1917	10	-13.1	19.9
USNM: 256000	1920	13	-13.0	20.8
USNM: 256000	1923	16	-12.7	20.3
USNM: 256000	1926	19	-12.9	19.6
USNM: 256000	1929	22	-12.9	19.2
USNM: A13018	1855	4	-12.3	18.7
USNM: A13018	1856	5	-12.8	18.5
USNM: A13018	1857	6	-13.1	18.9

Table 4.4. Summary statistics for the stable isotope values of dentin from 36 transient killer whales sampled in this study. We first calculated a mean for each individual animal from all growth layer groups (GLGs) sampled, and then we averaged the individual means to identify the '*Means of individual means*' for killer whales collected in California ('CA)' and in Alaska, Oregon, or Washington ('AK'). Within the AK transients, we also report the mean of all individual GLGs before 1970 and after (inclusive of) 1970. We were unable to calculate individual means pre-and post-1970 since some individuals lived before and after 1970.

	δ^{13}C (‰)						δ^{15}N (‰)				
	Median	Mean	SD	Min	Max		Median	Mean	SD	Min	Max
Means of individual means											
CA transients (n = 14)	-12.8	-12.8	0.6	-14.1	-11.6		18.9	19.3	1.5	17.2	22.3
AK transients (n = 22)	-12.8	-12.7	1.0	-15.3	-11.0		19.8	19.4	1.4	15.5	21.5
Mean of all GLGs											
AK transients pre-1970	-12.3	-12.3	1.2	-14.9	-10.7		19.3	19.0	1.3	15.7	20.8
AK transients post-1970	-12.8	-12.9	1.2	-16.5	-10.9		19.7	19.3	1.7	14.8	21.7

Table 4.5. Results from ANOVAs of four separate linear mixed models (LMMs) to investigate the effect of time (categorical) and age (continuous), with all possible interactions, on transient killer whale δ^{13}C and δ^{15}N values. Specimen ID was used as a random factor to account for multiple samples within an individual tooth. We used data from 36 total individuals. Significance codes are: *** < 0.001, ** < 0.01, * < 0.05.

Response variable and model	*SS*	*NumDF*	*DenDF*	*F*	*p*	
AK transients, δ^{15}N (‰)						
Time	2.81	1	143.23	14.23	0.00	***
Age	0.31	1	140.10	1.55	0.22	
Time:Age	0.50	1	137.87	2.52	0.12	
AK transients, δ^{13}C (‰)						
Time	0.35	1	142.00	4.46	0.04	*
Age	0.02	1	139.55	0.24	0.63	
Time:Age	0.11	1	137.81	1.40	0.24	
CA transients, δ^{15}N (‰)						
Time	0.27	1	101.24	1.78	0.18	
Age	2.11	1	97.19	13.79	0.00	***
Time:Age	1.67	1	96.89	10.94	0.00	**
CA transients, δ^{13}C (‰)						
Time	0.04	1	100.17	0.43	0.51	
Age	0.00	1	103.10	0.02	0.87	
Time:Age	0.27	1	102.75	3.18	0.08	

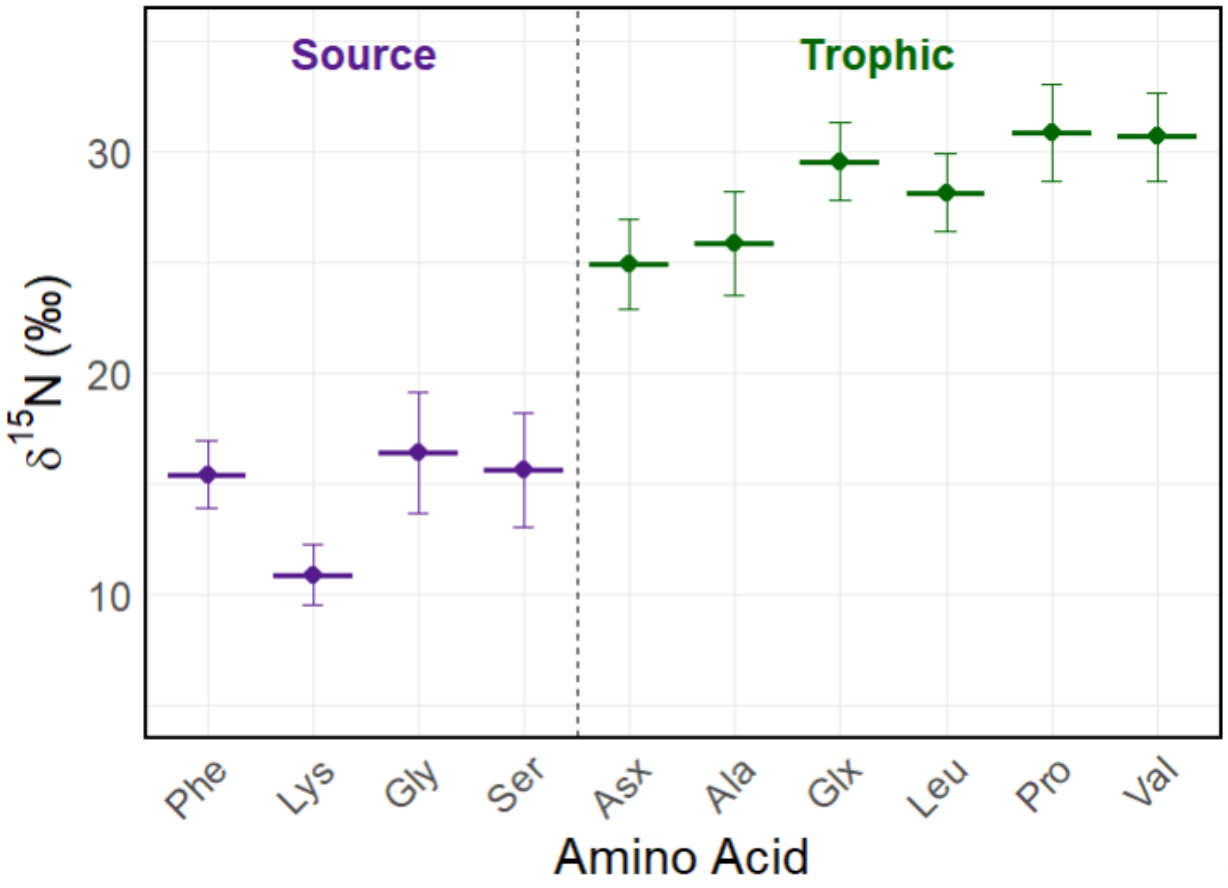


Figure S4.1. The mean δ^{15}N values with standard deviation error bars are shown for each of 10 amino acids: four source amino acids (left, purple) and six trophic amino acids (right, green).

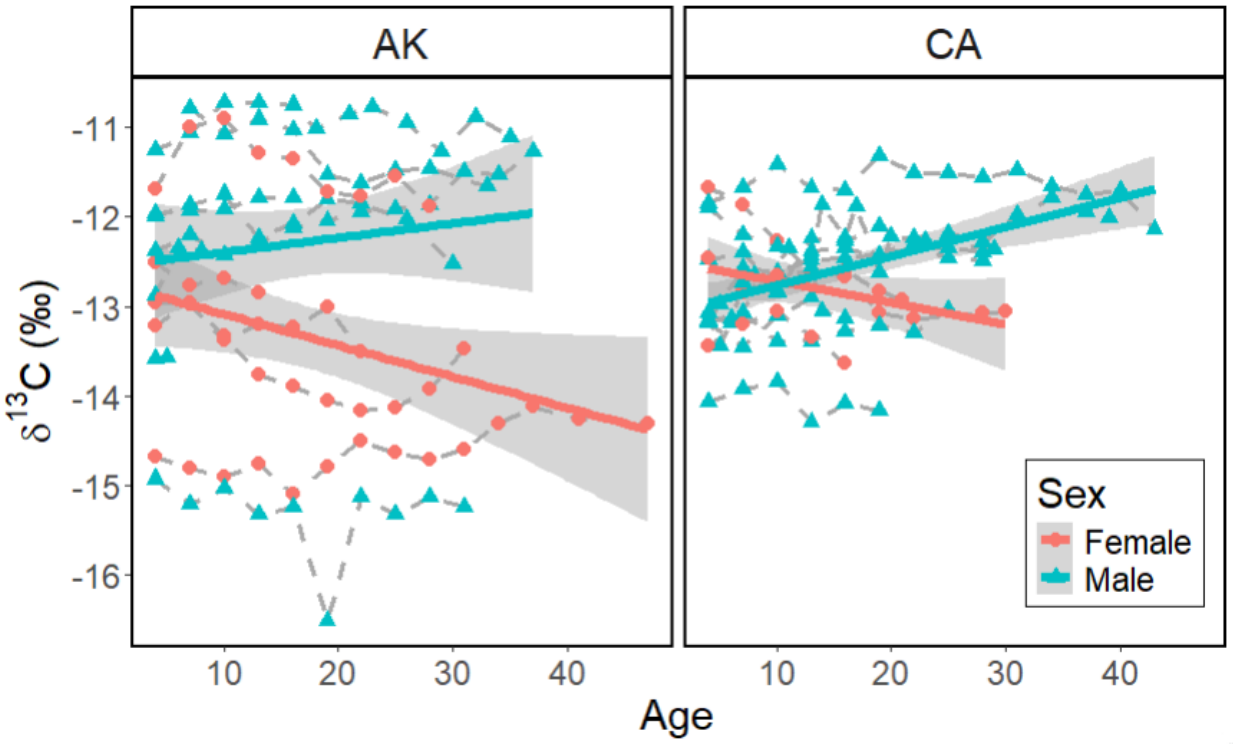


Figure S4.2. The δ^{13}C values of both Alaska (AK) and California (CA) transient killer whales are shown across ages for males (blue triangles) and females (red circles). Trend lines are shown for all data points in that category, and dashed grey lines indicate sampled growth layer groups within an individual.

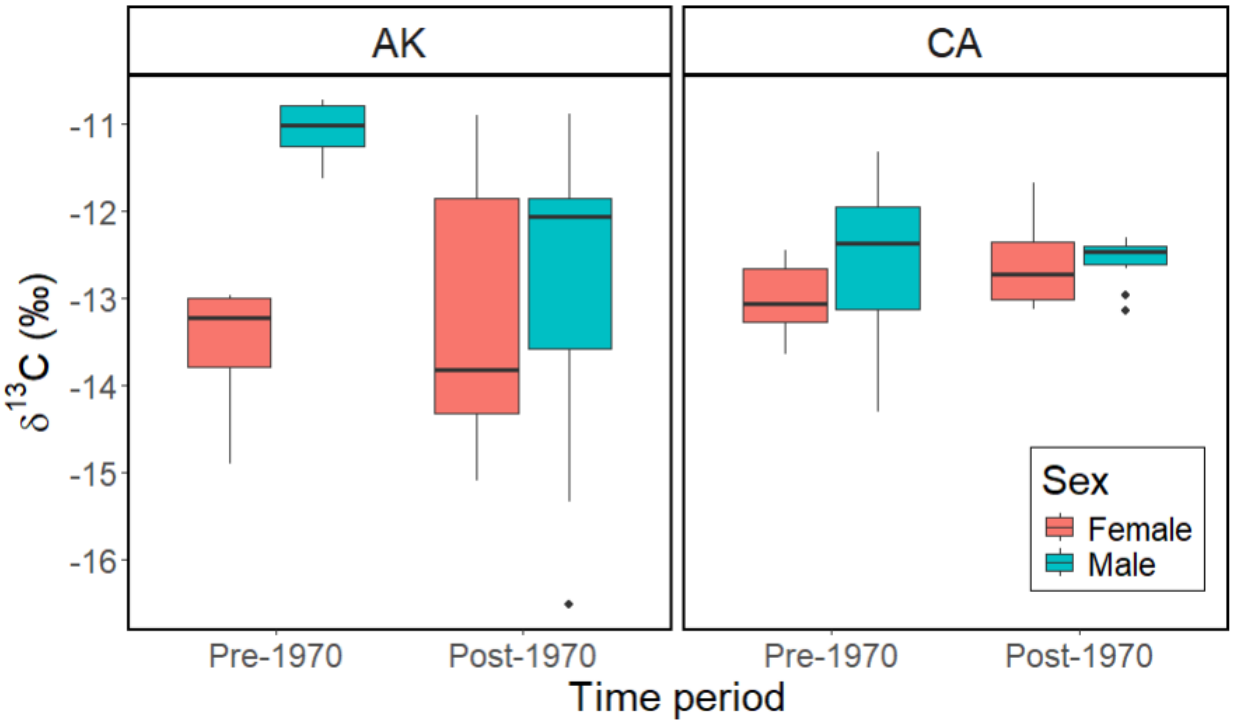


Figure S4.3. Boxplots of the δ^{13}C values (all sampled growth layer groups) pre- and post-1970 for males (blue) and females (red) in both Alaska (AK) and California (CA) transient killer whale populations.

Table S4.1. The specimen IDs (* = from external sources not measured in our study), ecotype (O = offshore, R = resident, T = transient), sex (NA = not available, F = female, M = male), and the δ^{13}C and δ^{15}N values of the specimen used in our ecotype prediction model.

Specimen ID	Ecotype	Sex	δ^{13}C (‰)	δ^{15}N (‰)
AMNH: 80294	O	NA	-11.5	16.4
CAS: 20749	O	F	-13.6	16.0
CAS: 29219	O	M	-14.1	17.5
LACM: 1790	O	F	-12.8	16.9
MML-1964-986	O	F	-13.6	16.5
NMML: 80	O	F	-13.6	16.3
NMML: 87	O	M	-13.2	18.0
PGNHM: 2540A	O	F	-13.6	16.7
RBCM: 5214	O	F	-13.1	16.8
UWBM: 82332	O	F	-14.9	16.0
UWBM: 82333	O	M	-15.0	15.6
UWBM: 82688	O	F	-13.3	17.2
AF_57355*	R	NA	-14.3	15.3
BBM: C21	R	F	-13.3	17.8
BBM: J18	R	M	-13.2	17.2
MML: 3265	R	F	-11.8	18.0
MML: 3266	R	M	-12.0	18.2
NMML: 1903	R	F	-12.8	17.7
NMML: 77	R	M	-11.7	17.8
NMML: 88	R	M	-12.7	17.2
NMML: 89	R	M	-12.1	18.0
NMML: 90 (594675)	R	F	-13.6	17.7
Namu	R	M	-11.7	17.5
RBCM: 16006	R	F	-11.7	17.6
RBCM: 16814	R	M	-12.0	18.1
RBCM: 8386	R	M	-12.5	17.5
USNM: 16488	R	NA	-12.8	17.1
USNM: 16625	R	NA	-12.1	17.6
USNM: 239357	R	NA	-12.9	17.1

Table S4.1. Continued. The specimen IDs (* = from external sources not measured in our study), ecotype (O = offshore, R = resident, T = transient), sex (NA = not available, F = female, M = male), and the $\delta^{13}C$ and $\delta^{15}N$ values of the specimen used in our ecotype prediction model.

Specimen ID	Ecotype	Sex	$\delta^{13}C$ (‰)	$\delta^{15}N$ (‰)
UWBM: 12030	R	NA	-11.8	18.1
UWBM: 26183	R	F	-11.8	17.7
AMMSN: 2020_192	T	M	-12.9	20.0
BBM: "Eyak"	T	M	-12.9	20.2
HSU_8404	T	F	-12.8	19.7
LACM: 54444	T	F	-13.1	20.9
MML: 1963-832	T	M	-12.0	21.3
MML: 1965-4	T	M	-14.8	17.5
MML: 1967-157	T	M	-13.4	19.6
MML: 1967-175	T	M	-13.7	19.0
MML: US-61-1k	T	M	-13.2	18.6
MVZ: 129686	T	M	-12.4	22.3
NGOS_1*	T	NA	-12.6	20.1
NGOS_2*	T	NA	-12.2	20.0
NMML: 1850	T	F	-14.1	19.5
NMML: 1865	T	F	-15.1	16.5
NMML: 78	T	M	-12.6	18.6
NMML: 79	T	M	-11.8	21.2
NMML: 81	T	M	-14.3	17.2
NMML: 82	T	M	-13.4	18.2
NMML: 84	T	M	-13.2	19.4
NMML: 85	T	F	-13.6	18.8
PW	T	NA	-13.7	20.0
RBCM: 10001	T	M	-11.6	18.6
RBCM: 10402	T	M	-13.0	20.2
RBCM: 12844	T	M	-11.2	20.0
RBCM: 21479	T	M	-12.8	21.1
RBCM: 21490	T	M	-16.0	15.5
RBCM: 21491	T	F	-12.2	20.6
SBNHM-1546*	T	NA	-12.5	20.2
UAM: 101796	T	NA	-13.6	19.7
UAM: 134310	T	NA	-14.1	19.0
UAM: 134311	T	NA	-14.2	19.0
USNM: A13018	T	NA	-12.8	18.7

Table S4.2. The output of our ecotype prediction model from stable isotope data using a multinomial regression analysis with input data from known ecotypes (Table S4.1). Offshore, resident, and transient columns show the probability that the specimen belongs to that ecotype. The classification column is the ecotype determined by the highest probability (T = transient, O = offshore, R = resident).

Specimen ID	Offshore	Resident	Transient	Classification
2020_023	0.023	0.014	0.963	T
2020_063	0.762	0.044	0.194	O
AMMSN: 2020_246	0.000	0.000	1.000	T
AMMSN: 2021_010	0.000	0.000	1.000	T
AMMSN: 2021_017	0.932	0.060	0.008	O
AMNH: 34276	0.746	0.254	0.000	O
AMNH: 34844	0.030	0.110	0.860	T
CAS: 20754	0.000	0.000	1.000	T
CAS: 30729	0.091	0.230	0.679	T
CRC: 1932	0.988	0.011	0.001	O
HSU: 4107	0.005	0.028	0.967	T
LACM: 30461	0.207	0.588	0.205	R
MML: 1966-145	0.020	0.065	0.915	T
MML: 3204	0.126	0.272	0.603	T
MML: 99-1	0.000	0.002	0.998	T
MML: 3264	0.240	0.622	0.138	R
MML: 3774	0.076	0.240	0.684	T
MML: 1984-1	0.002	0.027	0.972	T
MML: 60-1	0.129	0.828	0.044	R
MVZ: 208592	0.000	0.000	1.000	T
UAM: 101747	0.000	0.000	1.000	T
UAM: 85504	0.928	0.071	0.000	O
USNM: 256000	0.000	0.001	0.999	T
USNM: 504965	0.720	0.208	0.072	O
UWBM: 81700	0.001	0.005	0.994	T

Table S4.3. The δ^{15}N values from compound-specific isotope analysis of amino acids (CSIA-AA) separated into 'source' amino acids and 'trophic' amino acids.

Specimen ID	Alternate ID	Location	Est. age	Est. year	"Source" amino acids				"Trophic" amino acids					
					Phe	*Lys*	*Gly*	*Ser*	*Asx*	*Ala*	*Glx*	*Leu*	*Pro*	*Val*
RBCM: 12844		AK	28	1969	14.9	10.8	16.7	16.9	26.4	27.5	30.3	28.9	32.3	30.5
NMML: 1865		AK	15	1972	13.1	8.3	10.5	9.4	22.5	23.7	27.7	27.2	30.8	29.0
NMML: 1850		AK	15	1977	15.4	11.7	15.1	14.4	24.2	24.9	29.8	28.4	30.8	29.9
PWTooth		AK	12	1986	15.5	10.1	17.4	16.3	25.1	25.6	29.0	27.1	30.5	30.5
RBCM: 21479		AK	12	1994	15.0	9.6	17.0	16.7	26.9	28.1	30.6	29.9	32.8	32.2
RBCM: 21491		AK	17	2001	16.8	10.5	16.5	16.1	26.0	28.0	30.1	28.8	31.4	31.4
NMML: 78		CA	23	1944	14.7	11.6	16.0	15.4	23.5	24.2	28.7	27.5	29.1	29.5
NMML: 79		CA	30	1948	17.5	13.0	20.3	19.2	27.1	28.4	31.5	29.5	32.9	33.1
MVZ: 129686		CA	13	1954	17.2	12.7	20.4	18.5	27.2	27.8	32.1	30.7	33.3	33.5
NMML: 81		CA	15	1959	12.8	10.9	14.1	14.3	21.2	21.0	25.9	24.3	25.8	26.6
HSU: 8404		CA	11	1981	16.6	10.4	16.0	14.3	23.7	25.2	29.1	27.2	29.5	31.0

Table S4.4. The mean and standard deviation (SD) for the $\delta^{13}C$ and the $\delta^{15}N$ values of two primary prey groups we examined in our study, pinnipeds and mysticetes, used as input for a MixSIAR analysis. Values were calculated from the meta-analysis in Chapter 3.

Prey group	**Mean $\delta^{13}C$ (‰)**	**SD**	**Mean $\delta^{15}N$ (‰)**	**SD**	**n**
Pinnipeds	-15.95	1.70	17.64	1.29	1139
Mysticetes	-18.16	1.57	11.70	2.15	3672

Table S4.5. Results of linear mixed models used to investigate the effects of sex, time, and age on Alaska (AK) and California (CA) killer whales. Significance codes are: *** < 0.001, ** < 0.01, * < 0.05.

Response variable and model	*Estimate*	*SE*	*DF*	*t-value*	*p*	
AK transients, δ^{15}N (‰)						
Intercept	18.29	0.84	12.86	21.68	0.00	***
Time (Post-1970)	0.71	0.33	87.81	2.17	0.03	*
Estimated age	0.04	0.02	88.09	1.58	0.12	
Sex (Male)	-0.40	1.10	14.11	-0.36	0.73	
Time (Post-1970):Estimated age	-0.03	0.03	87.84	-1.02	0.31	
Time (Post-1970):Sex (Male)	0.76	0.51	89.07	1.48	0.14	
Estimated age:Sex (Male)	0.01	0.03	87.84	0.23	0.82	
Time (Post-1970):Estimated age:Sex (Male)	-0.02	0.03	87.80	-0.66	0.51	
AK transients, δ^{13}C (‰)						
Intercept	-12.81	0.60	13.11	-21.29	0.00	***
Time (Post-1970)	-0.44	0.25	87.89	-1.77	0.08	
Estimated age	-0.02	0.02	88.22	-1.27	0.21	
Sex (Male)	0.87	0.79	14.54	1.10	0.29	
Time (Post-1970):Estimated age	0.03	0.02	87.92	1.49	0.14	
Time (Post-1970):Sex (Male)	-0.24	0.39	89.33	-0.63	0.53	
Estimated age:Sex (Male)	0.01	0.02	87.93	0.55	0.59	
Time (Post-1970):Estimated age:Sex (Male)	-0.01	0.02	87.89	-0.39	0.70	
CA transients, δ^{15}N (‰)						
Intercept	18.61	0.95	13.90	19.58	0.00	***
Time (Post-1970)	0.74	0.74	91.91	1.00	0.32	
Estimated age	0.04	0.03	86.33	1.48	0.14	
Sex (Male)	0.17	1.08	13.45	0.16	0.88	
Time (Post-1970):Estimated age	-0.04	0.03	88.77	-1.05	0.30	
Time (Post-1970):Sex (Male)	-0.50	0.89	93.12	-0.57	0.57	
Estimated age:Sex (Male)	0.01	0.03	86.34	0.52	0.60	
Time (Post-1970):Estimated age:Sex (Male)	-0.01	0.04	89.23	-0.33	0.74	
CA transients, δ^{13}C (‰)						
Intercept	-12.76	0.41	18.55	-31.35	<2e-16	***
Time (Post-1970)	1.13	0.47	96.72	2.42	0.02	*
Estimated age	-0.02	0.02	86.52	-1.31	0.20	
Sex (Male)	-0.08	0.46	17.24	-0.18	0.86	
Time (Post-1970):Estimated age	-0.04	0.02	92.00	-1.97	0.05	
Time (Post-1970):Sex (Male)	-1.47	0.55	96.99	-2.67	0.01	**
Estimated age:Sex (Male)	0.03	0.02	86.56	1.95	0.05	
Time (Post-1970):Estimated age:Sex (Male)	0.05	0.02	92.69	2.13	0.04	*

Table S4.6. Results from Analysis of Variance tests (ANOVAs) used to assess which variables in the linear mixed model (Table S4.5) were significant predictors of $\delta^{13}C$ and $\delta^{15}N$ values in Alaska (AK) and California (CA) killer whales. Significance codes are: *** < 0.001, ** < 0.01, * < 0.05.

Response variable and model	*SS*	*NumDF*	*DenDF*	*F*	*p*	
AK transients, $\delta^{15}N$ (‰)						
Time	2.81	1	89.07	18.00	0.00	***
Age	1.48	1	88.17	9.46	0.00	**
Sex	0.00	1	11.66	0.00	0.99	
Time:Age	0.89	1	87.80	5.67	0.02	*
Time:Sex	0.34	1	89.07	2.20	0.14	
Age:Sex	0.01	1	88.17	0.05	0.82	
Time:Age:Sex	0.07	1	87.80	0.43	0.51	
AK transients, $\delta^{13}C$ (‰)						
Time	0.75	1	89.33	8.28	0.01	**
Age	0.08	1	88.30	0.83	0.36	
Sex	0.09	1	11.72	1.00	0.34	
Time:Age	0.41	1	87.89	4.52	0.04	*
Time:Sex	0.04	1	89.33	0.39	0.53	
Age:Sex	0.03	1	88.30	0.38	0.54	
Time:Age:Sex	0.01	1	87.89	0.15	0.70	
CA transients, $\delta^{15}N$ (‰)						
Time	0.19	1	93.12	1.24	0.27	
Age	0.85	1	88.91	5.46	0.02	*
Sex	0.00	1	12.93	0.01	0.94	
Time:Age	0.76	1	89.23	4.87	0.03	*
Time:Sex	0.05	1	93.12	0.32	0.57	
Age:Sex	0.02	1	88.91	0.14	0.71	
Time:Age:Sex	0.02	1	89.23	0.11	0.74	
CA transients, $\delta^{13}C$ (‰)						
Time	0.13	1	96.99	1.98	0.16	
Age	0.32	1	92.06	4.86	0.03	*
Sex	0.22	1	15.50	3.39	0.08	
Time:Age	0.13	1	92.69	1.95	0.17	
Time:Sex	0.46	1	96.99	7.11	0.01	**
Age:Sex	1.48	1	92.06	22.60	0.00	***
Time:Age:Sex	0.30	1	92.69	4.54	0.04	*

4.7 References

1. Lindeman RL. The trophic-dynamic aspect of ecology. *Ecology*. 1942;23(4):399-417. doi:10.2307/1930126

2. Paine RT. Food web complexity and species diversity. *The Am Nat*. 1966;100(910):65-75.

3. Polis G, Strong D. Food web complexity and community dynamics. *The Am Nat*. 1966;147(5):813-846.

4. Estes JA, Palmisano JF. Sea otters: Their role in structuring nearshore communities. *Science*. 1974;185(4156):1058-1060. doi:10.1126/science.185.4156.1058

5. Estes JA, Tinker MT, Williams TM, Doak DF. Killer whale predation on sea otters linking oceanic and nearshore ecosystems. *Science*. 1998;282(5388):473-476. doi:10.1126/science.282.5388.473

6. Österblom H, Hansson S, Larsson U, Hjerne O, Wulff F, Elmgren R, Folke C. Human-induced trophic cascades and ecological regime shifts in the Baltic Sea. *Ecosystems*. 2007;10(6):877-889. doi:10.1007/s10021-007-9069-0

7. Williams TM, Estes JA, Doak DF, Springer AM. Killer appetites: assessing the role of predators in ecological communities. *Ecology*. 2004;85(12):3373-3384. doi:10.1890/03-0696

8. Pan CW, Chen MH, Chou LS, Lin HJ. The trophic significance of the Indo-Pacific humpback dolphin, *Sousa chinensis*, in Western Taiwan. Li S, ed. *PLoS ONE*. 2016;11(10):e0165283. doi:10.1371/journal.pone.0165283

9. Jefferson TA, Stacey PJ, Baird RW. A review of killer whale interactions with other marine mammals: predation to co-existence. *Mamm Rev*. 1991;21(4):151-180. doi:10.1111/j.1365-2907.1991.tb00291.x

10. Ford JKB. Killer Whales: Behavior, Social Organization, and Ecology of the Oceans' Apex Predators. In: Würsig B, ed. *Ethology and Behavioral Ecology of Odontocetes*. Ethology and Behavioral Ecology of Marine Mammals. Springer International Publishing; 2019:239-259. doi:10.1007/978-3-030-16663-2_11

11. Towner AV, Watson RG, Kock AA, Papastamatiou Y, Sturup M, Gennari E, Baker K, Booth T, Dicken M, Chivell W, Elwen S. Fear at the top: killer whale predation drives white shark absence at South Africa's largest aggregation site. *Afr J Mar Sci*. 2022;44(2):139-152. doi:10.2989/1814232X.2022.2066723

12. Jorgensen SJ, Anderson S, Ferretti F, Tietz JR, Chapple T, Kanive P, Bradley RW, Moxley JH, Block BA. Killer whales redistribute white shark foraging pressure on seals. *Sci Rep*. 2019;9(6153). doi:https://doi.org/10.1038/s41598-019-39356-2

13. Breed GA, Matthews CJ, Marcoux M, Higdon JW, LeBlanc B, Petersen SD, Orr J, Reinhart NR, Ferguson SH. Sustained disruption of narwhal habitat use and behavior in the presence of Arctic killer whales. *Proc Natl Acad Sci USA*. 2017;114(10):2628-2633. doi:10.1073/pnas.1611707114

14. Bigg M. *An Assessment of Killer Whale (*Orcinus Orca*) Stocks off Vancouver Island, British Columbia*. Report of the International Whaling Commission; 1982:655-666.

15. Baird RW, Stacey PJ. Variation in saddle patch pigmentation in populations of killer whales (*Orcinus orca*) from British Columbia, Alaska, and Washington State. *Can J Zool*. 1988;66(11):2582-2585. doi:10.1139/z88-380

16. Bigg MA, Olesiuk PF, Ellis GM, Ford JKB, Balcomb KC. Social organization and genealogy of resident killer whales (*Orcinus orca*) in the coastal waters of British Columbia and Washington State. *Rep Int Whale Commn*. 1990;(12):383-405.

17. Barrett-Lennard LG, Ford JKB, Heise KA. The mixed blessing of echolocation: differences in sonar use by fish-eating and mammal-eating killer whales. *Anim Behav*. 1996;51(3):553-565. doi:10.1006/anbe.1996.0059

18. Ford JK, Ellis GM, Barrett-Lennard LG, Morton AB, Palm RS, Balcomb KC. Dietary specialization in two sympatric populations of killer whales (*Orcinus orca*) in coastal British Columbia and adjacent waters. *Can J Zool*. 1998;76(8):1456-1471. doi:10.1139/z98-089

19. Herman DP, Burrows DG, Wade PR, Durban JW, Matkin CO, LeDuc RG, Barrett-Lennard LG, Krahn MM. Feeding ecology of eastern North Pacific killer whales Orcinus orca from fatty acid, stable isotope, and organochlorine analyses of blubber biopsies. *Mar Ecol Prog Ser*. 2005;302:275-291. doi:10.3354/meps302275

20. Best PB, Meÿer MA, Lockyer C. Killer whales in South African waters—a review of their biology. *Afr J Mar Sci*. 2010;32(2):171-186. doi:10.2989/1814232X.2010.501544

21. De Bruyn PJN, Tosh CA, Terauds A. Killer whale ecotypes: is there a global model? *Biol Rev*. 2013;88(1):62-80. doi:10.1111/j.1469-185X.2012.00239.x

22. Morin PA, Parsons KM, Archer FI, Ávila-Arcos MC, Barrett-Lennard LG, Dalla Rosa L, Duchêne S, Durban JW, Ellis GM, Ferguson SH, Ford JK. Geographic and temporal dynamics of a global radiation and diversification in the killer whale. *Mol Ecol*. 2015;24(15):3964-3979. doi:10.1111/mec.13284

23. Jourdain E, Ugarte F, Víkingsson GA, Samarra FI, Ferguson SH, Lawson J, Vongraven D, Desportes G. North Atlantic killer whale *Orcinus orca* populations: a review of current knowledge and threats to conservation. *Mamm Rev*. 2019;49(4):384-400. doi:10.1111/mam.12168

24. Morin PA, McCarthy ML, Fung CW, Durban JW, Parsons KM, Perrin WF, Taylor BL, Jefferson TA, Archer FI. Revised taxonomy of eastern North Pacific killer whales (*Orcinus orca*): Bigg's and resident ecotypes deserve species status. *R Soc Open Sci*. 2024;11(3):231368. doi:10.1098/rsos.231368

25. Muto MM, Helker VT, Delean BJ, Young NC, Freed JC, Angliss RP, Friday NA, Boveng PL, Breiwick JM, Brost BM, Cameron MF. Alaska marine mammal stock assessments, 2020. Published online 2021. doi:10.25923/YN3S-N786

26. McInnes J, Mathieson C, West-Stap P, et al. Transient killer whales of central and northern California and Oregon: A catalog of photo-identified individuals. Published online 2021. doi:10.25923/60Y3-5M49

27. Dahlheim ME, White PA. Ecological aspects of transient killer whales *Orcinus orca* as predators in southeastern Alaska. *Wildl Biol*. 2010;16(3):308-322. doi:10.2981/09-075

28. Matkin C, Barrett-Lennard L, Ellis G. *Steller Sea Lion Decline: Is It Food II: Proceedings of the Workshop Is It Food II, Alaska Sealife Center, Seward, Alaska, May 2001*. (DeMaster DP, Alaska Sealife Center, eds.). Univ. of Alaska, Sea Grant College Program; 2002.

29. Black NA, Talty CM, Schulman-Janiger A, Srinivasan M. Mammal Hunting Killer Whales off Monterey, California: A 30-Year Synthesis. In: Srinivasan M, Würsig B, eds. *Social Strategies of Carnivorous Mammalian Predators*. Fascinating Life Sciences. Springer International Publishing; 2023:283-333. doi:10.1007/978-3-031-29803-5_8

30. McInnes JD, Lester KM, Dill LM, Mathieson CR, West-Stap PJ, Marcos SL, Trites AW. Foraging behaviour and ecology of transient killer whales within a deep submarine canyon system. Hyrenbach D, ed. *PLoS ONE*. 2024;19(3):e0299291. doi:10.1371/journal.pone.0299291

31. Barrett-Lennard L, Matkin C, Durban J, Saulitis E, Ellifrit D. Predation on gray whales and prolonged feeding on submerged carcasses by transient killer whales at Unimak Island, Alaska. *Mar Ecol Prog Ser*. 2011;421:229-241. doi:10.3354/meps08906

32. Springer AM, Estes JA, Van Vliet GB, Williams TM, Doak DF, Danner EM, Forney KA, Pfister B. Sequential megafaunal collapse in the North Pacific Ocean: An ongoing legacy of industrial whaling? *Proc Natl Acad Sci USA*. 2003;100(21):12223-12228. doi:10.1073/pnas.1635156100

33. Hanson MB, Baird RW, Ford JK, Hempelmann-Halos J, Van Doornik DM, Candy JR, Emmons CK, Schorr GS, Gisborne B, Ayres KL, Wasser SK. Species and stock identification of prey consumed by endangered southern resident killer whales in their summer range. *Endang Species Res*. 2010;11:69-82. doi:10.3354/esr00263

34. Ford J, Ellis G. Selective foraging by fish-eating killer whales *Orcinus orca* in British Columbia. *Mar Ecol Prog Ser*. 2006;316:185-199. doi:10.3354/meps316185

35. Merrick RL, Brown R, Calkins D, Loughlin T. A comparison of Steller sea lion, *Eumetopias jubatus*, pup masses between rookeries with increasing and decreasing populations. *Oceanogr Lit Rev*. 1996;9(43):926-927.

36. Adams T. *Foraging Differences and Early Maternal Investment in Adult Female Alaskan Steller Sea Lions (*Eumetopias Jubatus*)*. Ph.D. thesis. Texas A&M University; 2000.

37. Rea LD, Castellini MA, Fadely BS, Loughlin TR. Health status of young Alaska Steller sea lion pups (*Eumetopias jubatus*) as indicated by blood chemistry and hematology. *Comp Biochem Physiol Part A: Mol Integr Physiol*. 1998;120(4):617-623. doi:10.1016/S1095-6433(98)10074-0

38. National Research Council. *The Decline of the Steller Sea Lion in Alaskan Waters: Untangling Food Webs and Fishing Nets*. National Academies Press; 2003:10576. doi:10.17226/10576

39. Springer AM, Estes JA, Van Vliet GB, Williams TM, Doak DF, Danner EM, Pfister B. Mammal-eating killer whales, industrial whaling, and the sequential megafaunal collapse in the North Pacific Ocean: A reply to critics of Springer *et al*. 2003. *Mar Mamm Sci*. 2008;24(2):414-442. doi:10.1111/j.1748-7692.2008.00185.x

40. DeMaster DP, Trites AW, Clapham P, Mizroch S, Wade P, Small RJ, Ver Hoef J. The sequential megafaunal collapse hypothesis: Testing with existing data. *Prog Oceanogr*. 2006;68(2-4):329-342. doi:10.1016/j.pocean.2006.02.007

41. Mizroch S, Rice D. Have North Pacific killer whales switched prey species in response to depletion of the great whale populations? *Mar Ecol Prog Ser*. 2006;310:235-246. doi:10.3354/meps310235

42. Ford JKB, Reeves RR. Fight or flight: antipredator strategies of baleen whales. *Mamm Rev*. 2008;38(1):50-86. doi:10.1111/j.1365-2907.2008.00118.x

43. Wade PR, Burkanov VN, Dahlheim ME, Friday NA, Fritz LW, Loughlin TR, Mizroch SA, Muto MM, Rice DW, Barrett-Lennard LG, Black NA. Killer whales and marine mammal trends in the North Pacific—a re-examination of evidence for sequential megafauna collapse and the prey-switching hypothesis. *Mar Mamm Sci*. 2007;23(4):766-802. doi:10.1111/j.1748-7692.2006.00093.x

44. Hobson KA, Sease JL. Stable isotope analyses of tooth annuli reveal temporal dietary records: an example using Steller sea lions. *Mar Mamm Sci*. 1998;14(1):116-129. doi:10.1111/j.1748-7692.1998.tb00694.x

45. Walker JL, Macko SA. Dietary studies of marine mammals using stable carbon and nitrogen isotopic ratios of teeth. *Mar Mamm Sci*. 1999;15(2):314-334. doi:10.1111/j.1748-7692.1999.tb00804.x

46. Clementz MT, Koch PL. Differentiating aquatic mammal habitat and foraging ecology with stable isotopes in tooth enamel. *Oecologia*. 2001;129(3):461-472. doi:10.1007/s004420100745

47. Hamilton V, Evans K. Establishing growth chronologies from marine mammal teeth: A method applicable across species. *J Exp Mar Biol Ecol*. 2018;505:24-34. doi:10.1016/j.jembe.2018.04.006

48. Newsome S, Etnier M, Monson D, Fogel M. Retrospective characterization of ontogenetic shifts in killer whale diets via δ^{13}C and δ^{15}N analysis of teeth. *Mar Ecol Prog Ser*. 2009;374:229-242. doi:10.3354/meps07747

49. Newsome SD, Clementz MT, Koch PL. Using stable isotope biogeochemistry to study marine mammal ecology. *Mar Mamm Sci*. Published online January 2010. doi:10.1111/j.1748-7692.2009.00354.x

50. Hanson N, Jones EL, Harris RN. Multi-decadal and ontogenetic trophic shifts inferred from stable isotope ratios of pinniped teeth. *Oikos*. 2018;127(1):134-146. doi:10.1111/oik.04441

51. Teixeira CR, Troina GC, Daura-Jorge FG, Simões-Lopes PC, Botta S. A practical guide on stable isotope analysis for cetacean research. *Mar Mamm Sci*. 2022;38(3):1200-1228. doi:10.1111/mms.12911

52. Post DM. Using stable isotopes to estimate trophic position: models, methods, and assumptions. *Ecology*. 2002;83(3):703-718. doi:10.1890/0012-9658(2002)083[0703:USITET]2.0.CO;2

53. Roughgarden J. Evolution of niche width. *The Am Nat*. 1972;106(952):683-718. doi:10.1086/282807

54. Bolnick DI, Svanbäck R, Fordyce JA, Yang LH, Davis JM, Hulsey CD, Forister ML. The ecology of individuals: incidence and implications of individual specialization. *The Am Nat*. 2003;161(1):1-28.

55. Newsome SD, Tinker MT, Monson DH, Oftedal OT, Ralls K, Staedler MM, Fogel ML, Estes JA. Using stable isotopes to investigate individual diet specialization in California sea otters (*Enhydra lutris nereis*). *Ecology*. 2009;90(4):961-974. doi:10.1890/07-1812.1

56. Rossman S, Ostrom PH, Stolen M, Barros NB, Gandhi H, Stricker CA, Wells RS. Individual specialization in the foraging habits of female bottlenose dolphins living in a trophically diverse and habitat rich estuary. *Oecologia*. 2015;178(2):415-425. doi:10.1007/s00442-015-3241-6

57. Stock BC, Jackson AL, Ward EJ, Parnell AC, Phillips DL, Semmens BX. Analyzing mixing systems using a new generation of Bayesian tracer mixing models. *PeerJ*. 2018;6:e5096. doi:10.7717/peerj.5096

58. McMahon KW, Hamady LL, Thorrold SR. A review of ecogeochemistry approaches to estimating movements of marine animals. *Limnol Oceanogr*. 2013;58(2):697-714. doi:10.4319/lo.2013.58.2.0697

59. McMahon KW, McCarthy MD. Embracing variability in amino acid $\delta^{15}N$ fractionation: mechanisms, implications, and applications for trophic ecology. *Ecosphere*. 2016;7(12):e01511. doi:10.1002/ecs2.1511

60. Popp BN, Graham BS, Olson RJ, Hannides CC, Lott MJ, López-Ibarra GA, Galván-Magaña F, Fry B. Insight into the Trophic Ecology of Yellowfin Tuna, *Thunnus albacares*, from Compound-Specific Nitrogen Isotope Analysis of Proteinaceous Amino Acids. In: *Terrest Ecol*. Vol 1. Elsevier; 2007:173-190. doi:10.1016/S1936-7961(07)01012-3

61. Baird R. *Foraging Behaviour and Ecology of Transient Killer Whales (*Orcinus Orca*)*. Ph.D. thesis. Simon Fraser University; 1994. https://summit.sfu.ca/_flysystem/fedora/sfu_migrate/5048/b14873187.pdf

62. Ford JKB, Ellis GM, Balcomb KC. *Killer Whales: The Natural History and Genealogy of Orinus Orca in British Columbia and Washington*. 2nd ed. UBC Press ; University of Washington Press; 2000.

63. Turner Tomaszewicz CN, Seminoff JA, Avens L, Kurle CM. Methods for sampling sequential annual bone growth layers for stable isotope analysis. Fisher D, ed. *Methods Ecol Evol*. 2016;7(5):556-564. doi:10.1111/2041-210X.12522

64. Lockyer C, Hohn AA, Hobbs R, Stewart RE. Report of the workshop on age estimation in beluga: Beaufort, North Carolina, US 5-9 December 2011. *NAMMCOSP*. 2016;8. doi:10.7557/3.3731

65. Hohn AA. Age estimation. In: *Encyclopedia of Marine Mammals*. Academic Press; 2009:11-17.

66. Perrin WF, Myrick AC. *Age Determination of Toothed Whales and Sirenians*. International Conference on Determining Age of Odontocete Cetaceans and Sirenians. International Whaling Commission; 1980.

67. Evans K, Robertson K. A note on the preparation of sperm whale (*Physeter macrocephalus*) teeth for age determination. *jcrm*. 2001;3(1):101-107. doi:10.47536/jcrm.v3i1.907

68. Watt CA, Stewart BE, Loseto L, Halldorson T, Ferguson SH. Estimating narwhal (*Monodon monoceros*) age using tooth layers and aspartic acid racemization of eye lens nuclei. *Mar Mamm Sci*. 2020;36(1):103-115. doi:10.1111/mms.12623

69. GIMP Development Team. Published online 2019. https://www.gimp.org

70. Mendes S, Newton J, Reid RJ, Frantzis A, Pierce GJ. Stable isotope profiles in sperm whale teeth: variations between areas and sexes. *J Mar Biol Ass*. 2007;87(2):621-627. doi:10.1017/S0025315407056019

71. Frie AK, Hammill MO, Hauksson E, Lind Y, Lockyer C, Stenman O, Svetocheva O. Error patterns in age estimation and tooth readability assignment of grey seals (*Halichoerus grypus):* results from a transatlantic, image-based, blind-reading study using known-age animals. *ICES J Mar Sci*. 2013;70(2):418-430. doi:10.1093/icesjms/fss169

72. Read FL, Hohn AA, Lockyer CH. A review of age estimation methods in marine mammals with special reference to monodontids. *NAMMCOSP*. 2018;10. doi:10.7557/3.4474

73. Nehasil S. *Examining Trophic Relationships between Top Predators and Their Prey in a Coastal Upwelling Ecosystem*. Ph.D. thesis. University of California San Diego; 2023. https://escholarship.org/uc/item/6245g9bm

74. Hanson N, Wurster C, Bird M, Reid K, Boyd I. Intrinsic and extrinsic forcing in life histories: patterns of growth and stable isotopes in male Antarctic fur seal teeth. *Mar Ecol Prog Ser*. 2009;388:263-272. doi:10.3354/meps08158

75. Brault EK, Koch PL, Gier E, Ruiz-Cooley RI, Zupcic J, Gilbert KN, McCarthy MD. Effects of decalcification on bulk and compound-specific nitrogen and carbon isotope analyses of dentin. *Rapid Comm Mass Spectrometry*. 2014;28(24):2744-2752. doi:10.1002/rcm.7073

76. Groom B. *Effects of Decalcification, Species, and Mammalian Order on Bulk Stable Isotope Values from Marine Mammal Teeth*. University of California San Diego; 2018. https://www.proquest.com/openview/7b61f9e80a3bd2171850ad4a04ac42f4/1?pq-origsite=gscholar&cbl=18750

77. Corr LT, Berstan R, Evershed RP. Optimisation of derivatisation procedures for the determination of $\delta^{13}C$ values of amino acids by gas chromatography/combustion/isotope ratio mass spectrometry. *Rapid Comm Mass Spectrometry*. 2007;21(23):3759-3771. doi:10.1002/rcm.3252

78. Yarnes CT, Herszage J. The relative influence of derivatization and normalization procedures on the compound-specific stable isotope analysis of nitrogen in amino acids. *Rapid Comm Mass Spectrometry*. 2017;31(8):693-704. doi:10.1002/rcm.7832

79. Keeling CD. The Suess effect: ^{13}Carbon-^{14}Carbon interrelations. *Environ Int*. 1979;2(4-6):229-300. doi:10.1016/0160-4120(79)90005-9

80. Clark CT, Cape MR, Shapley MD, Mueter FJ, Finney BP, Misarti N. SuessR: Regional corrections for the effects of anthropogenic CO_2 on $\delta^{13}C$ data from marine organisms. *Methods Ecol Evol*. 2021;12(8):1508-1520. doi:10.1111/2041-210X.13622

81. Clark C, Cape M, Shapley M, Mueter F, Finney B, Misarti N. SuessR: Suess and Laws corrections for marine stable carbon isotope data. Published online 2023. https://CRAN.R-project.org/package=SuessR

82. R Core Team. R: A language and environment for statistical computing. Published online 2022. https://www.R-project.org/

83. Ambrose SH. Preparation and characterization of bone and tooth collagen for isotopic analysis. *J Archaeol Sci*. 1990;17(4):431-451. doi:10.1016/0305-4403(90)90007-R

84. Post DM, Layman CA, Arrington DA, Takimoto G, Quattrochi J, Montaña CG. Getting to the fat of the matter: models, methods and assumptions for dealing with lipids in stable isotope analyses. *Oecologia*. 2007;152(1):179-189. doi:10.1007/s00442-006-0630-x

85. Pereira LB, Botta S, Teixeira CR, Fruet P, Simões-Lopes PC, Daura-Jorge FG. Feeding ecology of two subspecies of bottlenose dolphin: a tooth tale. *Aquat Ecol*. 2020;54(4):941-955. doi:10.1007/s10452-020-09785-7

86. Posit Team. RStudio: Integrated Development Environment for R. Published online 2024.

87. Hare SR, Mantua NJ. Empirical evidence for North Pacific regime shifts in 1977 and 1989. *Prog Oceanogr*. 2000;47(2-4):103-145. doi:10.1016/S0079-6611(00)00033-1

88. Kuznetsova A, Brockhoff PB, Christensen RHB. lmerTest Package: Tests in Linear Mixed Effects Models. *J Stat Soft*. 2017;82(13). doi:10.18637/jss.v082.i13

89. Jackson AL, Inger R, Parnell AC, Bearhop S. Comparing isotopic niche widths among and within communities: SIBER - Stable Isotope Bayesian Ellipses in R: Bayesian isotopic niche metrics. *Journal of Animal Ecology*. 2011;80(3):595-602. doi:10.1111/j.1365-2656.2011.01806.x

90. Jackson PA. SIBER: Stable Isotope Bayesian Ellipses in R. Published online 2023. https://CRAN.R-project.org/package=SIBER

91. Páez-Rosas D, Insuasti-Zarate P, Riofrío-Lazo M, Galván-Magaña F. Feeding behavior and trophic interaction of three shark species in the Galapagos Marine Reserve. *PeerJ*. 2018;6:e4818. doi:10.7717/peerj.4818

92. Brault EK, Koch PL, Costa DP, McCarthy MD, Hückstädt LA, Goetz KT, McMahon KW, Goebel ME, Karlsson O, Teilmann J, Harkonen T. Trophic position and foraging ecology of Ross, Weddell, and crabeater seals revealed by compound-specific isotope analysis. *Mar Ecol Prog Ser*. 2019;611:1-18. doi:10.3354/meps12856

93. Chikaraishi Y, Ogawa NO, Kashiyama Y, Takano Y, Suga H, Tomitani A, Miyashita H, Kitazato H, Ohkouchi N. Determination of aquatic food-web structure based on compound-

specific nitrogen isotopic composition of amino acids. *Limnol Oceanogr Meth*. 2009;7(11):740-750. doi:10.4319/lom.2009.7.740

94. Luo D, Ganesh S, Koolaard J. Predictmeans package. Published online 2024. https://cran.r-project.org/web/packages/predictmeans/predictmeans.pdf

95. Baylis AM, Orben RA, Arnould JP, Peters K, Knox T, Costa DP, Staniland IJ. Diving deeper into individual foraging specializations of a large marine predator, the southern sea lion. *Oecologia*. 2015;179(4):1053-1065. doi:10.1007/s00442-015-3421-4

96. Hückstädt LA, Koch PL, McDonald BI, Goebel ME, Crocker DE, Costa DP. Stable isotope analyses reveal individual variability in the trophic ecology of a top marine predator, the southern elephant seal. *Oecologia*. 2012;169(2):395-406. doi:10.1007/s00442-011-2202-y

97. Kernaléguen L, Cherel Y, Knox TC, Baylis AMM, Arnould JPY. Sexual niche segregation and gender-specific individual specialisation in a highly dimorphic marine mammal. Crocker DE, ed. *PLoS ONE*. 2015;10(8):e0133018. doi:10.1371/journal.pone.0133018

98. Moore JW, Semmens BX. Incorporating uncertainty and prior information into stable isotope mixing models. *Ecol Lett*. 2008;11(5):470-480. doi:10.1111/j.1461-0248.2008.01163.x

99. Stock B, Jackson A, Ward E, Venkiteswaran J. brianstock/MixSIAR 3.1.9. Published online March 29, 2018. doi:10.5281/ZENODO.1209993

100. Borrell A, Abad-Oliva N, Gómez-Campos E, Giménez J, Aguilar A. Discrimination of stable isotopes in fin whale tissues and application to diet assessment in cetaceans. *Rapid Comm Mass Spectrometry*. 2012;26(14):1596-1602. doi:10.1002/rcm.6267

101. Gelman A, Rubin DB. Inference from iterative simulation using multiple sequences. *Statist Sci*. 1992;7(4). doi:10.1214/ss/1177011136

102. Baird RW, Whitehead H. Social organization of mammal-eating killer whales: group stability and dispersal patterns. *Can J Zool*. 2000;78(12):2096-2105. doi:10.1139/z00-155

103. Black NA, Ternullo A, Schulman-Janiger A, Ellis GM, Dahlheim ME, Stapp P. Behavior and ecology of killer whales in Monterey Bay, California. (*Orcinus orca*). In: *Proceedings of the Fourth International Orca Symposium*; 2002:40-44. https://gowhales.com/Features/KillerWhaleEcology0210.html

104. Ternullo R, Black N. Predation Behavior of Transient Killer Whales in Monterey Bay, California.2002. https://www.montereybaywhalewatch.com/Features/KillerWhalePredation0210.html

105. Carretta JV, Oleson EM, Forney KA, Muto MM, Weller DW, Lang AR, Baker J, Hanson B, Orr AJ, Barlow J, Moore JE. *U.S. Pacific Marine Mammal Stock Assessments: 2022. U.S.*

Department of Commerce, NOAA Technical Memorandum.; 2022. https://doi.org/10.25923/5ysf-gt95

106. Canseco JA, Niklitschek EJ, Quezada-Romegialli C, Yarnes C, Harrod C. Comparing trophic position estimates using bulk and compound specific stable isotope analyses: applying new approaches to mackerel icefish *Champsocephalus gunnari*. *PeerJ*. 2024;12:e17372. doi:10.7717/peerj.17372

107. Rafter PA, Bagnell A, Marconi D, DeVries T. Global trends in marine nitrate N isotopes from observations and a neural network-based climatology. *Biogeosciences*. 2019;16(13):2617-2633. doi:10.5194/bg-16-2617-2019

108. Salton M, Raoult V, Jonsen I, Harcourt R. Niche partitioning and individual specialisation in resources and space use of sympatric fur seals at their range margin. *Oecologia*. 2024;204(4):815-832. doi:10.1007/s00442-024-05537-8

109. Riesch R, Barrett-Lennard LG, Ellis GM, Ford JKB, Deecke VB. Cultural traditions and the evolution of reproductive isolation: ecological speciation in killer whales? *Biol J Linn Soc*. 2012;106(1):1-17. doi:10.1111/j.1095-8312.2012.01872.x

Chapter 5 : Historical reconstruction of northern and southern resident killer whale (*Orcinus orca ater*) diets through stable isotope analysis of dentin

5.1 Abstract

Northern resident killer whales (NRKWs) and southern resident killer whales (SRKWs) are distinct population segments of the 'resident' killer whale (*Orcinus orca ater*) ecotype in the North Pacific Ocean. Despite similar ecology and prey sources, including a strong reliance on Chinook salmon, NRKWs have undergone an overall increase in abundance since the 1970s while the SRKWs have declined. Prey availability and foraging plasticity are among the proposed hypotheses for the differential population trajectories. NRKWs may be better able to adapt to low Chinook salmon abundance by supplementing their diets with other prey species, whereas SRKWs may be less flexible in their reliance on Chinook salmon and suffer in survival and reproduction when Chinook are less available.

Historical ecology aims to provide a temporal and spatial framework of ecosystem dynamics in the context of changing anthropogenic activity and environmental conditions. In addition, understanding past environmental and ecosystem conditions is imperative to establish baselines, which are in turn used to measure 1) changes in trophic ecology over time and 2) current and future success of management and conservation goals. Stable isotope analysis (SIA) utilizes the stable carbon ($\delta^{13}C$) and nitrogen ($\delta^{15}N$) isotope values in consumer tissues, which reflect those of their prey and foraging habitat. SIA of those consumer tissues allows for broad, long-term (potentially lifelong) dietary assessment, especially when analyzing biologically inert teeth or bone. We sampled annual growth layer groups (n = 270) within teeth (n = 17) of resident killer whales to study differences within individuals, among individuals, and throughout time. We used both bulk and compound-specific isotope analysis of amino acids (CSIA-AA) to

examine diet over the past ~60 years and test the hypothesis that NRKWs have a more flexible diet than SRKWs to adapt to low Chinook abundance.

We found mixed evidence to support that dietary plasticity may have contributed to the differences in population trajectories of resident killer whales. The overall δ^{13}C and δ^{15}N values were not significantly different among the residents, and neither resident diet measured through the δ^{15}N values appeared to be related to Chinook abundance. However, NRKWs did have a slightly larger range of stable isotope values and trophic position as determined through CSIA-AA throughout time, implying a more diverse diet than SRKWs. Our study helps enhance understanding of long-term dietary trends in resident killer whales and catalyzes future efforts to design and implement effective conservation strategies.

5.2 Introduction

Killer whales (*Orcinus orca*) are an apex marine predator found globally, but they have been organized into distinct ecotypes that differ genetically, morphologically, and ecologically[1–5]. There are currently three recognized ecotypes in the eastern North Pacific[6–11]: transients (aka Bigg's; *Orcinus orca rectipinnus*), offshores, and residents. The fish-eating residents have been further divided into three stocks[12]: the Alaska residents, the northern residents, and the southern residents, and our study focuses on the latter two.

The northern resident killer whales (NRKWs) are comprised of multiple pods that associate into three clans (A, G, and R clans), whereas the southern resident killer whales (SRKWs) consist of one clan defined by three pods (L, K, and J pods).[13] The NRKWs range from southeastern Alaska to Washington State, often overlapping during late spring, summer, and early fall with the SRKWs, which also seasonally inhabit the coastal waterways around British Columbia and Washington.[9,14–18] During the winter, both NRKWs and SRKWs expand

their range to the outer coast, with the NRKWs moving further north and the SRKWs occasionally moving as far south as California.[16–18] Even with some sympatric habitat, the two resident stocks are genetically and acoustically distinct and are not known to socialize.[9,13]

The range and seasonal movements of both NRKWs and SRKWs appear to be influenced by the occurrence of their mutual primary prey source, Chinook salmon (*Oncorhynchus tshawytscha*).[8,19–21] The killer whales are found more near the coast during the summer months as adult Chinook salmon return from the ocean to spawn in their natal rivers. At this time of year, Chinook salmon constitute ~80-100% of the diet for both killer whale populations.[20–23] Throughout winter, spring, and fall, resident killer whales expand their range presumably to increase access to Chinook salmon[24,25], though they also begin to consume a slightly greater diversity of prey. Chinook consumption can fall to 30-50% of the diet[21,26], while chum (*Oncorhynchus keta*) or coho (*Oncorhynchus kisutch*) salmon dominate[20,23,26,27]. Non-salmonid prey species, including pacific herring[20] (*Clupea pallasii*), lingcod[21] (*Ophiodon elongates*), and flatfish (Pleuronectiformes) such as pacific halibut[20] (*Hippoglossus stenolepis*) and English sole[21] (*Parophrys vetulus*), appear in their diet, albeit rarely. Chinook salmon is likely targeted by resident killer whales because of year-round availability, large body size, and high energy content[22,28], despite being far less abundant in the environment than other species such as pink (*Oncorhynchus gorbuscha*) and sockeye (*Oncorhynchus nerka)* salmon[22].

Since field studies first began documenting resident killer whales in the 1970s[29], SRKW and Chinook salmon populations have declined, whereas NRKWs have experienced fairly consistent growth. The SRKWs were declared endangered under the US Endangered Species Act in 2003[30] and under the Canada Species at Risk Act in 2005[31], as they displayed essentially no net growth over the past 50 years with 71 whales counted in 1974[32] and 75 whales in 2023[33].

Similarly, several Chinook salmon stocks are also listed as threatened or endangered in the US[30], have declined in abundance during recent years[34], and have exhibited decreased body size[35]. In contrast, the NRKWs have gradually increased from ~115 to ~330 individuals from 1974 to 2023, though they are also listed as threatened under the Species at Risk Act[36].

Exposure to toxins and pollutants (review in Noel *et al*.[37]), disturbance and mortality from ships (review in Ferrara *et al*.[38]), and reduced prey availability or accessibility[14,20,21,39–41] have been investigated as potential contributors to the differential population trajectories of SRKWs and NRKWs[42]. There is evidence that NRKWs and SRKWs may compete for dwindling Chinook salmon, with NRKWs at an advantage because their geographic location during salmon spawning season allows them to encounter salmon returning to their natal rivers before the SRKWs[21,43]. However, other studies suggest prey availability and/or nutritional stress may not be at the core of the declines in SRKW numbers. For example, Sato *et al*.[44] found that SRKW habitat harbored 4 - 6 times the density of large fish prey than NRKW habitat during the summer of 2018 and 2019, and therefore prey availability could not explain why SRKWs were observed less frequently in coastal waters at those times. Additionally, Stewart *et al*.[45] showed an inconsistent effect of prey abundance on metrics of health for the SRKWs during the summer as salmon abundance of two major stocks predicted the body condition for individuals in the J-pod, but did so less for those in L-pod, and not at all for individuals in K-pod.

Both resident types seem capable of supplementing their diets with other fish species to some degree, especially during the winter when Chinook salmon are less available[20,21,23,26,27], and dietary plasticity may differ between sexes and among age classes. Both males and females consume more Chinook salmon than any other prey species, but males may sometimes consume significantly more chum salmon[22]. In addition, foraging behavior between sexes sometimes

differs, with males diving deeper and occasionally independently[46–48], indicating the potential for differential prey targeting. Juveniles (<14 years) also consume a substantial amount of Chinook salmon, but they tend to consume smaller individuals and are the only age class shown to consume pink salmon[22].

Overall, knowledge of SRKW and NRKW diet is still understudied, especially during the winter season when they spend more time foraging further offshore[31] (but see Hanson *et al.*[21]). In addition, many previous dietary studies are limited in that the methods used (analyses of stomach contents, hard parts in killer whale scats, and observed predation events) provide relatively high taxonomic resolution, but are constrained temporally and reflect only recent meals and may be biased in the prey they represent[8,20–23,26].

A few studies[32,49–51] have utilized stable carbon (δ^{13}C) and nitrogen (δ^{15}N) isotope analyses (SIA) to study NRKW and SRKW diets. Predictable shifts in the δ^{13}C and δ^{15}N values from prey to predator tissue[52] allow for inferences about animal foraging habitats and diets at the trophic level[53,54] and can reflect longer-term foraging information. Previous SIA studies[32,49–51] investigating resident killer whale diets utilized skin or blubber biopsies that were nearly all collected from killer whales after the year 2000 and focused on diets of SRKWs in summer and fall seasons. These data indicate some inconsistent interannual variability in the δ^{15}N values from SRKWs[32,51], but their results could not determine if observed changes in the δ^{15}N values from the killer whales were driven by diet choices, variations in the isotope values in their prey, or variations at the base of the food web.

Here, we use bulk stable carbon and nitrogen isotope analysis of annual growth layer groups (GLGs) from archived killer whale teeth to reconstruct ~60 years of NRKW and SRKW foraging ecology (technique review in Read *et al.*[55] , see also Bowen and Kurle in prep and

Bowen and Kurle in review). Our specimens date back to ~1950, over 20 years before consistent research on these killer whale populations began[29]. Our first aim was to investigate the degree to which isotope values collected from the teeth of NRKWs and SRKWs vary over decades and compare those values with published stable isotope values from multiple potential prey groups. Given their disparate population trajectories (NRKWs increasing and SRKWs decreasing), we hypothesized that the stable isotope values from the killer whales would demonstrate greater dietary plasticity over time for NRKWs, indicating they are better adapted to consuming alternate prey during times of lower Chinook salmon abundances than SRKWs. Second, we conducted SIA on material collected from multiple GLGs (each layer reflects dietary information from a different year in the killer whale's life) within each individual tooth in order to determine the potential for ontogenetic changes in killer whale diets. Third, we used our SIA data to examine potential sex-based differences in killer whale foraging. We also conducted compound-specific stable isotope analysis of amino acids (CSIA-AA) on material from a subset of the teeth to calculate killer whale trophic positions and determine if any variations in measured SI values were influenced by changes in the isotope values at the base of the food web; this could confound interpretations of the bulk SI values measured in the teeth, a challenge for previous studies using bulk SIA of killer whale tissues[32,50,51]. Finally, we investigated the trophic positions of NRKW and SRKW throughout time with baseline context determined by CSIA-AA.

5.3 Materials and Methods

-Specimen collection

We sampled 87 annual GLGs from the teeth of 17 killer whales, with 65 GLGs from 11 SRKWs (five female, six male) and 22 GLGs from 6 NRKWs (three female, three male; Table

5.1, Figure 5.1).The GLGs from the SRKW and NRKW teeth represented years from 1947 to 2006 (59 years) and 1951 to 1999 (48 years), respectively.

Some of our specimens were collected during the era in which capture of wild killer whales for display in aquaria was allowed. Our study includes a tooth from "Namu", the male NRKW whose capture in 1965 spurred a commercial market for killer whales[56]. We include four specimens who spent some amount of time in captivity (three SRKWs in addition to "Namu", details in Table 5.1), however we removed years (*i.e.*, GLGs) in which the animals would have been confined. Capturing killer whales for aquaria was mostly ended in the US Northwest Pacific Ocean after the passage of the Marine Mammal Protection Act in 1972[56]. Shortly after, dedicated efforts to research wild killer whale populations began[29]. Accordingly, our specimens also include six wild individuals that were identified as part of these research efforts (two NRKWs and four SRKWs, Table 5.1). Ecotypes and resident designations of all specimens were confirmed via genetics, photo-identification, or acoustics.

-Specimen preparation

More details on specimen preparation, age estimation, and dentin sampling are provided in Chapter 4, but overviews are provided here.

All teeth in this study except BBM-C21 were stored dry. The BBM-C21 tooth was stored in olive oil for an unknown amount of time (likely <10 years) in an effort to prevent desiccation and cracking, so we soaked it in soapy water for 24 hours, rinsed it under running deionized water for one hour, and soaked it overnight in ultra-pure water (MilliQ, Darmstadt, Germany). Note that there is a potential effect of storage medium on the readability of GLGs[57], although qualitatively we found the distinction of GLGs in C21 comparable with other killer whale teeth.

To access the internal GLGs, whole killer whale teeth were bisected longitudinally. We accomplished this with a Bosch® TC10 wet tile saw (Farmington Hills, MI, USA) that we modified with a custom tooth-mounting and motorized pulley system (described in Bowen and Bowen in prep). This setup allowed us to automate the sawing and control the angle of the cut. We also controlled the speed at which the tooth was sectioned by the 10-inch diamond blade to a rate of ~0.50 cm per minute, in line with existing protocols[57] and sufficiently slow to avoid burning the surface of the tooth.

After the teeth were bisected, we manually polished the cut surface of the half-tooth we intended to sample with individual wet sandpaper discs to remove saw marks. We used 400 grit sandpaper, then 600 grit sandpaper until the surface was visibly free of saw marks.

To enhance the visibility of GLGs, we 'etched' the surface of the half-teeth in 10% formic acid[58] to a depth of 0.5 - 1.0 cm[59] for 12 hours[60] in individual glass dishes. After etching, we rinsed the half-teeth in running tap water for approximately one hour and soaked them overnight in ultra-pure water[61]. After removing the half-teeth from submersion, it is important to dry the teeth slowly to reduce potential cracking. We first wrapped the teeth in damp paper towels and sealed them individually in glass dishes with a lid for 24 hours. Then, we loosened the paper towels, draped them over the teeth and rested the lid on top of the glass dishes without clasping it for another 24 hours. Finally, we removed the lids for approximately 12 hours, then removed the paper towels. When the teeth were completely dry, we rubbed a soft graphite pencil (6B) gently on the surface of the tooth to highlight the ridges that were produced from the acid-etching.

In a separate study (Bowen and Kurle in review), we demonstrated that the formic acid and graphite protocol we used here (in combination with the parameters we describe below in

'Dentin sampling') did not significantly affect the $\delta^{13}C$ and $\delta^{15}N$ values of killer whale dentin. Note that Stukonytė *et al*.[62] concluded formic acid did bias the $\delta^{13}C$ and $\delta^{15}N$ values of sperm whale teeth in their study, so researchers might consider the potential impacts of acid-etching on stable isotope sampling of dentin.

-Age estimation

We captured high-resolution (800-1200 dpi) scans of all half-teeth and processed those images in GIMP[63]. We first generated a duplicate layer of the image so the original would remain unmodified. To the duplicate layer, we sharpened the image by using the "High Pass" and "Sharpen" tools to enhance overall clarity. Then, we added a third layer for annotations. We marked the GLGs that we identified and counted them to estimate the age of the tooth. After at least 14 days, with the previous annotated layer toggled 'off', we added a fourth layer and generated another GLG reading. We repeated that process once more for a total of three aging sessions (*i.e.*, annotated layers). Lastly, all three readings were evaluated together to form a consensus on GLG boundaries, with reference to the physical half-tooth under a microscope when needed to address discrepancies. Our goal was to define each GLG boundary, rather than estimate an overall age, since it was important we sampled particular GLGs and could relate them to calendar year through the life of the animal. All teeth were aged by one reader (KB) blindly (*i.e*, with no reference to metadata of the specimens such as ecotype, sex, or body size), with the exception of BBM-J18 which was used as a known-age reference. Age estimation of marine mammal teeth is an ongoing area of research, but see Bowen and Kurle in prep for a discussion on the particulars relating to aging killer whale teeth.

-Dentin sampling

We used a computer-controlled micromill (MicroMill2, Elemental Scientific Lasers, Omaha, NE, USA) at the NOAA Southwest Fisheries Science Center (La Jolla, CA) to collect dentin from individual GLGs of half-teeth. We used carbide drill bits that ranged from 300 µm to 1200 µm (Brasseler USA Dental Instruments, Savannah, GA, USA), depending on the width of the target GLG. We used the computer interface to map a desired drill path, which was typically ~8-10 mm in length and ~200-350 µm in depth to yield ~1-2 mg of dentin. We discarded the outermost ~25 µm of drilled dentin with compressed air to reduce surface contamination. However this may be unnecessary as the presence of formic acid and graphite does not influence the δ^{13}C and δ^{15}N values of killer whale dentin, even without discarding any surface material (Bowen and Kurle in prep). We sampled from the middle region of each tooth when possible because the GLGs are narrower and thinner at the root and crown of the tooth, and sampling from those regions could increase the risk of accidentally sampling an underlying GLG due to the conical nature of the teeth. If sampling into underlying layers is avoided, data from Bowen and Kurle (in review) demonstrate that the δ^{13}C and δ^{15}N values from killer whale teeth are consistent, regardless of the exact sampling location within the GLG. For all teeth, we began sampling at GLG 4 as the first year representing wild foraging after weaning[60]. If the tooth was aged 10 years or younger, we sampled every other GLG (*e.g.*, GLG 4, 6, 8, 10). If the tooth was aged older than 10 years, we sampled every 3rd GLG (*e.g.*, GLG 4, 7, 10, *etc*.).

We also sampled 11 half-teeth (seven SRKW and four NRKW) for CSIA-AA to better understand potential isotopic variation at the base of the food web to contextualize killer whale foraging trends. For temporal coverage, we aimed to sample one GLG from two individuals per decade (Table 5.2), though we had limited NRKW representation. When possible, we sampled

one GLG to represent the first half of a decade (*e.g.*, 1980-1984) and one to represent the second half of the decade (*e.g.*, 1985 - 1989). We made four considerations when choosing samples for CSIA-AA: 1) we prioritized teeth that were from known-age individuals to reduce potential aging errors, 2) we chose GLGs that corresponded to years of neutral oceanographic conditions, meaning neither El Niño nor La Niña years, for consistency, 3) we then chose the oldest GLGs when possible because the oldest GLG corresponds to the known collection year, again reducing potential error associated with aging, and 4) we did not sample any GLGs representing younger than age 10, to reduce variation from comparing juvenile and adult years. As CSIA-AA is time and resource intensive, we were confined to a relatively small sample size.

For CSIA-AA, which requires substantially more tissue than bulk isotope analysis, our drill path was ~30 mm in length and ~1,100 - 1,400 µm in depth with either a 500 µm or 800 µm drill bit to collect ~35 - 40 mg of dentin. As previously described, we attempted to sample from the middle of the tooth and minimize the depth so as to avoid drilling into an underlying layer, and we discarded the top ~25 µm of dentin. We then demineralized collected dentin samples in individual micro-centrifuge tubes with ~1 mL of 0.5N hydrochloric acid (HCl) for approximately one hour at room temperature and 23 hours at 4C in a refrigerator (Brault et al. 2014). We then centrifuged the samples at 12,000 rpm for five minutes, aspirated the HCl with a pipette, and rinsed the sample five times with ultra-pure water. After removing the water from the last rinse, we lyphophilized the samples for 48 hours. We packaged the resulting 1.0 - 1.3 mg of demineralized dentin to be analyzed by the University of California Davis - Stable Isotope Facility.

-Stable isotope analyses

For bulk isotope analysis, we packaged approximately 1.2 mg of untreated dentin into 5x9 mm tin capsules. Our samples were analyzed in three laboratories: the University of California Santa Cruz - Stable Isotope Laboratory using a CE Instruments NC2500 elemental analyzer coupled to a Thermo Scientific DELTAplus XP isotope ratio mass spectrometer via a Thermo-Scientific ConFlo III, and the University of New Mexico Center for Stable Isotopes using a Costech 4010 elemental analyzer coupled to a Thermo Scientific Delta V mass spectrometer via a Thermo-Scientific ConFlo IV, and the University of California Davis - Stable Isotope Facility using a PDZ Europa ANCA-GSL elemental analyzer coupled to a PDZ Europa 20-20 isotope ratio mass spectrometer. We report stable isotope values using delta-notation in units of per mil using the equation:

$$\delta X = [(R_{sample} \div R_{standard}) - 1] \times 1000$$

where X is $\delta^{13}C$ or $\delta^{15}N$ and R is the heavy:light isotope ratio for the given element. International standards referred to in the equation were Vienna Peedee Belemnite (VPDB) for the $\delta^{13}C$ values and atmospheric nitrogen for the $\delta^{15}N$ values. Precision was evaluated using several externally-calibrated reference materials: IAEA-600, IU acetanilide, Pugel, USGS 40, USGS 41, and USGS 61. The overall standard deviations for all reference materials were ≤0.2‰ for $\delta^{13}C$ values and ≤0.3‰ for $\delta^{15}N$ values.

See Chapter 4 for details of the CSIA-AA analyses.

-Corrections to the $\delta^{13}C$ values for Suess effect and lipids

We made corrections to all $\delta^{13}C$ values to account for the Suess effect, and we corrected a subset of samples when needed for the presence of lipids.

The Suess effect describes a decrease in global $\delta^{13}C$ values from an increase in carbon dioxide emissions[64], particularly due to the onset of the industrial revolution, which needs to be accounted for when measuring the $\delta^{13}C$ values of specimens from different time periods[65]. We used the R[66] package called SuessR[67] to correct the $\delta^{13}C$ values for both the Suess and Laws effects (a related change in phytoplankton fractionation[65]). These corrections are location-specific, and three regions in the North Pacific are currently available in SuessR: the Bering Sea, the Aleutian Islands, and the Gulf of Alaska. The difference in overall net corrections between the three regions differed by less than 0.01% in Clark *et al.*[65], thus we assumed the corrections would be highly similar for samples collected for our study from neighboring waters. Therefore, we prioritized the modern and accurate calculations provided by SuessR and used it to correct the $\delta^{13}C$ values from our study to the standard pre-industrial year of 1850 using the Gulf of Alaska as it is the region closest to our collection sites.

A subset of our samples (23/87 samples) measured C:N values higher than 3.6 (mean C:N = 3.7 + 0.06), which is the upper limit of pure collagen[68] and indicates potential lipid contamination. In an abundance of caution, we applied the correction described in Post *et al.*[69] for aquatic organisms to these $\delta^{13}C$ values as needed.

-Statistical analyses

All analyses were conducted in R[66] version 4.2.1 using the RStudio[70] interface. We used one-way ANOVAs ($\delta^{15}N$ ~ Sample ID) to examine differences among the $\delta^{15}N$ values of individuals for both populations separately after verifying the assumptions of normality (Shapiro-Wilk tests: $W > 0.93$, $p > 0.11$) and homogeneity of variances (Levene's tests: SRKWs, $F_{(10,54)} = 1.19$, $p = 0.32$; NRKWs, $F_{(5,16)} = 0.83$, $p = 0.55$). We followed the same process for the

δ^{13}C values as well (Shapiro-Wilk tests: W > 0.93, p > 0.10; Levene's tests: SRKWs, $F_{(10,54)}$ = 1.03, p = 0.43; NRKWs, $F_{(5,16)}$ = 2.10, p = 0.12).

We also calculated the mean δ^{13}C and δ^{15}N values for each individual whale from multiple GLG measurements, and the means were consistent with a normal distribution (Shapiro-Wilk tests: δ^{13}C values, W > 0.90 and p > 0.22; δ^{15}N values, W > 0.93 and p > 0.40). Although the population variances between SRKWs and NRKWs were equal (Levene's tests: δ^{13}C values, $F_{(1, 15)}$ = 0.35, p = 0.56; δ^{15}N values, $F_{(1,15)}$ = 0.00075, p = 0.98), we conservatively used Welch's t-tests to compare the mean δ^{13}C and δ^{15}N values of SRKWs and NRKWs due to unequal sample sizes.

Effects of time, age, and sex

We used separate linear mixed models (via the lmerTest package[71]) to determine whether sex, age, and time were significant predictors of the δ^{13}C and δ^{15}N values, with sex as a categorical variable and age and time as continuous variables. The linear mixed models were followed by Type III Analysis of Variance (ANOVA) tests using Satterthwaite's method to determine which, if any, main and interaction effects were significant predictors of the δ^{13}C or δ^{15}N values. We re-scaled 'year' based on the minimum value in a model; for example, if 1950 was the minimum year, then 1950 became 1 and 1951 became 2, and so on. In addition to sex, age, and time as fixed predictors, we included specimen ID as a random effect because we sampled multiple GLGs within individuals. We assessed the assumptions of linear mixed models by visually assessing diagnostic plots and observed no substantial violations: residuals vs fitted (linearity), normal Q-Q (normality), scale-location (homoscedasticity), and residuals vs leverage (influential points).

We also tested for a correlation between the δ^{15}N values of resident killer whales and the abundance of spawning Chinook salmon in Puget Sound through time. We first calculated the average δ^{15}N value for a given year across all animals that were sampled for that year. We also obtained data on historical Chinook salmon abundance from 1949 to 2015[72] and filtered for the 'Puget Sound' domain, which included salmon abundance indices from multiple rivers. We then combined salmon abundance for all rivers to obtain a final Chinook abundance value for each year. Then, we were able to use Spearman's rank correlation test between the δ^{15}N values and the corresponding Chinook abundance index for sampled years.

MixSIAR diet estimation

We used the R package MixSIAR[73,74] to further investigate potential dietary trends with respect to Chinook salmon consumption for SRKWs and NRKWs. MixSIAR uses biotracers, such as stable isotope values, and a Bayesian statistical framework to calculate an estimated contribution of a priori determined prey groups to a predator's diet. MixSIAR requires information for three data categories: 1) predator isotope values, 2) prey isotope values, and 3) trophic discrimination factors (the predicted offset in isotope values between predator and prey[75]).

We used the bulk δ^{13}C and δ^{15}N values we measured from GLGs in NRKW and SRKW teeth as predator data. For the prey groups, we used a simplified system consisting of only two groups, Chinook salmon and miscellaneous salmon (*e.g.*, coho, chum, sockeye, and steelhead). We based this decision on the knowledge that resident killer whales rely heavily on Chinook when available[20–23] and that Chinook salmon are isotopically distinct from the other miscellaneous salmon species that are the preferred prey alternatives[51,76,77]. Our intent with the

MixSIAR model was to use the potential for differential Chinook salmon consumption between NRKWs and SRKWs as a proxy for dietary adaptability. The estimated prey contributions generated by our MixSIAR model are thus not to be taken as absolute interpretations of diet, but rather viewed as measures of dietary variability over time.

Warlick *et al*.[51] also constructed MixSIAR models of resident killer whale diet, and we referenced their stable isotope values for all five salmon species in the Pacific Northwest. We used PlotDigitizer[78,79] to extract mean and standard deviation values from Figure 1 within Warlick *et al*.[51] (sample sizes are also reported therein). We used the extracted Chinook salmon values directly as MixSIAR input (δ^{13}C = -15.3 ± 0.6‰; δ^{15}N = 17.9 ± 0.5‰; n = 111). However, based on a priori data indicating Chinook salmon have substantially higher stable isotope values than most other species of salmon[51] (Bowen and Kurle in review), we condensed coho, chum, steelhead, and sockeye into one group representative of salmonid prey other than Chinook salmon (although note some isotopic overlap between Chinook salmon and coho salmon). To accomplish this, we created a normal distribution of 2,000 values for each of the four species based on the extracted mean and standard deviation values[80] (Bowen and Kurle in prep). We then combined all four distributions into one cumulative normal distribution, and evaluated the mean and standard deviation to be used for the miscellaneous salmon prey group in MixSIAR (δ^{13}C = -17.6 ± 1.5‰; δ^{15}N = 14.9 ± 1.5‰; n = 145). Finally, we used trophic discrimination factors of 3.11 ± 0.27‰ for the δ^{13}C values and 2.03 ± 0.71‰ for the δ^{15}N values, which have been measured for bone protein in cetaceans and are a reasonable approximation for killer whale dentin[81].

Because we were interested in the relative changes in Chinook salmon contribution over time and between NRKWs and SRKWs, we did not use informative priors in the model. We

assigned ‘Specimen ID’ as a random factor and ‘Resident Type’ (NRKW or SRKW) as a fixed factor, and we ran three parallel Markov Chain Monte Carlo simulations using the “normal” run parameter (100,000 chain length with 50,000 burn-in and thinning interval of 50). The model converged by the Gelman-Rubin diagnostic (all R values less than 1.05[82]).

CSIA-AA analyses and trophic position

McMahon and McCarthy[83] describe three amino acids that reflect changes in the $\delta^{15}N$ values at the base of the food web and are considered ‘source’ amino acids: phenylalanine (Phe), methionine (Met), and lysine (Lys; see discussions in McMahon and McCarthy[83] regarding tyrosine (Tyr), glycine (Gly), and serine (Ser)). They also identify seven amino acids that are influenced by the consumer’s metabolism and are considered ‘trophic’ amino acids: Aspartic acid + asparagine (Asx), isoleucine (Ile), alanine (Ala), glutamic acid + glutamine (Glx), leucine (Leu), proline (Pro), and valine (Val). We summarize the $\delta^{15}N$ values for these amino acids in Table S5.1 and Figure S5.1, with the exception of Ile because those measurements fell below the limit of quantification.

We calculated trophic positions (TP) for the subset of killer whale specimens that were analyzed for CSIA-AA using the equation[84]:

$$TP = 1 + [(\delta^{15}N_{Pro} - \delta^{15}N_{Phe} - \beta_{Pro/Phe})/TDF_{Pro\text{-}Phe}]$$

Though Glx has traditionally been used as the trophic amino acid for TP calculations, we followed recommendations in Brault et al.[85] and Nehasil[86] to utilize Pro as the trophic acid for marine mammals and maintain use of Phe as the source amino acid. In the equation, the $\delta^{15}N_{Pro}$ and $\delta^{15}N_{Phe}$ values are our measurements from killer whale dentin, $\beta_{Pro/Phe}$ is a constant equal to 3.1‰ that represents the difference between the $\delta^{15}N_{Pro}$ and $\delta^{15}N_{Phe}$ values of the primary

producer in the ecosystem (*e.g.*, marine phytoplankton[84]), and $TDF_{Pro\text{-}Phe}$ ('trophic discrimination factor') is a constant equal to 4.5‰ that represents the difference in TDF (*i.e.*, the $\delta^{15}N$ offset between consumer and prey) for Pro minus that for Phe[85].

We then used Student's t-test to compare TP between NRKW and SRKW, as distributions were normal (Shapiro-Wilk test: W(4) = .96, p = .98 (NRKW); W(7) = .95, p = .81 (SRKW)), and variances were equal (Levene's test: $F_{(1,9)} = 4.1$, p = 0.07). We also calculated the effect size of differences between NRKW and SRKW populations following Coe[87] using the $\delta^{15}N_{Pro\text{-}Phe}$ values[88]:

$$\text{Effect size } (\delta^{15}N_{Pro\text{-}Phe}) = \frac{\text{[NRKW Mean]-[SRKW Mean]}}{\text{Pooled Standard Deviation}}$$

Finally, we used linear regression models to examine relationships between the $\delta^{15}N$ values from the bulk and CSIA-AA data, TP, and time.

5.4 Results

We measured the bulk $\delta^{13}C$ and $\delta^{15}N$ values (Table S5.2) and the CSIA-AA $\delta^{15}N$ values of GLGs within teeth of SRKWs (n = 11) and NRKWs (n = 6) to study the effects of sex, age, and time. The SRKW animals ranged from an estimated six to 24 years old, and the NRKW animals ranged from 10 to 20 years old (though we only sampled the 20 year-old animal to age 16 due to its capture and captivity during its older years). We sampled between two and 13 GLGs in the SKRW teeth and two and five GLGs in the NRKW teeth. There were significant differences among individuals for the $\delta^{15}N$ value of SRKWs (ANOVA: $F_{(10,54)} = 5.45$, $p < 0.001$) but not for NRKWs (ANOVA: $F_{(5, 16)} = 0.52$, $p = 0.76$). There were significant differences among individuals for the $\delta^{13}C$ values for both SRKWs ($F_{(10,54)} = 13.11$, $p < 0.001$) and NRKWs ($F_{(5, 16)} = 11.0$, $p < 0.001$). However, there were overall no significant differences between the

individual means of the $\delta^{13}C$ (Welch's t-test: t(7.62) = 1.62, p = 0.15) or $\delta^{15}N$ values (Welch's t-test: t(10.39) = 1.62, p = 0.26) between SRKWs and NRKWs (Table 5.3).

-Effects of time, age, and sex

The main effect of age and the interaction between age and time were found to be significant predictors of the $\delta^{13}C$ values from the SRKWs (Table 5.4, Table 5.5, Figure 5.2). Generally, animals that lived further in the past (*e.g.*, pre-1970) showed increased $\delta^{13}C$ values with age, whereas animals that lived more recently (*e.g.*, post-1970) showed the opposite trend of decreasing $\delta^{13}C$ values with age. In contrast, the $\delta^{13}C$ values of NRKWs were not predicted by age, sex, or time, though there was a slight trend of decreasing $\delta^{13}C$ values with time when accounting for all data points (R^2 = 0.056, $F_{(1,20)}$ = 1.2, p = 0.29; Figure 5.3).

The model suggested that sex, time, and age influenced the $\delta^{15}N$ values of SRKWs in a three-way interaction, meaning the interaction between age and time varied between males and females (Table 5.4, Table 5.5). Females showed a slight increase in their $\delta^{15}N$ values with age, but the $\delta^{15}N$ values of a juvenile individual in ~1965 were lower than animals of equivalent age near 1950 or 1980 (Figure 5.4). An individual that lived from ~1975 - 2000 also displayed more consistent $\delta^{15}N$ values throughout life than individuals that lived to a similar age in the past. Likewise, the most recently-lived male SRKW (~1980 - 2000) showed less variation over its life compared to the males that lived in the past, which showed a greater ontogenetic increase in their $\delta^{15}N$ values than females overall. The $\delta^{15}N$ values of NRKWs reflected a similar pattern: the three-way interaction between sex, age, and time was a significant predictor (Table 5.4, Table 5.5), where males (n = 3) showed more temporal and ontogenetic variation than females (n = 3), though the represented timeframe differed between the two (Figure 5.5). In contrast to the

juvenile female SRKW that exhibited below-average δ^{15}N values in ~1965, a juvenile male NRKW at the same time showed an elevated δ^{15}N value relative to 1950 or 1970. The 1965 juvenile male showed a decrease in δ^{15}N values with age, whereas a juvenile male in 1950 showed an increase in δ^{15}N values. Two female NRKWs showed the opposite trend, with a female born further in the past (~1960) showing a decrease in δ^{15}N values with age and a female born more recently (~2000) showing an increase.

We found no significant correlations between the mean δ^{15}N values of resident killer whales and the corresponding Chinook salmon abundance for a given year (Spearman's rank correlation: SRKWs, $r_s = -0.02$, $p = 0.93$; NRKWs, $r_s = 0.04$, $p = 0.90$; Figure 5.6).

-MixSIAR diet estimation

We used a MixSIAR model to evaluate how Chinook salmon consumption has differed over time between SRKWs and NRKWs when constrained to two simple groups, either Chinook salmon or miscellaneous salmon that are known to comprise much of the remaining diet. As expected, Chinook salmon comprised the vast majority of the diet when compared to miscellaneous salmon. The overall mean (± SD) contribution of Chinook salmon to the diets of NRKWs and SRKWs was 92.5 ± 0.1% and 98.4 ± 0.0%, respectively. The minimum estimated mean contribution of Chinook salmon to the diet of a single NRKW individual was 47.2 ± 0.1% compared to 70.5 ± 0.1% for a SRKW individual. Using the individual mean diet contribution of Chinook salmon for all 6 NRKW individuals, the group mean diet was 84.0 ± 0.2% Chinook salmon. For the 11 SRKW individuals, this calculation was 95.4 ± 0.1% Chinook salmon. When examining the relationship between Chinook contribution to the diet and year (Figure 5.7), SRKWs showed a slight decrease in Chinook salmon consumption over time in contrast to near

stable consumption by the NRKWs. However, the trend appeared to be driven by specimen ID BBM-J18 (see Discussion), and the slope of the SRKW trend line in Figure 5.7 is closer to zero than the NRKW trend line when J18 is excluded.

-CSIA-AA δ^{15}N analyses and trophic position

The average TP for NRKWs and SRKWs was 4.89±0.31 and 4.78±0.09, respectively, with the four NRKW samples covering 1963 – 2004 and the seven SRKW samples covering 1954 – 1994. Averaged over these timeframes, there were no significant differences between the TPs of both populations (Student's t-test: $t(9) = 0.90$, $p = 0.39$). However, linear regressions suggested a decrease in mean TP over time for NRKWs compared to the stable mean TPs of SRKWs (Figure 5.8). The ranges of TPs were also more constrained for SRKWs (4.65 – 4.90) than for NRKWs (4.57 – 5.31).

The effect size calculated from the $\delta^{15}N_{Pro\text{-}Phe}$ values to compare NRKWs to SRKWs was 0.60, meaning 73% of the SRKW population have a lower $\delta^{15}N_{Pro\text{-}Phe}$ value than the average NRKW (Coe 2002).For comparison, when the effect size is 0.0 (*i.e.*, the distributions of the values are the same), then 50% of one population has a lower value than the average of the other population.

We also examined linear relationships between the $\delta^{15}N_{Bulk}$ and $\delta^{15}N_{Phe}$ ($R^2 = 0.04$, $p = 0.80$; Figure 5.9A) values, the $\delta^{15}N_{Bulk}$ and $\delta^{15}N_{Pro}$ ($R^2 = 0.36$, $p = 0.40$; Figure 5.9B) values, and the $\delta^{15}N_{Phe}$ values and time ($R^2 = 0.72$, $p = 0.15$; Figure 5.10) for the isotope data from the NRKWs. We also examined these relationships for SRKWs: $\delta^{15}N_{Bulk}$ and $\delta^{15}N_{Phe}$ ($R^2 = 0.02$, $p = 0.76$; Figure 5.9A), $\delta^{15}N_{Bulk}$ and $\delta^{15}N_{Pro}$ ($R^2 = 0.23$, $p = 0.28$; Figure 5.9B), and $\delta^{15}N_{Phe}$ and time

($R^2 = 0.22$, $p = 0.29$; Figure 5.10). There were no significant correlations between any of the relationships.

5.5 Discussion

We used SIA to investigate the effects of time, age, and sex on historical resident killer whale diet, and we tested the hypothesis that NRKWs would show a greater degree of dietary plasticity than SRKWs. Although the mean $\delta^{13}C$ and $\delta^{15}N$ values for individuals were not significantly different between NRKWs and SRKWs, this could be expected given the primary reliance of both populations on Chinook salmon[8,19–21]. We did observe that NRKWs had a slightly greater range for both their $\delta^{13}C$ (2.5‰ compared to 2.0‰) and $\delta^{15}N$ (2.3‰ compared to 1.8‰) values than SRKWs. This finding could be the result of NRKWs incorporating more diverse prey into their diet than SRKWs, or it could reflect fluctuations in the isotope values of prey (see further discussions below). There were also significant differences among the $\delta^{15}N$ values of SRKWs, but not NRKWs. Our dataset included at least three known L-pod and one known J-pod SRKW, and J- and L-pod animals appear to utilize different ranges during the winter months[50], providing some possible reasoning for differences in the $\delta^{15}N$ values among individual SRKWs.

<u>-Effects of time, age, and sex</u>

The interaction between age and time was a significant predictor of the $\delta^{13}C$ values for SRKWs and we observed an overall historical trend of increasing $\delta^{13}C$ with age (Figure 5.2). Ford and Ellis[22] found that only juvenile killer whales (without distinguishing resident type), and not adults, consume pink salmon. Pink salmon, and other smaller species of salmon, exhibit lower $\delta^{13}C$ values than Chinook salmon (Bowen and Kurle in review), thus an ontogenetic shift

from pink or other smaller salmon species to Chinook salmon could contribute to this overall observation.

In contrast, recently-lived (post 1970s) killer whales tended to demonstrate decreasing δ^{13}C values with age (Figure 5.2), indicating the potential incorporation of resources from further offshore that are depleted in δ^{13}C values. Juvenile killer whales also consume smaller Chinook salmon more frequently than adults[22]. Smaller Chinook salmon may have higher δ^{13}C values because their isotope values still reflect their time spent in freshwater before they migrated to saltwater, whereas the tissues from larger adults reflect the incorporation of nutrients from prey ingested in the Puget Sound and these saltwater prey have lower δ^{13}C values[89–91]. This trend for the more recently-lived SRKW could also be related to their consumption of larger Chinook salmon with age, or to spending more time foraging on other prey in offshore habitats as δ^{13}C values are higher nearshore than in more pelagic regions. In contrast to the SRKWs, no terms in our model predicted the δ^{13}C values for NRKWs. Either NRKWs have been consistent in their foraging habitats and prey choices, or changes in these behaviors cannot be distinguished given the limitations of SIA.

For the δ^{15}N values, a three-way interaction between time, age, and sex influenced both SRKWs (Figure 5.4) and NRKWs (Figure 5.5). There was a general increase with age in the δ^{15}N values for both sexes, but the increase was greater for males of both resident types. Adult male NRKWs and SRKWs are known to forage in different locations and at deeper depths than females[27,46–48]. Large size Chinook salmon are capable of diving deeper[92] and show higher δ^{15}N values[90] than smaller salmon. As males mature and forage on these larger salmon at greater depths, they may exhibit higher δ^{15}N values than females. Additionally, while female killer whales often initiate prey-sharing behavior, it is rare for males to do so[22,93]. Consequently, males

may consume some distinct prey species contributing to differences in their δ^{15}N values relative to females. The ontogenetic increase in the δ^{15}N values of female killer whales could also be attributed to the positive relationship between body size and the δ^{15}N values in Chinook salmon[90], since female killer whales can likely also capture larger fish as they age, but perhaps not to the same degree as males.

Time was among the significant predictors in the three-way interaction, but with no apparent pattern. There were fluctuations in the δ^{15}N values throughout time that could, as previously noted, be driven by changes in the diet or fluctuations in the δ^{15}N values of Chinook salmon resulting from different geographic stocks, migration behaviors, seasons, ages, sizes, or hatchery vs. wild origins[21,23,44,94,95].

In an effort to better understand the potential role of Chinook salmon over time, we tested for a correlation between Chinook abundance in Puget Sound and the δ^{15}N values of resident killer whales, but found no significance for either resident type. This finding was in contrast to our expectation that the δ^{15}N values from NRKWs in particular would be higher with greater Chinook salmon abundance because all other salmon species have lower δ^{15}N values[51,76]. We hypothesized that killer whales would consume salmon species with lower δ^{15}N values when their preferred Chinook are encountered less frequently. Indeed, Couture *et al.*[41] predicted that SRKWs would consume more chum salmon than Chinook salmon when the latter were low in abundance. It is possible that our analysis did not support that prediction because we limited Chinook abundance to spawning adults in Puget Sound. There were also significant differences among individual SRKWs, but we combined the δ^{15}N values of all individuals for a given year, which may have introduced a source of bias. Nonetheless, we would likely still expect to observe a correlation given the indiscriminate reliance of residents on Chinook salmon. The lack of

correlation between Chinook salmon abundance and δ^{15}N values in our study could support the suggestion by Sato *et al*.[44] that prey limitation is not the primary cause of the population decline exhibited by the SRKWs.

-MixSIAR diet estimation

Although by a minimal margin, our MixSIAR results support the hypothesis that NRKWs have a more diverse diet than SRKWs. On average, SRKWs were estimated to consume more Chinook salmon than NRKWs. Additionally, the minimum estimated contribution of Chinook salmon to a NRKW was 47.2 ± 0.1% compared to 70.5 ± 0.1% for the SRKWs.

We also examined how estimated Chinook contribution changed over time, and though the magnitudes were again small, there was a slight increase for NRKWs (slope = 0.0006) and decrease for SRKWs (slope = -0.0026). BBM-J18 was an influential point, however, and the change in Chinook consumption for SRKWs was less than that of the NRKWs (slope = 0.0003) when the point was excluded. BBM-J18 died of a bacterial infection in 2000 and was highly contaminated with pollutants. The δ^{15}N values from this animal declined during its last three years to the lowest value measured in our study. The δ^{15}N values of a nutritionally stressed animal would be expected to increase[96], but it is possible BBM-J18 exhibited decreased δ^{15}N values as a result of targeting prey species that require less effort than large Chinook salmon at depths. The other species of salmon, smaller Chinook salmon, and other known non-salmonid prey have lower δ^{15}N values in comparison to large adult Chinook salmon[21,51] (Bowen and Kurle in review).

-Trophic position as determined from CSIA-AA

The sample size for our CSIA-AA data was limited by available specimens and the time and cost intensive nature of these analyses. Nevertheless, the results are useful for estimating predator TP and they allow us to better understand the differential contributions of killer whale prey vs. nitrogen dynamics at the base of the food web to the bulk $\delta^{15}N$ values from killer whales[97]. Similar to what we observed with our bulk $\delta^{15}N$ data, overall TPs were not significantly different between resident types, though a wider range of TPs for NRKWs provided some evidence of their potential for greater dietary plasticity. However, the mean TP, maximum TP, and effect size calculation supported that NRKWs may forage at a higher trophic level than SRKWs, which could be contrary to our hypothesis that NRKWs supplement their diets with prey species that have lower $\delta^{15}N$ values compared to those from Chinook salmon. The TPs of adult Chinook salmon near Vancouver Island, BC ranged from 3.54 to 3.80[98], and our data fit the general expectation that resident killer whales should have TPs approximately one level higher than Chinook salmon.

Interestingly, in a broader analysis of historical TP trends for all three North Pacific ecotypes (transients, residents, and offshores), we found SRKWs had the narrowest range of TPs (0.25; Bowen and Kurle in prep). Our results also corroborate previous findings through SIA that L-pod SRKWs did not substantially shift trophic level between 1996 and 2006[50].

For both NRKWs and SRKWs, the $\delta^{15}N_{Phe}$ values explained very little of the variation in the $\delta^{15}N_{Bulk}$ values, whereas the $\delta^{15}N_{Pro}$ values explained 36% and 23% of variation in the $\delta^{15}N_{Bulk}$ values, respectively. This suggests that the variability observed in the $\delta^{15}N_{Bulk}$ values reflect changes in killer whale diets more than potential isotopic changes at the baseline of the ecosystem. There was an association with time and the $\delta^{15}N_{Phe}$ values from all residents sampled, but the ranges we observed (range of 2.2‰ for SRKWs, 3.5‰ for NRKWs) are within the level

of variation that would be expected due to variations in ecosystem baseline $\delta^{15}N$ values that would result when killer whales traverse latitudinally or closer or further from shore in the course of their movements across their habitat[99]. In any case, these changes in the $\delta^{15}N_{Phe}$ values over time did not seem to influence the $\delta^{15}N_{Bulk}$ values we observed, given the very low R^2 (explained variation) values in the linear correlation.

-Conclusions

We used analyses of bulk $\delta^{13}C$ and $\delta^{15}N$ values from killer whale dentin, along with analysis of the $\delta^{15}N$ values from individual amino acids from a subset of those killer whales, to reconstruct the foraging ecology of two subpopulations of resident killer whales (NRKWs and SRKWs) in the eastern North Pacific Ocean over the past ~60 years. One of our primary aims was to evaluate the hypothesis that the positive population trajectory observed for NRKWs is due to their increased ability to prey-switch when the abundance of their preferred prey, Chinook salmon, is reduced. In addition, we hypothesized that the negative population trend observed for SRKWs is due to their failure to target alternative prey when Chinook salmon are scarce. We hypothesized a greater range of the $\delta^{15}N$ values for NRKWs, implying NRKWs consume more lower- $\delta^{15}N$ prey species than SRKWs. We also expected SRKWs to have consistent, higher $\delta^{15}N$ values than NRKWs, either as a result of a stricter reliance on Chinook salmon or perhaps as a response to increased frequency of nutritional stress events when Chinook salmon are low in abundance. The MixSIAR analysis would show a greater contribution of Chinook salmon to SRKW diet than NRKW diet. Lastly, we expected a higher and less variable TP over time for SRKWs than NRKWs.

We found evidence to both support and refute our hypothesis that NRKWs would exhibit more flexibility in diet than SRKWs as a response to low Chinook abundance. In opposition to our hypothesis, there were no significant differences between the bulk $\delta^{13}C$ or $\delta^{15}N$ values of SRKWs and NRKWs over time, suggesting little diet differentiation between the two populations. The $\delta^{15}N$ values of both resident types were related to time, age, and sex, again suggesting that both resident types respond to environmental variation and/or changes in prey availability in similar ways. Additionally, there were significant differences among the bulk $\delta^{15}N$ values measured from individual SRKWs, but not for NRKWs, which could signal less dietary uniformity for the SRKWs. The $\delta^{15}N$ values of both resident types showed no relationship to the changing abundances of spawning adult Chinook salmon in Puget Sound, in contrast to our expectation that the $\delta^{15}N$ values from NRKW would reliably shift to reflect the incorporation of different prey during times of low Chinook salmon abundance. The SRKWs also exhibited a lower $\delta^{15}N$ mean and maximum value than NRKWs, which we would not expect if SRKWs were more reliant on large Chinook and more nutritionally stressed.

However, several of our findings support the notion that NRKWs may be less reliant on Chinook salmon than SRKWs. The $\delta^{15}N$ values and TPs of our NRKW specimens were more variable than those of the SRKWs, suggesting a more diverse diet. It is particularly noteworthy that SRKWs appeared to remain at a more stable TP than any other North Pacific killer whale ecotype (Bowen and Kurle in prep). Our CSIA-AA data supported that the variability we observed in the bulk $\delta^{15}N$ values was more likely driven by true dietary changes rather than by variation in the nitrogen dynamics that could shift the $\delta^{15}N$ values at the base of the marine food web. Our study enhances the understanding of historical ecological trends for resident killer

whales in the eastern North Pacific and contributes to future conservation and management strategies for these threatened and endangered populations.

5.6 Acknowledgements

We are grateful to the natural history collections and all the staff/curators who made this work possible through generous specimen loans, including: the Beaty Biodiversity Museum – University of British Columbia (M. deRoos, C. Stinson); the California Academy of Sciences (M. Flannery); Cal Poly Humboldt (formerly Humboldt State University, T. Danufsky, M. Hawkins, P. Goley, A. Bronson, A. Semerdjian); the Natural History Museum of Los Angeles County (D. Janiger, J. Velez-Juarbe, S. Robson); the NOAA Marine Mammal Laboratory (P. Clapham, P. Wade); the Museum of the North – University of Alaska (A. Gunderson, L. Olson); the Smithsonian National Museum of Natural History (M. Hawkins, D. Lunde, M. McGowen, J. Ososky); the Burke Museum of Natural History and Culture – University of Washington (J. Bradley); the Royal British Columbia Museum (G. Hanke, C. Davies, L. Golding).
Our thanks also to the following for assistance with sample measurements: University of California Santa Cruz Stable Isotope Laboratory (D. Andreasen, C. Carney, and E. Cano); the University of New Mexico Center for Stable Isotopes (S. Newsome, V. Atudorei); University of Florida - Light Stable Isotope Mass Spec Lab (J. Curtis); University of California Davis - Stable Isotope Facility (C. Yarnes, E. Schick).

Finally, we extend our greatest appreciation to numerous researchers at NOAA's Southwest Fisheries Science Center for support that made this work possible, including: D. Weller, J. Seminoff, C. Turner Tomaszewicz, T. Chen, R. Schnug. Also thanks to L. Ballance, J. Shurin, S. Nehasil, and J. Bowen for invaluable additional project support. Funding and support for K.B. and C.K. were provided by the University of California San Diego (UCSD), the NIH

Cell & Molecular Genetics Graduate Training Program, the PADI Foundation, the Lerner-Gray Fund for Marine Research by the American Museum of Natural History, the Jeanne Marie Messier Memorial Endowed Fund (UCSD), the American Cetacean Society Los Angeles Chapter John E. Heyning Research Grant, and the Association for Women in Science San Diego Chapter.

Chapter 5, in full, is currently being prepared for submission for publication of the material. Bowen, Kelly; Kurle, Carolyn. The dissertation author was the primary investigator and author of this material.

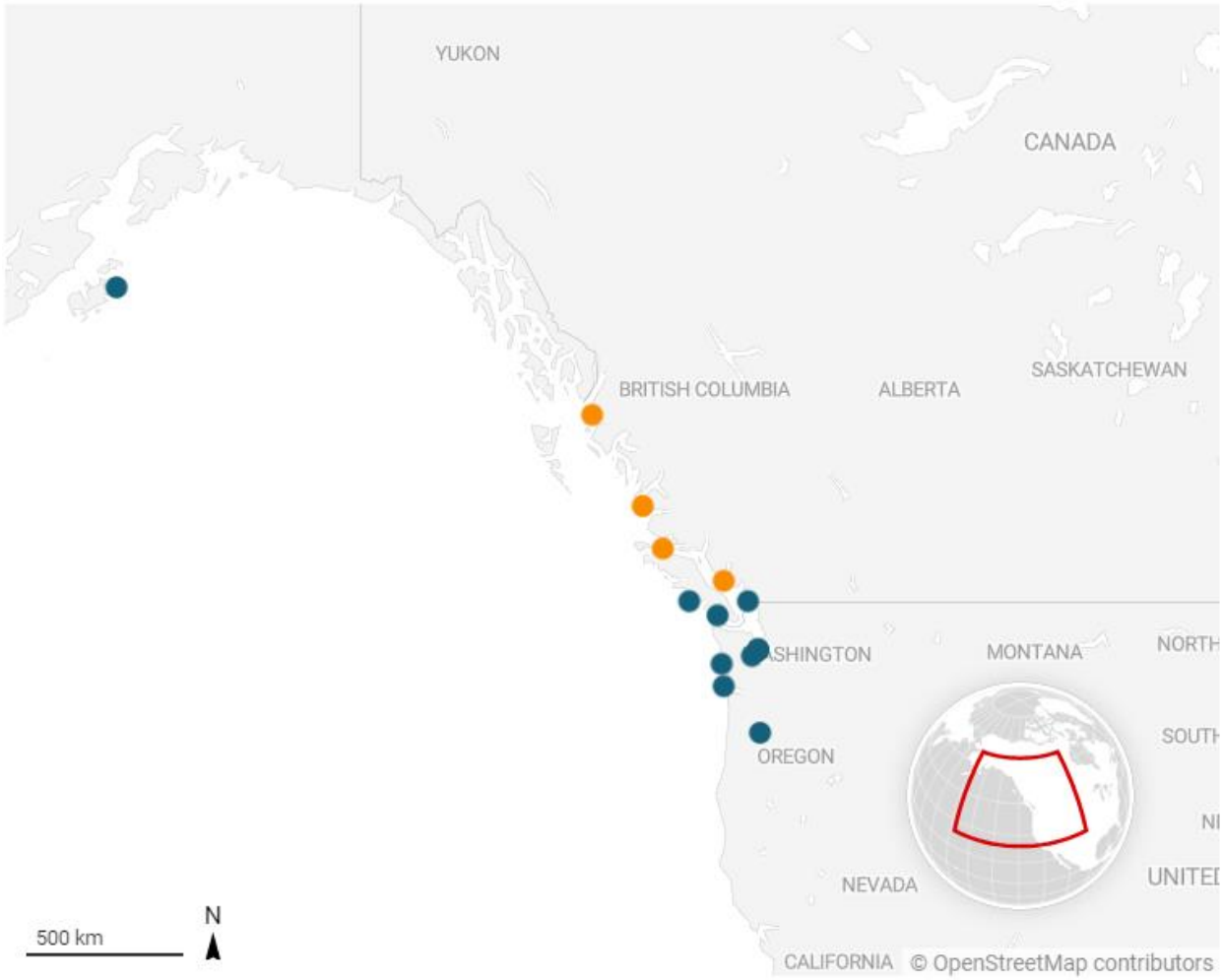


Figure 5.1. Map centered on the west coast of the United States showing collection location of resident killer whale specimens (blue = Southern resident, orange = Northern resident). Map created using Datawrapper.

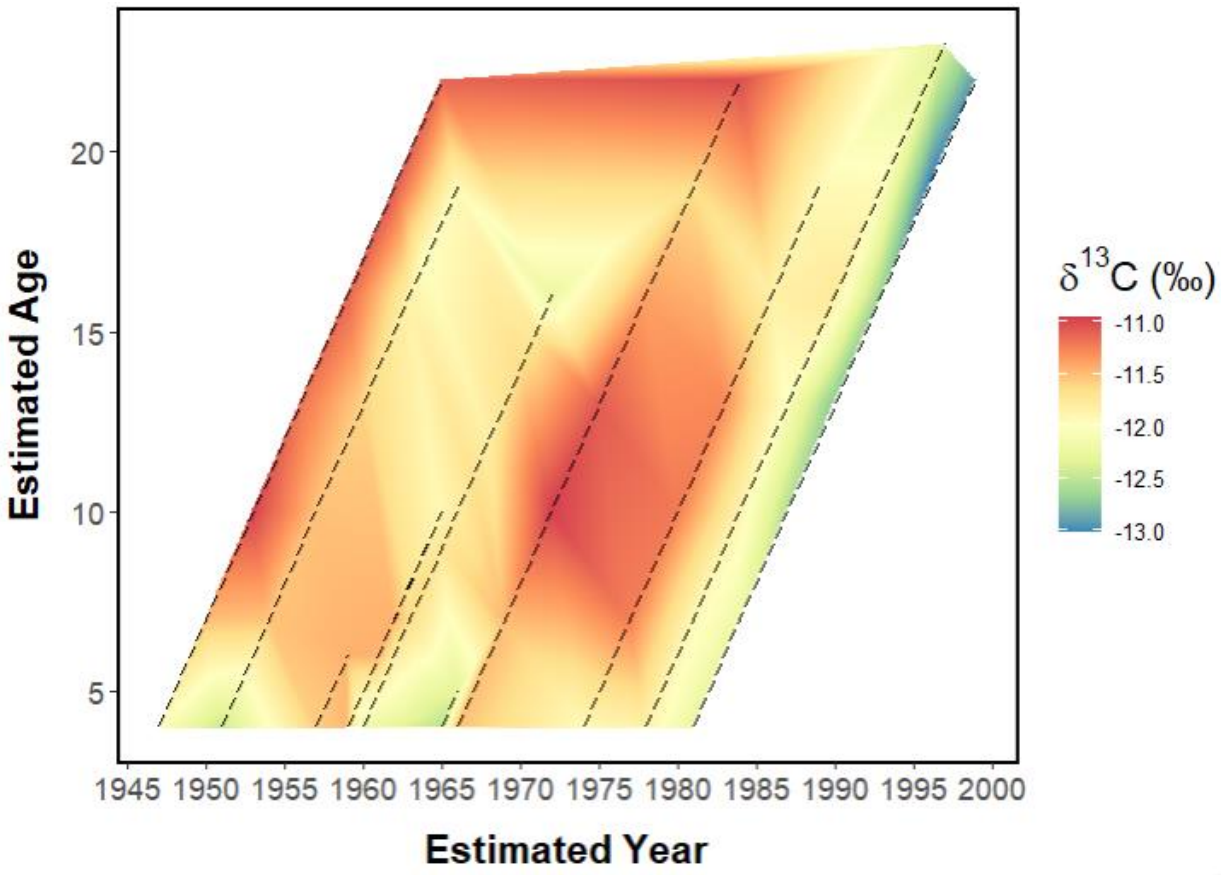


Figure 5.2. A visual representation of the two-way interaction (time:age) that significantly predicted the δ^{13}C values from dentin collected from the growth layer groups (GLGs) in teeth from archived Southern resident killer whale (SRKW) skulls (n = 11 individuals; 65 GLGs). Animals that lived pre-1970 tended to have increasing δ^{13}C values with age, whereas animals after 1970 showed the opposite.

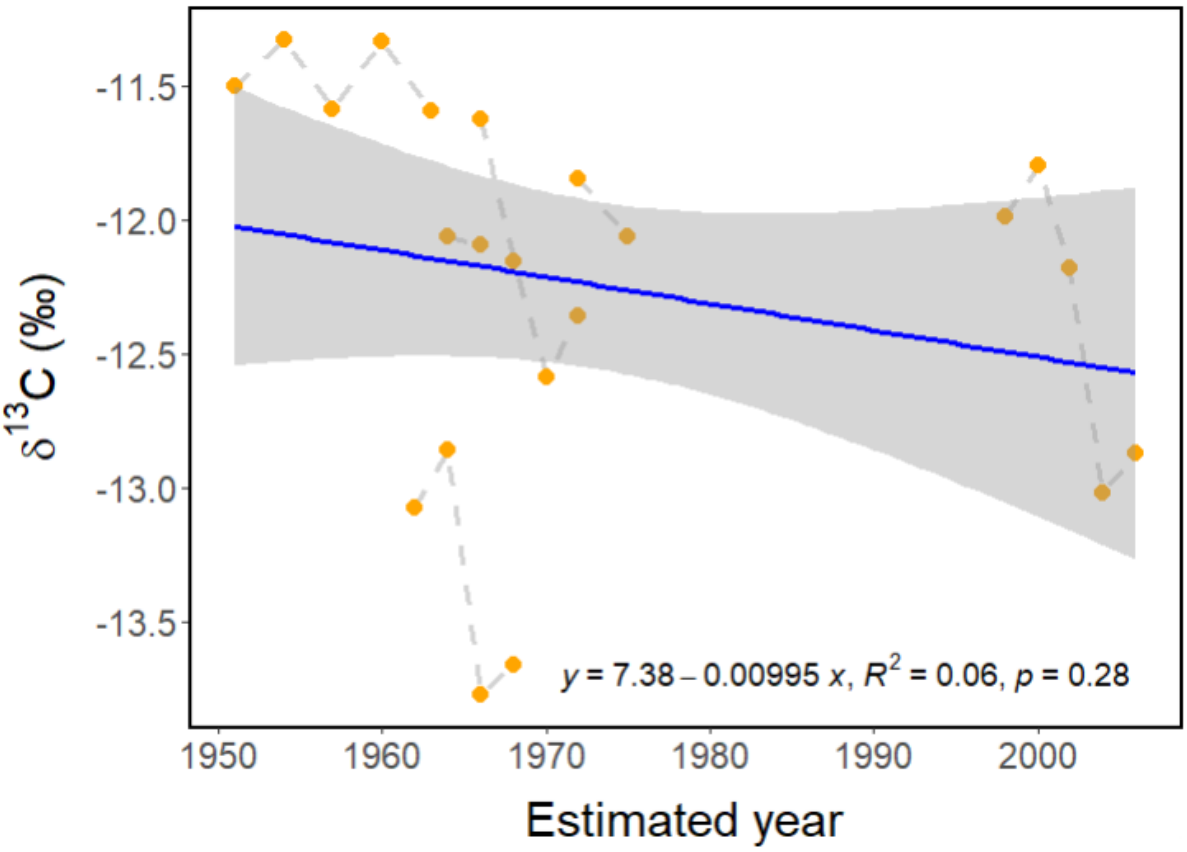


Figure 5.3. The $\delta^{13}C$ values from dentin collected from the growth layer groups (GLGs) in teeth from archived Northern resident killer whale NRKW skulls (n = 6 individuals; 22GLGs) are shown across the years each sampled GLG was estimated to represent. Each connected line represents one individual. There was a non-significant negative trend between the $\delta^{13}C$ values and estimated year.

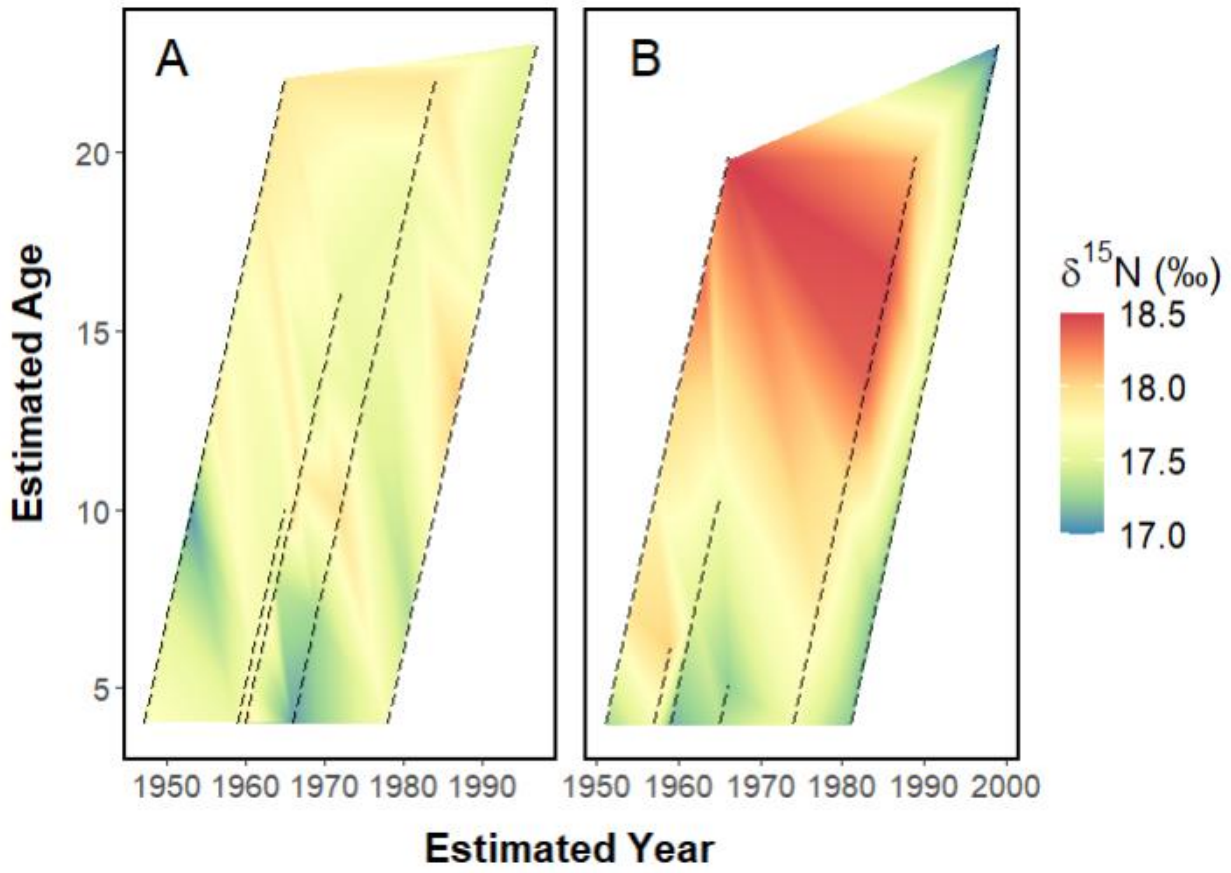


Figure 5.4. A visual representation of the three-way interaction (time:age:sex) that significantly predicted the δ^{15}N values from dentin collected from the growth layer groups (GLGs) in teeth from archived Southern resident killer whale (SRKW) skulls (n = 11 individuals; 65 GLGs). Females (A) and males (B) showed an overall increase in their δ^{15}N values with age, but the ontogenetic shift was weaker for females.

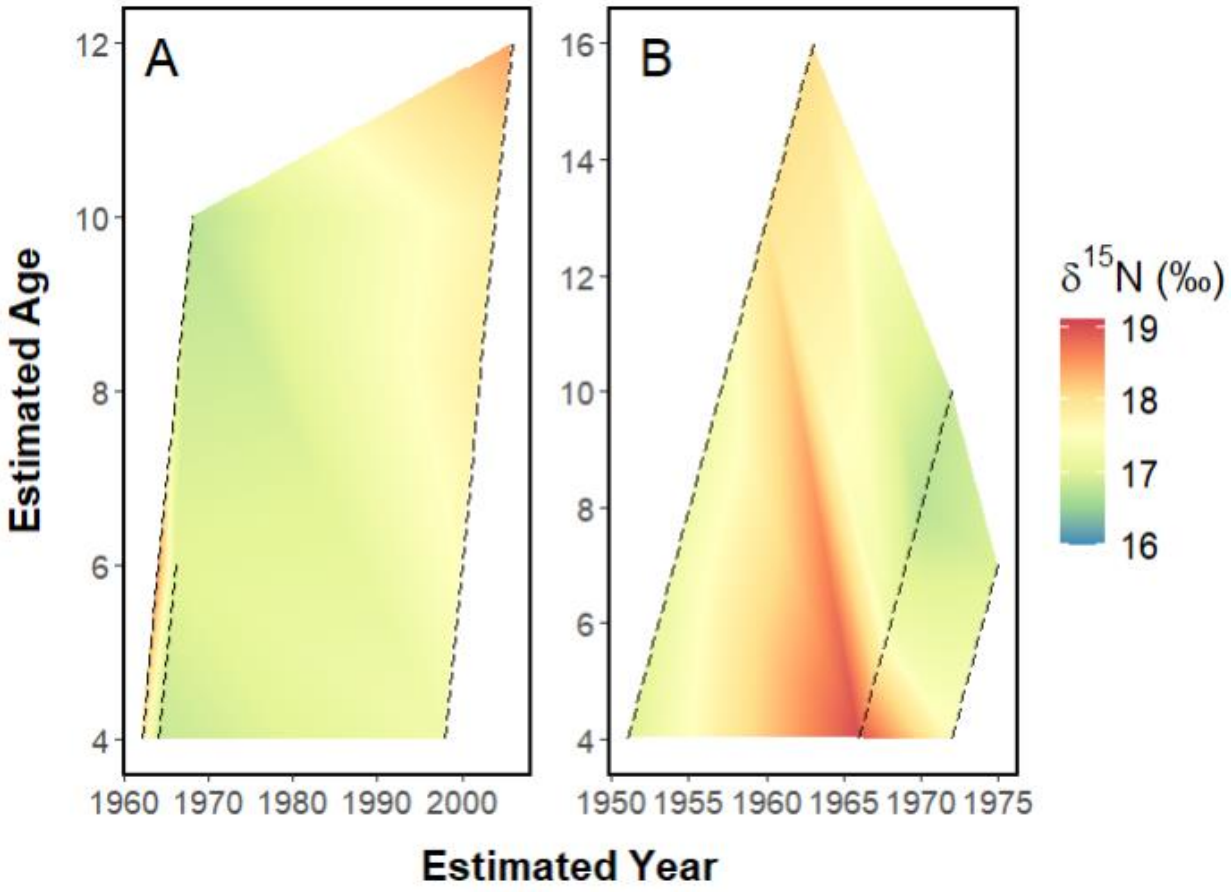


Figure 5.5. A visual representation of the three-way interaction (time:age:sex) that significantly predicted the δ^{15}N values from dentin collected from the growth layer groups (GLGs) in teeth from archived Northern resident killer whale (NRKW) skulls (n = 6 individuals; 22 GLGs). For both females (A) and males (B), there were individuals that exhibited a decrease in their δ^{15}N values with age near the 1960s and 1970s. There were also individuals that exhibited an increase in their δ^{15}N values, but during different time periods (1990s for the female, 1950s for the male), perhaps due to limitations in our represented time periods.

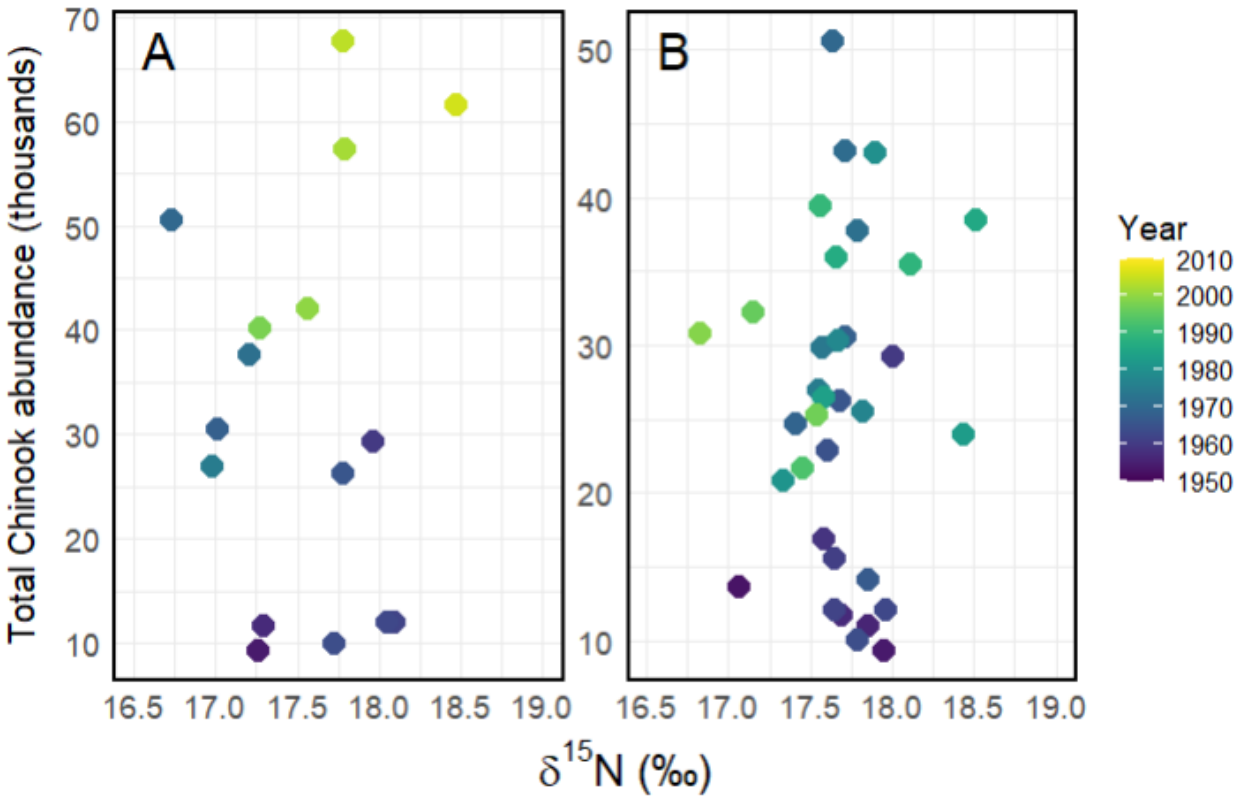


Figure 5.6. There were no significant relationships between total adult spawning Chinook salmon abundance in Puget Sound and the δ^{15}N values from dentin collected from the growth layer groups (GLGs) in teeth from archived (A) Northern resident and (B) Southern resident killer whale skulls.

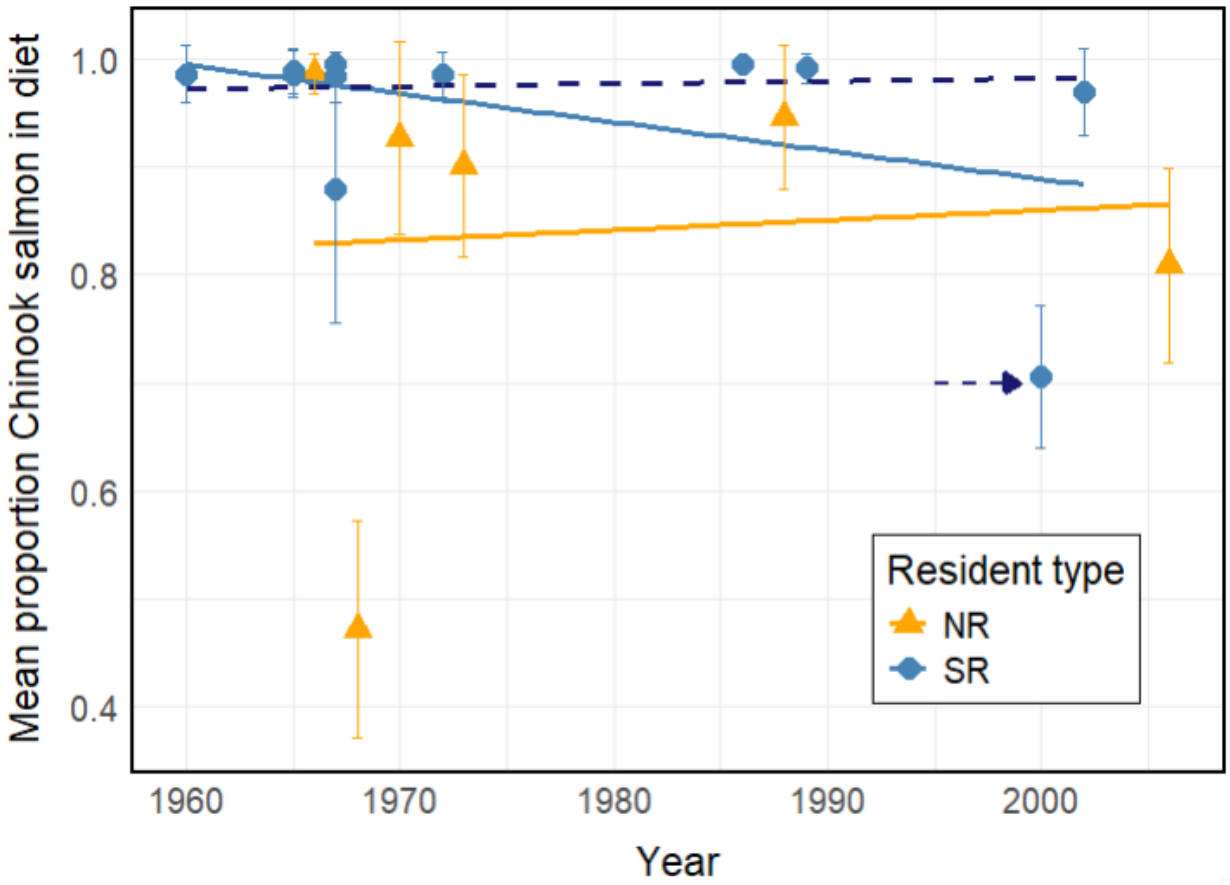


Figure 5.7. Estimations of the mean contribution of Chinook salmon to the diets of individual Northern resident (NR; orange triangles) and Southern resident (SR; blue circles) over time using MixSIAR. Error bars represent the standard deviations. The dashed dark blue trend line represents the relationship for SRs when BBM-J18 (year 2000, dark blue dashed arrow) is excluded.

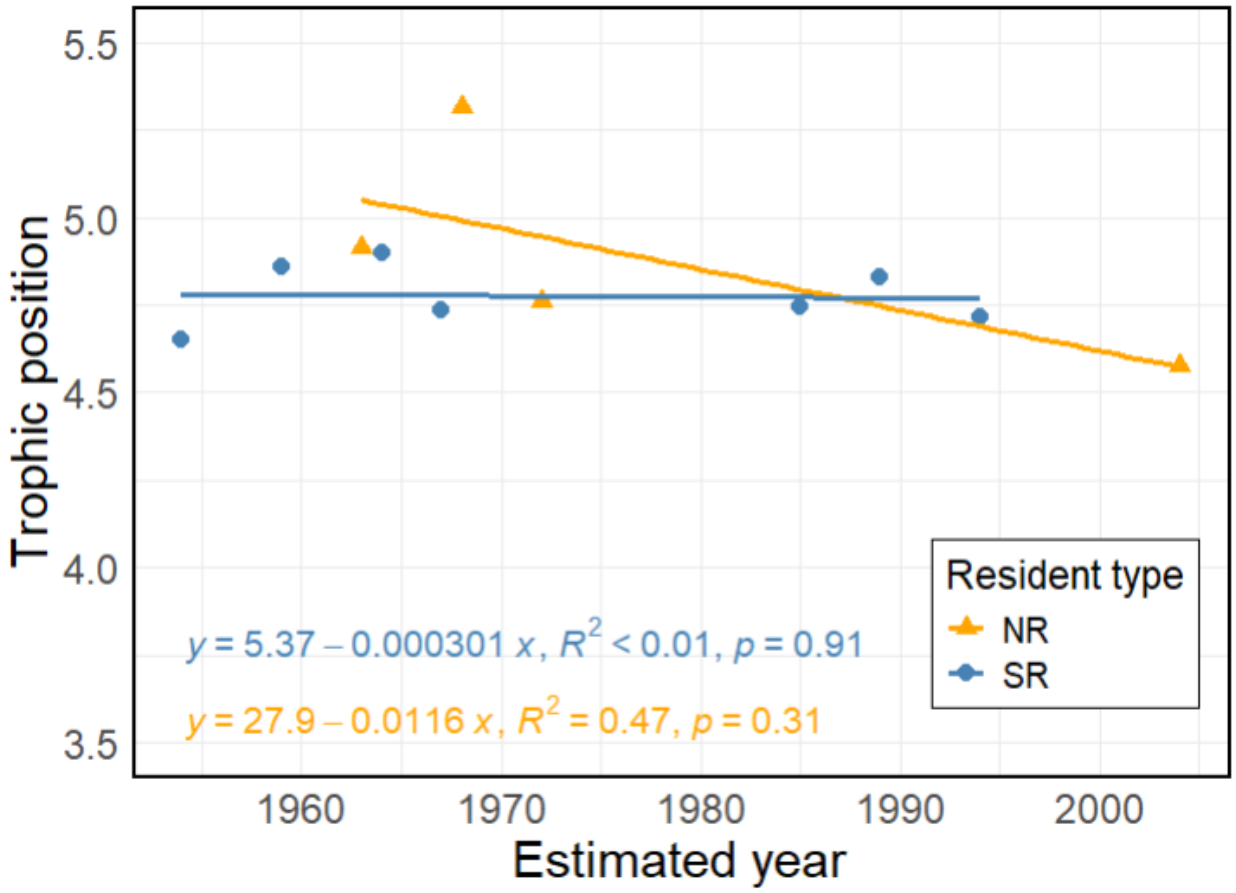


Figure 5.8. Trophic positions are shown across time for both Northern resident (NR; orange triangles) and Southern resident (SR; blue circles) killer whales.

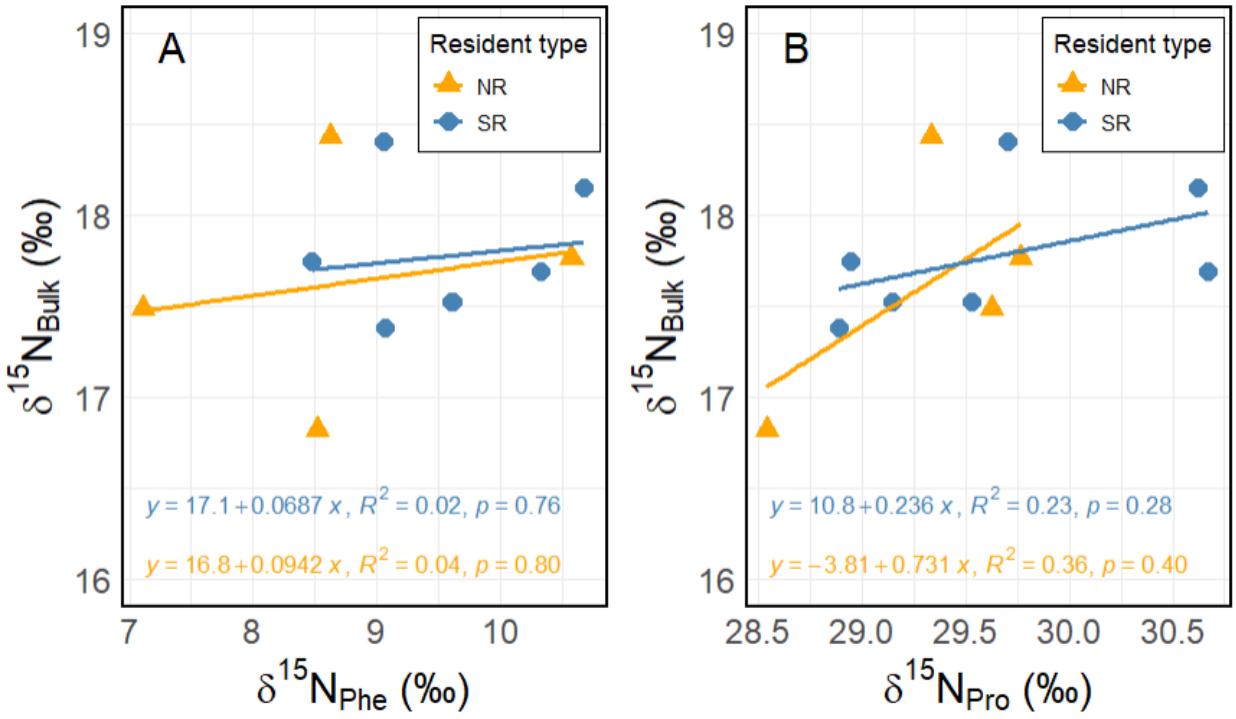


Figure 5.9. The relationship between (A) the $\delta^{15}N_{bulk}$ and $\delta^{15}N_{Phe}$ (source amino acid values and (B) the $\delta^{15}N_{bulk}$ and $\delta^{15}N_{Pro}$ (trophic amino acid) values from dentin collected from the growth layer groups (GLGs) in teeth from archived Northern resident (NR; orange triangles) and Southern resident (SR; blue circles) killer whale skulls.

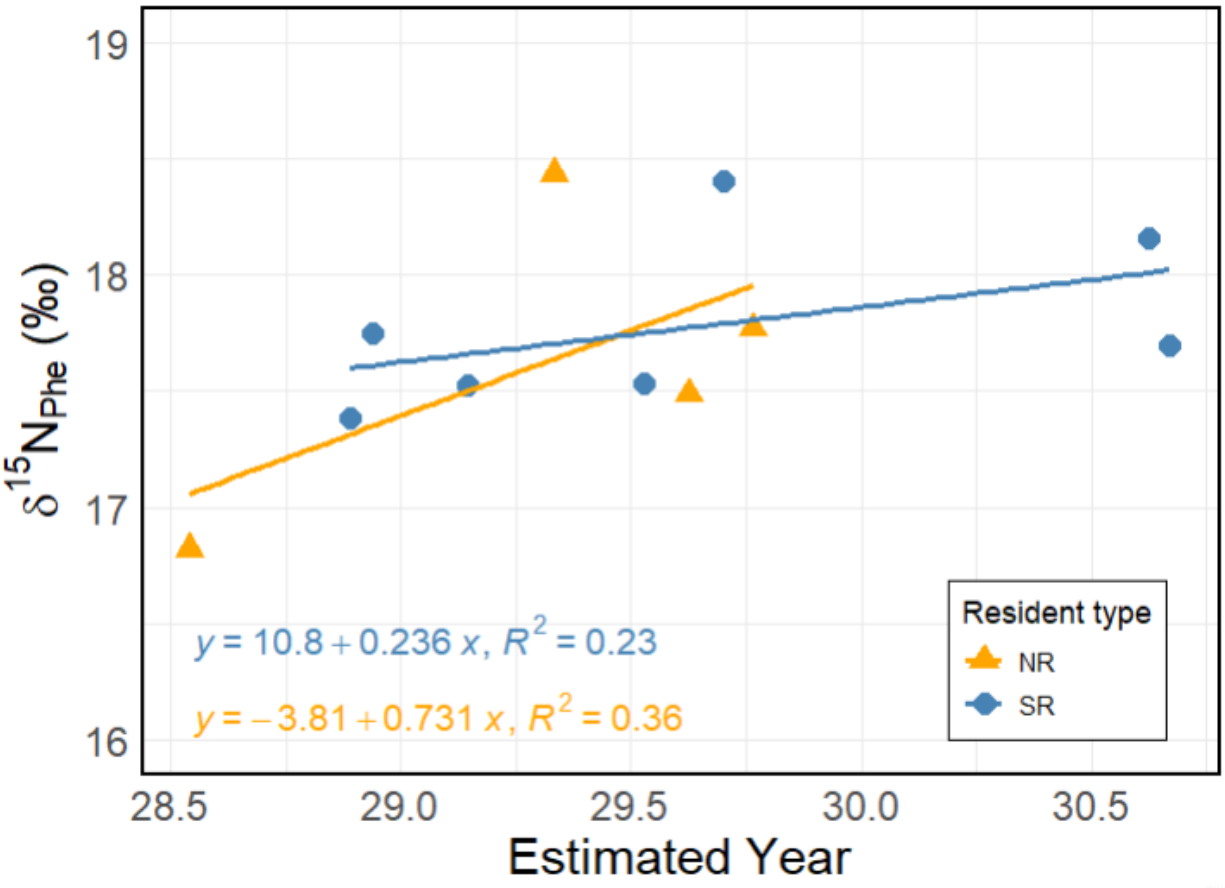


Figure 5.10. The $\delta^{15}N_{Phe}$ (source amino acid) values from dentin collected from the growth layer groups (GLGs) in teeth from archived Northern resident (NR; orange triangles) and Southern resident (SR; blue circles) killer whale skulls shown across time.

Table 5.1. Metadata for the killer whale specimens used in this study. * = animals that spent some amount of time in captivity, with those years being excluded from our analyses. † = Known wild animals with an assigned pod number.

Specimen ID	Alternate ID	Sex	Resident type	Collection year
AMNH: 214946*	"Lupa"	F	SR	1968
BBM: C21 †	"Quadra"	F	NR	2006
CAS: 16464*	"Ahab"	M	SR	1968 (capture)
BBM: J18 †	"Everett"	M	SR	2000
LACM: 52479		F	NR	1968 (capture)
MML: 1977*	"Sandy"	F	SR	1973 (capture)
MML-1966*	"Namu"	M	NR	1965 (capture)
NMML: 1903 †	L60, "Rascal"	F	SR	2002
RBCM: 16006 †	L66, "Mata Hari"	F	SR	1986
RBCM: 16814 †	L14, "Cordy"	M	SR	1989
RBCM: 8386 †	B4	M	NR	1973
USNM: 607013	NMML: 77, MML-60-1	M	SR	1960
USNM: 594670	NMML: 88, MML: 3264	M	SR	1967
USNM: 594672	NMML: 89, MML: 3266	M	SR	1967
USNM: 594675	NMML: 90	F	NR	1968
UWBM: 26183		F	SR	1967

Table 5.2. The killer whales from which tooth specimens were used for measuring the $\delta^{15}N$ values of amino acids through compound-specific isotope analysis of amino acids (CSIA-AA). GLG = growth layer group removed from each tooth, NR = Northern resident killer whales, SR = Southern resident killer whales.

Specimen sampled	Targeted GLG year	Estimated age	Resident type
MML: 1966	1963	16	NR
USNM: 594675	1968	10	NR
RBCM: 8386	1972	10	NR
BBM: C21	2004	10	NR
UWBM: 26183	1954	11	SR
USNM: 594672	1959	12	SR
MML-3265	1964	15	SR
AMNH: 214946	1967	12	SR
RBCM: 16814	1985	15	SR
NMML: 1903	1989	15	SR
BBM: J18	1994	17	SR

Table 5.3. The stable isotope values of dentin collected from the growth layer groups (GLGs) in teeth from archived Northern resident killer whale (NRKW) and Southern resident killer whale (SRKW) skulls.

	δ^{13}C (‰)						δ^{15}N (‰)				
	Median	Mean	SD	Min	Max		Median	Mean	SD	Min	Max
Means of individual means											
NRKW (n = 6)	-12.1	-12.2	0.6	-13.3	-11.5		17.5	17.4	0.3	16.9	17.8
SRKW (n = 11)	-11.7	-11.8	0.4	-12.6	-11.3		17.7	17.6	0.3	17.2	18.1
Mean of all GLGs											
NRKW (n = 22)	-12.1	-12.2	0.7	-13.8	-11.3		17.3	17.5	0.6	16.7	19.0
SRKW (n = 65)	-11.7	-11.8	0.5	-13.0	-11.0		17.6	17.7	0.4	16.8	18.6

Table 5.4. Results of linear mixed models to assess the effect of time (year), age, and sex on the $\delta^{13}C$ and $\delta^{15}N$ values from dentin collected from the growth layer groups in teeth from archived Southern resident killer whale (SRKW) and Northern resident killer whale (NRKW) skulls. Significance levels: *** = 0.001 – 0, ** = 0.01 – 0.001, * = 0.05 – 0.01

Response variable and model	*Estimate*	*SE*	*DF*	*t-value*	*p*	
SRKW, $\delta^{15}N$ (‰)						
Intercept	17.43	0.25	17.50	68.99	< 2e-16	***
Year	0.00	0.01	10.29	0.21	0.84	
Age	0.02	0.02	29.47	1.19	0.24	
Sex(M)	-0.68	0.37	18.92	-1.83	0.08	
Year : Age	0.00	0.00	50.20	-0.72	0.48	
Year : Sex(M)	0.01	0.02	10.74	0.37	0.72	
Age : Sex(M)	0.12	0.03	38.16	3.87	0.00	***
Year : Age : Sex (M)	0.00	0.00	51.83	-2.86	0.01	**
SRKW, $\delta^{13}C$ (‰)						
Intercept	-11.95	0.32	13.57	-37.65	0.00	***
Year	0.00	0.02	9.10	0.25	0.81	
Age	0.07	0.02	21.58	2.89	0.01	**
Sex(M)	0.01	0.46	14.56	0.03	0.98	
Year : Age	0.00	0.00	50.17	-2.98	0.00	**
Year : Sex(M)	-0.01	0.02	9.38	-0.21	0.84	
Age : Sex(M)	-0.01	0.04	30.24	-0.41	0.69	
Year : Age : Sex (M)	0.00	0.00	51.31	-0.04	0.97	
NRKW, $\delta^{15}N$ (‰)						
Intercept	19.21	1.20	12.48	15.98	0.00	***
Year	-0.05	0.03	8.55	-1.35	0.21	
Age	-0.32	0.17	13.65	-1.82	0.09	
Sex(M)	-3.44	1.63	12.67	-2.11	0.06	
Year : Age	0.01	0.00	12.85	2.06	0.06	
Year : Sex(M)	0.17	0.09	11.31	2.01	0.07	
Age : Sex(M)	0.59	0.23	13.82	2.62	0.02	*
Year : Age : Sex (M)	-0.03	0.01	12.94	-2.59	0.02	*

Table 5.4. Continued. Results of linear mixed models to assess the effect of time (year), age, and sex on the $\delta^{13}C$ and $\delta^{15}N$ values from dentin collected from the growth layer groups in teeth from archived Southern resident killer whale (SRKW) and Northern resident killer whale (NRKW) skulls. Significance levels: *** = 0.001 – 0, ** = 0.01 – 0.001, * = 0.05 – 0.01

Response variable and model	*Estimate*	*SE*	*DF*	*t-value*	*p*	
NRKW, $\delta^{13}C$ (‰)						
Intercept	-12.18	0.68	7.20	-17.79	0.00	***
Year	0.02	0.02	4.16	1.06	0.35	
Age	-0.14	0.08	13.37	-1.71	0.11	
Sex(M)	0.28	0.92	7.34	0.30	0.77	
Year : Age	0.00	0.00	12.29	-0.28	0.79	
Year : Sex(M)	-0.01	0.05	5.74	-0.25	0.81	
Age : Sex(M)	0.24	0.11	13.99	2.12	0.05	
Year : Age : Sex (M)	-0.01	0.01	12.29	-1.24	0.24	

Table 5.5. Results of linear mixed models used to determine the significance of time (year), age, and sex on the $\delta^{13}C$ and $\delta^{15}N$ values from dentin collected from the growth layer groups in teeth from archived Southern resident killer whale (SRKW) and Northern resident killer whale (NRKW) skulls.

Response variable and model	*SS*	*NumDF*	*DenDF*	*F*	*p*	
SRKW, $\delta^{15}N$ (‰)						
Year	0.02	1	10.74	0.46	0.51	
Age	1.38	1	38.16	28.90	0.00	***
Sex	0.16	1	18.92	3.33	0.08	
Year : Age	0.70	1	51.83	14.60	0.00	***
Year : Sex	0.01	1	10.74	0.14	0.72	
Age : Sex	0.71	1	38.16	14.95	0.00	***
Year : Age : Sex	0.39	1	51.83	8.20	0.01	**
SRKW, $\delta^{13}C$ (‰)						
Year	0.00	1	9.38	0.03	0.88	
Age	0.63	1	30.24	11.10	0.00	**
Sex	0.00	1	14.56	0.00	0.98	
Year : Age	0.91	1	51.31	16.11	0.00	***
Year : Sex	0.00	1	9.38	0.04	0.84	
Age : Sex	0.01	1	30.24	0.16	0.69	
Year : Age : Sex	0.00	1	51.31	0.00	0.97	
NRKW, $\delta^{15}N$ (‰)						
Year	0.30	1	11.31	0.86	0.37	
Age	0.01	1	13.82	0.03	0.86	
Sex	1.54	1	12.67	4.46	0.06	
Year : Age	0.44	1	12.94	1.28	0.28	
Year : Sex	1.40	1	11.31	4.06	0.07	
Age : Sex	2.36	1	13.82	6.84	0.02	*
Year : Age : Sex	2.31	1	12.94	6.70	0.02	*

Table 5.5. Continued. Results of linear mixed models used to determine the significance of time (year), age, and sex on the $\delta^{13}C$ and $\delta^{15}N$ values from dentin collected from the growth layer groups in teeth from archived Southern resident killer whale (SRKW) and Northern resident killer whale (NRKW) skulls.

Response variable and model	*SS*	*NumDF*	*DenDF*	*F*	*p*
NRKW, $\delta^{13}C$ (‰)					
Year	0.03	1	5.74	0.43	0.54
Age	0.01	1	13.99	0.20	0.66
Sex	0.01	1	7.34	0.09	0.77
Year : Age	0.15	1	12.29	2.05	0.18
Year : Sex	0.00	1	5.74	0.06	0.81
Age : Sex	0.34	1	13.99	4.50	0.05
Year : Age : Sex	0.11	1	12.29	1.53	0.24

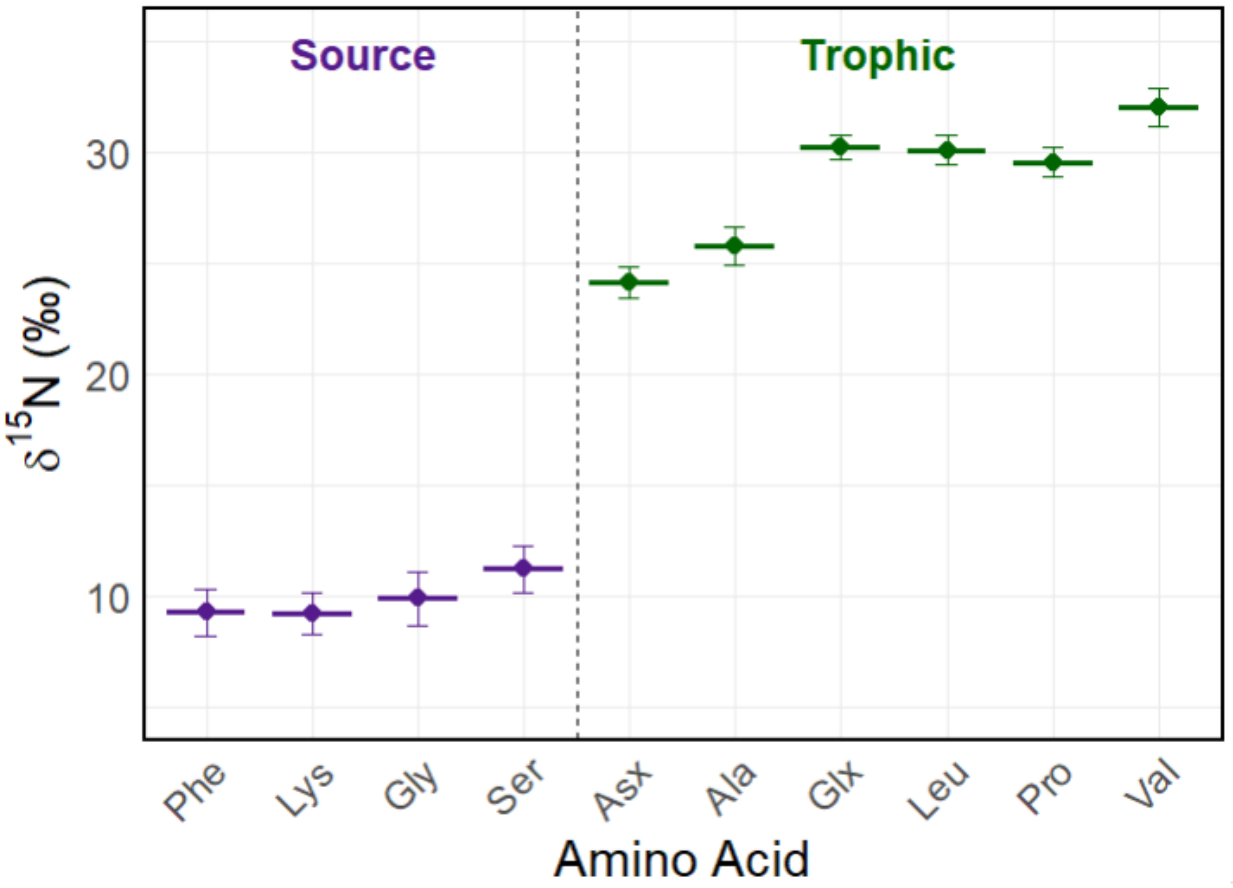


Figure S5.1. The mean δ^{15}N values with standard deviation error bars are shown for each of 10 amino acids: four source amino acids (left, purple) and six trophic amino acids (right, green).

Table S5.1. We report details for the compound-specific isotope analysis of amino acids (CSIA-AA) results for each of the 11 specimens sampled, including specimen ID (* = specimen not included in the linear mixed model analyses of bulk isotope analyses), alternate catalogue IDs, resident type (NR = Northern resident, SR = Southern resident), the estimated age of the sampled growth layer group (GLG), the estimated year that GLG represents, and the δ^{15}N values for the "source" and "trophic" amino acids.

Specimen	**Alternate**	**Resident**	**Est.**	**Est.**	**"Source" amino acids**					**"Trophic" amino acids**				
ID	**ID**	**type**	**age**	**year**	*Phe*	*Lys*	*Gly*	*Ser*	*Asx*	*Ala*	*Glx*	*Leu*	*Pro*	*Val*
MML-1966	"Namu"	NR	16	1963	8.6	11.3	9.8	11.0	25.4	26.9	30.4	29.9	29.3	31.9
USNM: 594675	NMML: 90	NR	10	1968	7.1	9.2	8.5	10.8	24.9	24.0	29.3	29.1	29.6	30.3
RBCM: 8386	B4	NR	10	1972	8.5	8.5	10.9	10.2	23.2	25.8	29.5	29.4	28.5	31.9
BBM: C21	"Quadra"	NR	10	2004	10.6	9.8	11.1	9.8	24.1	26.6	30.7	31.0	29.8	33.4
UWBM: 26183		SR	11	1954	9.6	8.7	8.3	11.9	24.2	25.2	30.0	29.7	29.1	31.5
USNM: 594672	NMML: 89, MML: 3266	SR	12	1959	8.5	8.7	9.6	11.4	23.8	25.1	29.7	30.0	28.9	31.9
MML-3265*		SR	15	1964	9.1	8.4	9.8	12.6	24.2	27.0	30.4	30.1	29.7	31.8
AMNH: 214946	"Lupa"	SR	12	1967	9.6	9.2	10.1	9.5	23.5	26.0	30.3	30.8	29.5	33.1
RBCM: 16814	L14	SR	15	1985	10.7	9.9	12.2	12.2	24.5	26.0	30.9	31.2	30.6	32.9
NMML: 1903	L60; "Rascal"	SR	15	1989	10.3	9.4	8.4	11.5	24.0	25.6	30.9	30.0	30.7	31.5
BBM: J18	"Everett"	SR	17	1994	9.1	8.1	9.8	12.2	23.3	25.4	29.8	29.7	28.9	31.9

Table S5.2. We report the specimens used in this study (* = time in captivity, † = assigned wild ID), alternate catalogue IDs, the sex of the individual, resident type (SR = Southern resident, NR = Northern resident), the estimated age of the growth layer group (GLG) from which dentin was extracted, the estimated year the GLG represents, and the bulk $\delta^{13}C$ and $\delta^{15}N$ values for each GLG. The $\delta^{13}C$ values are corrected for the Suess effect, Laws effect, and lipid content.

Specimen ID	Alternate ID	Sex	Resident type	Est. age	Est. year	$\delta^{13}C$ (‰)	$\delta^{15}N$ (‰)
AMNH: 214946*	"Lupa"	F	SR	4	1959	-11.6	17.6
		F	SR	6	1961	-11.5	17.7
		F	SR	8	1963	-11.7	17.6
		F	SR	10	1965	-11.9	17.6
BBM: C21 †	"Quadra"	F	NR	4	1998	-12.0	17.3
		F	NR	6	2000	-11.8	17.6
		F	NR	8	2002	-12.2	17.8
		F	NR	10	2004	-13.0	17.8
		F	NR	12	2006	-12.9	18.5
CAS: 16464*	"Ahab"	M	SR	4	1959	-11.4	17.0
		M	SR	7	1962	-11.5	17.4
		M	SR	10	1965	-11.9	17.6
BBM: J18 †	"Everett"	M	SR	4	1981	-12.2	17.1
		M	SR	7	1984	-12.2	17.0
		M	SR	10	1987	-12.5	17.2
		M	SR	13	1990	-12.7	17.4
		M	SR	16	1993	-12.6	17.4
		M	SR	19	1996	-13.0	17.2
		M	SR	22	1999	-12.9	16.8
LACM: 52479		F	NR	4	1964	-12.1	16.8
		F	NR	6	1966	-12.1	17.0
		M	NR	4	1972	-11.8	17.6
		M	NR	7	1975	-12.1	17.0

Table S5.2. Continued. We report the specimens used in this study (* = time in captivity, † = assigned wild ID), alternate catalogue IDs, the sex of the individual, resident type (SR = Southern resident, NR = Northern resident), the estimated age of the growth layer group (GLG) from which dentin was extracted, the estimated year the GLG represents, and the bulk $\delta^{13}C$ and $\delta^{15}N$ values for each GLG. The $\delta^{13}C$ values are corrected for the Suess effect, Laws effect, and lipid content.

Specimen ID	Alternate ID	Sex	Resident type	Est. age	Est. year	$\delta^{13}C$ (‰)	$\delta^{15}N$ (‰)
MML: 1977*	"Sandy"	F	SR	4	1960	-12.1	18.0
		F	SR	5	1961	-11.9	17.6
		F	SR	6	1962	-11.8	17.6
		F	SR	7	1963	-11.6	17.8
		F	SR	8	1964	-11.6	17.4
		F	SR	9	1965	-11.7	17.6
		F	SR	10	1966	-11.8	18.0
		F	SR	11	1967	-11.7	17.9
		F	SR	12	1968	-11.8	17.7
		F	SR	13	1969	-11.7	17.5
		F	SR	14	1970	-11.7	17.6
		F	SR	15	1971	-11.7	17.7
		F	SR	16	1972	-12.2	17.6
MML-1966*	"Namu"	M	NR	4	1951	-11.5	17.0
		M	NR	7	1954	-11.3	17.3
		M	NR	10	1957	-11.6	17.3
		M	NR	13	1960	-11.3	18.0
		M	NR	16	1963	-11.6	18.0
NMML: 1903 †	L60; "Rascal"	F	SR	4	1978	-11.8	17.7
		F	SR	7	1981	-11.9	17.3
		F	SR	10	1984	-11.9	17.8
		F	SR	13	1987	-12.0	18.1
		F	SR	16	1990	-11.8	17.7
		F	SR	19	1993	-11.9	17.5
		F	SR	23	1997	-12.3	17.5
USNM: 607013	NMML: 77, MML-60-1	M	SR	4	1957	-11.6	17.6
		M	SR	6	1959	-11.5	18.0
USNM: 594670	NMML: 88, MML: 3264	M	SR	4	1965	-12.5	17.2
		M	SR	5	1966	-12.3	17.1

Table S5.2. Continued. We report the specimens used in this study (* = time in captivity, † = assigned wild ID), alternate catalogue IDs, the sex of the individual, resident type (SR = Southern resident, NR = Northern resident), the estimated age of the growth layer group (GLG) from which dentin was extracted, the estimated year the GLG represents, and the bulk $\delta^{13}C$ and $\delta^{15}N$ values for each GLG. The $\delta^{13}C$ values are corrected for the Suess effect, Laws effect, and lipid content.

Specimen ID	Alternate ID	Sex	Resident type	Est. age	Est. year	$\delta^{13}C$ (‰)	$\delta^{15}N$ (‰)
USNM: 594672	NMML: 89, MML: 3266	M	SR	4	1951	-12.5	17.1
		M	SR	7	1954	-11.5	18.0
		M	SR	10	1957	-11.5	17.8
		M	SR	13	1960	-11.6	18.0
		M	SR	16	1963	-11.8	18.4
		M	SR	17	1964	-12.0	18.2
		M	SR	19	1966	-11.9	18.6
USNM: 594675	NMML: 90	F	NR	4	1962	-13.1	18.1
		F	NR	6	1964	-12.9	18.6
		F	NR	8	1966	-13.8	17.3
		F	NR	10	1968	-13.7	16.7
RBCM: 16006 †	L66	F	SR	4	1966	-11.5	17.1
		F	SR	7	1969	-11.5	17.3
		F	SR	10	1972	-11.0	18.0
		F	SR	13	1975	-11.1	17.5
		F	SR	16	1978	-11.4	17.6
		F	SR	19	1981	-11.6	17.6
		F	SR	22	1984	-11.0	17.9
RBCM: 16814 †	L14	M	SR	4	1974	-11.9	17.6
		M	SR	7	1977	-11.2	17.8
		M	SR	10	1980	-11.2	17.9
		M	SR	13	1983	-11.3	18.4
		M	SR	16	1986	-11.8	18.5
		M	SR	19	1989	-11.9	18.1

Table S5.2. We report the specimens used in this study (* = time in captivity, † = assigned wild ID), alternate catalogue IDs, the sex of the individual, resident type (SR = Southern resident, NR = Northern resident), the estimated age of the growth layer group (GLG) from which dentin was extracted, the estimated year the GLG represents, and the bulk $\delta^{13}C$ and $\delta^{15}N$ values for each GLG. The $\delta^{13}C$ values are corrected for the Suess effect, Laws effect, and lipid content.

Specimen ID	Alternate ID	Sex	Resident type	Est. age	Est. year	$\delta^{13}C$ (‰)	$\delta^{15}N$ (‰)
RBCM: 8386 †	B4	M	NR	4	1966	-11.6	19.0
		M	NR	6	1968	-12.2	17.3
		M	NR	8	1970	-12.6	16.7
		M	NR	10	1972	-12.4	16.8
UWBM: 26183		F	SR	4	1947	-12.0	17.8
		F	SR	7	1950	-11.5	17.5
		F	SR	10	1953	-11.0	17.1
		F	SR	13	1956	-11.2	17.9
		F	SR	16	1959	-11.1	17.7
		F	SR	19	1962	-11.0	17.9
		F	SR	22	1965	-11.1	17.9

5.7 References

1. Pitman RL, Ensor P. Three forms of killer whales (*Orcinus orca*) in Antarctic waters. *jcrm*. 2023;5(2):131-139. doi:10.47536/jcrm.v5i2.813

2. Foote AD, Newton J, Piertney SB, Willerslev E, Gilbert MTP. Ecological, morphological and genetic divergence of sympatric North Atlantic killer whale populations. *Mol Ecol*. 2009;18(24):5207-5217. doi:10.1111/j.1365-294X.2009.04407.x

3. Morin PA, Archer FI, Foote AD, Vilstrup J, Allen EE, Wade P, Durban J, Parsons K, Pitman R, Li L, Bouffard P. Complete mitochondrial genome phylogeographic analysis of killer whales (*Orcinus orca*) indicates multiple species. *Genome Res*. 2010;20(7):908-916. doi:10.1101/gr.102954.109

4. Foote AD, Morin PA, Durban JW, Willerslev E, Orlando L, Gilbert MTP. Out of the Pacific and Back Again: Insights into the Matrilineal History of Pacific Killer Whale Ecotypes. Demuth J, ed. *PLoS ONE*. 2011;6(9):e24980. doi:10.1371/journal.pone.0024980

5. De Bruyn PJN, Tosh CA, Terauds A. Killer whale ecotypes: is there a global model? *Biol Rev*. 2013;88(1):62-80. doi:10.1111/j.1469-185X.2012.00239.x

6. Bigg MA, Olesiuk PF, Ellis GM, Ford JKB, Balcomb KC. Social organization and genealogy of resident killer whales (*Orcinus orca*) in the coastal waters of British Columbia and Washington State. *Rep Int Whale Commn*. 1990;(12):383-405.

7. Olesiuk PF, Bigg MA, Ellis GM. Life history and population dynamics of resident killer whales (*Orcinus orca*) in the coastal waters of British Columbia and Washington State. *Rep Int Whale Commn*. (12):209-243.

8. Ford JK, Ellis GM, Barrett-Lennard LG, Morton AB, Palm RS, Balcomb KC. Dietary specialization in two sympatric populations of killer whales (*Orcinus orca*) in coastal British Columbia and adjacent waters. *Can J Zool*. 1998;76(8):1456-1471. doi:10.1139/z98-089

9. Ford JKB, Ellis GM, Balcomb KC. *Killer Whales: The Natural History and Genealogy of Orinus Orca in British Columbia and Washington*. 2nd ed. UBC Press ; University of Washington Press; 2000.

10. Ford J, Ellis G, Matkin C, Wetklo M, Barrett-Lennard L, Withler R. Shark predation and tooth wear in a population of northeastern Pacific killer whales. *Aquat Biol*. 2011;11(3):213-224. doi:10.3354/ab00307

11. Morin PA, McCarthy ML, Fung CW, Durban JW, Parsons KM, Perrin WF, Taylor BL, Jefferson TA, Archer FI. Revised taxonomy of eastern North Pacific killer whales (*Orcinus orca*): Bigg's and resident ecotypes deserve species status. *R Soc Open Sci*. 2024;11(3):231368. doi:10.1098/rsos.231368

12. Carretta JV, Oleson EM, Forney KA, Muto MM, Weller DW, Lang AR, Baker J, Hanson B, Orr AJ, Barlow J, Moore JE. *U.S. Pacific Marine Mammal Stock Assessments: 2022. U.S. Department of Commerce, NOAA Technical Memorandum*.; 2022. https://doi.org/10.25923/5ysf-gt95

13. Riesch R, Ford JKB, Thomsen F. Stability and group specificity of stereotyped whistles in resident killer whales, *Orcinus orca*, off British Columbia. *Anim Behav*. 2006;71(1):79-91. doi:10.1016/j.anbehav.2005.03.026

14. Krahn MM, Wade PR, Kalinowski ST, Dahlheim ME, Taylor BL, Hanson MB, Ylitalo GM, Angliss RP, Stein JE, Waples RS. *2004 Status Review of Southern Resident Killer Whales (*Orcinus Orca*) under the Endangered Species Act*. U.S. Dep. Commer., NOAA Tech. Memo; 2004:73.

15. Hilborn R, Cox SP, Gulland FMD, Hankin DG, Hobbs NT, Schindler DE, Trites AW. *The Effects of Salmon Fisheries on Southern Resident Killer Whales: Final Report of the Independent Science Panel*. National Marine Fisheries Service (Seattle. WA) and Fisheries and Oceans Canada (Vancouver. BC); 2012:xv + 61 pp. + Appendices. https://www.noaa.gov/sites/default/files/legacy/document/2020/Oct/07354626726.pdf

16. Rice A, Deecke VB, Ford JK, Pilkington JF, Oleson EM, Hildebrand JA. Spatial and temporal occurrence of killer whale ecotypes off the outer coast of Washington State, USA. *Mar Ecol Prog Ser*. 2017;572:255-268. doi:10.3354/meps12158

17. Hanson M, Ward E, Emmons C, Holt M. *Modeling the occurrence of endangered killer whales near a U.S. Navy training range in Washington State using satellite-tag locations to improve acoustic detection data*. National Oceanic and Atmospheric Administration, Northwest Fisheries Science Center; 2018:33.

18. Emmons C, Hanson M, Lammers M. Passive acoustic monitoring reveals spatiotemporal segregation of two fish-eating killer whale *Orcinus orca* populations in proposed critical habitat. *Endang Species Res*. 2021;44:253-261. doi:10.3354/esr01099

19. Nichol LM, Shackleton DM. Seasonal movements and foraging behaviour of northern resident killer whales (*Orcinus orca*) in relation to the inshore distribution of salmon (*Oncorhynchus* spp.) in British Columbia. *Can J Zool*. 1996;74(6):983-991. doi:10.1139/z96-111

20. Ford JKB, Ellis GM, Olesiuk PF, Balcomb KC. Linking killer whale survival and prey abundance: food limitation in the oceans' apex predator? *Biol Lett*. 2010;6(1):139-142. doi:10.1098/rsbl.2009.0468

21. Hanson MB, Emmons CK, Ford MJ, Everett M, Parsons K, Park LK, Hempelmann J, Van Doornik DM, Schorr GS, Jacobsen JK, Sears MF. Endangered predators and endangered prey: Seasonal diet of Southern Resident killer whales. Hyrenbach D, ed. *PLoS ONE*. 2021;16(3):e0247031. doi:10.1371/journal.pone.0247031

22. Ford J, Ellis G. Selective foraging by fish-eating killer whales *Orcinus orca* in British Columbia. *Mar Ecol Prog Ser*. 2006;316:185-199. doi:10.3354/meps316185

23. Hanson MB, Baird RW, Ford JK, Hempelmann-Halos J, Van Doornik DM, Candy JR, Emmons CK, Schorr GS, Gisborne B, Ayres KL, Wasser SK. Species and stock identification of prey consumed by endangered southern resident killer whales in their summer range. *Endang Species Res*. 2010;11:69-82. doi:10.3354/esr00263

24. Zamon J, Guy T, Balcomb K, Ellifrit D. Winter observations of southern resident killer whales (*Orcinus orca*) near the Columbia River plume during the 2005 spring Chinook salmon (*Oncorhynchus tshawytscha*) spawning migration. *Northwest Nat*. 2007;88:193-198.

25. Weitkamp LA. Marine distributions of Chinook salmon from the west coast of North America determined by coded wire tag recoveries. *Trans Am Fish Soc*. 2010;139(1):147-170. doi:10.1577/T08-225.1

26. Ford MJ, Hempelmann J, Hanson MB, Ayres KL, Baird RW, Emmons CK, Lundin JI, Schorr GS, Wasser SK, Park LK. Estimation of a killer whale (*Orcinus orca*) population's diet using sequencing analysis of DNA from feces. Crocker DE, ed. *PLoS ONE*. 2016;11(1):e0144956. doi:10.1371/journal.pone.0144956

27. Tennessen JB, Holt MM, Wright BM, Hanson MB, Emmons CK, Giles DA, Hogan JT, Thornton SJ, Deecke VB. Divergent foraging strategies between populations of sympatric matrilineal killer whales. Pinter-Wollman N, ed. *Behav Ecol*. Published online March 4, 2023:arad002. doi:10.1093/beheco/arad002

28. O'Neill S, Ylitalo G, West J. Energy content of Pacific salmon as prey of northern and southern resident killer whales. *Endang Species Res*. 2014;25(3):265-281. doi:10.3354/esr00631

29. Bigg MA, MacAskie I, Ellis G. *Abundance and Movements of Killer Whales off Eastern and Southern Vancouver Island with Comments on Management*. Arctic Biological Station; 1976.

30. NMFS. *Endangered and Threatened Species: Final Listing Determinations for 16 ESUs of West Coast Salmon, and Final 4(d) Protective Regulations for Threatened Salmonid ESUs*.; 2005. www.nwr.noaa.gov/Publications/FR-Notices/2005/upload/ 70FR37160.pdf

31. Heise KA. *Recovery Strategy for the Northern and Southern Resident Killer Whales (*Orcinus Orca*) in Canada*. Fisheries and Oceans Canada; 2008.

32. Krahn MM, Hanson MB, Schorr GS, Emmons CK, Burrows DG, Bolton JL, Baird RW, Ylitalo GM. Effects of age, sex and reproductive status on persistent organic pollutant concentrations in "Southern Resident" killer whales. *Mar Pollut Bull*. 2009;58(10):1522-1529. doi:10.1016/j.marpolbul.2009.05.014

33. Stocking J. *Periodic Status Review for the Orca*. Washington Department of Fish and Wildlife; 2023:iii + 24.

34. Schindler D, Krueger C, Bisson P, Bradford M, Clark B, Conitz J, Howard K, Jones M, Murphy J, Myers K, Scheuerell M. *Evidence of Decline of Chinook Salmon Populations and Recommendations for Future Research. Arctic-Yukon-Kuskokwim Chinook Salmon Research Action Plan*. AYK Sustainable Salmon Initiative; 2013. http://www.aykssi.org/wp-content/uploads/AYK-SSI-Chinook-Salmon-Action-Plan-83013.pdf

35. Ohlberger J, Ward EJ, Schindler DE, Lewis B. Demographic changes in Chinook salmon across the Northeast Pacific Ocean. *Fish Fish*. 2018;19(3):533-546. doi:10.1111/faf.12272

36. DFO. *Population Status Update for the Northern Resident Killer Whale (*Orcinus Orca*) in 2021*. Can. Sci. Advis. Sec. Sci. Resp; 2022.

37. Noel M, Ylitalo GM, Hanson B, Towers J, Ross P. PCB and PBDE levels in southern and northern resident killer whales: update on contaminant levels and related health effects. In: ; 2018. https://cedar.wwu.edu/ssec/2018ssec/allsessions/30

38. Ferrara G, Mongillo T, Barre L. *Reducing Disturbance from Vessels to Southern Resident Killer Whales: Assessing the Effectiveness of the 2011 Federal Regulations in Advancing Recovery Goals*.; 2017:76.

39. Ward EJ, Holmes EE, Balcomb KC. Quantifying the effects of prey abundance on killer whale reproduction. *J Appl Ecol*. 2009;46(3):632-640. doi:10.1111/j.1365-2664.2009.01647.x

40. Wasser SK, Lundin JI, Ayres K, Seely E, Giles D, Balcomb K, Hempelmann J, Parsons K, Booth R. Population growth is limited by nutritional impacts on pregnancy success in endangered Southern Resident killer whales (*Orcinus orca*). Deng ZD, ed. *PLoS ONE*. 2017;12(6):e0179824. doi:10.1371/journal.pone.0179824

41. Couture F, Oldford G, Christensen V, Barrett-Lennard L, Walters C. Requirements and availability of prey for northeastern pacific southern resident killer whales. Fujiwara M, ed. *PLoS ONE*. 2022;17(6):e0270523. doi:10.1371/journal.pone.0270523

42. Murray CC, Hannah LC, Doniol-Valcroze T, Wright BM, Stredulinsky EH, Nelson JC, Locke A, Lacy RC. A cumulative effects model for population trajectories of resident killer whales in the Northeast Pacific. *Biol Conserv*. 2021;257:109124. doi:10.1016/j.biocon.2021.109124

43. Chasco BE, Kaplan IC, Thomas AC, Acevedo-Gutiérrez A, Noren DP, Ford MJ, Hanson MB, Scordino JJ, Jeffries SJ, Marshall KN, Shelton AO. Competing tradeoffs between increasing marine mammal predation and fisheries harvest of Chinook salmon. *Sci Rep*. 2017;7(1):15439. doi:10.1038/s41598-017-14984-8

44. Sato M, Trites AW, Gauthier S. Southern resident killer whales encounter higher prey densities than northern resident killer whales during summer. *Can J Fish Aquat Sci*. 2021;78(11):1732-1743. doi:10.1139/cjfas-2020-0445

45. Stewart JD, Durban JW, Fearnbach H, Barrett-Lennard LG, Casler PK, Ward EJ, Dapp DR. Survival of the fattest: linking body condition to prey availability and survivorship of killer whales. *Ecosphere*. 2021;12(8):e03660. doi:10.1002/ecs2.3660

46. Bain D. *An Evaluation of Evolutionary Processes: Studies of Natural Selection, Dispersal, and Cultural Evolution in Killer Whales (*Orcinus Orca*)*. Ph.D. thesis. University of California Santa Cruz; 1989.

47. Baird RW, Hanson MB, Dill LM. Factors influencing the diving behaviour of fish-eating killer whales: sex differences and diel and interannual variation in diving rates. *Can J Zool*. 2005;83(2):257-267. doi:10.1139/z05-007

48. Beerman A, Ashe E, Preedy K, Williams R. Sexual segregation when foraging in an extremely social killer whale population. *Behav Ecol Sociobiol*. 2016;70(1):189-198. doi:10.1007/s00265-015-2038-2

49. Herman DP, Burrows DG, Wade PR, Durban JW, Matkin CO, LeDuc RG, Barrett-Lennard LG, Krahn MM. Feeding ecology of eastern North Pacific killer whales *Orcinus orca* from fatty acid, stable isotope, and organochlorine analyses of blubber biopsies. *Mar Ecol Prog Ser*. 2005;302:275-291. doi:10.3354/meps302275

50. Krahn MM, Hanson MB, Baird RW, Boyer RH, Burrows DG, Emmons CK, Ford JK, Jones LL, Noren DP, Ross PS, Schorr GS. Persistent organic pollutants and stable isotopes in biopsy samples (2004/2006) from Southern Resident killer whales. *Mar Pollut Bull*. 2007;54(12):1903-1911. doi:10.1016/j.marpolbul.2007.08.015

51. Warlick A, Ylitalo G, O'Neill S, Hanson M, Emmons C, Ward E. Using Bayesian stable isotope mixing models and generalized additive models to resolve diet changes for fish-eating killer whales *Orcinus orca*. *Mar Ecol Prog Ser*. 2020;649:189-200. doi:10.3354/meps13452

52. Newsome SD, Clementz MT, Koch PL. Using stable isotope biogeochemistry to study marine mammal ecology. *Mar Mamm Sci*. 2010. doi:10.1111/j.1748-7692.2009.00354.x

53. DeNiro MJ, Epstein S. Influence of diet on the distribution of carbon isotopes in animals. *Geochimica et Cosmochimica Acta*. 1978;42(5):495-506. doi:10.1016/0016-7037(78)90199-0

54. Deniro MJ, Epstein S. Influence of diet on the distribution of nitrogen isotopes in animals. *Geochimica et Cosmochimica Acta*. 1981;45(3):341-351. doi:10.1016/0016-7037(81)90244-1

55. Read FL, Hohn AA, Lockyer CH. A review of age estimation methods in marine mammals with special reference to monodontids. *NAMMCOSP*. 2018;10. doi:10.7557/3.4474

56. Ventre J, Jett J. Killer Whales, Theme Parks and Controversy: An Exploration of the Evidence. In: Markwell K, ed. *Animals and Tourism*. Multilingual Matters; 2015:128-145. doi:10.21832/9781845415051-012

57. Lockyer C, Hohn AA, Hobbs R, Stewart RE. Report of the workshop on age estimation in beluga: Beaufort, North Carolina, US 5-9 December 2011. *NAMMCOSP*. 2016;8. doi:10.7557/3.3731

58. Pierce K, Kajimura H. *Acid Etching and Highlighting for Defining Growth Layers in Cetacean Teeth*. International Whaling Commission; 1980:99-103.

59. Evans K, Robertson K. A note on the preparation of sperm whale (*Physeter macrocephalus*) teeth for age determination. *jcrm*. 2023;3(1):101-107. doi:10.47536/jcrm.v3i1.907

60. Newsome S, Etnier M, Monson D, Fogel M. Retrospective characterization of ontogenetic shifts in killer whale diets via $\delta^{13}C$ and $\delta^{15}N$ analysis of teeth. *Mar Ecol Prog Ser*. 2009;374:229-242. doi:10.3354/meps07747

61. Watt CA, Stewart BE, Loseto L, Halldorson T, Ferguson SH. Estimating narwhal (*Monodon monoceros*) age using tooth layers and aspartic acid racemization of eye lens nuclei. *Mar Mamm Sci*. 2020;36(1):103-115. doi:10.1111/mms.12623

62. Stukonytė L, Borrell A, Drago M, Lockyer C, Víkingsson G, Aguilar A. Effect of formic acid treatment on carbon and nitrogen stable isotope ratios in sperm whale teeth dentine. *Rapid Comm Mass Spectrometry*. 2023;37(10):e9500. doi:10.1002/rcm.9500

63. GIMP Development Team. Published online 2019. https://www.gimp.org

64. Keeling CD. The Suess effect: ^{13}Carbon-^{14}Carbon interrelations. *Environ Int*. 1979;2(4-6):229-300. doi:10.1016/0160-4120(79)90005-9

65. Clark CT, Cape MR, Shapley MD, Mueter FJ, Finney BP, Misarti N. SuessR: Regional corrections for the effects of anthropogenic CO_2 on $\delta^{13}C$ data from marine organisms. *Methods Ecol Evol*. 2021;12(8):1508-1520. doi:10.1111/2041-210X.13622

66. R Core Team. R: A language and environment for statistical computing. Published online 2022. https://www.R-project.org/

67. Clark C, Cape M, Shapley M, Mueter F, Finney B, Misarti N. SuessR: Suess and Laws Corrections for Marine Stable Carbon Isotope Data. Published online 2023. https://CRAN.R-project.org/package=SuessR

68. Ambrose SH. Preparation and characterization of bone and tooth collagen for isotopic analysis. *J Archaeol Sci*. 1990;17(4):431-451. doi:10.1016/0305-4403(90)90007-R

69. Post DM, Layman CA, Arrington DA, Takimoto G, Quattrochi J, Montaña CG. Getting to the fat of the matter: models, methods and assumptions for dealing with lipids in stable isotope analyses. *Oecologia*. 2007;152(1):179-189. doi:10.1007/s00442-006-0630-x

70. Posit Team. RStudio: Integrated Development Environment for R. Published online 2024.

71. Kuznetsova A, Brockhoff PB, Christensen RHB. lmerTest Package: Tests in Linear Mixed Effects Models. *J Stat Soft*. 2017;82(13). doi:10.18637/jss.v082.i13

72. NOAA Fisheries Salmon Population Summary. Salmonid and Steelhead Population Abundance Summary from 1949 to 2010 for Washington, Oregon, and Idaho. Published online 2015. https://www.webapps.nwfsc.noaa.gov/apex/f?p=261:1

73. Moore JW, Semmens BX. Incorporating uncertainty and prior information into stable isotope mixing models. *Ecol Lett*. 2008;11(5):470-480. doi:10.1111/j.1461-0248.2008.01163.x

74. Stock BC, Jackson AL, Ward EJ, Parnell AC, Phillips DL, Semmens BX. Analyzing mixing systems using a new generation of Bayesian tracer mixing models. *PeerJ*. 2018;6:e5096. doi:10.7717/peerj.5096

75. Post DM. Using stable isotopes to estimate trophic position: models, methods, and assumptions. *Ecology*. 2002;83(3):703-718. doi:10.1890/0012-9658(2002)083[0703:USITET]2.0.CO;2

76. Satterfield FR, Finney BP. Stable isotope analysis of Pacific salmon: insight into trophic status and oceanographic conditions over the last 30 years. *Prog Oceanogr*. 2002;53(2-4):231-246. doi:10.1016/S0079-6611(02)00032-0

77. Quinn TP. *The Behavior and Ecology of Pacific Salmon and Trout*. Second edition. University of Washington Press ; In association with American Fisheries Society; 2018.

78. Huwaldt J, Steinhorst S. Plot digitizer. Published online 2020. http://plotdigitizer.sourceforge.net

79. Aydin O, Yassikaya MY. Validity and reliability analysis of the PlotDigitizer software program for data extraction from single-case graphs. *Perspect Behav Sci*. 2022;45(1):239-257. doi:10.1007/s40614-021-00284-0

80. Carlisle AB, Goldman KJ, Litvin SY, Madigan DJ, Bigman JS, Swithenbank AM, Kline Jr TC, Block BA. Stable isotope analysis of vertebrae reveals ontogenetic changes in habitat in an endothermic pelagic shark. *Proc R Soc B*. 2015;282(1799):20141446. doi:10.1098/rspb.2014.1446

81. Borrell A, Abad-Oliva N, Gómez-Campos E, Giménez J, Aguilar A. Discrimination of stable isotopes in fin whale tissues and application to diet assessment in cetaceans. *Rapid Comm Mass Spectrometry*. 2012;26(14):1596-1602. doi:10.1002/rcm.6267

82. Gelman A, Rubin DB. Inference from iterative simulation using multiple sequences. *Statist Sci*. 1992;7(4). doi:10.1214/ss/1177011136

83. McMahon KW, McCarthy MD. Embracing variability in amino acid δ^{15}N fractionation: mechanisms, implications, and applications for trophic ecology. *Ecosphere*. 2016;7(12):e01511. doi:10.1002/ecs2.1511

84. Chikaraishi Y, Ogawa NO, Kashiyama Y, Takano Y, Suga H, Tomitani A, Miyashita H, Kitazato H, Ohkouchi N. Determination of aquatic food-web structure based on compound-specific nitrogen isotopic composition of amino acids. *Limnol Oceanogr Methods*. 2009;7(11):740-750. doi:10.4319/lom.2009.7.740

85. Brault EK, Koch PL, Costa DP, McCarthy MD, Hückstädt LA, Goetz KT, McMahon KW, Goebel ME, Karlsson O, Teilmann J, Harkonen T. Trophic position and foraging ecology of Ross, Weddell, and crabeater seals revealed by compound-specific isotope analysis. *Mar Ecol Prog Ser*. 2019;611:1-18. doi:10.3354/meps12856

86. Nehasil S. *Examining Trophic Relationships between Top Predators and Their Prey in a Coastal Upwelling Ecosystem*. Ph.D. thesis. University of California San Diego; 2023. https://escholarship.org/uc/item/6245g9bm

87. Coe R. It's the effect size, stupid: What effect size is and why it is important. A paper presented at the Annual Conference of the British Educational Research Association, University of Exeter, Exeter, Devon, England.

88. Morra KE, Chikaraishi Y, Gandhi H, James HF, Rossman S, Wiley AE, Raine AF, Beck J, Ostrom PH. Trophic declines and decadal-scale foraging segregation in three pelagic seabirds. *Oecologia*. 2019;189(2):395-406. doi:10.1007/s00442-018-04330-8

89. Hertz E, Trudel M, Brodeur RD, Daly EA, Eisner L, Farley Jr EV, Harding JA, MacFarlane RB, Mazumder S, Moss JH, Murphy JM. Continental-scale variability in the feeding ecology of juvenile Chinook salmon along the coastal Northeast Pacific Ocean. *Mar Ecol Prog Ser*. 2015;537:247-263. doi:10.3354/meps11440

90. Litz MN, Miller JA, Copeman LA, Teel DJ, Weitkamp LA, Daly EA, Claiborne AM. Ontogenetic shifts in the diets of juvenile Chinook Salmon: new insight from stable isotopes and fatty acids. *Environ Biol Fish*. 2017;100(4):337-360. doi:10.1007/s10641-016-0542-5

91. Wolf N, Garcia S, Harris BP, Howard KG. Stable isotopes, morphology, and body condition metrics suggest similarity in the trophic level and diversity in the carbon sources of freshwater and early marine diets of Chinook salmon. *Mar Biol*. 2024;171(4):75. doi:10.1007/s00227-024-04392-8

92. Candy JR, Quinn TP. Behavior of adult Chinook salmon (*Oncorhynchus tshawytscha*) in British Columbia coastal waters determined from ultrasonic telemetry. *Can J Zool*. 1999;77(7):1161-1169. doi:10.1139/z99-043

93. Wright BM, Stredulinsky EH, Ellis GM, Ford JKB. Kin-directed food sharing promotes lifetime natal philopatry of both sexes in a population of fish-eating killer whales, *Orcinus orca*. *Anim Behav*. 2016;115:81-95. doi:10.1016/j.anbehav.2016.02.025

94. Quinn TP, Seamons TR, Johnson SP. Stable isotopes of carbon and nitrogen indicate differences in marine ecology between wild and hatchery-produced steelhead. *Trans Am Fish Soc*. 2012;141(2):526-532. doi:10.1080/00028487.2012.670188

95. Davis MJ, Woo I, Ellings CS, Hodgson S, Beauchamp DA, Nakai G, De La Cruz SE. Integrated diet analyses reveal contrasting trophic niches for wild and hatchery juvenile chinook salmon in a large river delta. *Trans Am Fish Soc*. 2018;147(5):818-841. doi:10.1002/tafs.10088

96. Doi H, Akamatsu F, González AL. Starvation effects on nitrogen and carbon stable isotopes of animals: an insight from meta-analysis of fasting experiments. *R Soc open sci*. 2017;4(8):170633. doi:10.1098/rsos.170633

97. McMahon KW, Hamady LL, Thorrold SR. A review of ecogeochemistry approaches to estimating movements of marine animals. *Limnol Oceanogr*. 2013;58(2):697-714. doi:10.4319/lo.2013.58.2.0697

98. Lerner JE, Hunt BPV. Seasonal variation in the lipid content of Fraser River Chinook Salmon (*Oncorhynchus tshawytscha*) and its implications for Southern Resident killer whale (*Orcinus orca*) prey quality. *Sci Rep*. 2023;13(1):2675. doi:10.1038/s41598-023-28321-9

99. Rafter PA, Bagnell A, Marconi D, DeVries T. Global trends in marine nitrate N isotopes from observations and a neural network-based climatology. *Biogeosciences*. 2019;16(13):2617-2633. doi:10.5194/bg-16-2617-2019

CONCLUSIONS

Stable isotope analysis of consumer tissues is a powerful technique to reconstruct foraging ecology and habitat use. This is especially true for elusive, at-sea marine mammals such as killer whales. However, appropriate and tissue-specific pre-treatment conditions must be identified. I address these questions in Chapters 1 and 2 for killer whale bone and teeth, respectively. This will provide a foundation for any future work involving stable isotope analyses of these tissues. In Chapter 3, I review and synthesize stable isotope values for numerous consumer species in the North Pacific. This dataset will be useful for any trophic ecology studies using stable isotope analyses in this region. That chapter provided context for Chapters 4 and 5, in which I explored how killer whales exert top-down effects in food webs as apex predators, but are also susceptible to bottom-up effects such as limited prey availability. This dissertation describes historical baseline information for killer whales, which will inform that which we continue to learn about them in the future.